Technische Universität München
Fakultät für Physik
Lehrstuhl für theoretische Physik IV (T31)

Anatomy and Phenomenology of Flavor and CP Violation in Supersymmetric Theories

Wolfgang Altmannshofer

Vollständiger Abdruck der von der Fakultät für Physik der Technischen Universität München zur Erlangung des akademischen Grades eines

Doktors der Naturwissenschaften

genehmigten Dissertation.

Vorsitzender:	Univ.-Prof. Dr. Stephan Paul
Prüfer der Dissertation:	1. Univ.-Prof. Dr. Andrzej J. Buras
	2. Hon.-Prof. Dr. Wolfgang F. L. Hollik

Die Dissertation wurde am 08.07.2010 bei der Technischen Universität München eingereicht und durch die Fakultät für Physik am 20.07.2010 angenommen.

Zusammenfassung

Gegenstand dieser Doktorarbeit ist eine umfangreiche und systematische Untersuchung von Flavor und CP verletzenden Niederenergieprozessen im Rahmen des MSSM, der minimalen supersymmetrischen Erweiterung des Standard Modells. Supersymmetrische (SUSY) Modelle gehören zu den am besten motivierten und am gründlichsten untersuchten Modellen für Neue Physik (NP). Es wird erwartet, dass die neuen Freiheitsgrade, die die Supersymmetrie vorhersagt, Massen von der Größenordnung der TeV Skala besitzen und die direkte Suche nach diesen Teilchen ist eines der Hauptziele am LHC. Ein komplementärer Ansatz das MSSM zu testen, besteht in der Untersuchung von Präzisionsobservablen bei niedrigen Energien, die durch die virtuellen Effekte der neuen Freiheitsgrade beeinflusst werden können. Von besonderer Bedeutung in diesem Zusammenhang sind sogenannte Flavor Changing Neutral Current (FCNC) Prozesse, die im Standard Modell nicht auf Tree Niveau vorkommen und deshalb höchst sensitiv auf die Flavorstruktur von NP Modellen sind.

Zuerst untersuchen wir modellunabhängig Niederenergieprozesse, die eine hohe Sensitivität auf die Flavor und CP verletzenden Strukturen besitzen, die im MSSM enthalten sind. Als nächstes diskutieren wir im Detail die reichhaltige Flavorstruktur des MSSM und die resultierenden SUSY Beiträge zu FCNC und CP verletzenden Observablen und zwar sowohl für große und kleine Werte für $\tan\beta$. In der Tat schränken genau gemessene Niederenergieobservable den MSSM Parameterraum außergewöhnlich stark ein, was oft als SUSY Flavor Problem bezeichnet wird. Wir skizzieren Möglichkeiten die gefährlich großen SUSY Effekte in diesen Observablen zu kontrollieren und untersuchen die daraus resultierenden Vorhersagen für jene Niederenergieprozesse, die noch nicht mit hoher Präzision gemessen sind. Wir berücksichtigen sowohl das MSSM mit minimaler Flavor Verletzung als auch SUSY Modelle die auf abelschen und nicht-abelschen Flavor Symmetrien basieren und deren "weiche" SUSY Brechungsterme repräsentative Flavorstrukturen aufweisen. Wir identifizieren die markanten Muster von Flavoreffekten in den Niederenergieprozessen, wobei wir uns insbesonders auf CP verletzende Observable im $b \to s\gamma$ Übergang, die B_s Mischungsphase, das Verzweigungsverhältnis des seltenen $B_s \to \mu^+\mu^-$ Zerfalls, CP Verletzung in $D^0 - \bar{D}^0$ Mischung Und elektrische Dipolmomente konzentrieren. Wir betonen, dass es die charkteristischen Korrelationen zwischen den SUSY Effekten in diesen Observablen erlauben, die verschiedenen Modelle von einander zu unterscheiden.

Abstract

The main subject of this PhD thesis is a comprehensive and systematic analysis of flavor and CP violating low energy processes in the framework of the MSSM, the minimal supersymmetric extension of the Standard Model. Supersymmetric (SUSY) models are among the best motivated and most thoroughly analyzed New Physics (NP) models. The new degrees of freedom predicted by Supersymmetry are expected to have masses of the order of the TeV scale and the direct search for these particles is one of the major goals at the LHC. A complementary strategy to probe the MSSM is given by the analysis of low energy high-precision observables, that can be modified through virtual effects of the new degrees of freedom. Of particular importance in this respect are so-called Flavor Changing Neutral Current (FCNC) processes that, forbidden in the Standard Model at the tree level, are highly sensitive probes of the flavor structure of NP models.

We first analyze model independently low energy processes that show high sensitivity to the new sources of flavor and CP violation contained in the MSSM. Next, we discuss in detail the rich flavor structure of the MSSM and the implied SUSY contributions to FCNC and CP violating observables both in the low and high $\tan\beta$ regime. In fact, well measured low energy observables lead to remarkably strong constraints on the MSSM parameter space, which is often referred to as the SUSY flavor problem. We outline possibilities to control dangerously large SUSY effects in such observables and analyze the implied predictions for those low energy processes that are not measured with high precision, yet. We consider both the Minimal Flavor Violating MSSM and SUSY models based on abelian and non-abelian flavor symmetries that show representative flavor structures in the soft SUSY breaking terms. We identify the distinctive patterns of SUSY effects in the low energy observables, focussing in particular on CP violation in the $b \to s\gamma$ transition, the B_s mixing phase, the branching ratio of the rare $B_s \to \mu^+\mu^-$ decay, CP violation in $D^0 - \bar{D}^0$ mixing and electric dipole moments. We emphasize that the characteristic correlations among the SUSY effects in these processes allow to distinguish between the different models.

Contents

1 Introduction

The era of the Large Hadron Collider has started. On March 30, 2010, the first long physics run of the LHC at a center of mass energy of 7 TeV was initiated and with confidence the clarification of the mechanism of electroweak symmetry breaking is expected in the coming years. In fact, the Standard Model (SM) of elementary particle physics with its presently discovered particle content becomes inconsistent at a scale of around 1 TeV, and without doubts, the experimental discovery of the last missing piece in the Standard Model, the Higgs boson (or whatever dynamics takes its role), is the main goal of the LHC experiment. Moreover, arguments based on the *gauge hierarchy problem* suggest that the Standard Model also has to be extended with New Physics (NP) around the TeV scale [1] and the direct exploration of this energy scale will have profound impact on our understanding of particle physics.

As the Standard Model does not include a description of gravity, it is necessarily incomplete and has to be considered as a low energy effective theory of a still to be determined fundamental theory. As the Higgs boson is a scalar particle and its mass m_h is not protected by any symmetry in the SM, m_h, that is roughly set by the electroweak scale $v \simeq 246$ GeV, is quadratically sensitive to the highest scale contained in the fundamental theory, i.e. the scale of gravity, the Planck mass $M_{\rm Pl} \simeq 10^{19}$ GeV. In other words, quantum corrections to the Higgs mass are generically of the order of the Planck mass, and the huge hierarchy between the electroweak scale and the scale of gravity is unstable at the quantum level. Unless a tremendous amount of fine tuning is assumed, the natural value of the electroweak scale would be given by the Planck mass. This is usually referred to as the gauge hierarchy problem.

Numerous mechanisms to stabilize the electroweak scale against large quantum corrections have been investigated. Supersymmetry (SUSY) [2, 3] for example is an extension of Poincaré symmetry and relates bosonic and fermionic degrees of freedom thus leading to scalar masses that are protected from quadratically divergent quantum corrections as fermion masses are. Also in the so-called Technicolor theories [4, 5] where electroweak symmetry is broken dynamically by the condensate of a strongly coupled sector, a large hierarchy between the electroweak scale and some high NP scale is natural. In theories with large extra dimensions [6, 7, 8] the hierarchy problem can be solved by lowering the scale of gravity down to the electroweak scale and attributing the observed weakness of gravity to several large spatial extra dimensions. Models with warped extra dimensions [9] generate the electroweak scale from the Planck scale through an exponential hierarchy that arises from an AdS_5 background metric. Finally, so-called little and littlest Higgs models [10, 11, 12] address the hierarchy problem, assuming the Higgs particle of the Standard Model to be a pseudo Nambu-Goldstone boson of a collectively broken global symmetry.

In order to address the gauge hierarchy problem, all these New Physics theories predict new phenomena at the TeV scale, the energy scale that will be directly explored for the first time at the LHC. On the other hand, also high-precision low energy experiments allow

to indirectly probe NP theories predicting new degrees of freedom at the TeV scale. In particular, Flavor Changing Neutral Current (FCNC) processes, forbidden in the SM at the tree level [13], are highly sensitive probes of the flavor structure of such new degrees of freedom.

Among the many possible extensions of the SM, the most popular is still the Minimal Supersymmetric Standard Model (MSSM). Theories with TeV scale Supersymmetry are in fact able to address the gauge hierarchy problem and provide for example also a dark matter candidate. They remain perturbative up to high scales and achieve gauge coupling unification at a Grand Unification scale of around 10^{16} GeV. However, the rich flavor structure of the MSSM generically leads to large contributions to FCNC processes in conflict with available experimental data: the so-called *SUSY flavor problem*. A thorough understanding of the SUSY contributions to FCNCs – their origin, their structure and their implied phenomenology – is therefore crucial in order to test SUSY theories.

In this thesis we will discuss in detail the anatomy and phenomenology of flavor and CP violation in the quark sector of the MSSM. The presented results will mostly be based on our analyses published in [14, 15, 16, 17, 18, 19, 20, 21, 22, 23].

In chapter 2 we briefly review the status of flavor violation in the SM and sketch the SM flavor puzzle and the New Physics flavor problem. In chapter 3 we discuss selected low energy observables concentrating on but not restricting ourselves to FCNC processes. In particular, our presentation contains $\Delta F = 2$ processes as $D^0 - \bar{D}^0$, $K^0 - \bar{K}^0$, $B_d - \bar{B}_d$ and $B_s - \bar{B}_s$ mixing, $\Delta F = 1$ rare Kaon and B meson decays as e.g. the radiative $B \to X_s\gamma$ decay, the semileptonic $B \to K^*\ell^+\ell^-$ decay, the hadronic $B \to \phi K_S$ and $B \to \eta' K_S$ decays, the purely leptonic $B_{s,d} \to \mu^+\mu^-$ decays, the several rare decays based on the $b \to s\nu\bar{\nu}$ and $s \to d\nu\bar{\nu}$ transition and the tree level $B \to \tau\nu$ decay, as well as $\Delta F = 0$ processes as the anomalous magnetic moment of the muon, $(g-2)_\mu$, and electric dipole moments (EDMs). We collect the most updated SM predictions of these observables and present their current experimental situation and the expected future prospects. We also discuss in a model independent way how these observables can be affected by generic NP contributions. In chapter 4 we introduce the concept of Supersymmetry, concentrating directly on the MSSM. We briefly review its field content and consider in detail the flavor structure of the MSSM in the quark sector. Chapter 5 is devoted to the MSSM in the large $\tan\beta$ regime. A detailed analysis of SUSY contributions to low energy observables then follows in chapter 6. We give a very comprehensive presentation of the relevant SUSY induced effects in the low energy observables introduced in chapter 3, pointing out the main dependencies on the MSSM parameters. In chapter 7 we then discuss the SUSY flavor problem. In an example MSSM scenario we impose the bounds coming from FCNC processes and derive the allowed ranges for the SUSY flavor structures. Possibilities to address the SUSY flavor problem are also reviewed. Finally in chapter 8, we present an extensive numerical analysis of low energy processes in concrete SUSY models. In particular we consider the MSSM with Minimal Flavor Violation as well as SUSY flavor models based on abelian and non-abelian flavor symmetries that show representative flavor structures in the soft SUSY breaking terms and demonstrate how their distinct predictions for low energy observables allow to distinguish between these different models. We conclude in chapter 9 with a summary and outlook.

2 The Standard Model and New Physics Flavor Problems

2.1 The Success of the SM CKM Mechanism of Flavor and CP Violation

The Standard Model provides an extremely successful description of basically all experimental data in particle physics. It is based on the $\mathrm{SU}(3)_c \times \mathrm{SU}(2)_L \times \mathrm{U}(1)_Y$ gauge group that is spontaneously broken to $\mathrm{SU}(3)_c \times \mathrm{U}(1)_{\mathrm{em}}$ by the vacuum expectation value of a single Higgs scalar with quantum numbers $(1,2)_{1/2}$. The matter content of the SM consists of five different representations of the gauge group: left handed quarks q_L^I $(3,2)_{1/6}$, right handed up quarks u_R^I $(3,1)_{2/3}$, right handed down quarks d_R^I $(3,1)_{-1/3}$, left handed leptons ℓ_L^I $(1,2)_{-1/2}$ and right handed charged leptons e_R^I $(1,1)_{-1}$. These matter fields come in three generations or *flavors*, I = 1,2,3. Concerning their gauge interactions, the three flavors are identical copies and behave in exactly the same way. They can be only distinguished by their Yukawa couplings to the Higgs field that are in general 3×3 matrices in flavor space. Diagonalizing the Yukawa matrices to get diagonal quark masses after electroweak symmetry breaking, one is left with the the Cabibbo-Kobayashi-Maskawa (CKM) matrix, V_{CKM} [24, 25], that appears in the flavor changing coupling of the W boson with the quarks.

Within the SM all flavor changing effects in the quark sector are induced by the CKM matrix, that parameterizes the misalignment between the up and down quark mass eigenstates in flavor space. It is a unitary matrix that depends on three real angles and one single complex phase. A very convenient parameterization of the CKM matrix is given by the Wolfenstein parameterization [26] in terms of λ, A, $\bar{\varrho}$ and $\bar{\eta}$

$$V_{\mathrm{CKM}} \simeq \begin{pmatrix} 1-\frac{1}{2}\lambda^2 & \lambda & A\lambda^3(\varrho - i\eta) \\ -\lambda & 1-\frac{1}{2}\lambda^2 & A\lambda^2 \\ A\lambda^3(1-\bar{\varrho}-i\bar{\eta}) & -A\lambda^2 & 1 \end{pmatrix} + O(\lambda^4) \ , \tag{2.1}$$

where the Cabibbo angle $\lambda \simeq 0.23$ plays the role of an expansion parameter and the CP violating phase is represented by the parameter $\bar{\eta}$. Unitarity of the CKM matrix implies various relations between its entries, in particular so-called Unitarity Triangles. The most important Unitarity Triangle (UT) is

$$V_{ud}V_{ub}^* + V_{cd}V_{cb}^* + V_{td}V_{tb}^* = 0 \tag{2.2}$$

and it can directly be visualized as a triangle in the $\bar{\varrho} - \bar{\eta}$ plane.

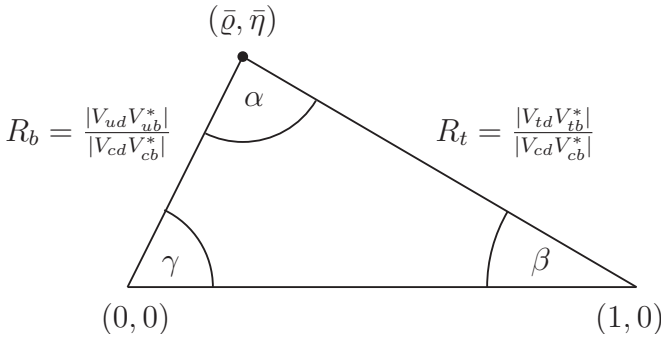

Its sides R_t and R_b as well its angles α, β and γ are accessible in many flavor changing observables and using the available experimental information on these observables allows to overconstrain the $\bar{\varrho} - \bar{\eta}$ plane.

Within the last years the SM CKM mechanism of flavor and CP violation has been fully experimentally established. Global fits to the data on flavor changing processes (see [27] and [28]) all lead consistently to a single solution in the $\bar{\varrho} - \bar{\eta}$ plane and there is basically no doubt anymore that the SM CKM matrix is the main source of flavor and CP violation in the processes entering the UT analysis [29]. Correspondingly, New Physics effects to such processes can only be small corrections and are strongly bounded by existing data.

A very close look to the analyses of the Unitarity Triangle however reveals some tensions [30, 31, 32, 33, 34]. In particular, the measured amount of CP violation in $B_d - \bar{B}_d$ mixing ($S_{\psi K_S}$) seems insufficient to fully explain CP violation in $K^0 - \bar{K}^0$ mixing (ϵ_K).

While this tension can be fully analyzed by means of the standard UT analysis in the $\bar{\varrho} - \bar{\eta}$ plane (see e.g. [30, 34]), it can be displayed particularly transparent in the $R_b - \gamma$ plane [35, 14, 31, 21]. In the upper left plot of figure 2.1 we show the $R_b - \gamma$ plane in the SM, imposing the constraints from $S_{\psi K_S}$ (blue), $\Delta M_d/\Delta M_s$ (yellow) and ϵ_K (red) at the 1σ level. The solid black line corresponds to $\alpha = 90^\circ$ close to the result from the SM UT fits [27, 28] and the direct determination from the isospin analysis of $B \to \pi\pi, \rho\rho, \rho\pi$ [36].

The numerical input parameter that we use to obtain this plot are collected in appendix A.3. It is evident that there is a tension between the three constraints, as dependently on which two constraints are used to fix R_b and γ, three distinct regions in the plane are chosen. Possible solutions to this tension can be achieved by assuming NP contributions in one of the three observables ϵ_K, $S_{\psi K_S}$ or $\Delta M_d/\Delta M_s$:

1) If $S_{\psi K_S}$ and $\Delta M_d/\Delta M_s$ are used to determine R_b and γ (see upper right plot in figure 2.1), the resulting prediction for ϵ_K reads $\epsilon_K = (1.82 \pm 0.26) \times 10^{-3}$, much below the experimental value $\epsilon_K^{\rm exp} = (2.228 \pm 0.011) \times 10^{-3}$. A positive NP effect in ϵ_K at the level of +22% compared to its SM value is then required to fit exactly the measurement.

2) If ϵ_K and $\Delta M_d/\Delta M_s$ are assumed to be NP free and used to fix the UT parameters as shown in the lower left plot of figure 2.1, then $\sin 2\beta$ is predicted to be $\sin 2\beta = 0.81 \pm 0.09$, which is considerably larger than the measured $S_{\psi K_S}^{\rm exp} = 0.672 \pm 0.023$. This tension can be solved by a NP phase in B_d mixing of -6.1°.

3) If instead ϵ_K and $S_{\psi K_S}$ are used for a determination of R_b and γ, then R_t comes out as $R_t = 1.02^{+0.06}_{-0.07}$ which in the SM corresponds to $\Delta M_d/\Delta M_s = 0.036 \pm 0.005$. In order to agree exactly with the experimental central value of $\Delta M_d^{\rm exp}/\Delta M_s^{\rm exp} = 0.0285 \pm 0.0005$,

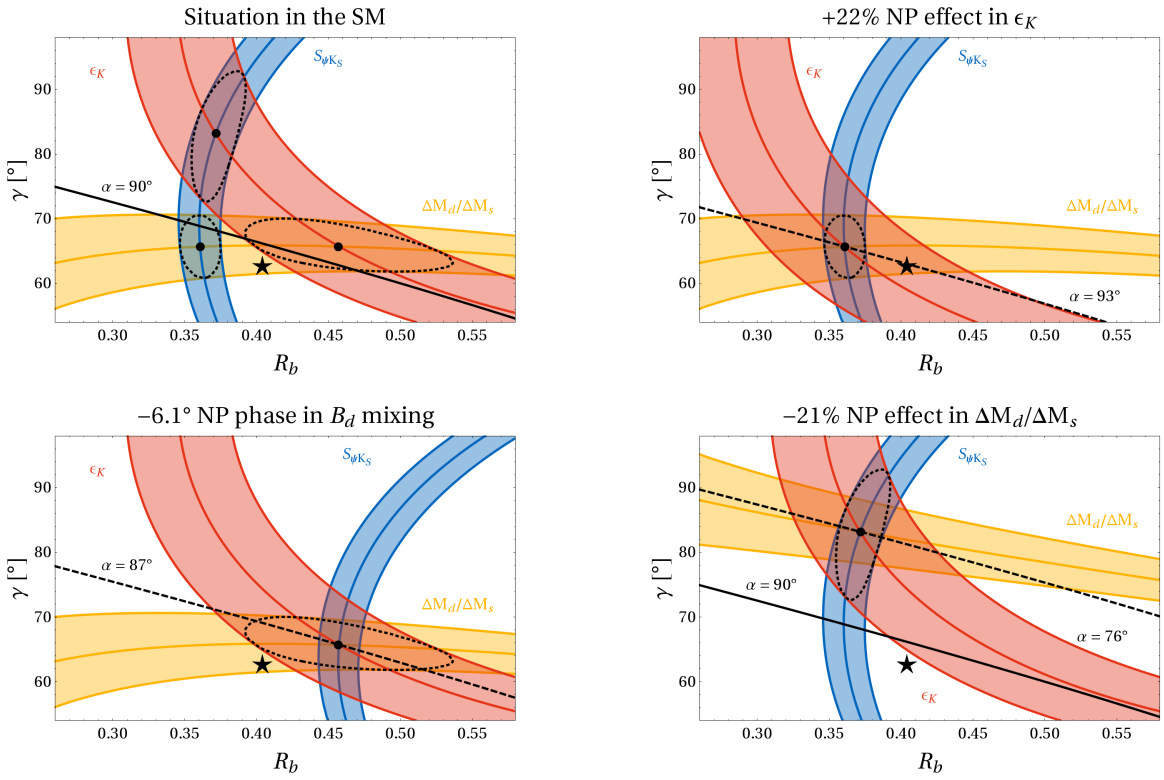

Figure 2.1: The $R_b - \gamma$ plane assuming: i) $\sin 2\beta$, R_t and ϵ_K not affected by NP effects (upper left), ii) $\sin 2\beta$ and R_t NP free while ϵ_K affected by a positive NP effect at the level of $+22\%$ compared to the SM contribution (upper right), iii) ϵ_K and R_t NP free while $\sin 2\beta$ affected by a NP phase in B_d mixing of $-6.1°$ (lower left), iv) ϵ_K and $\sin 2\beta$ NP free while $\Delta M_d/\Delta M_s$ affected by a negative NP effect at the level of -21% compared to the SM contribution (lower right). The black star indicates the values for R_b and γ obtained in the NP UT fit of [28].

one then needs a NP contribution to $\Delta M_d/\Delta M_s$ at the level of -21%. Such a situation is shown in the lower right plot of figure 2.1.

In table 2.1 we list the values of the relevant CKM parameters corresponding to each case. We observe

- **Solution 1)** corresponds to $\gamma \simeq 66°$, $R_b \simeq 0.36$ and $\alpha \simeq 93°$ in accordance with the usual SM UT analysis.
- **Solution 2)** is characterized by a large value of $R_b \simeq 0.47$, that is significantly larger than its exclusive determinations but still compatible with the inclusive determinations. The angles $\gamma \simeq 66°$ and $\alpha \simeq 87°$ agree with the usual SM UT analysis.
- **Solution 3)** finally is characterized by a large value of $\gamma \simeq 84°$ and α much below $90°$. The latter fact could be problematic for this solution given the improving determinations of α.

As one can see from table 2.1, the three NP scenarios characterized by black points in figure 2.1 can be distinguished from each other through precise tree level measurements of γ

	$\bar{\rho}$	$\bar{\eta}$	$\alpha[^\circ]$	$\gamma[^\circ]$	R_b	$\lvert V_{ub}\rvert \times 10^3$
1)	$0.149^{+0.029}_{-0.029}$	$0.329^{+0.018}_{-0.017}$	$93.2^{+5.0}_{-5.0}$	$65.7^{+4.9}_{-4.9}$	$0.361^{+0.014}_{-0.014}$	$3.44^{+0.17}_{-0.16}$
2)	$0.188^{+0.057}_{-0.048}$	$0.417^{+0.062}_{-0.054}$	$87.1^{+4.2}_{-3.8}$	$65.7^{+4.3}_{-3.9}$	$0.457^{+0.077}_{-0.064}$	$4.37^{+0.74}_{-0.62}$
3)	$0.044^{+0.063}_{-0.062}$	$0.369^{+0.023}_{-0.024}$	$75.7^{+10.0}_{-9.1}$	$83.2^{+9.4}_{-10.2}$	$0.372^{+0.020}_{-0.017}$	$3.55^{+0.22}_{-0.19}$
UTfit	0.177 ± 0.044	0.360 ± 0.031	92 ± 7	63 ± 7	0.404 ± 0.025	3.87 ± 0.23

Table 2.1: Predictions of several CKM parameters in the three scenarios as discussed in the text. For comparison, in the last line results are also shown from a global NP fit of the UT [28].

and R_b that are expected to be basically unaffected by NP effects and that will eventually be performed at a superB factory [37, 38, 39].

Instead of choosing now one of these three scenarios, for definiteness we will in the rest of this work use the CKM parameters from a global NP fit of the UT [28] that are also listed in appendix A.3.

2.2 The Standard Model Flavor Puzzle

While the identification of tensions and possible inconsistencies in the Unitarity Triangle provides valuable insight, the main goal of the SM UT analysis is to give a determination of the CKM parameters as precise as possible. The global fits seem to be consistent to a large extent and as mentioned above, the CKM picture of flavor and CP violation in the SM appears to be a very good description of the data.

As already evident from the parameterization (2.1), the measured entries in the CKM matrix show a strongly hierarchical pattern and range over three orders of magnitude

$$\begin{array}{lll} |V_{ud}| \simeq 0.97 \ , & |V_{us}| \simeq 0.23 \ , & |V_{ub}| \simeq 3.8 \times 10^{-3} \ , \\ |V_{cd}| \simeq 0.23 \ , & |V_{cs}| \simeq 0.97 \ , & |V_{cb}| \simeq 4.1 \times 10^{-2} \ , \\ |V_{td}| \simeq 8.4 \times 10^{-3} \ , & |V_{ts}| \simeq 4.1 \times 10^{-2} \ , & |V_{tb}| \simeq 1 \ . \end{array} \tag{2.3}$$

Similarly, also the remaining flavor parameters in the SM, i.e. the fermion masses are strongly hierarchical. Even leaving aside neutrinos, the SM fermion masses range over almost six order of magnitude between the electron mass and the top quark mass

$$\begin{array}{lll} m_t \simeq 164 \text{ GeV} \ , & m_c \simeq 1.2 \text{ GeV} \ , & m_u \simeq 3 \text{ MeV} \ , \\ m_b \simeq 4.2 \text{ GeV} \ , & m_s \simeq 0.1 \text{ GeV} \ , & m_d \simeq 5 \text{ MeV} \ , \\ m_\tau \simeq 1.8 \text{ GeV} \ , & m_\mu \simeq 0.1 \text{ GeV} \ , & m_e \simeq 0.5 \text{ MeV} \ . \end{array} \tag{2.4}$$

Only the top quark mass has a "natural" value of the order of the electroweak scale, while all the other fermion masses are very small and look unnatural.

The lack of a theoretical understanding of the huge hierarchies among the masses and mixing angles is often referred to as the *SM flavor puzzle*.

2.3 The New Physics Flavor Problem

New Physics models typically introduce additional sources of flavor and CP violation to the ones contained already in the SM CKM matrix. Employing a generic effective theory approach, the NP effects in flavor observables can be analyzed in a model independent way (see e.g. [40] for a recent review). Under the assumption that the NP degrees of freedom are heavier than the SM fields, they can be integrated out and their effects can be described by higher dimensional operators. The effective Lagrangian contains then the SM Lagrangian and an infinite tower of operators with dimension $d > 4$, constructed out of SM fields and suppressed by inverse powers of an effective NP scale $\Lambda_{\rm NP}$

$$\mathcal{L}_{\rm eff} = \mathcal{L}_{\rm SM} + \sum_{i,\, d>4} \frac{C_i^d}{\Lambda_{\rm NP}^{d-4}}\, \mathcal{O}_i^d \ , \tag{2.5}$$

where C_i^d are unknown couplings.

The term with the higher dimensional operators in (2.5) contains dimension six $\Delta F = 2$ four quark operators (see (3.3) below) that lead to contributions to neutral meson mixing. The good agreement between the SM predictions for meson mixing and the experimental data can then be translated into bounds on the combination $C_i/\Lambda_{\rm NP}^2$ [41, 42, 40].

The general picture that emerges is the following:

- If the coefficients C_i are assumed to be generic, i.e. all of O(1), then the most stringent bounds on the NP scale $\Lambda_{\rm NP}$, that come from CP violation in $K^0 - \bar{K}^0$ mixing, are at the level of $10^4 - 10^5$ TeV. This scale is far above the scale of NP that one expects from naturalness arguments.

- If on the other hand the NP scale is fixed to 1 TeV as suggested by a natural solution to the hierarchy problem, the couplings C_i that are responsible for CP violation in $K^0 - \bar{K}^0$ mixing are constrained at the level of $10^{-9} - 10^{-11}$. Slightly less stringent bounds arise from $D^0 - \bar{D}^0$, $B_d - \bar{B}_d$ and $B_s - \bar{B}_s$ mixing where the most stringent constraints on the corresponding couplings are at the level of 10^{-8}, 10^{-7} and 10^{-5} respectively.

This is the so-called *NP flavor problem*: NP with generic flavor structure is forced to be far above the natural TeV scale, while NP at the TeV scale necessarily has to possess a highly non-generic and unnatural flavor structure.

An elegant way to avoid this problem is provided by the Minimal Flavor Violation (MFV) hypothesis [43, 44, 45], where the only source of flavor violation, even beyond the SM, are the SM Yukawa couplings. As a result, flavor violating processes are determined by the same CKM elements as in the SM, i.e. the couplings C_i are suppressed, and a low NP scale at the level of few TeV is still compatible with the flavor data within this minimalistic scenario [41, 46].

Minimal flavor violation is however not a theory of flavor. While it naturally suppresses NP contributions to flavor violating process, it does not provide an explanation for the hierarchical flavor structure that is already present in the SM. Much more ambitious in this respect are models that try to explain the pattern of fermion masses and mixings based on the spontaneous breaking of flavor symmetries through the Froggatt-Nielsen mechanism [47].

Supersymmetric versions of flavor models have been widely discussed in the literature and we will only briefly present the main concepts of these SUSY flavor models in section 7.2. The flavor phenomenology of the MSSM with MFV and of representative SUSY flavor models will then be analyzed in chapter 8.

3 Low Energy Probes of Flavor and CP Violation

In the coming years, the LHC will probe the TeV scale. If new degrees of freedom exist at that scale, they will be produced directly and their production and decay mechanisms can be studied in an immediate way. A strategy complementary to the direct search is provided by low energy high-precision experiments where NP could be detected through the virtual effects of the NP degrees of freedom. In particular, Flavor Changing Neutral Current (FCNC) processes, that are forbidden in the SM at tree level, are highly sensitive to possible NP degrees of freedom and constitute of one of the best tools to investigate the flavor structure of NP theories.

In this chapter we discuss selected low energy observables concentrating on but not restricting ourselves to FCNC processes. We review their SM predictions as well as their present experimental situation and the expected future prospects. We also discuss in a model independent way how these observables can be affected by generic NP contributions.

We start with the $\Delta F = 2$ sector and discuss observables in the four neutral meson systems, i.e. in $D^0 - \bar{D}^0$, $K^0 - \bar{K}^0$, $B_d - \bar{B}_d$ and $B_s - \bar{B}_s$ mixing. We cover both well measured observables that lead to strong constraints on the NP flavor structure as well as observables where experimental data is still poor and large NP effects are still possible. In particular the observable $S_{\psi\phi}$ that measures the phase of the B_s mixing amplitude has recently attracted a lot of attention as recent data from Tevatron seems to hint at large non-standard contributions to B_s mixing.

In the $\Delta F = 1$ sector we first concentrate on processes sensitive to NP effects in flavor changing dipole operators, including the radiative $b \to s\gamma$ decay as well as the semileptonic $b \to s\ell^+\ell^-$ and the non-leptonic $B \to \phi K_s$ and $B \to \eta' K_S$ decay modes. Apart from the extremely important $B \to X_s\gamma$ branching ratio, we focus in particular on observables that are theoretically clean as e.g. CP asymmetries. We then turn to the purely leptonic $B_s \to \mu^+\mu^-$ and $B_d \to \mu^+\mu^-$ decays that are especially sensitive probes of flavor changing scalar currents that can arise in NP models. Subsequently we consider rare B and K decays with two neutrinos in the final state, i.e. $B \to X_s\nu\bar{\nu}$, $B \to K^{(*)}\nu\bar{\nu}$, $K^+ \to \pi^+\nu\bar{\nu}$ and $K_L \to \pi^0\nu\bar{\nu}$, that are among the theoretically cleanest FCNC processes. Finally we also discuss the tree level $B^+ \to \tau^+\nu$ decay that constitutes an essential probe of extended Higgs sectors of NP models.

In the end we also consider $\Delta F = 0$ observables, i.e. observables that do not require any source of flavor violation. We discuss the anomalous magnetic moment of the muon, $(g-2)_\mu$, and electric dipole moments (EDMs). The EDMs are particular interesting observables as the corresponding SM predictions are extremely small and any experimental evidence for them would be a clear signal of New Physics.

The most important observables are then conveniently collected in table 3.2 at the end of this chapter.

3.1 $\Delta F = 2$ Processes

3.1.1 Basics of Meson Mixing and the $\Delta F = 2$ Effective Hamiltonian

Before discussing in detail observables accessible in $D^0 - \bar{D}^0$, $K^0 - \bar{K}^0$, $B_d - \bar{B}_d$ and $B_s - \bar{B}_s$ mixing, we briefly make some general comments about the basics of meson mixing and the $\Delta F = 2$ effective Hamiltonian.

The amplitude for the transition of a neutral meson $\bar{M}^0$ into its antiparticle M^0 can be written as follows

$$\langle M^0|\mathcal{H}_{\rm eff}|\bar{M}^0\rangle = M_{12} - \frac{i}{2}\Gamma_{12} \ , \quad \langle \bar{M}^0|\mathcal{H}_{\rm eff}|M^0\rangle = M_{12}^* - \frac{i}{2}\Gamma_{12}^* \ , \tag{3.1}$$

where M_{12} is the dispersive part and Γ_{12} the absorptive part of the amplitude. The phases of M_{12} and Γ_{12} are phase convention dependent but their relative phase is a physical observable. The three fundamental theory parameters describing meson - antimeson mixing are then

$$|M_{12}| \ , \quad |\Gamma_{12}| \ , \quad \phi_{12} = {\rm Arg}(M_{12}/\Gamma_{12}) \ . \tag{3.2}$$

While in most models beyond the SM the absorptive part Γ_{12} is hardly affected by NP, the dispersive part M_{12} is sensitive to new short distance dynamics that can be encoded in the Wilson coefficients of the $\Delta F = 2$ effective Hamiltonian

$$\mathcal{H}_{\rm eff} = -\sum_{i=1}^{5} C_i O_i - \sum_{i=1}^{3} \tilde{C}_i \tilde{O}_i + \text{h.c.} \ , \tag{3.3}$$

with the operators defined as

$$\begin{aligned}
O_1 &= (\bar{u}_\alpha \gamma_\mu P_L c_\alpha)\,(\bar{u}_\beta \gamma^\mu P_L c_\beta) \ , & \tilde{O}_1 &= (\bar{u}_\alpha \gamma_\mu P_R c_\alpha)\,(\bar{u}_\beta \gamma^\mu P_R c_\beta) \ , \\
O_2 &= (\bar{u}_\alpha P_L c_\alpha)\,(\bar{u}_\beta P_L c_\beta) \ , & \tilde{O}_2 &= (\bar{u}_\alpha P_R c_\alpha)\,(\bar{u}_\beta P_R c_\beta) \ , \\
O_3 &= (\bar{u}_\alpha P_L c_\beta)\,(\bar{u}_\beta P_L c_\alpha) \ , & \tilde{O}_3 &= (\bar{u}_\alpha P_R c_\beta)\,(\bar{u}_\beta P_R c_\alpha) \ , \\
O_4 &= (\bar{u}_\alpha P_L c_\alpha)\,(\bar{u}_\beta P_R c_\beta) \ , & & \\
O_5 &= (\bar{u}_\alpha P_L c_\beta)\,(\bar{u}_\beta P_R c_\alpha) \ , & &
\end{aligned} \tag{3.4}$$

Here, α and β are color indices and $P_{R,L} = \frac{1}{2}(1 \pm \gamma_5)$. For definiteness we quoted here the Hamiltonian for the $c\bar{u} \to \bar{u}c$ transition. Completely analogous expressions hold of course also in the case of the $s\bar{d} \to \bar{s}d$, $b\bar{d} \to \bar{b}d$ and $b\bar{s} \to \bar{b}s$ transitions.

Integrating out the heavy degrees of freedom of models beyond the SM, the NP contributions to the Wilson coefficients C_i and $\tilde{C}_i$ in (3.3) can be determined at a high matching scale $\mu_{\rm NP}$. Renormalization group running from this high scale down to the low hadronic scales, $\mu_l \simeq m_b$ for $B_d - \bar{B}_d$ and $B_s - \bar{B}_s$ mixing and $\mu_l \simeq 2$ GeV for $K^0 - \bar{K}^0$ and $D^0 - \bar{D}^0$ mixing, where the mixing amplitudes are evaluated can be performed using the results from [48, 49, 50]. The NP contributions to the mixing amplitude are then given by

$$M_{12}^{\rm NP} = \langle M^0|\mathcal{H}_{\rm eff}^{\rm NP}|\bar{M}^0\rangle = -\sum_{i}^{5} C_i^{\rm NP}(\mu_l)\langle O_i(\mu_l)\rangle - \sum_{i}^{3} \tilde{C}_i^{\rm NP}(\mu_l)\langle \tilde{O}_i(\mu_l)\rangle \ . \tag{3.5}$$

The operator matrixelements $\langle O_i \rangle$ and $\langle \tilde{O}_i \rangle$ can be evaluated at the low scale with lattice QCD methods. They are commonly written in the following way

$$\begin{aligned}
\langle O_1 \rangle &= \langle \tilde{O}_1 \rangle = \frac{1}{3} M_D F_D^2 B_1^D \ , & \langle O_4 \rangle &= \frac{1}{4} R_D^2 M_D F_D^2 B_4^D \ , \\
\langle O_2 \rangle &= \langle \tilde{O}_2 \rangle = -\frac{5}{24} R_D^2 M_D F_D^2 B_2^D \ , & \langle O_5 \rangle &= \frac{1}{12} R_D^2 M_D F_D^2 B_5^D \ , \\
\langle O_3 \rangle &= \langle \tilde{O}_3 \rangle = \frac{1}{24} R_D^2 M_D F_D^2 B_3^D \ , & &
\end{aligned} \tag{3.6}$$

where R_D is a chiral factor given by $R_D = m_D/(m_c+m_u)$ and the so-called Bag parameter B_i^D parameterize the deviation of the matrix elements from the vacuum insertion approximation. In (3.6) we restricted ourselves again to the case of $D^0 - \bar{D}^0$ mixing. The hadronic matrix elements for $K^0 - \bar{K}^0$, $B_d - \bar{B}_d$ and $B_s - \bar{B}_s$ mixing can be obtained in exact analogy. We remark that the factor R is particularly large in the case of $K^0 - \bar{K}^0$ mixing, $R_K^2 \simeq 20$ and leads to a strong chiral enhancement of NP contributions to the corresponding operators. All the relevant quark and meson masses, the decay constants and the Bag parameter needed for numerical studies are collected in appendix A.3.

In the remainder of this section we now discuss observables accessible in neutral meson mixing in terms on the mixing amplitude. The NP contributions to the Wilson coefficients in the effective Hamiltonian (3.3) in the MSSM will be discussed in detail in section 6.4.

3.1.2 $D^0 - \bar{D}^0$ Mixing

The neutral D meson mass eigenstates D_1 and D_2 are linear combinations of the strong interaction eigenstates, D^0 and $\bar{D}^0$

$$|D_{1,2}\rangle = p|D^0\rangle \pm q|\bar{D}^0\rangle \ , \quad \frac{q}{p} = \sqrt{\frac{M_{12}^{D*} - \frac{i}{2}\Gamma_{12}^{D*}}{M_{12}^D - \frac{i}{2}\Gamma_{12}^D}} \ . \tag{3.7}$$

Their normalized mass and width differences, x_D and y_D, are given by

$$x_D = \frac{\Delta M_D}{\Gamma_D} = 2\tau_D \mathrm{Re}\left[\frac{q}{p}\left(M_{12}^D - \frac{i}{2}\Gamma_{12}^D\right)\right] \ , \tag{3.8}$$

$$y_D = \frac{\Delta \Gamma_D}{2\Gamma_D} = -2\tau_D \mathrm{Im}\left[\frac{q}{p}\left(M_{12}^D - \frac{i}{2}\Gamma_{12}^D\right)\right] \ . \tag{3.9}$$

Experimentally, $D^0 - \bar{D}^0$ mixing is now firmly established with the non-mixing hypothesis $x_D = y_D = 0$ excluded at 10.2σ [36, 51]. Still, at the current level of sensitivity, there is no evidence for CP violation in $D^0 - \bar{D}^0$ mixing. The experimental data on both $|q/p|$ and $\phi_D = \mathrm{Arg}(q/p)$ is compatible with CP conservation, i.e. $|q/p| = 1$ and $\phi_D = 0$. The most recent world averages as obtained by HFAG read [36, 51]

$$x_D^{\mathrm{exp}} = (0.98^{+0.24}_{-0.26})\% \ , \qquad y_D^{\mathrm{exp}} = (0.83 \pm 0.16)\% \ , \tag{3.10}$$

$$|q/p|^{\mathrm{exp}} = 0.87^{+0.17}_{-0.15} \ , \qquad \phi_D^{\mathrm{exp}} = (-8.5^{+7.4}_{-7.0})^\circ \ . \tag{3.11}$$

In the usual CKM conventions, the SM contributions to the dispersive and absorptive part of the mixing amplitude are predicted to be real to an excellent approximation, but their

magnitude cannot be calculated in a reliable way, for they are dominated by long distance effects [52, 53]. Still, the experimental values for x_D and y_D are within estimated ranges of the SM predictions. Therefore the mass and width difference in $D^0 - \bar{D}^0$ mixing can only be used to bound possible New Physics contributions [54, 55, 56, 57]. However, any experimental signal for CP violation in $D^0 - \bar{D}^0$ mixing above the per mill level would unambiguously point towards a NP effect as in the SM it is predicted to be at the level of $\mathrm{O}((V_{cb}V_{ub})/(V_{cs}V_{us})) \simeq 10^{-3}$.[1] Thus, $D^0 - \bar{D}^0$ mixing offers excellent opportunities to probe CP violation in NP models [59, 60, 61, 62].

In the remainder of this section we will therefore focus on two CP violating observables: the time dependent CP asymmetry in decays of D^0 and $\bar{D}^0$ to CP eigenstates, S_f^D, and the semileptonic asymmetry, a_{SL}^D.

Time Dependent CP Asymmetry

The decay rates of neutral D mesons decaying to CP eigenstates f are to a good approximation given by [54, 61, 63]

$$\Gamma(D^0(t) \to f) \propto \exp\left[-\hat{\Gamma}_{D^0\to f}t\right] \ , \quad \Gamma(\bar{D}^0(t) \to f) \propto \exp\left[-\hat{\Gamma}_{\bar{D}^0\to f}t\right] \ , \tag{3.12}$$

with effective decay widths

$$\hat{\Gamma}_{D^0\to f} = \Gamma_D\left[1 + \eta_f^{\mathrm{CP}}\left|\frac{q}{p}\right|(y\cos\phi - x\sin\phi)\right] \ , \tag{3.13}$$

$$\hat{\Gamma}_{\bar{D}^0\to f} = \Gamma_D\left[1 + \eta_f^{\mathrm{CP}}\left|\frac{p}{q}\right|(y\cos\phi + x\sin\phi)\right] \ . \tag{3.14}$$

Here η_f^{CP} is the CP parity of the final state f. One then defines the following CP violating combination [54, 64, 63]

$$S_f^D = 2\Delta Y_f = \frac{1}{\Gamma_D}\left(\hat{\Gamma}_{\bar{D}^0\to f} - \hat{\Gamma}_{D^0\to f}\right) \ , \tag{3.15}$$

that is given by

$$\eta_f^{\mathrm{CP}} S_f^D = x\left(\left|\frac{q}{p}\right| + \left|\frac{p}{q}\right|\right)\sin\phi - y\left(\left|\frac{q}{p}\right| - \left|\frac{p}{q}\right|\right)\cos\phi \ . \tag{3.16}$$

This expression gets in principle modified in the presence of new weak phases in the decay [64, 63], that one could expect e.g. in singly Cabibbo suppressed decay modes [62]. However, as shown in [63], such effects are severely constrained by the existing data on time integrated CP asymmetries. To an excellent approximation (3.16) holds therefore also in the presence of new weak phases in the decay, i.e. $\eta_f^{\mathrm{CP}} S_f^D$ and $\eta_f^{\mathrm{CP}}\Delta Y_f$ are universal for all final states and practically independent of direct CP violation in the decays.

In fact, time dependent CP asymmetries are currently determined from the singly Cabibbo suppressed decay modes $D^0 \to K^+K^-$ and $D^0 \to \pi^+\pi^-$ and one has [36]

$$\eta_f^{\mathrm{CP}} S_f^D = (-0.248 \pm 0.496)\% \ . \tag{3.17}$$

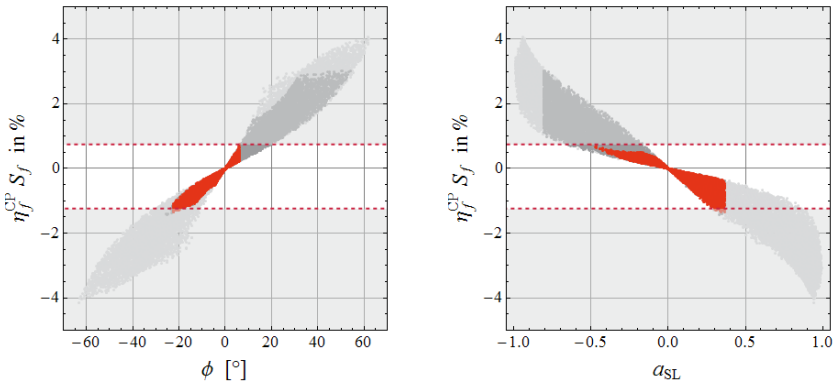

Figure 3.1: Model independent correlations between S_f^D and ϕ_D (left) and $a_{\rm SL}^D$ and S_f^D (right). Light gray points satisfy the constraints from x_D and y_D while darker gray points further satisfy the constraint from $|q/p|$. Red points are compatible with all constraints listed in (3.10) and (3.11) and the dashed lines stand for the allowed range (3.17) for S_f^D. From [22].

Concerning Cabibbo favored decay modes, the most promising channel seems to be $D^0 \to K_S\phi$ as advertised in [64].

The left plot of figure 3.1 shows the dependence of the asymmetry S_f^D on ϕ_D. The light gray points only fulfill the constraints from x_D and y_D, darker gray points in addition also the constraint from $|q/p|$. Red points finally are compatible with all constraints listed in (3.10) and (3.11). The range (3.17) for S_f^D is also shown as dashed lines. In fact the measured value for S_f^D determines to a large extent the allowed range for ϕ_D in (3.11).

To take into account the uncertainties coming from the unknown long distance contributions to the mixing amplitude in the SM, we follow [65] and scan $M_{12}^{\rm SM}$ flatly in the range $[-0.02, 0.02]{\rm ps}^{-1}$, so that the SM contribution alone can saturate the experimental bound on the mass difference. Moreover, we scan $\Gamma_{12}^{\rm SM}$ flatly in the range $[-0.04, 0.04]{\rm ps}^{-1}$.

The Semileptonic Asymmetry

The semileptonic asymmetry in the decay to "wrong sign" leptons is defined as

$$a_{\rm SL}^D = \frac{\Gamma(D^0 \to K^+\ell^-\nu) - \Gamma(\bar{D}^0 \to K^-\ell^+\nu)}{\Gamma(D^0 \to K^+\ell^-\nu) + \Gamma(\bar{D}^0 \to K^-\ell^+\nu)} = \frac{|q|^4 - |p|^4}{|q|^4 + |p|^4} \tag{3.18}$$

and is a direct measure of CP violation in the mixing.

The model independent relation between x, y, $|q/p|$ and ϕ identified in [66] implies the following correlation between the universal time dependent CP asymmetry S_f^D and the semileptonic asymmetry $a_{\rm SL}^D$ [64, 63]

$$S_f^D = 2\Delta Y_f = -\eta_f^{\rm CP}\, \frac{x_D^2 + y_D^2}{|y_D|}\, a_{\rm SL}^D\ , \tag{3.19}$$

In the right plot of figure 3.1 we show exactly this correlation as a result of the numerical scan described above. We observe that the constraints coming from q/p and ϕ_D limit the allowed range for $a_{\rm SL}^D$ in a model independent way. The remaining range reads $-0.5 \lesssim a_{\rm SL}^D \lesssim +0.35$. We will study this correlation in the context of abelian flavor models in section 8.6.

[1] See however [58] for a more conservative point of view.

3.1.3 $K^0 - \bar{K}^0$ Mixing

The two main observables in $K^0 - \bar{K}^0$ mixing are the mass difference ΔM_K and the parameter ϵ_K that is a measure of CP violation in $K^0 - \bar{K}^0$ mixing. In terms of the mixing amplitude M_{12}^K they can be written as

$$\Delta M_K = 2\mathrm{Re}(M_{12}^K) \ , \quad |\epsilon_K| = \frac{\kappa_\epsilon}{\sqrt{2}} \frac{\mathrm{Im}(M_{12}^K)}{\Delta M_K} \ , \tag{3.20}$$

While the SM prediction for ΔM_K has a large uncertainty due to unknown long distance contributions, the ϵ_K parameter is dominated by short distance physics and can be predicted with good accuracy. Long distance contributions to ϵ_K are only at the percent level and included in the factor $\kappa_\epsilon \simeq 0.94$ [31, 67].

Using the expression for M_{12}^K in the SM one finds

$$|\epsilon_K|^{\mathrm{SM}} = \kappa_\epsilon C_\epsilon \hat{B}_K \lambda^2 |V_{cb}|^2 \Big(\frac{1}{2} |V_{cb}|^2 R_t^2 \sin 2\beta \eta_{tt} S_0(x_t) + R_t \sin\beta \left(\eta_{ct} S_0(x_c, x_t) - \eta_{cc} x_c \right) \Big) \ , \tag{3.21}$$

where the SM loop function S_0 can be found e.g. in [68] and depends on $x_i = m_i^2/M_W^2$, with m_i the running $\overline{\mathrm{MS}}$ mass at the scale m_i. The factors η_{tt}, η_{ct} and η_{cc} are QCD correction factors known at NLO [69, 70, 71, 72] and the factor C_ϵ is given by

$$C_\epsilon = \frac{G_F^2 M_W^2 F_K^2 M_K}{6\sqrt{2}\pi^2 \Delta M_K} \simeq 3.655 \times 10^4 \ . \tag{3.22}$$

Expression (3.21) transparently shows the correlation between $|\epsilon_K|$ and $\sin 2\beta$ in the SM. Indeed, as detailed in section 2.1, using the experimental value of $S_{\psi K_S}$ to determine directly $\sin 2\beta$ leads to a SM expectation for ϵ_K almost 2σ below the experimental value [73]

$$|\epsilon_K|^{\mathrm{exp}} = (2.229 \pm 0.010) \times 10^{-3} \ . \tag{3.23}$$

Using instead the values for the CKM parameter from the NP UTfit [28] that are also collected in appendix A.3, we find

$$|\epsilon_K|^{\mathrm{SM}} = (1.94 \pm 0.30) \times 10^{-3} \ , \tag{3.24}$$

which is in agreement with the experimental number at the 1σ level and leads to strong constraints on the flavor structure of NP models.

3.1.4 $B_d - \bar{B}_d$ Mixing

The two most important observables in the B_d system are the mass difference ΔM_d and the time-dependent CP asymmetry in the tree level decay $B_d \to \psi K_S$

$$\frac{\Gamma(\bar{B}_d(t) \to \psi K_S) - \Gamma(B_d(t) \to \psi K_S)}{\Gamma(\bar{B}_d(t) \to \psi K_S) + \Gamma(B_d(t) \to \psi K_S)} = S_{\psi K_S} \sin(\Delta M_d t) \ , \tag{3.25}$$

where we neglected CP violation in the $B_d \to \psi K_S$ decay amplitude.

Parameterizing the $B_d - \bar{B}_d$ mixing amplitude M_{12}^d in the following way

$$M_{12}^d = (M_{12}^d)^{\mathrm{SM}} + (M_{12}^d)^{\mathrm{NP}} = |(M_{12}^d)^{\mathrm{SM}}| e^{2i\beta_d} + |(M_{12}^d)^{\mathrm{NP}}| e^{i\theta_d} = C_d e^{2i\phi_d} (M_{12}^d)^{\mathrm{SM}} \ , \tag{3.26}$$

the mass difference ΔM_d and the coefficient $S_{\psi K_S}$ can be written as

$$\Delta M_d = 2|M_{12}^d| = C_d(\Delta M_d)^{\rm SM} \ , \quad S_{\psi K_S} = -\sin\left(\text{Arg}(M_{12}^d)\right) = \sin\left(2\beta + 2\phi_d\right) \ . \tag{3.27}$$

While ΔM_d measures the absolute value of the mixing amplitude, $S_{\psi K_S}$ measures its phase that, in the SM, is determined by the CKM angle β, i.e. the phase of the CKM element V_{td}. In fact in the SM one has

$$(M_{12}^d)^{\rm SM} = \frac{G_F^2 M_W^2}{12\pi^2}\eta_B M_{B_d} F_{B_d}^2 \hat{B}_{B_d} S_0(x_t)\left(V_{tb}V_{td}^*\right)^2 \ , \tag{3.28}$$

and, using the input parameter from appendix A.3, we obtain

$$\Delta M_d^{\rm SM} = (0.53 \pm 0.13)\ \text{ps}^{-1} \ , \quad S_{\psi K_S}^{\rm SM} = \sin 2\beta = 0.734 \pm 0.038 \ . \tag{3.29}$$

The SM prediction for the mass difference is in perfect agreement with the measured value [36]

$$\Delta M_d^{\rm exp} = (0.507 \pm 0.005)\ \text{ps}^{-1} \ , \tag{3.30}$$

while the measurement of $S_{\psi K_S}$ [36]

$$S_{\psi K_S}^{\rm exp} = 0.672 \pm 0.023 \ , \tag{3.31}$$

is quite on the lower side of the SM prediction as already mentioned in section 2.1.

3.1.5 $B_s - \bar{B}_s$ Mixing

In the B_s system we will consider three observables: i) the mass difference ΔM_s, ii) the time dependent CP asymmetry in the tree level decay $B_s \to \psi\phi$,

$$\frac{\Gamma(\bar{B}_s(t) \to \psi\phi) - \Gamma(B_s(t) \to \psi\phi)}{\Gamma(\bar{B}_s(t) \to \psi\phi) + \Gamma(B_s(t) \to \psi\phi)} = S_{\psi\phi}\sin(\Delta M_s t) \ , \tag{3.32}$$

where we set to zero CP violation in the decay amplitude and iii) the semileptonic asymmetry

$$A_{\rm SL}^s = \frac{\Gamma(\bar{B}_s \to \ell^+ X) - \Gamma(B_s \to \ell^- X)}{\Gamma(\bar{B}_s \to \ell^+ X) + \Gamma(B_s \to \ell^- X)} \ . \tag{3.33}$$

Both asymmetries are induced in the SM by $\beta_s \simeq -1^\circ$, the tiny phase of the CKM element V_{ts}, and therefore very small. Consequently, both $S_{\psi\phi}$ and $A_{\rm SL}^s$ represent very promising observables where to look for NP effects.

To discuss the observables in $B_s - \bar{B}_s$ mixing, we use a parameterization of the mixing amplitude M_{12}^s analogous to the one in (3.26) in the B_d case

$$M_{12}^s = (M_{12}^s)^{\rm SM} + (M_{12}^s)^{\rm NP} = |(M_{12}^s)^{\rm SM}|e^{2i\beta_s} + |(M_{12}^s)^{\rm NP}|e^{i\theta_s} = C_s e^{2i\phi_s}(M_{12}^s)^{\rm SM} \ . \tag{3.34}$$

As it is the case in $B_d - \bar{B}_d$ mixing, the mass difference measures the absolute value of the mixing amplitude, while the coefficient $S_{\psi\phi}$ measures its phase

$$\Delta M_s = 2|M_{12}^s| = C_s(\Delta M_s)^{\rm SM} \ , \quad S_{\psi\phi} = -\sin\left(\text{Arg}(M_{12}^s)\right) = \sin\left(2|\beta_s| - 2\phi_s\right) \ . \tag{3.35}$$

In presence of NP the semileptonic asymmetry $A_{\rm SL}^s$ is strongly correlated with $S_{\psi\phi}$ [74]

$$A_{\rm SL}^s = -\left|{\rm Re}\left(\frac{\Gamma_{12}^s}{M_{12}^s}\right)^{\rm SM}\right| \frac{1}{C_s} S_{\psi\phi} \ , \tag{3.36}$$

where we have neglected a small contribution proportional to ${\rm Im}(\Gamma_{12}^s/M_{12}^s)^{\rm SM}$.

The mixing amplitude in the SM is given by

$$(M_{12}^s)^{\rm SM} = \frac{G_F^2 M_W^2}{12\pi^2} \eta_B M_{B_s} F_{B_s}^2 \hat{B}_{B_s} S_0(x_t) \left(V_{tb}V_{ts}^*\right)^2 \ . \tag{3.37}$$

Using the input parameter from appendix A.3 we find the following SM predictions

$$\Delta M_s^{\rm SM} = (18.3 \pm 5.1)\ {\rm ps}^{-1} \ , \quad S_{\psi\phi}^{\rm SM} = 0.038 \pm 0.003 \ , \tag{3.38}$$

while the semileptonic asymmetry $A_{\rm SL}^s$ is at the level of 10^{-5} [75].

Concerning the experimental situation, the SM prediction for the mass difference ΔM_s agrees very well with the value measured at CDF [76]

$$\Delta M_s^{\rm exp} = (17.77 \pm 0.12)\ {\rm ps}^{-1} \ . \tag{3.39}$$

However, data on $S_{\psi\phi}$ from CDF [77] and D0 [78] has attracted a lot of attention recently, as several analyses found tensions with the tiny SM prediction at the level of 2-3σ [75, 79, 80, 36]. In the following we will use the HFAG result [36, 21]

$$S_{\psi\phi}^{\rm exp} = 0.81^{+0.12}_{-0.32} \quad \text{and} \quad 0.20 \leq S_{\psi\phi}^{\rm exp} \leq 0.98 \quad @\ 95\%\ \text{C.L.} \ . \tag{3.40}$$

We mention that a very recent result from D0 on the like-sign dimuon charge asymmetry in semileptonic b-hadron decays leads to $A_{\rm SL}^s = (-14.6 \pm 7.5) \times 10^{-3}$ [81] which supports the idea of a large $B_s - \bar{B}_s$ mixing phase. An even more recent analysis from CDF however finds again a smaller $S_{\psi\phi}$, compatible with the SM expectation at the 1σ level [82]. At LHCb, the expected sensitivity to $S_{\psi\phi}$ is at the level of 0.01 for an integrated luminosity of 10 fb^{-1} [83] and one can expect that the value of $S_{\psi\phi}$ will be clarified in the near future.

In chapters 7 and 8 we will discuss how a large value for $S_{\psi\phi}$ can be accommodated for in various MSSM frameworks.

3.2 $\Delta F = 1$ Processes

3.2.1 The radiative $b \to s\gamma$ Decay

The good agreement between the experimental data on the branching ratio of the inclusive radiative $B \to X_s\gamma$ decay [36]

$${\rm BR}(B \to X_s\gamma)_{\rm exp} = (3.52 \pm 0.25) \times 10^{-4} \ , \tag{3.41}$$

and the corresponding NNLO SM prediction [84]

$${\rm BR}(B \to X_s\gamma)_{\rm SM} = (3.15 \pm 0.23) \times 10^{-4} \ , \tag{3.42}$$

leads to severe constraints on the flavor sectors of many NP models (see e.g. [85] for a review). Combining (3.41) and (3.42) one gets immediately

$$R_{bsg} = \frac{\mathrm{BR}(B \to X_s\gamma)_{\mathrm{exp}}}{\mathrm{BR}(B \to X_s\gamma)_{\mathrm{SM}}} = 1.13 \pm 0.12 \ , \tag{3.43}$$

which leaves only small room for possible NP contributions to the $b \to s\gamma$ transition. The suitable framework for the theoretical description of the $b \to s\gamma$ decay (see e.g. [86, 87]) is given by an effective Hamiltonian

$$\mathcal{H}_{\mathrm{eff}} = -\frac{4G_F}{\sqrt{2}} V_{tb}V_{ts}^* \sum_i \left(C_i Q_i + C_i' Q_i' \right) . \tag{3.44}$$

The operators in (3.44) that are most sensitive to NP effects are the magnetic and chromomagnetic dipole operators Q_7 and Q_8 as well as their primed counterparts Q_7' and Q_8'

$$Q_7 = \frac{e}{16\pi^2} m_b \left(\bar{s}\sigma^{\mu\nu} F_{\mu\nu} P_R b\right) \ , \qquad Q_7' = \frac{e}{16\pi^2} m_b \left(\bar{s}\sigma^{\mu\nu} F_{\mu\nu} P_L b\right) \ , \tag{3.45}$$

$$Q_8 = \frac{g_s}{16\pi^2} m_b \left(\bar{s}\sigma^{\mu\nu} G^A_{\mu\nu} T^A P_R b\right) \ , \qquad Q_8' = \frac{g_s}{16\pi^2} m_b \left(\bar{s}\sigma^{\mu\nu} G^a_{\mu\nu} T^a P_L b\right) \ . \tag{3.46}$$

These operators are helicity flipping. In the SM the amplitudes corresponding to the unprimed operators are therefore necessarily proportional to the bottom quark mass, which is made explicit in the definitions of the operators above. In the SM and models with MFV the primed operators are even suppressed by the strange quark mass and completely negligible. In generic NP models this suppression can be lifted and in general large NP contributions to the corresponding Wilson coefficients $C_7^{(\prime)}$ and $C_8^{(\prime)}$ are expected.

The prediction for the $B \to X_s\gamma$ branching ratio in the presence of arbitrary NP contributions to the Wilson coefficients $C_7^{(\prime)}$ and $C_8^{(\prime)}$ can be well approximated by the following expression [88]

$$\begin{aligned} R_{bs\gamma} \ &\simeq \ \frac{\mathrm{BR}(B \to X_s\gamma)}{\mathrm{BR}(B \to X_s\gamma)_{\mathrm{SM}}} = 1 + \hat{a}_{77} \left(\left|C_7^{\mathrm{NP}}\right|^2 + \left|C_7'^{\mathrm{NP}}\right|^2 \right) + \hat{a}_{88} \left(\left|C_8^{\mathrm{NP}}\right|^2 + \left|C_8'^{\mathrm{NP}}\right|^2 \right) \\ &+ \ \mathrm{Re}\left(\hat{a}_7\, C_7^{\mathrm{NP}}\right) + \mathrm{Re}\left(\hat{a}_8\, C_8^{\mathrm{NP}}\right) + \mathrm{Re}\left(\hat{a}_{78} \left[C_7^{\mathrm{NP}} C_8^{*\,\mathrm{NP}} + C_7'^{\mathrm{NP}} C_8'^{*\,\mathrm{NP}} \right]\right) \ , \end{aligned} \tag{3.47}$$

where the coefficients $\hat{a}_i$ are given by $\hat{a}_7 = -2.41 + 0.21i$, $\hat{a}_8 = -0.75 - 0.19i$, $\hat{a}_{77} = 1.59$, $\hat{a}_{88} = 0.26$ and $\hat{a}_{78} = 0.82 - 0.30i$ [88]. The Wilson coefficients entering (3.47) have to be evaluated at a scale $\mu_h = 160$ GeV and explicit expressions for their five and six flavor running can be found in e.g. in [68] and [89], respectively.

The primed Wilson coefficients C_7' and C_8' cannot interfere with the SM contributions to C_7 and C_8 in the branching ratio of the inclusive $B \to X_s\gamma$ decay. Therefore they appear only quadratically in (3.47), while the NP contributions to the unprimed coefficients also appear linearly. New Physics contributions to C_7 and C_8 are thus expected to be stronger constrained as contributions to C_7' and C_8'. If C_7^{NP} and C_8^{NP} are however complex, the constraint from $\mathrm{BR}(B \to X_s\gamma)$ can be relaxed to a large extent [90].

The Direct CP Asymmetry in $B \to X_s\gamma$

An observable very sensitive to CP violating effects in the $b \to s\gamma$ transition is the direct CP asymmetry of the $B \to X_s\gamma$ decay [91, 92]

$$A_{\mathrm{CP}}(b \to s\gamma) = \frac{\Gamma(B \to X_{\bar{s}}\gamma) - \Gamma(\bar{B} \to X_s\gamma)}{\Gamma(B \to X_{\bar{s}}\gamma) + \Gamma(\bar{B} \to X_s\gamma)} \ . \tag{3.48}$$

The direct CP asymmetry arises first at the next-to-leading order and the SM prediction, that is strongly CKM and GIM suppressed, reads [93]

$$A_{\rm CP}^{\rm SM}(b\to s\gamma) = \left(-0.44^{+0.14}_{-0.24}\right)\,\% \ . \tag{3.49}$$

While sensitivity to the SM prediction has not been reached yet experimentally, data from Belle [94] and BaBar [95, 96] lead to the following world average [36]

$$A_{\rm CP}^{\rm exp}(b\to s\gamma) = (1.2\pm 2.8)\% \ , \tag{3.50}$$

which is compatible with a vanishing CP asymmetry and fully consistent with the SM prediction. At a future superB factory it is expected to reach a sensitivity of $\sim 0.5\%$ [37, 38, 39].

Complex NP contributions to the Wilson coefficients $C_7^{(\prime)}$ and $C_8^{(\prime)}$ can lead to large modifications of the SM prediction for $A_{\rm CP}(b\to s\gamma)$. If NP effects dominate over the tiny SM contribution the following expression holds [92]

$$\begin{aligned} A_{\rm CP}(b\to s\gamma) \ \simeq \ & -\frac{1}{|0.31-C_7^{\rm NP}|^2+|C_7^{\prime\,\rm NP}|^2}\Big(2.84\ {\rm Im}(C_8^{\rm NP}) - 2.79\ {\rm Im}(C_7^{\rm NP}) \\ & -9.52\ {\rm Im}\big(C_8^{\rm NP}C_7^{*\,\rm NP}+C_8^{\prime\,\rm NP}C_7^{\prime *\,\rm NP}\big)\Big) \quad (\text{in }\%) \ , \end{aligned} \tag{3.51}$$

where the Wilson coefficients are evaluated at the scale $\mu\simeq m_b$. If there is a single dominant source of CP violation leading to complex phases in C_7' and C_8', as it is in particular the case in the SUSY frameworks that we will study in this work, then the phases of C_7' and C_8' are quasi aligned, such that $A_{\rm CP}(b\to s\gamma)$ is sensitive to phases in C_7 and C_8 only.

The Time Dependent CP Asymmetry in $B\to K^*\gamma$

An observable that is complementary in this respect is the time-dependent CP asymmetry in the exclusive decay $B\to K^*\gamma$ [97, 98]

$$\frac{\Gamma(\bar B^0(t)\to \bar K^{*0}\gamma)-\Gamma(B^0(t)\to K^{*0}\gamma)}{\Gamma(\bar B^0(t)\to \bar K^{*0}\gamma)+\Gamma(B^0(t)\to K^{*0}\gamma)} = S_{K^*\gamma}\sin(\Delta M_d t) - C_{K^*\gamma}\cos(\Delta M_d t) \ , \tag{3.52}$$

where K^{*0} and $\bar K^{*0}$ are observed through their decay into the CP eigenstate $K_S\pi^0$. The coefficient $S_{K^*\gamma}$ in (3.52) is highly sensitive to right handed currents as it vanishes for $C_7'\to 0$. As a consequence its SM prediction is very small [98]

$$S_{K^*\gamma}^{\rm SM} = -0.022\pm 0.015^{+0}_{-0.01} \ , \tag{3.53}$$

and experimental evidence for a large $S_{K^*\gamma}$ would be a clear indication of NP effects through right handed currents. On the experimental side one has presently [99, 100, 73]

$$S_{K^*\gamma}^{\rm exp} = -0.15\pm 0.22 \ , \tag{3.54}$$

which, due to the still large errors, is fully consistent with zero. The experimental situation is expected to improve significantly with a superB factory where the sensitivity to $S_{K^*\gamma}$ is estimated to be at the level of ~ 0.03 [37, 38, 39].

In presence of generic NP contributions to C_7 and C_7' one finds

$$S_{K^*\gamma} \simeq \frac{2}{|C_7|^2 + |C_7'|^2} \mathrm{Im}\left(e^{-2i(\beta+\phi_{B_d})} C_7 C_7'\right) \ , \tag{3.55}$$

where ϕ_{B_d} is a possible NP physics phase in B_d mixing (see (3.26)). The Wilson coefficients in (3.55) refer to the sum of SM and NP contributions $C_7 \simeq -0.31 + C_7^{\rm NP}$, $C_7' \simeq C_7'^{\rm NP}$ and have to be evaluated at a scale $\mu = m_b$. As it is clearly shown by (3.55), the observable $S_{K^*\gamma}$ is highly sensitive to CP violation in the C_7' Wilson coefficient.

3.2.2 The semileptonic $b \to s\ell^+\ell^-$ Decays

Also semileptonic decays based on the $b \to s\ell^+\ell^-$ transition are sensitive probes of NP contributions to the magnetic dipole operators $Q_7^{(\prime)}$ given in (3.45). In addition, such decays are also very sensitive to semileptonic four fermion operators in the effective Hamiltonian

$$Q_9 = \frac{e^2}{16\pi^2} (\bar{s}\gamma_\mu P_L b)\left(\bar{\ell}\gamma^\mu \ell\right) \ , \qquad Q_9' = \frac{e^2}{16\pi^2} (\bar{s}\gamma_\mu P_R b)\left(\bar{\ell}\gamma^\mu \ell\right) \ , \tag{3.56}$$

$$Q_{10} = \frac{e^2}{16\pi^2} (\bar{s}\gamma_\mu P_L b)\left(\bar{\ell}\gamma^\mu \gamma_5 \ell\right) \ , \qquad Q_{10}' = \frac{e^2}{16\pi^2} (\bar{s}\gamma_\mu P_R b)\left(\bar{\ell}\gamma^\mu \gamma_5 \ell\right) \ . \tag{3.57}$$

However, in the MSSM, the Wilson coefficients of the semileptonic operators, $C_9^{(\prime)}$ and $C_{10}^{(\prime)}$, are typically SM-like. Non-negligible effects arise only in C_{10} in certain corners of the parameter space. Therefore we will concentrate on the effects on the $b \to s\ell^+\ell^-$ decays coming from NP contributions to the dipole operators.

There are several meson decays that are based on the $b \to s\ell^+\ell^-$ transition at the parton level. They include the inclusive $B \to X_s\ell^+\ell^-$ decay as well as the exclusive $B \to K\ell^+\ell^-$, $B \to K^*\ell^+\ell^-$ and $B_s \to \phi\ell^+\ell^-$ decays. The NP sensitivity of these decay modes has been extensively studied in the literature (see e.g. [101, 102, 103, 104, 105, 106, 107, 88, 108, 109, 110, 19]) and in the following we will restrict our discussion to the $B \to K^*\ell^+\ell^-$ mode, following mainly our analysis in [19].

The exclusive $B \to K^*(\to K\pi)\ell^+\ell^-$ decay is regarded as a very important channel for B physics since its angular distribution gives access to a multitude of observables that offer new important tests of the Standard Model and its extensions. With an on-shell K^*, the decay is completely described by four independent kinematical variables: the dilepton invariant mass squared q^2 and three angles θ_K, θ_ℓ and ϕ as defined e.g. in [19]. The corresponding full angular decay distribution of $\bar{B}^0 \to \bar{K}^{*0}(\to K^-\pi^+)\mu^+\mu^-$ can be written as

$$\frac{d^4\Gamma}{dq^2\, d\cos\theta_\ell\, d\cos\theta_{K^*}\, d\phi} = \frac{9}{32\pi} I(q^2, \theta_\ell, \theta_{K^*}, \phi) \ , \tag{3.58}$$

where

$$\begin{aligned} I(q^2, \theta_\ell, \theta_K, \phi) = {} & I_1^s \sin^2\theta_K + I_1^c \cos^2\theta_K + (I_2^s \sin^2\theta_K + I_2^c \cos^2\theta_K)\cos 2\theta_\ell \\ & + I_3 \sin^2\theta_K \sin^2\theta_\ell \cos 2\phi + I_4 \sin 2\theta_K \sin 2\theta_\ell \cos\phi + I_5 \sin 2\theta_K \sin\theta_\ell \cos\phi \\ & + (I_6^s \sin^2\theta_K + I_6^c \cos^2\theta_K)\cos\theta_\ell + I_7 \sin 2\theta_K \sin\theta_\ell \sin\phi \\ & + I_8 \sin 2\theta_K \sin 2\theta_\ell \sin\phi + I_9 \sin^2\theta_K \sin^2\theta_\ell \sin 2\phi \ . \end{aligned} \tag{3.59}$$

The corresponding expression for the CP conjugated mode $B^0 \to K^{*0}(\to K^+\pi^-)\mu^+\mu^-$ is

$$\frac{d^4\bar{\Gamma}}{dq^2\, d\cos\theta_\ell\, d\cos\theta_{K^*}\, d\phi} = \frac{9}{32\pi}\bar{I}(q^2,\theta_\ell,\theta_{K^*},\phi) \tag{3.60}$$

and the function $\bar{I}(q^2,\theta_\ell,\theta_{K^*},\phi)$ is obtained from (3.59) by the replacements

$$I^{(a)}_{1,2,3,4,7} \to \bar{I}^{(a)}_{1,2,3,4,7}\ , \quad I^{(a)}_{5,6,8,9} \to -\bar{I}^{(a)}_{5,6,8,9}\ , \tag{3.61}$$

where $\bar{I}^{(a)}_i$ equals $I^{(a)}_i$ with all weak phases conjugated.

Taking into account effects from a non-vanishing lepton mass and including possible contributions to the $b \to s\ell^+\ell^-$ transitions from scalar operators, all the 24 angular coefficient functions $I^{(a)}_i$ and $\bar{I}^{(a)}_i$ are independent and physical observables.

From the theoretical side, the angular coefficients can be expressed in terms of transversity amplitudes, that in turn can be computed in terms of the Wilson coefficients of the effective Hamiltonian and the seven $B \to K^*$ form factors that can be evaluated in the low q^2 region, $q^2 < 6\ \text{GeV}^2$, with the method of QCD light-cone sum rules [111, 112, 19]. As argued in [19], the dominant power-suppressed corrections to the $B \to K^*\ell^+\ell^-$ decay are taken into account by using the full set of form factors in the naively factorized amplitude. Non-factorizable corrections can then be accounted for using QCD factorization methods [113, 114] with the reduced set of form factors in the heavy quark limit.

To separate CP conserving and CP violating NP effects, it is convenient to consider the twelve CP averaged angular coefficients $S^{(a)}_i$ as well as the twelve CP asymmetries $A^{(a)}_i$

$$S^{(a)}_i = \left(I^{(a)}_i + \bar{I}^{(a)}_i\right) \Big/ \frac{d(\Gamma+\bar{\Gamma})}{dq^2}\ , \quad A^{(a)}_i = \left(I^{(a)}_i - \bar{I}^{(a)}_i\right) \Big/ \frac{d(\Gamma+\bar{\Gamma})}{dq^2}\ , \tag{3.62}$$

where the normalization to the CP averaged dilepton mass distribution reduces both experimental and theoretical uncertainties in these observables. They offer a clean and comprehensive way to analyze the full richness of angular distributions in $B \to K^*(\to K\pi)\mu^+\mu^-$ decays. In our opinion, they are also the natural starting point for an experimental analysis. In [110] it was shown that with the large statistics that will become available at LHCb, a full angular fit is the preferred way to extract observables. Alternatively, $S^{(a)}_i$ and $A^{(a)}_i$ can be found by taking asymmetries and/or integrating $d^4(\Gamma \pm \bar{\Gamma})$ over the angles θ_ℓ, θ_K and ϕ [109]. This strategy will be particular important in the fist years of LHC where statistics will still be limited [115].

All established observables in $B \to K^*\mu^+\mu^-$ can be expressed in terms of $S^{(a)}_i$ and $A^{(a)}_i$. Neglecting the effect of a non-zero lepton mass and possible contributions from scalar operators that are strongly constrained by the $B_s \to \mu^+\mu^-$ decay, one finds for example

$$A_{\rm FB} = \frac{3}{4}S^s_6\ , \quad A^{\rm CP}_{\rm FB} = \frac{3}{4}A^s_6\ , \quad A_{\rm CP} = \frac{4}{3}A^s_1 + A^c_1\ , \quad F_L = -S^c_2\ , \quad F_T = 4S^s_2\ . \tag{3.63}$$

Here, $A_{\rm FB}$, $A^{\rm CP}_{\rm FB}$ and $A_{\rm CP}$ are the well known forward-backward asymmetry [116], the forward-backward CP asymmetry [117] and the CP asymmetry in the dilepton mass distribution, respectively, while F_L and F_T refer to the K^* longitudinal and transverse polarization fractions. Also the transverse asymmetries $A^{2,3,4}_T$ introduced in [107, 110] can be expressed in terms of $S^{(a)}_i$ and $A^{(a)}_i$ [19].

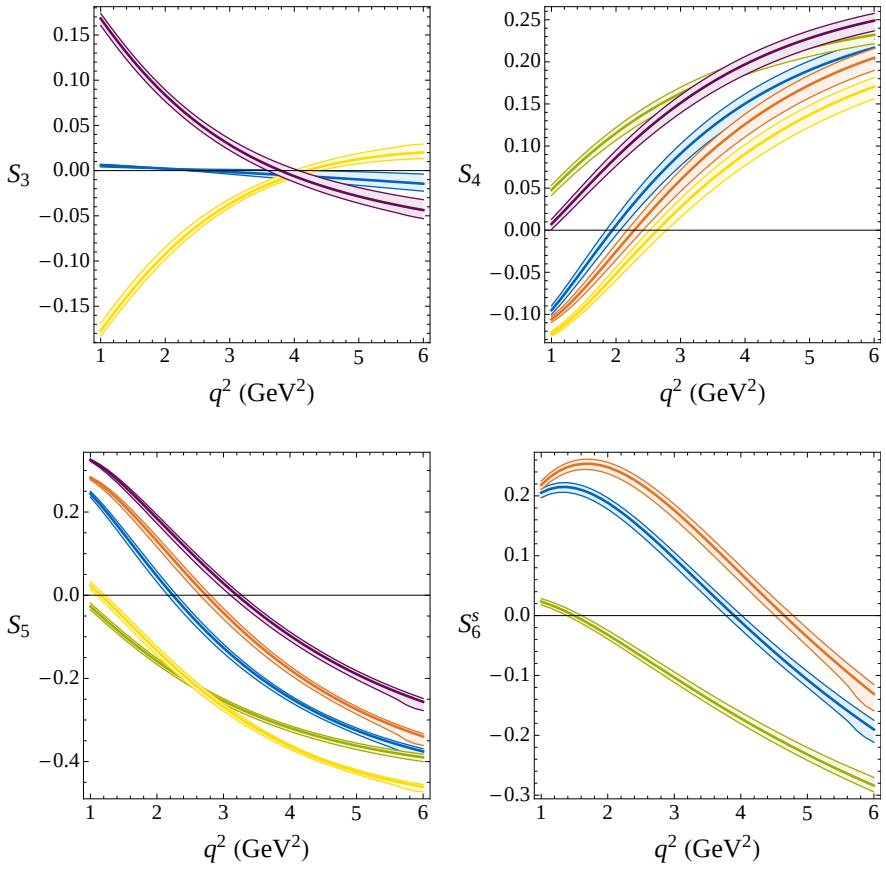

Figure 3.2: The CP averaged angular coefficients S_3, S_4, S_5 and S_6^s as functions of the dilepton invariant mass squared q^2. The blue bands correspond to the SM and the remaining colored bands to representative NP scenarios as described in the text.

Concerning the CP asymmetries $A_i^{(a)}$, they are tiny in the SM, as the effect of possible CP violating phases is doubly Cabibbo suppressed. Such a suppression is in general not present in generic NP models and large non-standard effects are in principle expected in the CP asymmetries. The $A_i^{(a)}$, $i = 1 \ldots 6$ are T-even and are only induced through an interference between strong and weak phases. Therefore they arise only at the NLO level and also in generic NP models they are not expected to be larger than $\alpha_s \simeq 0.1$. In contrast, A_7, A_8 and A_9 being T-odd, do not require any strong phases and can in principle be of O(1) [109].

Instead of discussing now in detail all 24 $S_i^{(a)}$ and $A_i^{(a)}$, we focus on the seven example observables S_3, S_4, S_5, S_6^s, A_7, A_8 and A_9 that show a particular characteristic and transparent pattern of deviations from their SM predictions in the presence of NP contributions to the Wilson coefficients of the magnetic dipole operators $Q_7^{(\prime)}$.

- The CP averaged coefficient S_6^s directly corresponds to the well known forward backward asymmetry and has a zero crossing in q^2 [118]. The same is true for the observables S_4 and S_5 and we find the following SM predictions for the positions of the zero crossings [19]

$$q_0^2(S_4)_{\rm SM} = 1.94^{+0.12}_{-0.10}\ {\rm GeV}^2\ , \quad q_0^2(S_5)_{\rm SM} = 2.24^{+0.06}_{-0.08}\ {\rm GeV}^2\ ,$$
$$q_0^2(S_6^s)_{\rm SM} = 3.90^{+0.11}_{-0.12}\ {\rm GeV}^2\ . \tag{3.64}$$

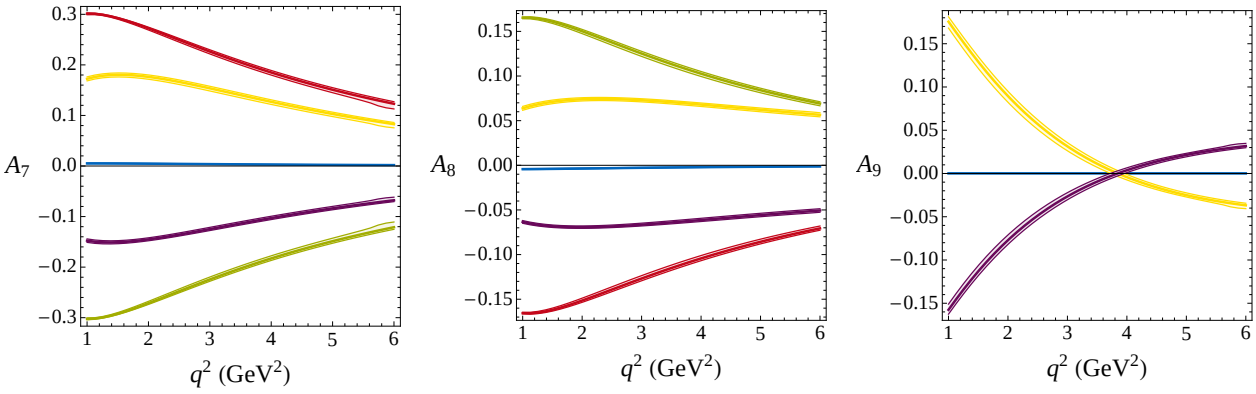

Figure 3.3: The CP asymmetries A_7, A_8 and A_9 as functions of the dilepton invariant mass squared q^2. The blue bands correspond to the SM and the remaining colored bands to NP scenarios as described in the text.

As we will see below, contributions from NP to the real parts of the $C_7^{(\prime)}$ Wilson coefficients will lead to characteristic shifts of these zero crossings.

- Another interesting observable is S_3, as it is approximately proportional to the real part of the Wilson coefficient C_7' and consequently very small in the SM. It corresponds directly to the transverse asymmetry A_T^2 discussed in [107, 88] and is a very sensitive probe of right handed currents in NP models.

- If the NP contributions to the Wilson coefficients also have CP violating phases, then the three T-odd asymmetries A_7, A_8 and A_9, that are approximately zero in the SM, can be strongly modified. While A_7 and A_8 are sensitive to the imaginary parts of both C_7 and C_7', A_9 can only be generated through an imaginary part of C_7' and is therefore a very interesting observable to probe CP violating right handed currents.

In figures 3.2 and 3.3 we show the q^2 distributions of these observables in the range 1 GeV^2 $< q^2 <$ 6 GeV^2 in the SM (blue) and 5 example scenarios with representative values of the NP contributions to the C_7 and C_7' Wilson coefficients at the electroweak scale, that are in agreement with the data on the BR($B \to X_s\gamma$) and BR($B \to X_s\ell^+\ell^-$)

$$\begin{aligned}
&\text{scenario 1 (orange):} && C_7^{\rm NP} = -0.13\ , && C_7'^{\rm NP} = \ \ 0\ ,\\
&\text{scenario 2 (green):} && C_7^{\rm NP} = \ \ 0.4 + 0.7i\ , && C_7'^{\rm NP} = \ \ 0\ ,\\
&\text{scenario 3 (red):} && C_7^{\rm NP} = \ \ 0.4 - 0.7i\ , && C_7'^{\rm NP} = \ \ 0\ ,\\
&\text{scenario 4 (yellow):} && C_7^{\rm NP} = \ \ 0\ , && C_7'^{\rm NP} = \ \ 0.33 + 0.33i\ ,\\
&\text{scenario 5 (purple):} && C_7^{\rm NP} = \ \ 0\ , && C_7'^{\rm NP} = -0.33 - 0.33i\ ,
\end{aligned}$$

The characteristic effects in the $B \to K^*\ell^+\ell^-$ observables that are induced by these NP contributions are conveniently summarized in table 3.1. The quantities $\langle A_7\rangle$ and $\langle A_8\rangle$ appearing in this table are the q^2 integrated versions of A_7 and A_8 and defined as

$$\langle A_i\rangle = \int_{1\,\text{GeV}^2}^{6\,\text{GeV}^2} dq^2\,\left(I_i - \bar{I}_i\right) \Big/ \int_{1\,\text{GeV}^2}^{6\,\text{GeV}^2} dq^2 \frac{d(\Gamma+\bar{\Gamma})}{dq^2}\ . \tag{3.65}$$

	$q_0^2(S_4)$	$q_0^2(S_5)$	$q_0^2(S_6^s)$	$\langle A_7 \rangle$	$\langle A_8 \rangle$	S_3	A_9
$\mathrm{Re}(C_7^{\mathrm{NP}}) > 0$	$\Downarrow$	$\Downarrow$	$\Downarrow$	–	–	–	–
$\mathrm{Re}(C_7^{\mathrm{NP}}) < 0$	$\Uparrow$	$\Uparrow$	$\Uparrow$	–	–	–	–
$\mathrm{Im}(C_7^{\mathrm{NP}}) > 0$	–	–	–	$\Downarrow$	$\Uparrow$	–	–
$\mathrm{Im}(C_7^{\mathrm{NP}}) < 0$	–	–	–	$\Uparrow$	$\Downarrow$	–	–
$\mathrm{Re}(C_7'^{\mathrm{NP}}) > 0$	$\Uparrow$	$\Downarrow$	–	–	–	$\Updownarrow$	–
$\mathrm{Re}(C_7'^{\mathrm{NP}}) < 0$	$\Downarrow$	$\Uparrow$	–	–	–	$\Updownarrow$	–
$\mathrm{Im}(C_7'^{\mathrm{NP}}) > 0$	–	–	–	$\Uparrow$	$\Uparrow$	–	$\Updownarrow$
$\mathrm{Im}(C_7'^{\mathrm{NP}}) < 0$	–	–	–	$\Downarrow$	$\Downarrow$	–	$\Updownarrow$

Table 3.1: Anatomy of effects in an example set of $B \to K^* \ell^+ \ell^-$ observables as induced by NP contributions to the Wilson coefficients C_7 and C_7'. The zero crossings of the CP averaged angular coefficients S_4, S_5 and S_6^s are shifted by the real parts of the Wilson coefficients, while the imaginary parts modify the asymmetries A_7, A_8 and A_9. Effects in the observables S_3 and A_9 only arise in the presence of the right handed Wilson coefficient C_7' and are also show in the corresponding figures 3.2 and 3.3.

We note a remarkably strict correlation between these two integrated CP asymmetries. In the left plot of figure 3.4 we show the possible effects in $\langle A_7 \rangle$ and $\langle A_8 \rangle$ that are generated by complex NP contributions to C_7 that is taken as a free parameter at the electroweak scale taking into account the constraints from $\mathrm{BR}(B \to X_s \gamma)$ and $\mathrm{BR}(B \to X_s \ell^+ \ell^-)$. In such a case, large positive values of $\langle A_7 \rangle$ necessarily imply large negative values for $\langle A_8 \rangle$ and vice versa. In the plot on the right hand side, the same situation is shown but now with the NP contributions in the right handed Wilson coefficient C_7', which leads to an exactly orthogonal correlation. The correlation between $\langle A_7 \rangle$ and $\langle A_8 \rangle$ thus allows for a clear distinction of these two cases.

We also make the following remark: While large negative values of $\mathrm{Re}(C_7^{\mathrm{NP}}) < -0.13$ are excluded by the constraint from the $\mathrm{BR}(B \to X_s \gamma)$, large positive values of $\mathrm{Re}(C_7^{\mathrm{NP}})$ that interfere destructively with the SM contribution C_7^{SM}, are in principle possible if simultaneously also the $\mathrm{Im}(C_7)$ is large. Large non-standard effects in the CP asymmetries A_7 and A_8 are therefore correlated with shifts of the zero crossings of S_4, S_5 and S_6^s towards smaller values, if NP affects only C_7.

The above discussion emphasizes the important role of the $B \to K^* \ell^+ \ell^-$ decay in testing physics beyond the SM. In particular, NP effects in the Wilson coefficients of the magnetic dipole operators that typically give the dominant contribution in the MSSM, lead to very characteristic modifications in the many observables that are accessible from its angular decay distribution. Measuring these observables at LHCb, will add valuable information to disentangle possible NP scenarios.

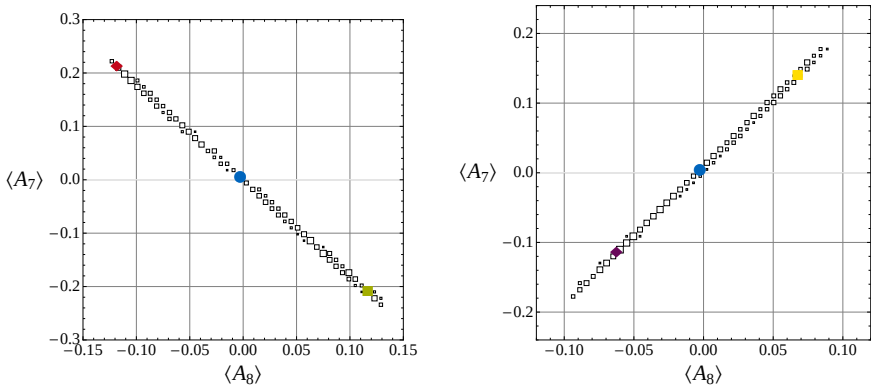

Figure 3.4: Correlation between the q^2 integrated CP asymmetries $\langle A_7 \rangle$ and $\langle A_8 \rangle$. In the plot on the left, NP contributions to the $B \to K^* \ell^+ \ell^-$ decay are only induced by C_7, while in the plot on the left, only NP contributions to the right handed Wilson coefficient C_7' are considered.

3.2.3 The $B \to \phi K_S$ and $B \to \eta' K_S$ Decays

Also non-leptonic decays of B mesons offer possibilities to probe the flavor and CP violating structure of NP models. While the theoretical predictions of the branching ratios of non-leptonic decays suffer from large hadronic uncertainties, the time dependent CP asymmetries in the decay into CP eigenstates for example can often be predicted with much higher accuracy. Here we concentrate on the time dependent CP asymmetries in the loop induced $B \to \phi K_S$ and $B \to \eta' K_S$ decays that are among the theoretical cleanest modes [119, 120, 121]. They can be written as follows

$$\frac{\Gamma(B_d(t) \to f) - \Gamma(B_d(t) \to f)}{\Gamma(B_d(t) \to f) + \Gamma(B_d(t) \to f)} = S_f \sin(\Delta M_d t) - C_f \cos(\Delta M_d t) \ , \tag{3.66}$$

where $f = \phi K_S$, or $f = \eta' K_S$. The coefficients S_f and C_f, are given by

$$S_f = \frac{2\mathrm{Im}(\lambda_f)}{1 + |\lambda_f|^2} \ , \quad C_f = \frac{1 - |\lambda_f|^2}{1 + |\lambda_f|^2} \ , \quad \lambda_f = e^{-2i(\beta + \phi_{B_d})} (\bar{A}_f / A_f) \ . \tag{3.67}$$

In the definition of the complex quantity λ_f, the phase ϕ_{B_d} is a possible NP phase in the B_d mixing amplitude (see (3.26)) and A_f ($\bar{A}_f$) is the decay amplitude for $B_d(\bar{B}_d) \to f$. Thus NP effects can enter either through the B_d mixing amplitude or directly in the $b \to sq\bar{q}$ decay amplitudes [122, 123].

In the SM it turns out that the ratio of the decay amplitudes $\bar{A}_f / A_f \simeq 1$ and S_f and C_f are to a good approximation universal for all $b \to sq\bar{q}$ transitions. In particular, in the SM it is predicted that both in the tree level $B_d \to \psi K_S$ as well as in the loop induced $B_d \to \phi K_S$ and $B_d \to \eta' K_S$ decay modes the coefficient S_f measures the angle β in the unitarity triangle $S_{\phi K_S} \simeq S_{\eta' K_S} \simeq S_{\psi K_S} \simeq \sin 2\beta \simeq 0.7$. Experimentally one finds [36]

$$S^{\mathrm{exp}}_{\phi K_S} = 0.44^{+0.17}_{-0.18} \ , \quad S^{\mathrm{exp}}_{\eta' K_S} = 0.59 \pm 0.07 \ , \quad S^{\mathrm{exp}}_{\psi K_S} = 0.672 \pm 0.023 \ , \tag{3.68}$$

which is roughly $1.5 - 2\sigma$ below the SM prediction. Both $S_{\phi K_S}$ and $S_{\eta' K_S}$ are expected to be measured with an accuracy of few % at a superB factory [37, 38, 39].

While a NP contribution to the B_d mixing phase leads to a common shift of all the coefficients S_f compared to the SM prediction, NP effects in the decay amplitudes can

modify them separately. In principle, the $b \to sq\bar{q}$ decay amplitudes are very sensitive to NP contributions of the so-called QCD penguin operators

$$\begin{aligned}
Q_3 &= (\bar{s}\gamma_\mu P_L b)\sum_q (\bar{q}\gamma_\mu P_L q) \ , & Q_3' &= (\bar{s}\gamma_\mu P_R b)\sum_q (\bar{q}\gamma_\mu P_R q) \ , \\
Q_4 &= (\bar{s}_\alpha\gamma_\mu P_L b_\beta)\sum_q (\bar{q}_\beta\gamma_\mu P_L q_\alpha) \ , & Q_4' &= (\bar{s}_\alpha\gamma_\mu P_R b_\beta)\sum_q (\bar{q}_\beta\gamma_\mu P_R q_\alpha) \ , \\
Q_5 &= (\bar{s}\gamma_\mu P_L b)\sum_q (\bar{q}\gamma_\mu P_R q) \ , & Q_5' &= (\bar{s}\gamma_\mu P_R b)\sum_q (\bar{q}\gamma_\mu P_L q) \ , \\
Q_6 &= (\bar{s}_\alpha\gamma_\mu P_L b_\beta)\sum_q (\bar{q}_\beta\gamma_\mu P_R q_\alpha) \ , & Q_6' &= (\bar{s}_\alpha\gamma_\mu P_R b_\beta)\sum_q (\bar{q}_\beta\gamma_\mu P_L q_\alpha) \ . \qquad (3.69)
\end{aligned}$$

In the concrete MSSM scenarios that we will consider in this work however, the main NP contributions to the decay amplitudes come from the chromomagnetic dipole operators $Q_8^{(\prime)}$ given already in (3.45). In terms of the Wilson coefficients of these operators, the decay amplitude A_f takes the generic form [120, 124]

$$A_f = A_f^c\left[1 + a_f^u e^{i\gamma} + \sum_i \left(b_{fi}^c + b_{fi}^u e^{i\gamma}\right)\left(C_i^{\rm NP*}(M_W) + \zeta C_i'^{\rm NP*}(M_W)\right)\right] \ , \qquad (3.70)$$

where $C_i^{\rm NP}(M_W)$ and $C_i'^{\rm NP}(M_W)$ are the NP contributions to the Wilson coefficients evaluated at the scale M_W. The parameters b_{fi}^u and b_{fi}^c have been calculated in [120] and $\zeta = \pm 1$ depending on the parity of the final state; for instance $\zeta = 1$ for $f = \phi K_S$ and $\zeta = -1$ for $f = \eta' K_S$ [125].

As just mentioned, in the MSSM scenarios to be considered below, the main role is played by the NP contributions to the chromomagnetic Wilson coefficients $C_8^{(\prime)}$, that will lead to characteristic modifications of the coefficients $S_{\phi K_S}$ and $S_{\eta' K_S}$ in the time dependent CP asymmetries in the $B \to \phi K_S$ and $B \to \eta' K_S$ decays.

3.2.4 The $B_s \to \mu^+\mu^-$ and $B_d \to \mu^+\mu^-$ Decays

The purely leptonic $B_s \to \mu^+\mu^-$ and $B_d \to \mu^+\mu^-$ decays are strongly helicity suppressed in the SM by the small muon mass, leading to tiny SM predictions for their branching ratios. Normalizing the branching ratios to the corresponding mass differences ΔM_s and ΔM_d as suggested in [126] to remove the dependence on the B meson decay constants and using the input parameter from appendix A.3, we obtain

$$\begin{aligned}
{\rm BR}(B_s \to \mu^+\mu^-)_{\rm SM} &= (3.47 \pm 0.37) \times 10^{-9} \ , & (3.71) \\
{\rm BR}(B_d \to \mu^+\mu^-)_{\rm SM} &= (1.06 \pm 0.11) \times 10^{-10} \ . & (3.72)
\end{aligned}$$

Experimentally, only upper bounds for the branching ratios of these decay modes have been obtained at CDF [127] and D0 [128]. The most stringent published bounds read

$$\begin{aligned}
{\rm BR}(B_s \to \mu^+\mu^-)_{\rm exp} &\lesssim 5.8 \times 10^{-8} \quad @\ 95\%\ {\rm C.L.} \ , & (3.73) \\
{\rm BR}(B_d \to \mu^+\mu^-)_{\rm exp} &\lesssim 1.8 \times 10^{-8} \quad @\ 95\%\ {\rm C.L.} \ , & (3.74)
\end{aligned}$$

and they are expected to be still improved down to a level of 3.3×10^{-8} and 9.1×10^{-9}, respectively [129] using data from Tevatron. The $B_s \to \mu^+\mu^-$ will then be one of the main channels at the LHCb experiment where one expects to reach a 5σ sensitivity to the SM prediction [130].

The strong suppression of these decays make them ideal probes to investigate the quark flavor structure of physics beyond the SM. In fact their helicity suppression can be lifted in the presence of scalar currents and even order of magnitude enhancements of the branching ratios are possible for example in the MSSM with large $\tan\beta$.

The operator that is responsible for the $B_s \to \mu^+\mu^-$ decay in the SM is the semileptonic operator Q_{10} already defined in (3.56). Possible scalar currents in NP models give rise to scalar and pseudo scalar operators

$$Q_S = \frac{e^2}{16\pi^2} m_b \left(\bar{s} P_R b\right)\left(\bar{\ell}\ell\right) \ , \qquad Q'_S = \frac{e^2}{16\pi^2} m_b \left(\bar{s} P_L b\right)\left(\bar{\ell}\ell\right) \ , \tag{3.75}$$

$$Q_P = \frac{e^2}{16\pi^2} m_b \left(\bar{s} P_R b\right)\left(\bar{\ell}\gamma_5\ell\right) \ , \qquad Q'_P = \frac{e^2}{16\pi^2} m_b \left(\bar{s} P_L b\right)\left(\bar{\ell}\gamma_5\ell\right) \ . \tag{3.76}$$

In terms of the Wilson coefficients of these operators, the branching ratio for the $B_s \to \mu^+\mu^-$ decay can be expressed in the following way[2]

$$\mathrm{BR}(B_s \to \mu^+\mu^-) = \tau_{B_s} \frac{G_F^2 \alpha_{\mathrm{em}}^2}{64\pi^3} F_{B_s}^2 M_{B_s}^3 |V_{tb}V_{ts}^*|^2 \sqrt{1 - \frac{4m_\mu^2}{M_{B_s}^2}} \left(|B|^2 \left(1 - \frac{4m_\mu^2}{M_{B_s}^2}\right) + |A|^2 \right) \ , \tag{3.77}$$

with A and B given by

$$A = 2\frac{m_\mu}{M_{B_s}} C_{10}^{\mathrm{SM}} + M_{B_s}\left(C_P - C'_P\right) \ , \quad B = M_{B_s}\left(C_S - C'_S\right) \ , \tag{3.78}$$

and $C_{10}^{\mathrm{SM}} \simeq -4.1$ [19]. In writing the above expressions, we neglected possible NP contributions to $C_{10}^{(\prime)}$ as they are negligible in all the MSSM frameworks that we will discuss below. The factor m_μ in front of C_{10}^{SM} clearly shows the above mentioned helicity suppression, that is lifted in the presence of the scalar and pseudoscalar operators. We also mention that through the explicit factor of m_b in the definition of the operators in (3.75), the anomalous dimension of these operators vanishes and in the expressions for the branching ratio (3.77) and (3.78) directly the Wilson coefficients at the high matching scale can be used.

The NP contributions to the Wilson coefficients $C_S^{(\prime)}$ and $C_P^{(\prime)}$ in the MSSM and the implied effects on the $B_s \to \mu^+\mu^-$ and $B_d \to \mu^+\mu^-$ decays will be discussed in section 6.3.

3.2.5 The $b \to s\nu\bar{\nu}$ Decays

In this section we discuss the inclusive $B \to X_s\nu\bar{\nu}$ as well as the two exclusive $B \to K^*\nu\bar{\nu}$ and $B \to K\nu\bar{\nu}$ decays that are all based on the $b \to s\nu\bar{\nu}$ transition at the parton level. These rare $b \to s\nu\bar{\nu}$ decays allow a transparent study of Z penguin effects in NP scenarios in the absence of dipole and scalar operator contributions that often dominate decay modes like $B \to X_s\gamma$, $B \to K^*\ell^+\ell^-$ or $B_s \to \mu^+\mu^-$ as discussed above. We will mostly follow our analysis [20], older discussions can be found e.g. in [131, 132, 133, 134].

[2] A fully analogous expressions holds of course also in the case of the $B_d \to \mu^+\mu^-$ decay.

The effective Hamiltonian for the $b \to s\nu\bar{\nu}$ transition is generally given by

$$\mathcal{H}_{\text{eff}} = -\frac{4G_F}{\sqrt{2}} V_{tb}V_{ts}^* \left(C_L^\nu \mathcal{O}_L^\nu + C_R^\nu \mathcal{O}_R^\nu\right) \; + \; \text{h.c.} \; , \tag{3.79}$$

with the operators

$$\mathcal{O}_L^\nu = \frac{e^2}{16\pi^2}(\bar{s}\gamma_\mu P_L b)(\bar{\nu}\gamma^\mu(1-\gamma_5)\nu) \; , \qquad \mathcal{O}_R^\nu = \frac{e^2}{16\pi^2}(\bar{s}\gamma_\mu P_R b)(\bar{\nu}\gamma^\mu(1-\gamma_5)\nu) \; . \tag{3.80}$$

In the SM, C_R^ν is negligible small while $(C_L^\nu)^{\text{SM}} = -6.38 \pm 0.06$ [135, 136, 20].

While the only observables in $B \to X_s\nu\bar{\nu}$ and $B \to K\nu\bar{\nu}$ are the respective branching ratios, the angular distribution of the K^* decay products in the $B \to K^*(\to K\pi)\nu\bar{\nu}$ decay allows to extract additional information about the polarization of the K^*, just like in $B \to K^*\mu^+\mu^-$ decays. The $B \to K^*(\to K\pi)\nu\bar{\nu}$ decay with an on-shell K^* is completely described by a double differential decay distribution in terms of the normalized dineutrino invariant mass squared $s_B = q^2/M_B^2$ and θ, the angle between the K^* flight direction in the B rest frame and the K flight direction in the $K\pi$ rest frame. This double differential spectrum can be written as

$$\frac{d^2\Gamma}{ds_B d\cos\theta} = \frac{3}{4}\frac{d\Gamma_T}{ds_B}\sin^2\theta + \frac{3}{2}\frac{d\Gamma_L}{ds_B}\cos^2\theta \; , \tag{3.81}$$

with the longitudinal and transverse polarization fractions

$$\frac{d\Gamma_L}{ds_B} = 3m_B^2|A_0|^2 \; , \quad \frac{d\Gamma_T}{ds_B} = 3m_B^2\left(|A_\perp|^2 + |A_\parallel|^2\right) \; . \tag{3.82}$$

The factor of 3 stems from the sum over neutrino flavors and A_0, $A_\perp$ and $A_\parallel$ are $B \to K^*$ transversity amplitudes that can be expressed in terms of the Wilson coefficients C_L^ν and C_R^ν and $B \to K^*$ form factors (see e.g. [20]). From the experimental perspective, $d\Gamma_L/ds_B$ and $d\Gamma_T/ds_B$ can be extracted by an angular analysis of the K^* decay products.

Instead of these two observables, one can choose the following two independent observables accessible from the double differential decay distribution: the dineutrino mass distribution $d\Gamma/ds_B$, where

$$\frac{d\Gamma}{ds_B} = \int_{-1}^{1} d\cos\theta \, \frac{d^2\Gamma}{ds_B d\cos\theta} = \frac{d\Gamma_L}{ds_B} + \frac{d\Gamma_T}{ds_B} = 3m_B^2\left(|A_\perp|^2 + |A_\parallel|^2 + |A_0|^2\right) \; , \tag{3.83}$$

and either of the K^* longitudinal or transverse polarization fractions $F_{L,T}$ also used in studies of $B \to K^*\ell^+\ell^-$ decays and defined as

$$F_{L,T} = \frac{d\Gamma_{L,T}/ds_B}{d\Gamma/ds_B} \; , \quad F_L = 1 - F_T \; . \tag{3.84}$$

The advantage of this choice of observables is twofold. First, the normalization of $F_{L,T}$ to the total dineutrino spectrum strongly reduces the hadronic uncertainties associated with the form factors as well as parametric uncertainties associated with CKM elements. Second, in the absence of right handed currents ($C_R^\nu = 0$), the dependence on the remaining Wilson coefficient C_L^ν drops out in $F_{L,T}$, making it a perfect observable to probe such right handed currents. We will also consider the s_B-integrated form of $F_{L,T}$, which we define as

$$\langle F_{L,T}\rangle = \frac{\Gamma_{L,T}}{\Gamma} \; , \qquad \text{where} \qquad \Gamma_{(L,T)} = \int_0^{1-\frac{M_{K^*}^2}{M_B^2}} ds_B \frac{d\Gamma_{(L,T)}}{ds_B} \; . \tag{3.85}$$

The four s_B-integrated observables in the $b \to s\nu\bar{\nu}$ transitions that we will consider then are the branching ratios of the $B \to X_s\nu\bar{\nu}$, the $B \to K\nu\bar{\nu}$ and the $B \to K^*\nu\bar{\nu}$ decays as well as the longitudinal polarization fraction $\langle F_L \rangle$ in the $B \to K^*(\to K\pi)\nu\bar{\nu}$ decay. For their SM predictions we find [20]

$$\begin{aligned}
\mathrm{BR}(B \to X_s\nu\bar{\nu})_{\mathrm{SM}} &= (2.7 \pm 0.2) \times 10^{-5} \,, && (3.86)\\
\mathrm{BR}(B^+ \to K^+\nu\bar{\nu})^{\mathrm{SD}}_{\mathrm{SM}} &= (4.5 \pm 0.7) \times 10^{-6} \,, && (3.87)\\
\mathrm{BR}(B \to K^*\nu\bar{\nu})_{\mathrm{SM}} &= (6.8^{+1.0}_{-1.1}) \times 10^{-6} \,, && (3.88)\\
\langle F_L \rangle(B \to K^*\nu\bar{\nu})_{\mathrm{SM}} &= 0.54 \pm 0.01 \,. && (3.89)
\end{aligned}$$

Few comments are in order

- With an estimated uncertainty of less than 10%, the decay $B \to X_s\nu\bar{\nu}$ is the theoretically cleanest branching ratio as it does not involve any form factors.
- For the $B \to K\nu\bar{\nu}$ and $B \to K^*\nu\bar{\nu}$ decays we use the form factors from [137] and [112, 19] respectively that are obtained with QCD light-cone sum rule techniques in the low q^2 regime. These formfactors are then fitted to parameterizations accounting for resonances in the form factors and extended to the high q^2 region (see also [138]).
- The SM prediction for $\mathrm{BR}(B^+ \to K^+\nu\bar{\nu})$ refers to the short distance contribution. For this *charged* mode also long distance contributions exist at tree level, coming from an intermediate τ lepton. These contributions have been analyzed in [139] and amount roughly to a 15% increase of the branching ratio prediction.
- As discussed in [140], the uncertainty in the prediction of the $\mathrm{BR}(B^+ \to K^+\nu\bar{\nu})$ can be reduced through a normalization to the branching ratio of the $B^+ \to K^+\ell^+\ell^-$ decay, leading to $\mathrm{BR}(B^+ \to K^+\nu\bar{\nu}) = (3.64 \pm 0.47) \times 10^{-6}$.

None of these three rare decays has been observed yet, and only experimental upper bounds on their branching ratios exist at present. They have been obtained by Aleph [141], Belle [142] and BaBar [143] and read

$$\begin{aligned}
\mathrm{BR}(B \to X_s\nu\bar{\nu})_{\mathrm{exp}} &\leq 64 \times 10^{-5} \quad @\ 90\%\ \mathrm{C.L.} \,, && (3.90)\\
\mathrm{BR}(B^+ \to K^+\nu\bar{\nu})_{\mathrm{exp}} &\leq 14 \times 10^{-6} \quad @\ 90\%\ \mathrm{C.L.} \,, && (3.91)\\
\mathrm{BR}(B \to K^*\nu\bar{\nu})_{\mathrm{exp}} &\leq 80 \times 10^{-6} \quad @\ 90\%\ \mathrm{C.L.} \,. && (3.92)
\end{aligned}$$

These bounds are still far above the SM predictions given in (3.86), (3.87) and (3.88). No experimental measurement of the longitudinal polarization fraction $\langle F_L \rangle$ in $B \to K^*\nu\bar{\nu}$ exists up to now. While the expected sensitivity of a superB factory should be sufficient to find evidence for the exclusive $B^+ \to K^+\nu\bar{\nu}$ and $B \to K^*\nu\bar{\nu}$ decays [37, 38, 39], the inclusive $B \to X_s\nu\bar{\nu}$ decay is most likely beyond the reach of such an experiment.

The four observables accessible in the three different $b \to s\nu\bar{\nu}$ decays are dependent on the two in principle complex Wilson coefficients C_L^ν and C_R^ν. However, only two combinations of these complex quantities enter the theoretical predictions of the observables [131, 133]

$$\epsilon = \frac{\sqrt{|C_L^\nu|^2 + |C_R^\nu|^2}}{|(C_L^\nu)^{\mathrm{SM}}|} \,, \quad \eta = \frac{-\mathrm{Re}(C_L^\nu C_R^{\nu *})}{|C_L^\nu|^2 + |C_R^\nu|^2} \,, \qquad (3.93)$$

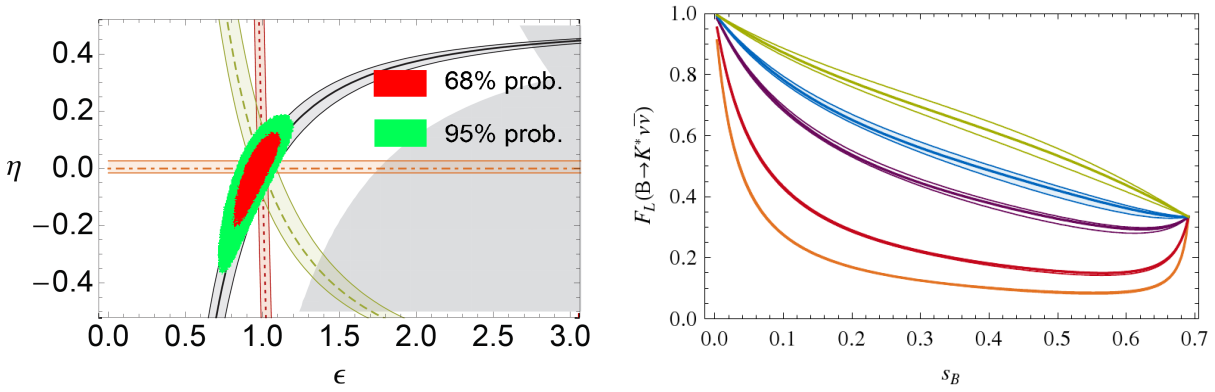

Figure 3.5: Left: Constraints in the $\epsilon - \eta$ plane. The light gray region is excluded by present experiments at the 90% C.L.. The colored bands assume that all four observables have been measured with infinite precision, taking into account only theoretical uncertainties. The green band (dashed line) represents $\mathrm{BR}(B \to K^*\nu\bar{\nu})$, the black band (solid line) $\mathrm{BR}(B \to K\nu\bar{\nu})$, the red band (dotted line) $\mathrm{BR}(B \to X_s\nu\bar{\nu})$ and the orange band (dot-dashed line) $\langle F_L \rangle$. The red and green areas are the projected sensitivity at a superB factory with $75\mathrm{ab}^{-1}$ integrated luminosity [144]. Right: The longitudinal polarization fraction F_L in the $B \to K^*\nu\bar{\nu}$ decay as a function of the normalized dineutrino invariant mass squared s_B for different values of η. From top to bottom: $\eta = 0.5$, $\eta = 0$, $\eta = -0.2$, $\eta = -0.4$, $\eta = -0.45$. From [145, 20].

with η lying in the range $[-1/2, 1/2]$. All four observables can then be expressed in terms of ϵ and η

$$\begin{aligned}
\mathrm{BR}(B \to X_s\nu\bar{\nu}) &= 2.7 \times 10^{-5}\ (1 + 0.09\eta)\epsilon^2\ , && (3.94)\\
\mathrm{BR}(B^+ \to K^+\nu\bar{\nu})_{\mathrm{SD}} &= 4.5 \times 10^{-6}\ (1 - 2\eta)\epsilon^2\ , && (3.95)\\
\mathrm{BR}(B \to K^*\nu\bar{\nu}) &= 6.8 \times 10^{-6}\ (1 + 1.31\eta)\epsilon^2\ , && (3.96)\\
\langle F_L \rangle(B \to K^*\nu\bar{\nu}) &= 0.54\ \frac{1 + 2\eta}{1 + 1.31\eta}\ . && (3.97)
\end{aligned}$$

As ϵ and η can be calculated in any model by means of (3.93), these four expressions can be considered as fundamental formulae for any phenomenological analysis of the decays in question. The experimental bounds on the branching ratios in (3.90), (3.91) and (3.92) can then be translated into excluded areas in the ϵ-η plane, where the SM corresponds to $(\epsilon, \eta) = (1, 0)$.

Since the four observables depend on only two parameters, a measurement of all of them would overconstrain the resulting (ϵ, η) point. To illustrate the theoretical cleanliness of the various observables, we show in the left plot of figure 3.5 the combined constraints after hypothetical measurements with infinite precision, assuming the SM. The expected sensitivity at a superB factory with $75\mathrm{ab}^{-1}$ integrated luminosity is also shown [144].

A special role is played by the observable $\langle F_L \rangle$. Since it only depends on η, it leads to a horizontal line in the ϵ-η plane. Although a similar constraint could be obtained by dividing two of the branching ratios to cancel the common factor of ϵ^2, the use of $\langle F_L \rangle$ is theoretically much cleaner since in this case, the hadronic uncertainties cancel, while they would add up when using the branching ratios. Since $\langle F_L \rangle$ only depends on η, the distribution $F_L(s_B)$ is universal for all models in which one of the Wilson coefficients C_L^ν or C_R^ν vanishes, as in the

SM and all models with minimal flavor violation. In the right plot of figure 3.5, we show $F_L(s_B)$ in the kinematically allowed range of s_B for several values of η. The blue curve is the universal curve for $\eta = 0$. Every experimentally observed deviation from this curve signals clearly the presence of right handed currents.

3.2.6 The $K \to \pi\nu\bar{\nu}$ Decays

The $K_L \to \pi^0\nu\bar{\nu}$ and $K^+ \to \pi^+\nu\bar{\nu}$ decays (see [146] for a review) are the theoretically cleanest processes among the many rare K and B decays. Their branching ratios have been calculated in the SM to an exceptionally high precision [147, 148]

$$\begin{aligned} \mathrm{BR}(K^+ \to \pi^+\nu\bar{\nu})_{\mathrm{SM}} &= (8.5 \pm 0.7) \times 10^{-11} \,, & (3.98)\\ \mathrm{BR}(K_L \to \pi^0\nu\bar{\nu})_{\mathrm{SM}} &= (2.5 \pm 0.4) \times 10^{-11} \,. & (3.99) \end{aligned}$$

On the experimental side, only a very loose upper bound from the E391a experiment at KEK exists for the neutral mode [149], while for the charged mode already seven candidate events have been reported at the E787 and E949 experiments at BNL [150] leading to

$$\begin{aligned} \mathrm{BR}(K^+ \to \pi^+\nu\bar{\nu})_{\mathrm{exp}} &= (1.73^{+1.15}_{-1.05}) \times 10^{-10} \,, & (3.100)\\ \mathrm{BR}(K_L \to \pi^0\nu\bar{\nu})_{\mathrm{exp}} &\leq 2.6 \times 10^{-8} \quad @\ 90\%\ \mathrm{C.L.} \,. & (3.101) \end{aligned}$$

While the central value in (3.100) is a factor of 2 above the SM prediction, it is perfectly consistent with the SM, given the huge experimental error at present. In the near future the NA62 experiment at CERN [151] and the K0TO experiment at JPARC [152] aim at SM sensitivity for the $K^+ \to \pi^+\nu\bar{\nu}$ and $K_L \to \pi^0\nu\bar{\nu}$ decays respectively.

Both decays, in particular the neutral $K_L \to \pi^0\nu\bar{\nu}$ mode that in the SM is purely induced by direct CP violation, are known to offer unique possibilities in testing the structure of flavor and CP violation in extensions of the SM [153, 154, 155].

The effective Hamiltonian relevant for these decays reads

$$\mathcal{H}_{\mathrm{eff}} = -\frac{4G_{\mathrm{F}}}{\sqrt{2}} \left[\mathcal{H}_{\mathrm{eff}}^{(c)} + V_{ts}^* V_{td} \left(C_L^K \mathcal{O}_L^K + C_R^K \mathcal{O}_R^K \right) \right] \ + \ \mathrm{h.c.} \,, \tag{3.102}$$

where $\mathcal{H}_{\mathrm{eff}}^{(c)}$ denotes the operators which encode physics below the electroweak scale and the remaining term consists of the part of the effective Hamiltonian sensitive to short distance dynamics. The operators in (3.102) read

$$\mathcal{O}_L^K = \frac{e^2}{16\pi^2} (\bar{s}\gamma_\mu P_L b)(\bar{\nu}\gamma^\mu(1-\gamma_5)\nu) \,, \quad \mathcal{O}_R^K = \frac{e^2}{16\pi^2} (\bar{s}\gamma_\mu P_R d)(\bar{\nu}\gamma^\mu(1-\gamma_5)\nu) \,. \tag{3.103}$$

The branching ratios of the $K_L \to \pi^0\nu\bar{\nu}$ and $K^+ \to \pi^+\nu\bar{\nu}$ decays can then be written as

$$\begin{aligned} \mathrm{BR}(K^+ \to \pi^+\nu\bar{\nu}) &= \kappa_+ \left[\left(\frac{\mathrm{Im}(\lambda_t X^K)}{\lambda^5} \right)^2 + \left(-P_{(u,c)} + \frac{\mathrm{Re}(\lambda_t X^K)}{\lambda^5} \right)^2 \right] \,, & (3.104)\\ \mathrm{BR}(K_L \to \pi^0\nu\bar{\nu}) &= \kappa_L \left(\frac{\mathrm{Im}(\lambda_t X^K)}{\lambda^5} \right)^2 \,, & (3.105) \end{aligned}$$

The κ factors originate mainly from the hadronic matrix elements and read $\kappa_+ = (5.27 \pm 0.03) \times 10^{-11}$ and $\kappa_L = (2.27 \pm 0.01) \times 10^{-10}$ [148]. The term $P_{(u,c)}$ accounts for contributions from charm and light quark loops and is given by $P_{(u,c)} = 0.41 \pm 0.05$ [156, 157, 158, 147]. Finally, X^K denotes the combination $-s_W^2(C_L^K + C_R^K)$ and is the quantity sensitive to NP contributions. In the SM $(C_R^K)^{\rm SM} \simeq 0$ and $(C_L^K)^{\rm SM} = (C_L^\nu)^{\rm SM} \simeq -6.38$. The most important contributions to the Wilson coefficients C_L^K and C_R^K in the MSSM will be discussed in section 6.5.

3.2.7 The $B^+ \to \tau^+\nu$ Decay

The helicity suppressed tree level $B^+ \to \tau^+\nu$ decay is not yet "observed" with a 5σ significance. Still, the current experimental world average for the branching ratio based on data from BaBar [159, 160] and Belle [161, 162] reads [80]

$$\mathrm{BR}(B^+ \to \tau^+\nu)_{\rm exp} = (1.73 \pm 0.35) \times 10^{-4} \ . \tag{3.106}$$

A superB factory can improve this result significantly and it is expected that a final accuracy at the level of 3-4% could be reached [37, 38, 39].

While in the SM the $B^+ \to \tau^+\nu$ decay is induced through the tree level exchange of a $W^\pm$, in models with extended Higgs sectors also non-negligible effects can be generated through the tree level exchange of charged Higgs bosons [163, 164, 165].

The SM prediction for the branching ratio of $B^+ \to \tau^+\nu$ is

$$\mathrm{BR}(B^+ \to \tau^+\nu)_{\rm SM} = \frac{G_F^2 M_{B^+} m_\tau^2}{8\pi} \left(1 - \frac{m_\tau^2}{M_{B^+}^2}\right)^2 F_{B^+}^2 |V_{ub}|^2 \tau_{B^+} \tag{3.107}$$

and is afflicted with large uncertainties from the B meson decay constant F_{B^+} and the CKM element V_{ub}. Using the input parameters collected in appendix A.3 one finds directly from (3.107)

$$\mathrm{BR}(B^+ \to \tau^+\nu)_{\rm SM} = (1.10 \pm 0.29) \times 10^{-4} \ , \tag{3.108}$$

which is slightly below the experimental result (3.106) but still compatible at the 2σ level. A much more accurate prediction of the branching ratio within the SM can be obtained by normalizing $\mathrm{BR}(B^+ \to \tau^+\nu)$ to ΔM_d, the mass difference in the B_d system, thus eliminating the dependence on the B meson decay constant [166, 165]. One finds

$$\mathrm{BR}(B^+ \to \tau^+\nu)_{\rm SM} = \frac{3\pi\ \Delta M_d}{4\eta_B S_0(x_t) \hat{B}_{B_d}} \frac{m_\tau^2}{M_W^2} \left(1 - \frac{m_\tau^2}{M_{B^+}^2}\right)^2 \left|\frac{V_{ub}}{V_{td}}\right|^2 \tau_{B^+} \ , \tag{3.109}$$

where we used $F_{B_d} \simeq F_{B^+}$ and $M_{B_d} \simeq M_{B^+}$. Furthermore, one can completely eliminate the dependence on the CKM elements through

$$\left|\frac{V_{ub}}{V_{td}}\right|^2 = \left(1 + \lambda^2\right) \left(1 + \frac{1}{R_t^2} - \frac{2}{R_t} \cos\beta\right) \ , \tag{3.110}$$

with R_t and β determined directly from experiment through $\Delta M_d / \Delta M_s$ and $S_{\psi K_S}$, by means of the SM relations

$$R_t = \frac{\xi}{\lambda} \sqrt{\frac{M_{B_s}}{M_{B_d}}} \sqrt{\frac{\Delta M_d^{\rm exp}}{\Delta M_s^{\rm exp}}} \ , \quad \sin 2\beta = S_{\psi K_S}^{\rm exp} \ . \tag{3.111}$$

The resulting SM prediction for the branching ratio is

$$\mathrm{BR}(B^+ \to \tau^+\nu)_{\mathrm{SM}} = (0.79 \pm 0.12) \times 10^{-4} \ , \tag{3.112}$$

that is in excellent agreement with predictions that are based on fits of the Unitarity Triangle [80, 167]. The result (3.112) is roughly 2.5σ below the experimental world average (3.106), which reflects an apparent tension between the rather low experimental value of $S_{\psi K_S}$ and the large measured $B^+ \to \tau^+\nu$ branching ratio in the SM.

In our numerical analysis of the supersymmetric frameworks in chapter 8 we will use the more conservative (3.108) which implies

$$R_{B\tau\nu} = \frac{\mathrm{BR}(B^+ \to \tau^+\nu)}{\mathrm{BR}(B^+ \to \tau^+\nu)_{\mathrm{SM}}} = 1.57 \pm 0.53 \ . \tag{3.113}$$

As will be detailed in section 6.1, in the MSSM the result (3.113) leads to strong constraints on the mass of the charged Higgs boson in the large $\tan\beta$ regime.

Similar to the $B \to \tau\nu$ decay, also $B \to D\tau\nu$ is a sensitive probe of extended Higgs sectors [168, 169, 170, 171]. Even so this decay is not helicity suppressed as $B \to \tau\nu$ is, the relevant hadronic uncertainties are below the level of 10% and tree level charged Higgs exchange can have a visible impact also on this decay mode. While the three body decay $B \to D\tau\nu$ allows in principle to study decay distributions [170], here we will restrict ourselves to the branching ratio. Combining the SM prediction from [171] with recent experimental data from BaBar [172] one finds

$$R_{BD\tau\nu} = \frac{\mathrm{BR}(B \to D\tau\nu)}{\mathrm{BR}(B \to D\tau\nu)_{\mathrm{SM}}} = 1.49 \pm 0.47 \ , \tag{3.114}$$

which will lead to further constraints on the MSSM Higgs sector.

Finally we mention that also the helicity suppressed $K \to \mu\nu$ decay can be used to probe models with extended Higgs sectors [173]. While the sensitivity to tree level charged Higgs effects is much smaller than in the case of the above-mentioned B decays, for $K \to \mu\nu$ one has a much higher experimental accuracy and much smaller theoretical uncertainties. One defines (see [173] for details)

$$R_{\ell 23} = \left| \frac{V_{us}(K_{\ell 2})}{V_{us}(K_{\ell 3})} \times \frac{V_{ud}(0^+ \to 0^+)}{V_{ud}(\pi_{\ell 2})} \right| \tag{3.115}$$

as the ratio of the CKM matrix element V_{us} determined from $K_{\ell 2}$ and $K_{\ell 3}$ decays. The normalization to the ratio of the CKM matrix element V_{ud} as obtained from $0^+ \to 0^+$ nuclear beta decays and $\pi_{\ell 2}$ decays serves to reduce theoretical uncertainties coming from the Kaon decay constant that enters the prediction for the $K_{\ell 2}$ decay. The quantity $R_{\ell 23}$ is then indeed sensitive to the charged Higgs exchange in the $K_{\ell 2}$ decays, i.e. in $K \to \mu\nu$.

Combining the experimental results on the CKM matrix elements with the corresponding theoretical uncertainties one finds the following constraint in the MSSM [174]

$$R_{\ell 32} = 0.999 \pm 0.007 \ , \tag{3.116}$$

and the corresponding bound on the MSSM Higgs sector will be also investigated in section 6.1.

3.3 $\Delta F = 0$ Processes

3.3.1 The Anomalous Magnetic Moment of the Muon

The anomalous magnetic moment of the muon, $a_\mu = \frac{1}{2}(g-2)_\mu$, is known to be a sensitive indirect probe of new short distance physics [175]. Both the experimental determination of this observable and its theory prediction in the SM have reached a truly remarkable level of accuracy [176, 177, 178, 179].

The current SM prediction for the anomalous magnetic moment of the muon reads [180]

$$a_\mu^{\rm SM} = (11\,659\,183.4 \pm 4.9) \times 10^{-10} \ . \tag{3.117}$$

Combined with the final experimental result from the Muon (g-2) Collaboration [181, 182]

$$a_\mu^{\rm exp} = (11\,659\,208.9 \pm 6.3) \times 10^{-10} \ , \tag{3.118}$$

one finds presently a discrepancy at the level of 3.2σ [180]

$$\Delta a_\mu = a_\mu^{\rm exp} - a_\mu^{\rm SM} = (25.5 \pm 8.0) \times 10^{-10} \ . \tag{3.119}$$

While this discrepancy cannot be interpreted as a clear signal of NP yet, the $g-2$ of the muon is nonetheless an important observable to be considered when one analyses the impact of NP models on low energy phenomenology.

In an effective theory formulation, the $g-2$ of the muon is generated by the following term in an effective Lagrangian

$$\mathcal{L}_{\rm eff} = \frac{e}{4m_\mu} \ a_\mu \ \bar{\mu} F_{\mu\nu} \sigma^{\mu\nu} \mu \ . \tag{3.120}$$

Analogous to the $b \to s\gamma$ operators in (3.45), the dimension 5 operator in the above expression is helicity flipping and consequently NP effects in a_μ generally decouple as $m_\mu^2/M_{\rm NP}^2$. The contributions to a_μ in the MSSM and the implications of the discrepancy (3.119) on the MSSM parameter space will be discussed in section 6.6.

3.3.2 Electric Dipole Moments

The SM predictions for electric dipole moments are very far from the present experimental resolutions. Any experimental observation of EDMs would therefore represent a very clean signal of the presence of NP effects [183]. The current experimental bounds on the most important experimentally accessible EDMs like the Thallium, Mercury and neutron EDM read [184, 185, 186, 187, 188]

$$d_{\rm Tl} \ \leq \ 9.4 \times 10^{-25} \ e\,{\rm cm} \quad @\ 90\%\ {\rm C.L.} \ , \tag{3.121}$$

$$d_{\rm Hg} \ \leq \ 3.1 \times 10^{-29} \ e\,{\rm cm} \quad @\ 95\%\ {\rm C.L.} \ , \tag{3.122}$$

$$d_n \ \leq \ 2.9 \times 10^{-26} \ e\,{\rm cm} \quad @\ 90\%\ {\rm C.L.} \ . \tag{3.123}$$

As the EDMs are CP violating observables, in the SM they can be generated only by the two sources of CP violation present in the SM: the QCD theta term $\bar{\theta}$ and the single physical

phase contained in the CKM matrix. Natural (order one) values for $\bar{\theta}$ are phenomenologically excluded since they would lead to unacceptably large contributions to the neutron EDM. Therefore, a Peccei-Quinn symmetry [189, 190] is commonly assumed to dynamically suppress the QCD theta term $\bar{\theta}$. In this way, EDMs can be generated only by the CP violating phase of the CKM matrix and they turn out to be highly suppressed. Quark EDMs for example are generated in the SM only at the three loop level and one finds a SM prediction for the neutron EDM at the level of $d_n \sim 10^{-32}\, e\,\mathrm{cm}$ [183] that is well below the current and expected future experimental sensitivities.

The main difficulty to fully exploit the NP sensitivity of the EDMs is, that experimentally one measures the EDMs of composite systems, as heavy atoms, molecules or the neutron, while on the theoretical side the EDMs of constituent particles, i.e. quarks and leptons are predicted.

The electric and chromoelectric dipole moments of quarks and leptons are described by the following effective CP-odd Lagrangian [183]

$$\mathcal{L}_{\text{eff}} = -i\frac{d_\ell}{2}\ \bar{\ell} F_{\mu\nu}\sigma^{\mu\nu}\gamma_5 \ell \tag{3.124}$$

$$-i\frac{d_q}{2}\ \bar{q} F_{\mu\nu}\sigma^{\mu\nu}\gamma_5 q - i\frac{d_q^c}{2} g_s\ \bar{q} G_{\mu\nu}\sigma^{\mu\nu}\gamma_5 q\ , \tag{3.125}$$

where the first line contains the EDMs of the leptons and the second line the EDMs and CEDMs of the quarks. In general also additional operators enter the prediction of the EDMs of composite systems such as the Weinberg three gluon operator [191] or scalar four fermion operators [192, 193]

$$\mathcal{L}_{\text{eff}} = \frac{1}{3} w\ f^{abc} G^a_{\mu\nu} \tilde{G}^{\nu\sigma,b} G_\sigma{}^{\mu,c} + \sum_{i,j} C_{ij}\ (\bar{\psi}_i \psi_i)(\bar{\psi}_j i\gamma_5 \psi_j) + \dots\ . \tag{3.126}$$

These operators however play only a subdominant role in our discussion of the EDMs in chapter 8 and therefore we restrict ourselves here to the quark and lepton (C)EDMs defined in (3.124) and (3.125).

Expressing the physical EDMs through the quark and lepton (C)EDMs induces sizable uncertainties related to QCD, nuclear and atomic interactions. Approximately one finds the following relations [183, 194]

$$d_{\text{Tl}} \simeq -585 d_e\ , \tag{3.127}$$

$$d_{\text{Hg}} \simeq 7\times 10^{-3} e(d_u^c - d_d^c) + 10^{-2} d_e\ , \tag{3.128}$$

$$d_n \simeq 1.4(d_d - 0.25 d_u) + 1.1 e(d_d^c + 0.5 d_u^c)\ . \tag{3.129}$$

The quark (C)EDMs in these expressions are understood to be evaluated at the hadronic scale 1 GeV. The running from the weak scale down to the hadronic scale is very good approximated by [195]

$$d_q(1\ \text{GeV}) \simeq 1.2 d_q(M_Z)\ , \quad d_q^c(1\ \text{GeV}) \simeq 0.91 d_q^c(M_Z)\ . \tag{3.130}$$

As Thallium is a paramagnetic atom, its EDM is primarily sensitive to the electron EDM, while the EDM of the diamagnetic atom Mercury mostly feels the CP-odd pion nucleon interaction induced by the chromoelectric dipole moments of the up and down quarks. Finally,

as a bound state of up and down quarks, the neutron EDM is obviously mostly sensitive to the up and down quark (C)EDMs. At a subleading level also the strange quark (C)EDM enters in principle the prediction for d_n. While the generic predictions for the strange quark (C)EDM $d_s^{(c)}$ is enhanced by $m_s/m_{u,d}$ it is presently not clear how important the effect from $d_s^{(c)}$ is, given the lack of reliable theoretical estimates of its contribution to the hadronic EDMs. Future lattice simulations might help in resolving this issue.

In NP models often additional sources of CP violation are present that generically induce EDMs that are in conflict with the experimental bounds in (3.127) - (3.129). Consequently, these bounds lead to strong constraints on the NP parameter spaces.

Models of New Physics can contain new sources of CP violation in form of flavor diagonal and flavor off-diagonal phases. Given that the EDMs are CP violating but flavor conserving observables, they do not require any source of flavor violation. Still they can also be generated by two complex $\Delta F = 1$ transitions, in which case one refers to *flavored* EDMs. In section 6.7 we discuss the most relevant contributions to the quark and lepton (C)EDMs in the MSSM, including both the case of flavor diagonal and flavor off-diagonal phases.

To summarize this chapter we show in table 3.2 a long (but of course incomplete) list of intersting low energy observables mostly in the quark flavor sector. We collect the SM predictions for these observables together with the present experimental results and the expected future experimental sensitivities. The well measured observables in the $\Delta F = 2$ sector, as well as for example the $B \to X_s\gamma$ branching ratio play an important role in constraining the parameter space of NP models, in particular the MSSM. Observables with tiny SM predictions, like the EDMs, the $B_s \to \mu^+\mu^-$ branching ratio, the $S_{\psi\phi}$ asymmetry or CP violation in $D^0 - \bar{D}^0$ mixing on the other hand can be considered as "discovery channels", where future measurements of large non-standard values would consist of unambiguous evidence of NP effects.

observable	SM prediction	present experiment	future sensitivity
x_D	$\lesssim$ few 10^{-2} [53]	$(0.98^{+0.24}_{-0.26})10^{-2}$ [36]	$\sim 0.09 \times 10^{-2}$ [37, 39]
y_D	$\lesssim$ few 10^{-2} [52]	$(0.83 \pm 0.16)10^{-2}$ [36]	$\sim 0.06 \times 10^{-2}$ [37, 39]
$1 - \lvert q/p \rvert$	$\lesssim 10^{-3}$ [59]	$0.13^{+0.15}_{-0.17}$ [36]	~ 0.03 [37, 39]
ϕ_D	$\lesssim 10^{-3}$ [59]	$(-8.5^{+7.4}_{-7.0})^\circ$ [36]	$1^\circ - 2^\circ$ [37, 39]
ΔM_K (ps^{-1})		$(5.292 \pm 0.009)10^{-3}$ [73]	
ΔM_d (ps^{-1})	0.53 ± 0.13	0.507 ± 0.005 [36]	
ΔM_s (ps^{-1})	18.3 ± 5.1	17.77 ± 0.12 [76]	
$\Delta M_d/\Delta M_s$	$(2.85 \pm 0.38)10^{-2}$	$(2.85 \pm 0.03)10^{-2}$	
$\lvert\epsilon_K\rvert$	$(1.94 \pm 0.30)10^{-3}$	$(2.229 \pm 0.010)10^{-3}$ [73]	
$S_{\psi\phi}$	0.038 ± 0.003	$0.81^{+0.12}_{-0.32}$ [36]	~ 0.01 [83]
$S_{\psi K_S}$	0.734 ± 0.038	0.672 ± 0.023 [36]	0.005-0.012 [37, 39]
$S_{\phi K_S}$	0.75 ± 0.04 [120]	0.44 ± 0.17 [36]	$0.02 - 0.03$ [37, 39]
$S_{\eta' K_S}$	0.74 ± 0.04 [120]	0.59 ± 0.07 [36]	$0.01 - 0.02$ [37, 39]
$S_{K^*\gamma}$	$-0.022 \pm 0.015^{+0}_{-0.01}$ [98]	-0.15 ± 0.22 [73]	$0.02 - 0.03$ [37, 39]
$A_{\mathrm{CP}}(b \to s\gamma)$	$\left(-0.44^{+0.14}_{-0.24}\right) 10^{-2}$ [93]	$(1.2 \pm 2.8)10^{-2}$ [36]	$(0.4 - 0.5)10^{-2}$ [37, 39]
$q_0^2(S_4)$ $(B \to K^*\ell^+\ell^-)$	$1.94^{+0.12}_{-0.10}$ GeV^2 [19]		
$q_0^2(S_5)$ $(B \to K^*\ell^+\ell^-)$	$2.24^{+0.06}_{-0.08}$ GeV^2 [19]		
$q_0^2(S_6^s)$ $(B \to K^*\ell^+\ell^-)$	$3.90^{+0.11}_{-0.12}$ GeV^2 [19]		
$\langle A_7 \rangle$ $(B \to K^*\ell^+\ell^-)$	$(3.4^{+0.4}_{-0.5})10^{-3}$ [19]		
$\langle A_8 \rangle$ $(B \to K^*\ell^+\ell^-)$	$(-2.6^{+0.4}_{-0.3})10^{-3}$ [19]		
$\langle A_9 \rangle$ $(B \to K^*\ell^+\ell^-)$	$(0.1^{+0.1}_{-0.1})10^{-3}$ [19]		
$\mathrm{BR}(B \to X_s\gamma)$	$(3.15 \pm 0.23)10^{-4}$ [84]	$(3.52 \pm 0.25)10^{-4}$ [36]	5% [37, 39]
$\mathrm{BR}(B \to X_s\ell^+\ell^-)$	$(1.59 \pm 0.11)10^{-6}$ [196]	$(1.59 \pm 0.49)10^{-6}$ [197, 198]	$4 - 6\%$ [37, 39]
$\mathrm{BR}(B_s \to \mu^+\mu^-)$	$(3.47 \pm 0.37)10^{-9}$	$\lesssim 5.8 \times 10^{-8}$ [127]	$\sim 10^{-9}$ [130]
$\mathrm{BR}(B_d \to \mu^+\mu^-)$	$(1.06 \pm 0.11)10^{-10}$	$\lesssim 1.8 \times 10^{-8}$ [127]	
$\mathrm{BR}(B \to \tau\nu)$	$(1.10 \pm 0.29)10^{-4}$	$(1.73 \pm 0.35)10^{-4}$ [80]	$3 - 4\%$ [37, 39]
$\mathrm{BR}(K_L \to \pi^0\nu\bar{\nu})$	$(2.49 \pm 0.39)10^{-11}$ [148]	$\lesssim 2.6 \times 10^{-8}$ [149]	$\sim 2 \times 10^{-11}$ [152]
$\mathrm{BR}(K^+ \to \pi^+\nu\bar{\nu})$	$(8.5 \pm 0.7)10^{-11}$ [147]	$(1.73^{+1.15}_{-1.05})10^{-10}$ [150]	$\sim 10^{-11}$ [151]
$\mathrm{BR}(B^+ \to K^+\nu\bar{\nu})_{\mathrm{SD}}$	$(3.64 \pm 0.47)10^{-6}$ [140]	$\lesssim 14 \times 10^{-6}$ [142]	$16 - 20\%$ [37, 39]
$\mathrm{BR}(B \to K^*\nu\bar{\nu})$	$(6.8^{+1.0}_{-1.1})10^{-6}$ [20]	$\lesssim 80 \times 10^{-6}$ [143]	$\sim 2 \times 10^{-6}$ [144]
$\langle F_L \rangle(B \to K^*\nu\bar{\nu})$	0.54 ± 0.01 [20]		~ 0.3 [144]
$\lvert d_{\mathrm{Tl}}\rvert$ $(e\,\mathrm{cm})$	$\sim 10^{-35}$ [183]	$< 9.4 \times 10^{-25}$ [184]	
$\lvert d_n\rvert$ $(e\,\mathrm{cm})$	$\sim 10^{-32}$ [183]	$< 2.9 \times 10^{-26}$ [188]	$\simeq 5 \times 10^{-27}$ [194]
$\lvert d_{\mathrm{Hg}}\rvert$ $(e\,\mathrm{cm})$		$< 3.1 \times 10^{-29}$ [186]	
$(g-2)_\mu \times 10^{10}$	$11\,659\,183.4 \pm 4.9$ [180]	$11\,659\,208.9 \pm 6.3$ [181, 182]	0.14 ppm [182]

Table 3.2: List of selected flavor observables.

4 Supersymmetry, the MSSM and its Flavor Structure

Supersymmetry (SUSY) [199, 200, 2, 201] is an extremely fascinating concept in particle physics. Supersymmetry relates bosonic and fermionic degrees of freedom and is know to be the only possible extension of Poincaré symmetry leading to a "meaningfull" quantum field theory [202, 203]. If Supersymmetry is promoted to a local symmetry one obtains so-called Supergravity theories [204] that contain General Relativity. In fact Supergravity theories arise in string theory that currently seems to be one of most promising approaches towards a consistent theory of quantum gravity. But also theories with global Supersymmetry show remarkable features. So-called non-renormalization theorems [205, 206] for example ensure that supersymmetric theories are free of any quadratic divergences.

In supersymmetric theories that are phenomenologically viable, Supersymmetry has necessarily to be broken. In fact, Supersymmetry predicts that for every fermionic degree of freedom there exists a bosonic partner with exactly the same mass and vice versa. As this situation is obviously not realized in nature, possible mechanisms of SUSY breaking have been investigated ever since (see e.g. [207, 208, 209, 210, 211, 212, 213, 214]). In most models, spontaneous SUSY breaking takes place in a *hidden sector* of particels that have no or only very small couplings to the *visible sector* of the model. However, if the two sectors share common interactions, SUSY breaking can be mediated from the hidden sector to the visible sector. The most popular mediation schemes are *Gravity mediation* [215, 216, 217, 218, 219], where SUSY breaking is communicated by Planck mass suppressed higher dimensional operators, and *Gauge mediation* [220, 221, 222, 223, 224, 225, 226], where messenger fields mediate the SUSY breaking through gauge interactions. Also extra dimensional setups have been considered leading to mediation schemes called *Gaugino mediation* [227, 228, 229] and *anomaly mediation* [230, 231].

It is important to note that quadratic divergences still remain absent also in theories with broken Supersymmetry, as long as the introduced breaking terms are *soft* [232], as it happens in theories with spontaneously broken SUSY. Adding all possible soft SUSY breaking terms to the "supersymmetrized" version of the Standard Model [233], one obtains the Minimal Supersymmetric Standard Model (MSSM). Without doubts, the MSSM is one of the best studied models beyond the Standard Model as it is naturally able to address several of the open issues in particle physics.

i) The gauge hierarchy problem is formally solved in the MSSM. While there is no explanation of the large hierarchy between the electroweak and the Planck scale, the absence of quadratic divergences ensures that the electroweak scale is stable against quantum corrections as long as the SUSY breaking terms (i.e. the masses of the SUSY partners of the SM particles) do not exceed the TeV scale.

ii) In the MSSM with TeV scale SUSY particles, gauge coupling unification works re-

markably well [234, 235, 236]. Running up the three SM gauge couplings, they unify with a high precision around a GUT scale of 3×10^{16} GeV. In fact, supersymmetric Grand Unified Theories (GUTs) [237, 238, 239] are very successfull and well investigated extensions of the SM.

iii) If so-called R-parity [240] is imposed, the lightest supersymmetric particle (LSP) is stable and thus the MSSM also provides a dark matter candidate [241, 242].

All these reasons make models with TeV scale SUSY very appealing extensions of the Standard Model. If TeV scale SUSY is indeed realized in nature then it should lead to many characteristic signals in high and low energy experiments [243]. In particular, the SUSY partners of the SM particles should be within the reach of LHC where they can be directly produced. Moreover, SUSY particles at the TeV scale are also expected to lead to visible effects in low energy observables as the ones discussed in chapter 3. In fact, the absence of any unambiguous hint of NP effects in these observables up to now has to be considered problematic for SUSY models[1] as the effects from TeV scale SUSY particles are naturally expected to be large. A thorough understanding of the SUSY contributions to low energy flavor and CP violating observables – their origin, their structure and their implied phenomenology – is therefore crucial to test the viability of SUSY models. Exactly this is the main subject of this work.

Instead of giving now a detailed presentation of the foundations of Supersymmetry, supersymmetric field theory and Supersymmetry breaking that can be found in numerous reviews [244, 3, 245, 246, 226, 247, 248] and text books [249, 250, 251, 252], we concentrate directly on the MSSM in the remainder of this chapter. In section 4.1 we briefly review its field content and give explicit expressions for the superpotential and the soft SUSY breaking terms, to fix our notation and conventions for the SUSY parameters. In the following sections we consider in detail the flavor structure of the MSSM in the quark sector (see also [253] for a review). We discuss the new sources of flavor violation present in the MSSM and briefly sketch their impact on flavor changing processes. Chapter 5 is devoted to the MSSM in the large $\tan\beta$ regime. A detailed analysis of supersymmetric contributions to flavor observables then follows in chapter 6.

4.1 The Minimal Supersymmetric Standard Model

Before presenting the particle content of the MSSM, its superpotential and the soft SUSY breaking terms, we mention that apart from few exceptions, we will mostly adopt the conventions of [254, 255] where the full MSSM Lagrangian and all MSSM Feynman rules have been worked out explicitly. A translation table between the notation and conventions used in the present work, the work of [254, 255] and the so-called SUSY Les Houches Accord [256, 257], a broadly accepted convention for MSSM parameter, can be found in appendix A.2.

The MSSM Particle Content

The Standard Model is based on the gauge group $\mathrm{SU}(3) \times \mathrm{SU}(2) \times \mathrm{U}(1)$. Correspondingly, the MSSM contains three vector superfields V_3, V_2 and V_1, which consist of the SM gauge

[1] As discussed in chapter 2, this is of course a problem for basically any NP model predicting new degrees of freedom at the TeV scale.

		superfields	fermions	vector bosons
gluons and gluinos	SU(3)	V_3	$\tilde{g}^a$	g^a_μ
W bosons and Winos	SU(2)	V_2	$\tilde{W}^\pm, \tilde{W}^3$	$W^\pm_\mu, W^3_\mu$
B boson and Bino	U(1)	V_1	$\tilde{B}$	B_μ

Table 4.1: The vector superfields of the MSSM. The SU(3) field contains the gluons and gluinos, the SU(2) field the W bosons and the Winos and the U(1) field the B and the Bino.

bosons (the gluons, the W bosons and the B) and their superpartners the so-called *gauginos* (the gluinos, the Winos and the Bino). The gauginos are Majorana fermions and as the gauge bosons they transform as adjoints under their respective gauge group. These fields are summarized in table 4.1.

The matter fermions of the SM are introduced through the chiral superfields listed in table 4.2. In addition to the quarks and leptons, they contain their spin 0 superpartners, the *squarks* and *sleptons*.

Finally, the Higgs sector of the MSSM consists of two Higgs doublets that are contained in the chiral superfields also shown in table 4.2. Apart from the spin 0 Higgs bosons, they also contain their spin 1/2 superpartners, the *Higgsinos*. In fact, in the MSSM two Higgs doublets with opposite hypercharge are required in order to have anomaly cancellation between the two Higgsinos.

The Superpotential

As usual, gauge interactions between the MSSM degrees of freedom directly arise from the kinetic terms of the chiral and vector superfields. Additional interactions are introduced through the *superpotential* which is a gauge invariant polynomial of the chiral superfields of mass dimension three. Supersymmetry requires the superpotential to be analytical in the fields and it leads to renormalizable interactions as long as it does not contain operators of dimension larger than three. The MSSM superpotential reads

$$\mathcal{W} = \mu \hat{H}_u \hat{H}_d - Y_\ell \hat{\ell}_L \hat{H}_d \hat{e}_R - Y_d \hat{q}_L \hat{H}_d \hat{d}_R + Y_u \hat{q}_L \hat{H}_u \hat{u}_R \ . \tag{4.1}$$

It contains the μ term, a supersymmetric mass parameter for the Higgs fields, and the usual Yukawa couplings between the matter fields and the Higgs fields that are responsible for giving masses to the matter fermions after electroweak symmetry breaking. We remark that analyticity of the superpotential ensures that at tree level the down Higgs couples only to down quarks and charged leptons, while the up Higgs couples only to up quarks. At tree level, the MSSM is therefore a so-called two Higgs doublet model of type II.

In fact one can construct additional gauge invariant and analytical terms for the superpotential. Such terms however violate baryon or lepton number and lead to fast proton decay. They can be forbidden by introducing an additional symmetry, R-parity, that distinguishes between the SM particles that have R-parity +1 and their supersymmetric partners

	superfields	scalars	fermions	$SU(3) \times SU(2) \times U(1)$
LH leptons and sleptons	$\hat{\ell}_L^I$	$\tilde{\ell}_L^I = \begin{pmatrix} \tilde{\nu}_L^I \\ \tilde{e}_L^I \end{pmatrix}$	$\ell_L^I = \begin{pmatrix} \nu_L^I \\ e_L^I \end{pmatrix}$	$(1,2)_{-1/2}$
RH electrons and selectrons	$\hat{e}_R^I$	$(\tilde{e}_R^I)^*$	$(e_R^I)^c$	$(1,1)_1$
LH quarks and squarks	$\hat{q}_L^I$	$\tilde{q}_L^I = \begin{pmatrix} \tilde{u}_L^I \\ \tilde{d}_L^I \end{pmatrix}$	$q_L^I = \begin{pmatrix} u_L^I \\ d_L^I \end{pmatrix}$	$(3,2)_{1/6}$
RH up quarks and squarks	$\hat{u}_R^I$	$(\tilde{u}_R^I)^*$	$(u_R^I)^c$	$(\bar{3},1)_{-2/3}$
RH down quarks and squarks	$\hat{d}_R^I$	$(\tilde{d}_R^I)^*$	$(d_R^I)^c$	$(\bar{3},1)_{1/3}$
up Higgs and higgsinos	$\hat{H}_u$	H_u	$\tilde{H}_u$	$(1,2)_{1/2}$
down Higgs and higgsinos	$\hat{H}_d$	H_d	$\tilde{H}_d$	$(1,2)_{-1/2}$

Table 4.2: The chiral multiplets of the MSSM. The matter fields contain the SM leptons and quarks. In addition there are the two Higgs doublets. The generation index on the matter fields runs from $I = 1, 2, 3$.

that have R-parity -1. As a consequence, the baryon and lepton number violating interactions are forbidden, supersymmetric particles can only be pair produced and the lightest supersymmetric particle is stable.

The Soft SUSY Breaking Lagrangian

To make the MSSM phenomenologically viable, one also has to introduce soft SUSY breaking terms. The most general soft SUSY breaking Lagrangian that is gauge invariant and respects R-parity reads

$$\begin{aligned} \mathcal{L}_{\text{soft}} &= \frac{1}{2} M_1 \lambda_B \lambda_B + \frac{1}{2} M_2 \lambda_W \lambda_W + \frac{1}{2} M_3 \lambda_g \lambda_g \\ &- m_{H_d}^2 H_d^* H_d - m_{H_u}^2 H_u^* H_u \\ &- m_Q^2 \tilde{q}_L^* \tilde{q}_L - m_D^2 \tilde{d}_R \tilde{d}_R^* - m_U^2 \tilde{u}_R \tilde{u}_R^* - m_L^2 \tilde{\ell}_L^* \tilde{\ell}_L - m_E^2 \tilde{e}_R \tilde{e}_R^* \\ &+ B\mu H_u H_d + \hat{A}_\ell \tilde{\ell} H_d \tilde{e}_R^* + \hat{A}_d \tilde{q} H_d \tilde{d}_R^* - \hat{A}_u \tilde{q} H_u \tilde{u}_R^* \,. \end{aligned} \tag{4.2}$$

The first line of (4.2) contains Majorana masses for the gauginos, the second and third line soft masses for the two Higgs boson doublets as well as the squarks and sleptons. The terms in last line finally exactly correspond to the terms in the superpotential and consist of the

$B\mu$ term that mixes the two Higgs bosons and the trilinear couplings between the Higgs bosons the squarks and sleptons. Even so we suppressed flavor indices on the sfermion fields in (4.2), the squark and slepton soft masses as well as the trilinear couplings are in general 3×3 matrices in flavor space.

In contrast to the superpotential (4.1), the soft SUSY breaking Lagrangian introduces a vast number of free parameters [258]. Many of them are sources of flavor and CP violation and lead to large SUSY contributions to the low energy observables discussed in chapter 3. Before discussing in detail these additional sources of flavor and CP violation in the next section, we first present briefly the physical MSSM particle spectrum. We will restrict ourselves here to the tree level. Comprehensive presentations of 1 loop corrections to the MSSM spectrum that are particularly important in the Higgs sector and sometimes also for gluinos and the light stop can be found for example in [259, 260].

The Higgs Spectrum

At tree level the Higgs sector of the MSSM is entirely determined by four parameters. The complex μ term, the $B\mu$ term (that can be always made real by an appropriate redefinition of the Higgs fields) and the two real soft masses $m^2_{H_u}$ and $m^2_{H_d}$. Of course these parameters have to be such that electroweak symmetry is broken by vacuum expectation values of the neutral components of the two Higgs doublets $v_{u,d} = \langle H^0_{u,d} \rangle$ and the Z boson mass is correctly reproduced. At tree level one finds

$$\sin 2\beta = \frac{B\mu}{m^2_{H_u} + m^2_{H_d} + 2|\mu|^2} \ , \quad \frac{M_Z^2}{2} = \frac{m^2_{H_u} \tan^2\beta - m^2_{H_d}}{1 - \tan^2\beta} - |\mu|^2 \ , \tag{4.3}$$

where $\tan\beta = v_u/v_d$ is the ratio between the two vacuum expectation values. The second relation in (4.3) visualizes the so-called μ *problem* of the MSSM. Even so μ is a superpotential parameter, it has to be of the order of the electroweak scale and the soft Higgs masses to reproduce M_Z without tremendous fine tuning. In singlet extensions of the MSSM like the so-called next-to Minimal Supersymmetric Standard Model (NMSSM) (see [261] for a recent review) this problem can be addressed by replacing μ with the vev of the singlet field. Here we do not follow this approach but simply assume that μ is around the TeV scale.

Out of the eight degrees of freedom that are contained in the two Higgs doublets of the MSSM, three take the role of the longitudinal components of the W and Z bosons after electroweak symmetry breaking. The remaining five consist of one light SM-like Higgs h, one additional neutral scalar Higgs H^0, a neutral pseudoscalar Higgs A^0 and two charged Higgs bosons $H^\pm$. Their tree level masses are approximately given by

$$M_A^2 = m^2_{H_u} + m^2_{H_d} + 2|\mu|^2 \ , \quad M_H^2 \simeq M_A^2 \ , \quad M_{H^\pm} = M_A^2 + M_W^2 \ . \tag{4.4}$$

Here we did not give an expression for the light higgs mass M_h. In fact, at tree level $M_h < M_Z$ which is phenomenologically excluded. Quantum corrections to the light Higgs boson mass are however large [262, 263, 264, 265] and can lift it above the LEP limit. As also the above relations 4.3 and in particular the first relation in (4.4) are subject to large loop corrections, in phenomenological applications it is then usually convenient to trade the original Lagrangian parameters $B\mu$ and $m^2_{H_u,d}$ for $\tan\beta$ and M_A. The full tree level Higgs spectrum is then expressed in terms of $v = \sqrt{v_u^2 + v_d^2}$, $\tan\beta$, M_A and μ. Loop corrections enter mainly in M_h and can be conveniently be taken into account using public available codes like `FeynHiggs` [266, 267, 268, 269].

Charginos, Neutralinos and Gluinos

After electroweak symmetry breaking, the Higgsinos, the Winos and the Bino mix to give so-called charginos and neutralinos as mass eigenstates. Charginos are Dirac fermions and are mixtures of the charged Higgsinos with the charged Winos. Their mass matrix reads

$$Z_-^{\mathrm{T}} \begin{pmatrix} M_2 & \frac{g_2}{\sqrt{2}} v_u \\ \frac{g_2}{\sqrt{2}} v_d & \mu \end{pmatrix} Z_+ = \mathrm{diag}(M_{\tilde{\chi}_1^\pm}, M_{\tilde{\chi}_2^\pm}) \ . \tag{4.5}$$

Neutralinos on the other hand are Majorana fermions and are composed out of neutral Higgsinos, Winos and the Bino. Their mass matrix reads

$$Z_N^{\mathrm{T}} \begin{pmatrix} M_1 & 0 & -\frac{g_1}{2} v_d & \frac{g_1}{2} v_u \\ 0 & M_2 & \frac{g_2}{2} v_d & -\frac{g_2}{2} v_u \\ -\frac{g_2}{2} v_d & \frac{g_2}{2} v_d & 0 & -\mu \\ \frac{g_2}{2} v_u & -\frac{g_2}{2} v_u & -\mu & 0 \end{pmatrix} Z_N = \mathrm{diag}(M_{\tilde{\chi}_1^0}, M_{\tilde{\chi}_2^0}, M_{\tilde{\chi}_3^0}, M_{\tilde{\chi}_4^0}) \ . \tag{4.6}$$

Gluinos finally do not mix with any other particles and their mass is directly given by the Lagrangian parameter $M_3 = M_{\tilde{g}}$. We chose conventions such that M_3 is real and positive.

Squarks and Sleptons

Turning to the squarks, we remark that after electroweak symmetry breaking the left and right handed up and down squarks mix, such that their masses are in general 6×6 matrices. In the super-CKM basis (see section 4.2 below) they read

$$Z_U^{\mathrm{T}} \begin{pmatrix} V^* (m_Q^2)^{\mathrm{T}} V^{\mathrm{T}} + \hat{m}_u^2 + D_{UL} & -(v_d \mu^* \hat{y}_u + v_u \hat{A}_u)/\sqrt{2} \\ -(v_d \mu \hat{y}_u + v_u \hat{A}_u^*)/\sqrt{2} & m_U^2 + \hat{m}_u^2 + D_{UR} \end{pmatrix} Z_U^* = \mathrm{diag}(m^2_{\tilde{U}_1}, \ldots, m^2_{\tilde{U}_6}) \ , \tag{4.7}$$

$$Z_D^\dagger \begin{pmatrix} (m_Q^2)^{\mathrm{T}} + \hat{m}_d^2 + D_{DL} & -(v_u \mu^* \hat{y}_d + v_d \hat{A}_d)/\sqrt{2} \\ -(v_u \mu \hat{y}_d + v_d \hat{A}_d^*)/\sqrt{2} & m_D^2 + \hat{m}_d^2 + D_{DR} \end{pmatrix} Z_D = \mathrm{diag}(m^2_{\tilde{D}_1}, \ldots, m^2_{\tilde{D}_6}) \ , \tag{4.8}$$

where $\hat{m}_{u,d}$ are diagonal matrices containing the quark masses and $\hat{y}_{u,d}$ are diagonal matrices with the corresponding Yukawa couplings. The D-term contributions to the masses D_{UL}, D_{UR}, D_{DL} and D_{DR} are flavor blind (i.e. proportional to the unit matrix) and given by

$$D_{UL} = M_Z^2 \ \cos 2\beta \ \left(\frac{1}{2} - \frac{2}{3} \sin^2 \theta_W \right) \ , \qquad D_{UR} = M_Z^2 \ \cos 2\beta \ \left(\frac{2}{3} \sin^2 \theta_W \right) \ , \tag{4.9}$$

$$D_{DL} = M_Z^2 \ \cos 2\beta \ \left(-\frac{1}{2} + \frac{1}{3} \sin^2 \theta_W \right) \ , \qquad D_{DR} = M_Z^2 \ \cos 2\beta \ \left(-\frac{1}{3} \sin^2 \theta_W \right) \ . \tag{4.10}$$

The D-term contributions as well as the $\hat{m}^2_{u,d}$ terms are all of the order of $\mathrm{O}(v^2/M^2_{\mathrm{SUSY}})$ and they are usually negligible. Only in scenarios with very light squarks, the m_t^2 term might play some role. The structure of the up and down squark mass matrices (4.7) and (4.8) and its implications are the main subject of the following section 4.2.

Similarly to the squarks, one has for the charged sleptons and sneutrinos

$$Z_\nu^\dagger \Big(m_L^2 + D_{\nu L} \Big) Z_\nu = \mathrm{diag}(m^2_{\tilde{\nu}_1}, \ldots, m^2_{\tilde{\nu}_3}) \ , \tag{4.11}$$

$$Z_L^\dagger \begin{pmatrix} (m_L^2)^{\mathrm{T}} + \hat{m}_\ell^2 + D_{LL} & -(v_u \mu^* \hat{y}_\ell + v_d \hat{A}_\ell)/\sqrt{2} \\ -(v_u \mu \hat{y}_\ell + v_d \hat{A}_\ell^*)/\sqrt{2} & m_E^2 + \hat{m}_\ell^2 + D_{LR} \end{pmatrix} Z_L = \mathrm{diag}(m^2_{\tilde{L}_1}, \ldots, m^2_{\tilde{L}_6}) \ . \tag{4.12}$$

Here, $\hat{m}_\ell$ is a diagonal matrix containing the lepton masses and $\hat{y}_\ell$ is a diagonal matrix with the corresponding Yukawa couplings. The D-term contributions $D_{\nu L}$, D_{LL} and D_{LR} are flavor blind and are given by

$$D_{\nu L} = M_Z^2 \ \cos 2\beta \ \frac{1}{2} \ , \tag{4.13}$$

$$D_{LL} = M_Z^2 \ \cos 2\beta \ \left(-\frac{1}{2} + \sin^2 \theta_W \right) \ , \qquad D_{LR} = M_Z^2 \ \cos 2\beta \ \left(-\sin^2 \theta_W \right) \ . \tag{4.14}$$

Both the D-term contributions and the $\hat{m}_\ell^2$ terms are basically always negligible.

4.2 Sources of Flavor and CP Violation in the MSSM

As gauge interactions are flavor blind, both the SM and the MSSM gauge sector are invariant under a large group G_F of flavor transformations. Concentrating on the quark sector and leaving aside possible U(1) factors, one has [270, 271, 44]

$$G_F = SU(3)^3 = SU(3)_Q \times SU(3)_U \times SU(3)_D \ . \tag{4.15}$$

In the MSSM, this flavor symmetry is broken by two different sources: the Yukawa couplings Y_u and Y_d that appear in the superpotential as well as the soft masses m_Q^2, m_U^2 and m_D^2 and trilinear couplings $\hat{A}_u$ and $\hat{A}_d$ in the soft SUSY breaking Lagrangian. All these terms can in principle be generic 3×3 matrices in flavor space.

The Yukawa Couplings and the CKM Matrix

Redefining the quark fields by unitary transformations, the Yukawa couplings can be diagonalized

$$u_L \to V_{UL} u_L \ , \quad u_R \to V_{UR} u_R \quad ; \quad V_{UL}^{\mathrm{T}} Y_u V_{UR}^* = \hat{y}_u = \mathrm{diag}(y_u, y_c, y_t) \ , \tag{4.16}$$

$$d_L \to V_{DL} d_L \ , \quad d_R \to V_{DR} d_R \quad ; \quad V_{DL}^{\mathrm{T}} Y_d V_{DR}^* = \hat{y}_d = \mathrm{diag}(y_d, y_s, y_b) \ . \tag{4.17}$$

This leads to diagonal mass matrices for the up and down quarks after electroweak symmetry breaking

$$\hat{m}_u = \mathrm{diag}(m_u, m_c, m_t) = \hat{y}_u \frac{v_u}{\sqrt{2}} \ , \quad \hat{m}_d = \mathrm{diag}(m_d, m_s, m_b) = \hat{y}_d \frac{v_d}{\sqrt{2}} \ . \tag{4.18}$$

In this procedure, the CKM matrix $V = V_{UL}^\dagger V_{DL}$ appears that basically parameterizes the misalignment between the up and down quark mass eigenstates in flavor space. The CKM matrix contains three mixing angles and a single physical CP violating phase. The CKM matrix is unitray and it determines the strength of flavor changing charged current interactions as the W boson quark and charged Higgs quark vertices shown in the upper row of figure 4.1. Neutral currents as the gluon quark or the Z boson quark vertices however remain flavor diagonal at the tree level [13]. Flavor changing neutral currents of quarks can only be introduced at the loop level through *weak* interactions.

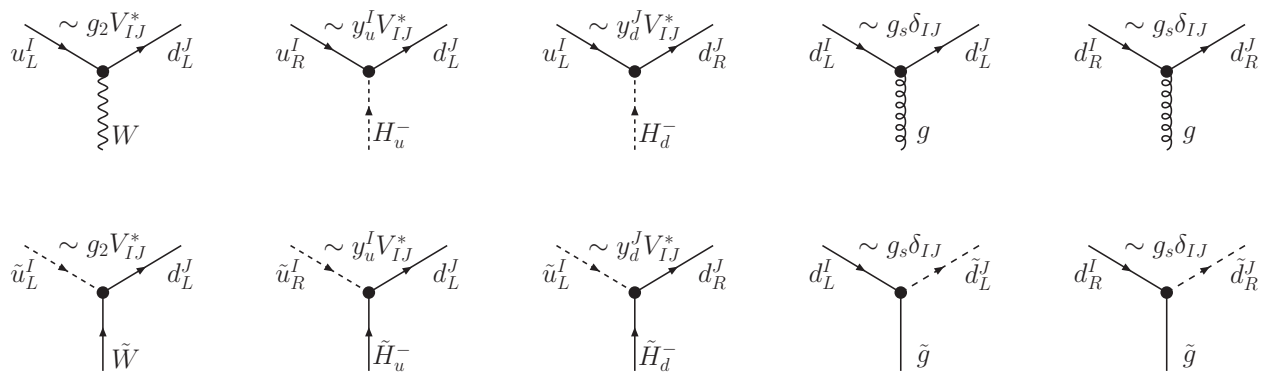

Figure 4.1: Example tree level vertices in the MSSM in the super-CKM basis. Charged current interactions are governed by the CKM matrix, while neutral currents are flavor diagonal. For simplicity only vertices with external down quarks are shown.

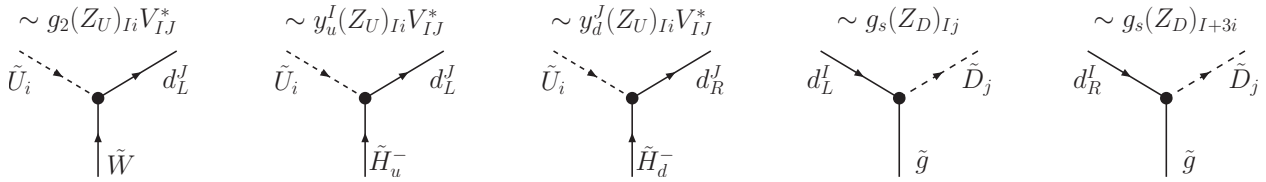

Figure 4.2: Example tree level vertices in the MSSM in the squark mass eigenstate basis. Vertices involving up and down squarks contain the Z_U and Z_D rotation matrices. In particular the gluino squark quark vertices are flavor violating. For simplicity only vertices with external downs quarks are shown.

Performing the same redefinitions of quark fields also for the *s*quarks, the resulting flavor basis is called *super-CKM basis*. In the super-CKM basis, the supersymmetrized versions of the above mentioned vertices share the same properties, i.e. the charged Wino quark squark as well as the charged Higgsino quark squark vertices are governed by the CKM matrix, while gluino quark squark vertices for example are flavor diagonal as shown in the diagrams in the lower row of figure 4.1.

The Mass Insertions and the Mass Insertion Approximation

However, the soft breaking terms and consequently the squark mass matrices are in general still flavor off-diagonal in the super-CKM basis. They can be diagonalized by a redefinition of the squark fields leading to each six up and down squark mass eigenstates $\tilde{U}_i$ and $\tilde{D}_i$. The unitary 6×6 rotation matrices Z_U and Z_D in (4.7) and (4.8) then appear in all vertices involving the up and down squarks respectively as shown in figure 4.2. In particular the gluino interactions are now flavor violating, leading to potentially large flavor changing neutral currents of quarks that are introduced at the loop level through *strong* interactions.

As the treatment of the squark flavor violation in terms of the 6×6 rotation matrices Z_U and Z_D often lacks transparency, it is usually much more convenient to work in the super-CKM basis and to treat the off-diagonal entries in the squark mass matrices as small perturbations. To do so, we first decompose the soft masses for up and down squarks m_Q^2, m_U^2 and m_D^2 in the super-CKM basis into universal diagonal parts and departures from

universality, the so-called mass insertions δ

$$\begin{aligned}(m_Q^2)^{\mathrm{T}} &= \mathrm{diag}(\tilde{m}_Q^2) + \tilde{m}_Q^2 \delta_d^{LL} \ , \\ m_U^2 &= \mathrm{diag}(\tilde{m}_U^2) + \tilde{m}_U^2 \delta_u^{RR} \ , \quad m_D^2 = \mathrm{diag}(\tilde{m}_D^2) + \tilde{m}_D^2 \delta_d^{RR} \ . \end{aligned} \tag{4.19}$$

We also define left-right mass insertions

$$\begin{aligned}\tilde{m}_Q \tilde{m}_U (\delta_u^{LR})_{IJ} &= -m_{u^I} \left(\hat{A}_u + \mu^* \cot\beta \right)_{IJ} \ , \\ \tilde{m}_Q \tilde{m}_D (\delta_d^{LR})_{IJ} &= -m_{d^I} \left(\hat{A}_d + \mu^* \tan\beta \right)_{IJ} \ . \end{aligned} \tag{4.20}$$

For the flavor diagonal parts of the trilinear couplings it is often convenient to factor out the Yukawa couplings explicitly $(\hat{A}_u)_{ii} = (y_u A_u, y_c A_c, y_t A_t)_i$ and $(\hat{A}_d)_{ii} = (y_d A_d, y_s A_s, y_b A_b)_i$ such that one can write

$$\begin{aligned}\tilde{m}_Q \tilde{m}_U (\delta_u^{LR})_{11} &= -m_u \left(A_u + \mu^* \cot\beta \right) \quad , \quad \tilde{m}_Q \tilde{m}_D (\delta_d^{LR})_{11} = -m_d \left(A_d + \mu^* \tan\beta \right) \ , \\ \tilde{m}_Q \tilde{m}_U (\delta_u^{LR})_{22} &= -m_c \left(A_c + \mu^* \cot\beta \right) \quad , \quad \tilde{m}_Q \tilde{m}_D (\delta_d^{LR})_{22} = -m_s \left(A_s + \mu^* \tan\beta \right) \ , \\ \tilde{m}_Q \tilde{m}_U (\delta_u^{LR})_{33} &= -m_t \left(A_t + \mu^* \cot\beta \right) \quad , \quad \tilde{m}_Q \tilde{m}_D (\delta_d^{LR})_{33} = -m_b \left(A_b + \mu^* \tan\beta \right) \ . \end{aligned} \tag{4.21}$$

At this point (4.19) and (4.20) are nothing but a convenient parameterization of the soft terms. For simplicity we will now and in the following assume $\tilde{m}_Q^2 = \tilde{m}_U^2 = \tilde{m}_D^2 = \tilde{m}^2$ [2], such that the 6×6 up and down squark masses can be written as

$$\mathcal{M}_d^2 = \mathrm{diag}(\tilde{m}^2) + \tilde{m}^2 \delta_d \ , \quad \mathcal{M}_u^2 = \mathrm{diag}(\tilde{m}^2) + \tilde{m}^2 \delta_u \tag{4.22}$$

where we neglected SU(2) breaking terms of the order $\mathrm{O}(v^2/M_{SUSY}^2)$ and decomposed the mass insertions according to the "chirality" of the squarks

$$\delta_q = \begin{pmatrix} \delta_q^{LL} & \delta_q^{LR} \\ \delta_q^{RL} & \delta_q^{RR} \end{pmatrix} \ , \quad q = u, d \ . \tag{4.23}$$

As the squark masses are hermitian one has the following relations among the mass insertions

$$(\delta_q^{LL}) = (\delta_q^{LL})^\dagger \ , \quad (\delta_q^{RR}) = (\delta_q^{RR})^\dagger \ , \quad (\delta_q^{RL}) = (\delta_q^{LR})^\dagger \ . \tag{4.24}$$

Due to SU(2) invariance also the left-left blocks of the up and down mass insertions are related (see (4.7) and (4.8)) such that

$$(\delta_u^{LL}) = V^* (\delta_d^{LL}) V^{\mathrm{T}} \ . \tag{4.25}$$

This relation will play a very important role in the discussion of the abelian flavor models in sections 7.2 and 8.6.

In the so-called Mass Insertion Approximation (MIA) [272] the δs in the squark mass matrices are then treated as perturbations and flavor changing amplitudes arise through mass

[2] While this might not necessarily lead to very accurate results for flavor changing amplitudes in case of large non-universalities between the overall scales of the soft masses, this approximation is absolutely sufficient for our purposes to show the main parametric dependencies of the flavor changing amplitudes in chapter 6. Whenever large non-universalities have important impact we will point this out explicitly.

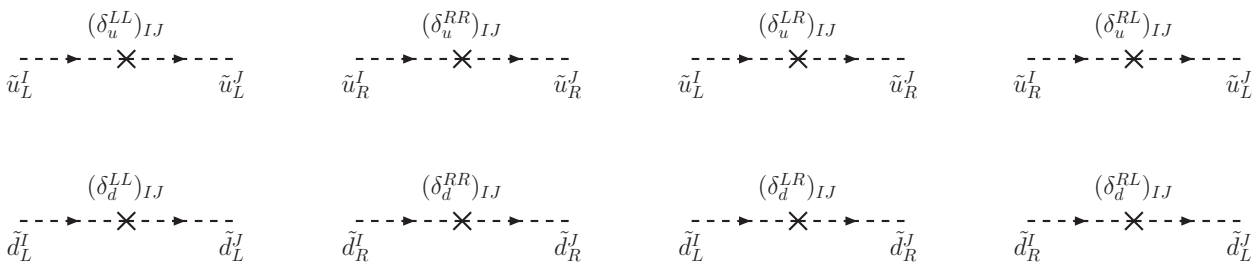

Figure 4.3: The Mass Insertion Approximation in the squark sector. Off-diagonal entries in the 6×6 squark mass matrices are treated as perturbations and flavor change occurs through mass insertions along squark propagators.

insertions along squark propagators as shown in figure 4.3. Similarly, also the off-diagonal elements in the chargino and neutralino mass matrices that are suppressed by $v/M_{\rm SUSY}$ can often be treated as perturbations [90], which corresponds to working directly with Winos, Binos and Higgsinos. Equivalently, one can also start with results that are obtained with squark, chargino and neutralino mass eigenstates and expand them in the mass insertions and $v/M_{\rm SUSY}$, respectively.

While the Mass Insertion Approximation is only an approximation and breaks down for mass insertions of O(1), it gives a very intuitive picture of the impact of the sources of flavor violation contained in the soft terms, and allows to transparently display the main dependencies of flavor changing amplitudes on the MSSM parameters. In the rest of this work we will indeed present the results for flavor changing amplitudes in the MIA. In our numerical analyses instead we always work with squark mass eigenstates.

New Sources of CP Violation

Before sketching the implications of the new sources of flavor violation in the MSSM for FCNC processes in the next section, we briefly also discuss the new sources of CP violation.

Out of the many free parameters of the MSSM a large part can in principle be complex. In particular, the supersymmetric μ term and the SUSY breaking $B\mu$ term, the gaugino masses M_1, M_2 and M_3, the full 3×3 trilinear coupling matrices $\hat{A}_u$, $\hat{A}_d$ and $\hat{A}_\ell$ as well as the off-diagonal entries of the soft sfermion masses m_Q^2, m_U^2, m_D^2, m_L^2 and m_E^2 are allowed to have arbitrary complex phases. However, not all of these phases are also physical. Redefining the involved fields appropriately, two of the above phases can be removed from the MSSM Lagrangian. In the commonly adopted conventions, $B\mu$ is chosen to be real (see also (4.3)). In addition we also chose a real and positive gluino mass $M_3 = M_{\tilde{g}} > 0$ in this work.

The remaining physical phases can be divided into two classes: i) *Flavor diagonal phases* of the μ parameter, the gaugino masses M_1 and M_2 and the diagonal parts of the trilinear couplings (A_u, A_c, A_t), (A_d, A_s, A_b) and (A_e, A_μ, A_τ) and ii) *flavored phases* of the flavor off-diagonal mass insertions.

The impact of these new sources of CP violation on electric dipole moments and the resulting *SUSY CP problem* is discussed in section 6.7.

4.3 Flavor Changing Neutral Currents in the MSSM

The several sources of flavor violation discussed in the previous section lead to potentially large flavor changing neutral currents for quarks at the loop level. While for definiteness we restrict the discussion here to a $\Delta F = 1$ transition from a left handed bottom to a left handed strange quark, the main conclusions remain true also in general.

Considering a generic $b_L \to s_L$ FCNC amplitude A_{bs} at the 1 loop level, it receives contributions from i) W boson up quark loops, ii) charged Higgs up quark loops, iii) chargino up squark loops, iv) neutralino down squark loops and v) gluino down squark loops. Both neutralino and gluino contribution obviously arise only if flavor off-diagonal entries are present in the down squark mass matrix. While gluinos are strongly interacting, neutralinos only interact weakly and therefore typically do not play a big role for FCNC processes in the quark sector. Concerning the chargino contributions we remind that charginos are linear combinations of Winos and Higgsinos and we consider Wino and Higgsino loops separately. We thus decompose the amplitude in the following way

$$A_{bs} = A_{bs}^{W^\pm} + A_{bs}^{H^\pm} + A_{bs}^{\tilde{W}^\pm} + A_{bs}^{\tilde{H}^\pm} + A_{bs}^{\tilde{g}} \ . \tag{4.26}$$

- The W boson contributions arise already in the SM and they can be written as[3]

$$A_{bs}^{W^\pm} \sim \frac{\alpha_2}{4\pi}\frac{1}{M_W^2}\Big(V^{\mathrm{T}} f(\hat{m}_u^2) V^*\Big)_{32} \simeq \frac{\alpha_2}{4\pi}\frac{1}{M_W^2}\ V_{tb}V_{ts}^*\ \big(f(m_t^2) - f(0)\big) \ . \tag{4.27}$$

  They arise at the 1 loop level through weak interactions and are induced by the CKM matrix. Their structure is governed by the breaking of the GIM mechanism [13] through the large top mass.

- Concerning the Higgs induced amplitude

$$A_{bs}^{H^\pm} \sim \frac{1}{16\pi^2}\frac{1}{M_{H^\pm}^2}\Big(V^{\mathrm{T}} \hat{y}_u f(\hat{m}_u^2) \hat{y}_u V^*\Big)_{32} \sim \frac{\alpha_2}{4\pi}\frac{1}{M_{H^\pm}^2}\frac{m_t^2}{M_W^2}\ V_{tb}V_{ts}^*\ f(m_t^2) \ , \tag{4.28}$$

  also here the source of flavor violation is the CKM matrix. In the considered case the involved Higgs couplings are proportional to the Yukawa couplings of the up quarks that run in the loop and as $m_u < m_c \ll m_t$, only the top contribution is relevant.

- The Higgsino amplitude is very similar in structure to the Higgs amplitude

$$A_{bs}^{\tilde{H}^\pm} \sim \frac{1}{16\pi^2}\frac{1}{\tilde{m}^2}\Big(V^{\mathrm{T}} \hat{y}_u f(M_u^2) \hat{y}_u V^*\Big)_{32} \sim \frac{\alpha_2}{4\pi}\frac{1}{\tilde{m}^2}\frac{m_t^2}{M_W^2}\ V_{tb}V_{ts}^*\ f(\tilde{m}^2) \ . \tag{4.29}$$

  It is only induced by the CKM matrix and insensitive to possible flavor off-diagonal terms in the soft sector. In contrast to the Higgs amplitude however, it does not decouple with the charged Higgs mass but of course with the SUSY scale.

[3] Here, f symbolizes a generic dimensionless loop function that should of course in general differ for the various contributions to the amplitudes considered below.

- As mentioned already at the beginning, the gluino contributions are only present for non-zero δ_d mass insertions

$$A_{bs}^{\tilde{g}} \sim \frac{\alpha_s}{4\pi}\frac{1}{\tilde{m}^2} f\Big(\tilde{m}^2(\mathbb{1}+\delta_d^{XY})\Big)_{32} \simeq \frac{\alpha_s}{4\pi}\frac{1}{\tilde{m}^2}\,(\delta_d^{XY})_{32}\,\partial f(\tilde{m}^2)\ . \tag{4.30}$$

  As they are induced by strong interactions, they are usually expected to give the dominant NP contributions to FCNC processes in the MSSM, whenever the down squark soft terms have a non-trivial flavor structure.

- Finally turning to the Wino contributions, they have at first sight a rather involved structure. If the left handed up squarks are all degenerate in mass, then the Wino contributions vanish due to the super-GIM mechanism. To have non-zero Wino induced FCNC amplitudes, δ_u^{LL} mass insertions therefore have to be present. A flavor changing $(\delta_u^{LL})_{32}$ mass insertion can lead directly to Wino contributions. However, also a flavor diagonal $(\delta_u^{LL})_{33}$ can provide a source of super-GIM breaking leading to Wino contributions through the CKM matrix. Explicitly one finds

$$\begin{aligned} A_{bs}^{\tilde{W}^\pm} &\sim \frac{\alpha_2}{4\pi}\frac{1}{\tilde{m}^2}\Big(V^{\mathrm{T}} f\Big(\tilde{m}^2(\mathbb{1}+\delta_u^{LL})\Big)V^*\Big)_{32} \\ &\simeq \frac{\alpha_2}{4\pi}\frac{1}{\tilde{m}^2}\partial f(\tilde{m}^2)\Big(V^{\mathrm{T}}\delta_u^{LL}V^*\Big)_{32} \simeq \frac{\alpha_2}{4\pi}\frac{1}{\tilde{m}^2}\,(\delta_d^{LL})_{32}\,\partial f(\tilde{m}^2)\ , \end{aligned} \tag{4.31}$$

  where in the last step we used the SU(2) relation (4.25). Interestingly, the Wino amplitude is proportional to the left-left mass insertions in the *down* sector and not in the up sector as one would naively expect. This implies in particular that Wino contributions are always accompanied by gluino contributions that are typically dominant.

The above presentation points out the main generic features of the MSSM flavor structure and its impact on FCNC amplitudes. Detailed and comprehensive discussions of the SUSY contributions to specific FCNC processes like $b \to s\gamma$, $B_s \to \mu^+\mu^-$, $K \to \pi\nu\bar{\nu}$ and neutral meson mixing will follow in chapter 6. However already form the above discussion it is clear that for a SUSY scale in the reach of LHC, the good agreement between the existing data on FCNC observables and the corresponding SM predictions leads to severe constraints on the flavor violating entries in the soft SUSY breaking terms. This so-called *SUSY flavor problem* will be the main subject of chapter 7.

4.4 The Minimal Flavor Violating MSSM and Beyond

One way to keep under control dangerously large SUSY contributions to flavor changing observables is to invoke the principle of Minimal Flavor Violation (MFV) [43, 44]. According to the symmetry based definition [44], the MFV hypothesis amounts to the assumption that the SM Yukawa couplings be, also in extensions of the SM, the only structures responsible for a breaking of the flavor group (4.15). In models with MFV, NP contributions to FCNC processes are thus suppressed by the same CKM factors as in the SM and therefore expected to be naturally small.

In the context of the MSSM, the MFV principle does *not* require that the soft SUSY breaking terms are completely flavor blind, but they have to be functions of the Yukawa

couplings. In the MSSM, Minimal Flavor Violation can be realized through the following, most general ansatz for the soft SUSY breaking sector at the electroweak scale in the super-CKM basis [44]

$$\begin{aligned} m_Q^2 &= \tilde{m}_Q^2 \left(1 + b_1 V^\dagger \hat{y}_u^2 V + b_2 \hat{y}_d^2 + b_3 \hat{y}_d^2 V^\dagger \hat{y}_u^2 V + b_3^* V^\dagger \hat{y}_u^2 V \hat{y}_d^2\right) \ , \\ m_U^2 &= \tilde{m}_U^2 \left(1 + b_4 \hat{y}_u^2\right) \ , \quad A_u = \tilde{A}_u \left(1 + b_6 V^* \hat{y}_d^2 V^{\mathrm{T}}\right) \hat{y}_u \ , \\ m_D^2 &= \tilde{m}_D^2 \left(1 + b_5 \hat{y}_d^2\right) \ , \quad A_d = \tilde{A}_d \left(1 + b_7 V^{\mathrm{T}} \hat{y}_u^2 V^*\right) \hat{y}_d \ . \end{aligned} \tag{4.32}$$

In fact the assumption of a flavor blind soft sector is not RGE invariant and the general structure in (4.32) is always generated in the running of the soft terms [273, 274].

In the above expressions (4.32), $\tilde{m}_Q^2$, $\tilde{m}_U^2$, $\tilde{m}_D^2$ and $\tilde{A}_u$, $\tilde{A}_d$ represent overall mass scales for the squark bilinear and trilinear terms that are at the leading order proportional to the unit matrix and the corresponding Yukawa couplings, respectively. The coefficients b_i are proportionality factors of O(1) for the higher order terms in the Yukawa couplings. The coefficients b_1, b_3 and b_7 lead to flavor non-diagonal terms in the down squark mass matrix. The most important effects comes usually from b_1 that induces a mass insertions $(\delta_d^{LL})_{ij} = b_1 y_t^2 V_{ti} V_{tj}^*$, which implies of course the existence of gluino contributions to FCNC processes that, however, are proportional to the respective CKM matrix elements. In addition, the coefficient b_1 leads to a splitting between the left handed stop mass $m_{\tilde{t}_L}^2 \simeq \tilde{m}_Q^2(1 + b_1 y_t^2)$ and the left handed up and charm squark masses $m_{\tilde{u}_L}^2 \simeq m_{\tilde{c}_L}^2 \simeq \tilde{m}_Q^2$. Such a splitting breaks the super-GIM mechanism and results also in Wino contributions to FCNC processes that are proportional to $(\delta_u^{LL})_{33} = b_1 y_t^2$. Detailed studies of the phenomenological impact of the general MFV ansatz for the soft terms can be found in [275, 14, 15, 276, 277].

We also note that the MFV principle does not forbid the presence of additional CP violating phases in the MSSM [274, 278, 279]. Both flavor blind parameters as the μ term, the gaugino masses and the trilinear couplings $\tilde{A}_u$, $\tilde{A}_d$ as well as the "flavored" parameters b_3, b_6 and b_7 are in principle allowed to be complex. The MFV MSSM with CP phases has been analyzed for example in [280, 281, 282, 283, 274, 18, 278, 279, 21] and in section 8.1 the main implications of this framework for the flavor and CP phenomenology as worked out by us in [18, 21] will be presented.

Going beyond the MFV framework, one has to ensure that the additional flavor structures do not spoil the good agreement between the SM predictions for FCNC observables and the experimental data, i.e. the SUSY flavor problem needs to be addressed. Several possibilities as the so-called degeneracy and alignment mechanisms are outlined in section 7.2. Such mechanisms can be realized for example in abelian and non-abelian flavor models and a comprehensive analysis of the characteristic phenomenology of flavor and CP violation of these frameworks will be presented in chapter 8.

5 The MSSM in the Large $\tan\beta$ Regime

Holomorphy of the superpotential ensures that at tree level the MSSM is a 2 Higgs doublet model of type II, i.e. down-type quarks and charged leptons only couple to the down-type Higgs and up-type quarks only couple to the up-type Higgs. In presence of soft SUSY breaking terms and the Peccei-Quinn breaking μ term, this is no longer true at the loop level. An often adopted strategy to take into account effects from the "wrong" Higgs couplings in a transparent way is to work in the so-called decoupling limit. The SUSY particles are integrated out leading to an effective 2 Higgs doublet model that contains both the holomorphic Yukawa couplings as well as loop induced non-holomorphic couplings of fermions to the "wrong" Higgs bosons.

In the large $\tan\beta$ regime of the MSSM, the loop induced couplings of down-type quarks and charged leptons to the up-type Higgs can lead to $\tan\beta$ enhanced $O(1)$ corrections to the corresponding masses [284, 285, 286], modify significantly CKM matrix elements [287] and strongly change also the couplings of charged and neutral Higgs bosons to fermions [288, 289]. All this has a profound impact on flavor phenomenology [288, 290, 291, 292, 293, 294, 295, 296, 297].

In this chapter we outline these effects and give approximate expressions for the non-holomorphic, i.e. $\tan\beta$ enhanced loop corrections, that are relevant for the discussion of the SUSY contributions to low energy observables in the next chapter. For this purpose, it is sufficient to work in the decoupling limit which is known to be an excellent approximation as long as the SUSY spectrum is not extremely light. Effects that go beyond the decoupling limit can be taken into account making use of the iteration procedure described in [295], which is consistently done in our numerical studies. An alternative, fully analytical approach has been adopted in [124].

5.1 Corrections to Quark and Lepton Masses

After electroweak symmetry breaking, the down-type quark and lepton masses arise at tree level from the coupling to the down-type Higgs, $\hat{m}^0_{d,\ell} = \hat{y}_{d,\ell}\frac{v_d}{\sqrt{2}}$. Non-holomorphic couplings to the up-type Higgs are generated at the loop level leading to $\tan\beta$ enhanced corrections to the tree level masses. In case of the τ and bottom mass one has for example

$$m_\tau = \frac{1}{\sqrt{2}}\left(y_\tau v_d + y'_\tau v_u\right) = m^0_\tau(1+\epsilon_\ell\tan\beta)\ , \qquad \epsilon_\ell = \epsilon_\ell^{\tilde{W}} + \epsilon_\ell^{\tilde{B}}\ , \tag{5.1}$$

$$m_b = \frac{1}{\sqrt{2}}\left(y_b v_d + y'_b v_u\right) = m^0_b(1+\epsilon_b\tan\beta)\ , \qquad \epsilon_b = \epsilon_b^{\tilde{g}} + \epsilon_b^{\tilde{W}} + \epsilon_b^{\tilde{B}} + \epsilon_b^{\tilde{H}}\ . \tag{5.2}$$

Instead of (4.18) one then has

$$y_\tau = \sqrt{2}\,\frac{m_\tau}{v}\frac{\tan\beta}{1+\epsilon_\ell\tan\beta}\ , \quad y_b = \sqrt{2}\,\frac{m_b}{v}\frac{\tan\beta}{1+\epsilon_b\tan\beta}\ , \tag{5.3}$$

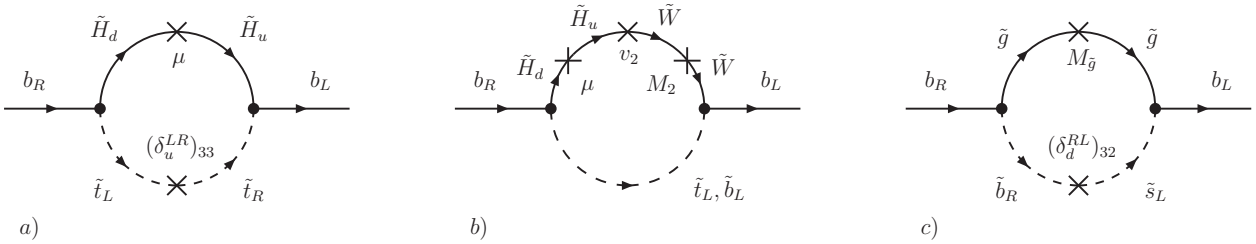

Figure 5.1: Most important non-holomorphic corrections to the bottom quark mass.

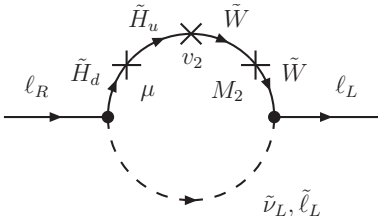

Figure 5.2: Most important non-holomorphic corrections to the lepton masses.

which resums the $\tan\beta$ enhanced beyond leading order corrections to all order [289].

The loop factors ϵ_ℓ and ϵ_b receive contributions from gluino, Wino, Bino and Higgsino loops. To transparently display the main dependencies on the SUSY parameters, we give approximate expressions for ϵ_ℓ and ϵ_b assuming all squarks and sleptons to have a common mass $\tilde{m}$. As the Bino contributions are parametrically suppressed by the small gauge coupling α_1 we do not give explicit expressions here. The diagrams corresponding to the remaining contributions are shown in figures 5.1 and 5.2 and lead to the following expressions[1]

$$\epsilon_b^{\tilde{g}} = \frac{\alpha_s}{4\pi}\frac{8}{3}\frac{\mu^* M_{\tilde{g}}}{\tilde{m}^2} f_1(x_g) \ , \qquad \epsilon_b^{\tilde{H}} = \frac{\alpha_2}{4\pi}\frac{m_t^2}{2M_W^2}\frac{\mu^* A_t^*}{\tilde{m}^2} f_1(x_\mu) \ ,$$

$$\epsilon_b^{\tilde{W}} = \epsilon_\ell^{\tilde{W}} = -\frac{\alpha_2}{4\pi}\frac{3}{2}\frac{\mu^* M_2^*}{\tilde{m}^2} f_2(x_2, x_\mu) \ , \tag{5.4}$$

The dominant correction to the bottom quark Yukawa is typically given by the gluino contribution $\epsilon_b^{\tilde{g}}$ which is positive (negative) for positive (negative) μ. As $\epsilon_b^{\tilde{g}}$ does not decouple with μ, the largest corrections to the bottom Yukawa are expected when $|\mu|$ is large. For large values of A_t (and light stops), also the Higgsino contribution $\epsilon_b^{\tilde{H}}$ can in principle become important and, depending on the sign of A_t, interfere constructively or destructively with the gluino contribution.

Concerning the tau Yukawa, due to the absence of gluino and Higgsino corrections, the Wino contribution $\epsilon_\ell^{\tilde{W}}$ is typically dominant and its sign is determined by $-\text{sign}(\mu M_2)$.

As these corrections are potentially of O(1) for large values of $\tan\beta$ it is essential to keep them into account when analyzing SUSY models in the large $\tan\beta$ regime and we will always

[1] We mention that in the presence of flavor off-diagonal entries in the squark and slepton soft masses, these expressions get in principle modified. Even so the flavor effects are suppressed by two powers of mass insertions, they can become relevant for light down quarks and leptons, where they feature enhancement factors of m_b/m_d, m_τ/m_e, etc. In the discussed case of the τ and bottom mass however, these flavor effects are usually negligible.

include them in the discussion of the SUSY contributions to low energy observables in the next chapter.

Of particular importance are these $\tan\beta$ enhanced corrections also in the context of SUSY GUTs that predict third generation Yukawa unification. As is well known, top-bottom-tau or bottom-tau Yukawa unification at the GUT scale implies $\tan\beta \simeq 50$ and only works with sizable threshold corrections to the bottom Yukawa coupling [298, 299, 300, 301, 302, 16, 17, 303, 304] implying a very particular SUSY spectrum and characteristic effects in flavor observables. Allowing for even larger values of $\tan\beta \gtrsim 50$ one can arrive at a situation where the down-type fermion masses are dominantly generated by the loop induced couplings to the up-type Higgs [305]. The viability of this so-called uplifted SUSY scenario [305] has recently been assessed by us in [23].

5.2 Flavor Off-Diagonal Corrections to the Quark Masses

Non-holomorphic corrections do not only lead to $\tan\beta$ enhanced modifications of the diagonal down quark masses as discussed in the section above. They also introduce flavor off-diagonal corrections to the 3×3 quark masses. The down quark mass matrix then has to be rediagonalized by an appropriate rotation of the left and right handed down quark fields which leads to modifications of the CKM matrix and charged Higgs quark couplings as well as to effective flavor changing neutral Higgs down quark vertices. Instead of giving now a detailed description of this procedure that can be found e.g. in [295], we restrict ourselves to giving the most relevant expressions for the flavor off-diagonal corrections to the down quark mass matrix. They can be written as

$$(\Delta\hat{m}_d)_{ji} = m_d^j \tan\beta\, \epsilon_b^{\tilde{H}}\, V_{ti}^0 V_{tj}^{0*} + m_d^j \tan\beta \left(\epsilon_{LL}^{\tilde{W}} + \epsilon_{LL}^{\tilde{g}}\right) (\delta_d^{LL})_{ij} + m_d^i \tan\beta\, \epsilon_{RR}^{\tilde{g}}\, (\delta_d^{RR})_{ij}\ , \quad (5.5)$$

with $i,j = d,s,b$ and $i \neq j$.

The most important diagrams leading to these corrections are shown in figure 5.3. The Higgsino diagram a) leads to a contribution proportional to the CKM elements $V_{ti}V_{tj}^*$ that is also present for a completely flavor blind soft sector. The corresponding loop factor $\epsilon_b^{\tilde{H}}$ has already been given in 5.4. Consequently, even in the absence of any sources of flavor violation apart from the SM CKM matrix, the corresponding term in (5.5) leads to flavor changing neutral higgs vertices in the effective 2 Higgs doublet model description of the MSSM, implying for example tree level contributions to FCNC processes like $B_s \to \mu^+\mu^-$ and $B_s - \bar{B}_s$ mixing [290, 292, 295]. This diagram also leads to a large renormalization of the CKM matrix. The relation between the bare CKM in the MSSM, V^0, that appears for example in chargino vertices, and the effective CKM in the 2 Higgs doublet model, V, that corresponds to the experimentally determined quantity, reads [124]

$$V^0 = \begin{pmatrix} V_{ud} & V_{us} & K^* V_{ub} \\ V_{cd} & V_{cs} & K^* V_{cb} \\ K V_{td} & K V_{ts} & V_{tb} \end{pmatrix}\ , \quad \text{with} \quad K = \frac{1+\epsilon_b \tan\beta}{1+\epsilon_0 \tan\beta}\ , \quad (5.6)$$

where $\epsilon_0 = \epsilon_b - \epsilon_b^{\tilde{H}}$.

If the soft masses of the down squarks contain non-trivial flavor structures, then also Wino and gluino loops contribute to the off-diagonal corrections to the down quark mass.[2] The

[2] As before, we neglect again contributions from Bino loops that are basically never relevant.

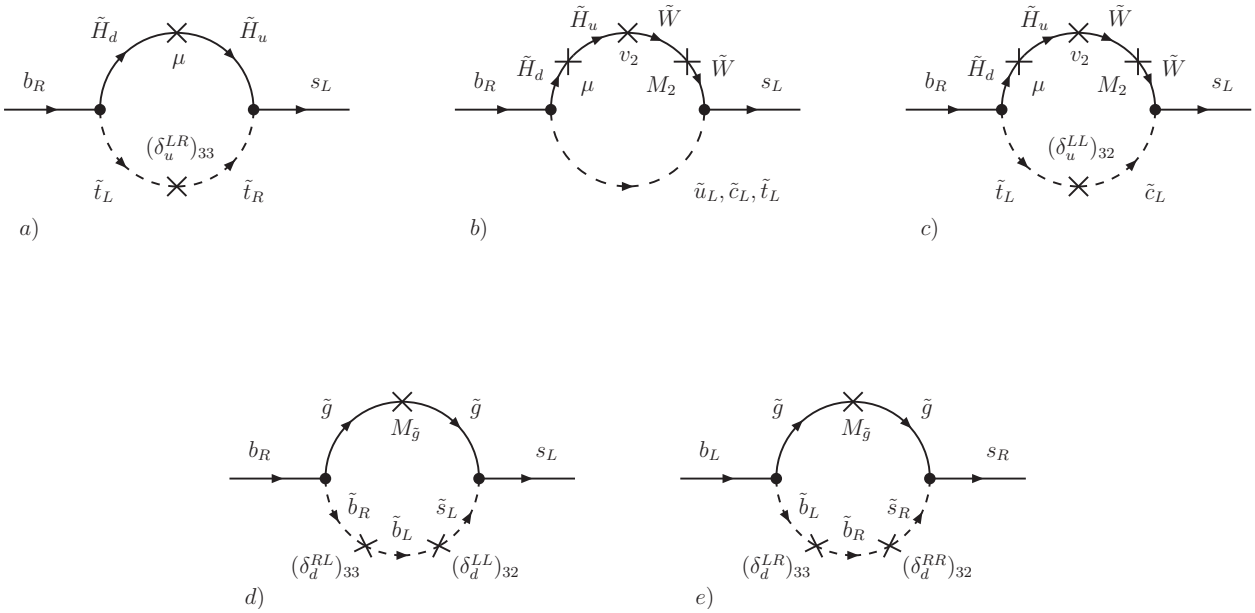

Figure 5.3: Most important non-holomorphic corrections to the off-diagonal entries of the down quark mass matrix. Shown is the example of a $b \to s$ transition.

factors $\epsilon_{LL}^{\tilde{W}}$, $\epsilon_{LL}^{\tilde{g}}$ and $\epsilon_{RR}^{\tilde{g}}$ are given by

$$\epsilon_{LL}^{\tilde{W}} = -\frac{\alpha_2}{4\pi}\frac{3}{2}\frac{\mu^* M_2^*}{\tilde{m}^2} f_4(x_2, x_\mu) \ , \quad \epsilon_{LL}^{\tilde{g}} = \epsilon_{RR}^{\tilde{g}} = \frac{\alpha_s}{4\pi}\frac{8}{3}\frac{\mu^* M_{\tilde{g}}}{\tilde{m}^2} f_3(x_g) \ , \tag{5.7}$$

We remark that the factor $\epsilon_{LL}^{\tilde{W}}$ contains both contributions from charged and neutral Winos. Shown in diagrams b) and c) of figure 5.3 are only the charged contributions that are split into two parts according to $(\delta_d^{LL})_{32} = \left(V^{\mathrm{T}}(\delta_u^{LL})V^*\right)_{32} \simeq \left((\delta_u^{LL})_{33} - (\delta_u^{LL})_{22}\right) V_{tb}V_{ts}^* + (\delta_u^{LL})_{32} V_{tb}V_{cs}^*$. Diagram c) is directly induced by the flavor changing $(\delta_u^{LL})_{32}$ mass insertion, while diagram b) arises from super-GIM breaking due to the mass difference of the left handed top and charm squarks.

Gluino loops are the only ones that can introduce the term proportional to δ_d^{RR} as shown in diagram e) of figure 5.3. This term leads to corrections of couplings of Higgs bosons with right handed down and strange quarks that are enhanced by factors of m_b/m_d and m_b/m_s, respectively. In fact, $\tan\beta$ enhanced corrections to Higgs vertices in the presence of δ_d^{RR} mass insertions have profound impact on flavor phenomenology (see e.g. [293, 297, 306, 307, 21]). This will be discussed in more detail, when we analyze the SUSY contributions to $B_s - \bar{B}_s$ mixing, $K \to \pi\nu\bar{\nu}$ and EDMs in sections 6.4, 6.5 and 6.7.

6 SUSY Contributions to Low Energy Observables

The various sources of flavor violation in the MSSM discussed in section 4.2, lead to NP contributions to flavor changing observables. In this chapter we present in detail the most important SUSY contributions to the low energy observables of chapter 3. Other comprehensive discussions can be found e.g. in [308, 309, 310, 311, 297, 312, 21].

We start in section 6.1 with the tree level $B^+ \to \tau^+\nu$ decay. In the MSSM there are additional charged Higgs contributions that can be sizable in the large $\tan\beta$ regime. In section 6.2 we then discuss SUSY contributions to the flavor changing $b \to s\gamma$ and $b \to s$ gluon dipole transitions, that play a crucial role for many FCNC processes, in particular the $B \to X_s\gamma$ decay as well as for example the semileptonic $B \to K^*\ell^+\ell^-$ and non-leptonic $B \to \phi K_S$ and $B \to \eta' K_S$ decays. Next, in section 6.3, we discuss Higgs penguin contributions to the purely leptonic $B_s \to \mu^+\mu^-$ and $B_d \to \mu^+\mu^-$ decays that are especially important in the large $\tan\beta$ regime of the MSSM. SUSY contributions to the $\Delta F = 2$ effective Hamiltonian, that are relevant for the discussion of meson mixing in the MSSM, are the main subject of section 6.4. In the following section 6.5, we discuss how sizable effects in the $b \to s\nu\bar{\nu}$ and $s \to d\nu\bar{\nu}$ transitions can be generated in the MSSM. Finally, in the last two sections 6.6 and 6.7 the most important SUSY contributions to the anomalous magnetic moment of the muon and the electric dipole moments of quark and leptons will be presented, respectively.

As mentioned in section 4.2 we will discuss the SUSY contributions to the low energy processes in the mass insertion approximation to display the main dependencies on the MSSM parameters in the most transparent way. Explicit expressions for the loop functions that will appear in various equations of this chapter are all conveniently collected in appendix A.1. These functions depend only on mass ratios that we define as

$$y_t = \frac{m_t^2}{M_{H^\pm}^2}\,, \quad x_\mu = \frac{|\mu|^2}{\tilde{m}^2}\,, \quad x_1 = \frac{|M_1|^2}{\tilde{m}^2}\,, \quad x_2 = \frac{|M_2|^2}{\tilde{m}^2}\,, \quad x_g = \frac{M_{\tilde{g}}^2}{\tilde{m}^2}\,. \tag{6.1}$$

6.1 Charged Higgs Effects in $B^+ \to \tau^+\nu$

The $B^+ \to \tau^+\nu$ decay is a sensitive probe of models with extended Higgs sectors [163]. Indeed, in the MSSM with large $\tan\beta$, its branching ratio can differ significantly from the SM prediction [164, 165]. Tree level charged Higgs contributions interfere destructively with the SM ones and lead to

$$R_{B\tau\nu} = \frac{\mathrm{BR}(B^+ \to \tau^+\nu)_{\mathrm{MSSM}}}{\mathrm{BR}(B^+ \to \tau^+\nu)_{\mathrm{SM}}} \simeq \left|1 - \frac{M_{B^+}^2}{M_{H^\pm}^2}\frac{\tan^2\beta}{(1+\epsilon_0^*\tan\beta)(1+\epsilon_\ell\tan\beta)}\right|^2 . \tag{6.2}$$

The suppression of the charged Higgs effects by the factor $M_{B^+}^2/M_{H^\pm}^2$ is compensated by the $\tan^2\beta$ enhancement and huge effects in $\mathrm{BR}(B^+ \to \tau^+\nu)$ are possible in the large $\tan\beta$

regime. The same is true for the $B \to D\tau\nu$ decay, where tree level charged Higgs effects result in [171]

$$R_{BD\tau\nu} = \frac{\mathrm{BR}(B \to D\tau\nu)_{\mathrm{MSSM}}}{\mathrm{BR}(B \to D\tau\nu)_{\mathrm{SM}}} \simeq 1 + 1.38(3)\mathrm{Re}(C^\tau_{\mathrm{NP}}) + 0.88(2)|C^\tau_{\mathrm{NP}}|^2 \ , \tag{6.3}$$

with the Wilson coefficient C^τ_{NP} given by

$$C^\tau_{\mathrm{NP}} \simeq -\frac{m_b m_\tau}{M^2_{H^\pm}} \frac{\tan^2\beta}{(1+\epsilon_0^*\tan\beta)(1+\epsilon_\ell\tan\beta)} \ . \tag{6.4}$$

Finally, charged Higgs exchange can also affect the $K \to \mu\nu$ decay. For the observable $R_{\ell 23}$ defined in section 3.2.7 one finds [173, 174]

$$R_{\ell 23} = \left| 1 - \frac{M^2_{K^+}}{M^2_{H^\pm}} \left(1 - \frac{m_d}{m_s}\right) \frac{\tan^2\beta}{(1+\epsilon_0^*\tan\beta)(1+\epsilon_\ell\tan\beta)} \right| \ . \tag{6.5}$$

The contributions to $K \to \mu\nu$ are strongly suppressed compared to the $B \to \tau\nu$ and $B \to D\tau\nu$ cases as they are proportional to $M^2_{K^+}$. Still, due to the much better experimental resolution and the much more accurate theoretical prediction of $R_{\ell 23}$, also the $K \to \mu\nu$ decay is comparatively sensitive to charged Higgs effects.

While at leading order, $R_{B\tau\nu}$, $R_{BD\tau\nu}$ and $R_{\ell 23}$ are only sensitive to the parameters $M_{H^\pm}$ and $\tan\beta$, sensitivity to the soft SUSY breaking parameters is introduced through the $\epsilon\tan\beta$ factors that resum the $\tan\beta$ enhanced beyond leading order corrections. The analytical expressions of these resummation factors have already been discussed in chapter 5.

In a non-supersymmetric two Higgs doublet model of type II, such $\tan\beta$ enhanced resummation factors are absent and the experimental data on the $B \to \tau\nu$, $B \to D\tau\nu$ and $K \to \mu\nu$ decays can directly be translated into bounds in the $M_{H^\pm} - \tan\beta$ plane as shown in the plots in the upper row of figure 6.1. As it is well know, $B \to \tau\nu$ alone cannot exclude a scenario where the SM contribution is overcompensated by a charged Higgs contribution more than twice as large as itself, leading to the small allowed strip for low charged Higgs masses. However, the experimental data on the $K \to \mu\nu$ and $B \to D\tau\nu$ decays exclude such a fine tuned situation [173, 313] as it is shown in the middle and right upper plots of figure 6.1.

Combining then the experimental information on the $B \to \tau\nu$, $B \to D\tau\nu$ and $K \to \mu\nu$ decays, stringent lower bounds on the charged Higgs mass follow in the large $\tan\beta$ regime. We find [23]

$$M_{H^\pm} > 9.6\,\mathrm{GeV} \times \tan\beta \quad @\ 95\%\ \mathrm{C.L.} \ , \tag{6.6}$$

which is less stringent than the bound found in [167], because of our more conservative SM prediction for $\mathrm{BR}(B^+ \to \tau^+\nu)$ (3.108).

Due to the presence of threshold corrections, the bound (6.6) can be relaxed in the MSSM, provided $\epsilon_0 > 0$ and/or $\epsilon_\tau > 0$. In the plots in the bottom row of figure 6.1 we show an exemplary situation with $\epsilon_0 \simeq 0.02$ and $\epsilon_\tau \simeq -0.002$ as it happens for an exemplary SUSY spectrum with all soft masses equal to $\tilde{m}$ and $\mu = +2\tilde{m}$. As one can see, the bound on the Higgs mass is indeed relaxed with $M_{H^\pm} > 370$ GeV for $\tan\beta = 50$ for example.

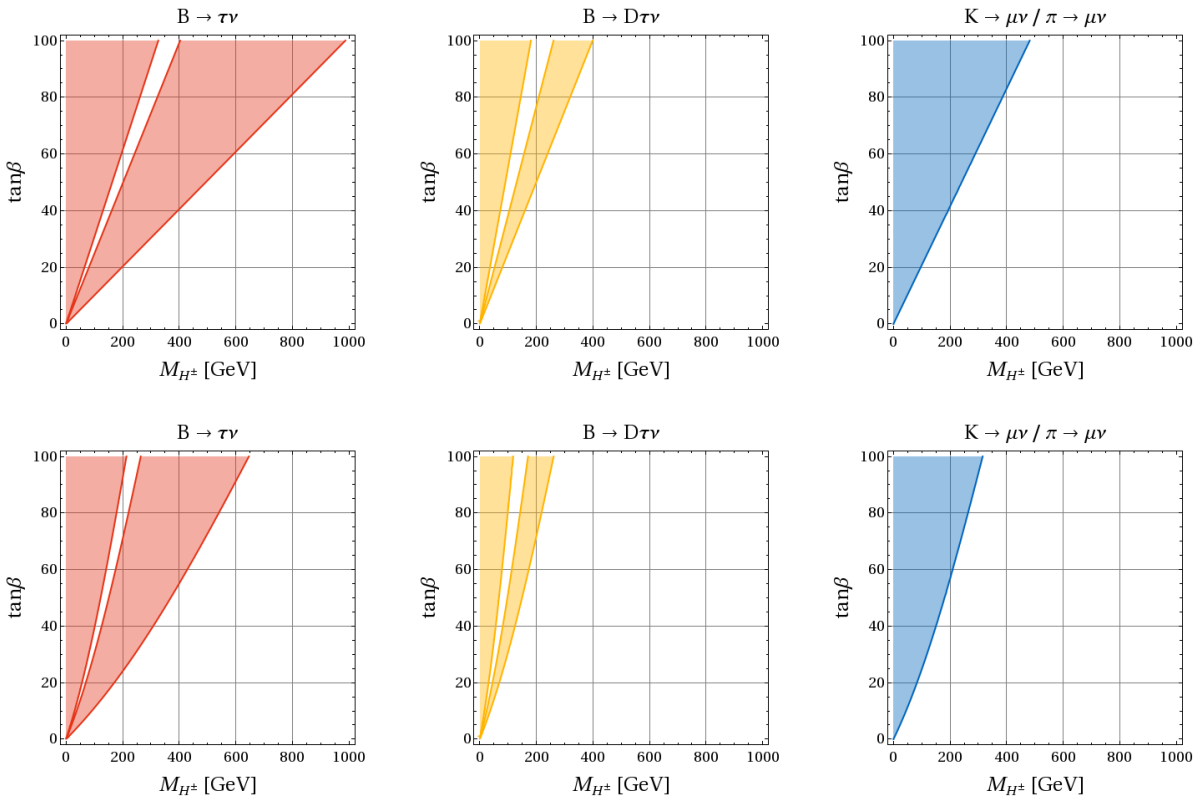

Figure 6.1: The $M_{H^\pm} - \tan\beta$ plane in a non-supersymmetric two Higgs doublet model of type II (upper row) and in the MSSM (lower row). Shown are the excluded ranges from $B \to \tau\nu$ (left), $B \to D\tau\nu$ (middle) and $K \to \mu\nu$ (right) at the 95% C.L. using the constraints given in section 3.2.7. For the MSSM plots, values of the threshold corrections $\epsilon_0 = 0.02$ and $\epsilon_\ell = -0.002$ are assumed.

6.2 The Magnetic and Chromomagnetic $b \to s\gamma$ Operators

The magnetic and chromomagnetic $b \to s\gamma$ operators (see (3.45)) require a helicity flip for the involved quarks. As only left handed fermions participate in the SM weak interactions, the SM contributions to the Wilson coefficients are necessarily suppressed by the bottom quark mass. This suppression can be circumvented in NP models which makes the $b \to s\gamma$ transition an excellent probe of the flavor structure of NP.

The SUSY contributions to the Wilson coefficients of the magnetic and chromomagnetic dipole operators can be decomposed according to the virtual particles that mediate the $b \to s\gamma$ transition

$$C_{7,8}^{(\prime)\,\mathrm{SUSY}} = C_{7,8}^{(\prime)\,H^\pm} + C_{7,8}^{(\prime)\,\tilde{\chi}^\pm} + C_{7,8}^{(\prime)\,\tilde{g}} + C_{7,8}^{(\prime)\,\tilde{\chi}^0} \,. \tag{6.7}$$

The various contributions on the r.h.s. arise from penguin diagrams with charged Higgs up type quarks, chargino up type squarks, gluino down type squarks and neutralino down type squarks, respectively. These contributions have been extensively studied in the literature for various SUSY frameworks both at LO and partly also at NLO (see e.g. [314, 315, 316, 317, 318, 319, 320, 291, 321, 89, 322, 323, 277]).

In the remainder of this section we qualitatively discuss the Higgs, the chargino and the gluino contributions to the $b \to s\gamma$ decay. As neutralino penguins always give a completely

negligible contribution they will be given no further consideration. We start with the case of low to moderate values of $\tan\beta$ and present all relevant expressions for a completely generic soft sector. In a second step we then discuss the contributions in the large $\tan\beta$ regime restricting the discussion to a flavor blind soft sector. Finally we also sketch the most involved case of large $\tan\beta$ and generic soft sector.

The case of moderate $\tan\beta$

For low to moderate values of $\tan\beta$ the charged Higgs top quark loops lead to the following contributions to the Wilson coefficients $C_{7,8}$

$$C_{7,8}^{H^\pm} = h_{7,8}(y_t) \ , \tag{6.8}$$

where here and in the following we neglect contributions suppressed by $\cot^2\beta$ with respect to the leading term. The sign of these contributions is such that they always interfere constructively with the SM contribution [324, 325]. The corresponding contributions to the primed Wilson coefficients $C'_{7,8}$ are suppressed by m_s/m_b and therefore negligibly small.

The chargino diagrams of figure 6.2 result in the following expressions

$$\begin{aligned}\frac{4G_F}{\sqrt{2}}V_{ts}^*V_{tb}\ C_{7,8}^{\tilde\chi^\pm} = {}& \frac{g_2^2}{\tilde m^2}V_{tb}V_{ts}^*\frac{m_t^2}{M_W^2}\left[f_{7,8}^{(4)}(x_\mu) + \left(\frac{A_t\mu}{\tilde m^2}\tan\beta + \frac{|\mu|^2}{\tilde m^2}\right) f_{7,8}^{(5)}(x_\mu)\right] \\ & + \frac{g_2^2}{\tilde m^2}(\delta_d^{LL})_{32}\left[f_{7,8}^{(1)}(x_2) + f_{7,8}^{(2)}(x_2,x_\mu) + \frac{\mu M_2}{\tilde m^2}\tan\beta\ f_{7,8}^{(3)}(x_2,x_\mu)\right] \ . \end{aligned} \tag{6.9}$$

The first line of (6.9) consists of the Higgsino contributions shown in diagrams a) and b) of figure 6.2. These contributions do not require any non-trivial flavor structure in the squark masses but are also present for a completely flavor blind soft sector. Even for moderate values of $\tan\beta$ the term proportional to $\tan\beta$ that stems from diagram b) is typically the by far most important one. Its sign/phase is determined by the sign/phase of $A_t\mu$.

The second line of (6.9) then contains all contributions involving also Winos shown in diagrams c) to h) of figure 6.2. Decomposing $(\delta_d^{LL})_{32} \simeq \left((\delta_u^{LL})_{33} - (\delta_u^{LL})_{22}\right) V_{tb}V_{ts}^* + (\delta_u^{LL})_{32}V_{tb}V_{cs}^*$ shows that for these diagrams to be non-vanishing either directly a $(\delta_u^{LL})_{32}$ mass insertion as shown in diagrams f) to h) or a splitting of the LH stop mass and the LH scharm mass are required. In fact the diagrams c) to e) vanish through the super-GIM mechanism if the involved LH up-type squarks are degenerate in mass. We remind that if the left-left soft mass matrix is aligned in the down sector, i.e. $(\delta_d^{LL})_{32} = 0$ then, the mass splitting and the $(\delta_u^{LL})_{32}$ mass insertion are correlated such that the Wino diagrams in the second and third line of figure 6.2 cancel each other.

As it was the case for the Higgs contributions, the leading order chargino contributions to the right handed coefficients $C'_{7,8}$ are suppressed by m_s/m_b and therefore can be neglected. Interestingly, at the leading order, the chargino contributions thus show no sensitivity to left-right, right-left or right-right mass insertions.

Turning finally to the gluino contributions, the relevant diagrams are shown in figure 6.3. All these diagrams always involve flavor off-diagonal mass insertions and lead to

$$\frac{4G_F}{\sqrt{2}}V_{ts}^*V_{tb}\ C_{7,8}^{\tilde g} = \frac{g_s^2}{\tilde m^2}\left[(\delta_d^{LL})_{32}\ g_{7,8}^{(1)}(x_g) + \frac{M_{\tilde g}}{m_b}(\delta_d^{RL})_{32}\ g_{7,8}^{(2)}(x_g)\right.$$

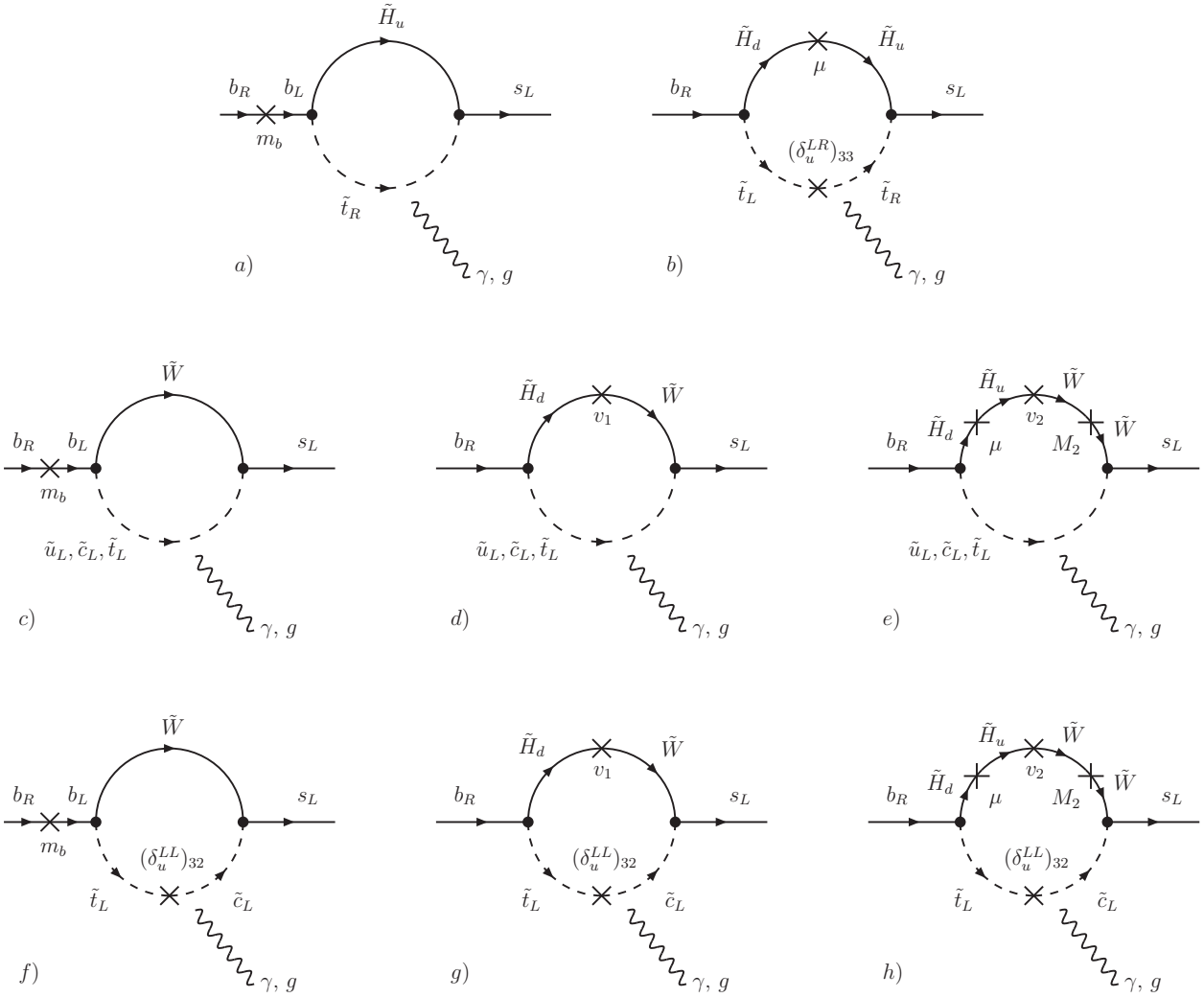

Figure 6.2: Leading order chargino contributions to the Wilson coefficients $C_{7,8}$. The photon/gluon is attached to the loop in all possible ways.

$$+\left(\frac{M_{\tilde{g}}\mu}{\tilde{m}^2}\tan\beta+\frac{M_{\tilde{g}}A_b^*}{\tilde{m}^2}\right)(\delta_d^{LL})_{32}\,g_{7,8}^{(3)}(x_g)\Bigg]\ , \quad (6.10)$$

$$\frac{4G_F}{\sqrt{2}}V_{ts}^*V_{tb}\,C_{7,8}^{\prime\tilde{g}}=\frac{g_s^2}{\tilde{m}^2}\Bigg[(\delta_d^{RR})_{32}\,g_{7,8}^{(1)}(x_g)+\frac{M_{\tilde{g}}}{m_b}(\delta_d^{LR})_{32}\,g_{7,8}^{(2)}(x_g)$$
$$+\left(\frac{M_{\tilde{g}}\mu^*}{\tilde{m}^2}\tan\beta+\frac{M_{\tilde{g}}A_b}{\tilde{m}^2}\right)(\delta_d^{RR})_{32}\,g_{7,8}^{(3)}(x_g)\Bigg]\ . \quad (6.11)$$

While diagrams a) to c) of figure 6.3 contribute to $C_{7,8}$ and are sensitive to $(\delta_d^{LL})_{32}$ and $(\delta_d^{RL})_{32}$ mass insertions, contributions to $C'_{7,8}$ are induced by the diagrams d) to f) that are instead sensitive to $(\delta_d^{RR})_{32}$ and $(\delta_d^{LR})_{32}$ mass insertions. As a matter of fact, gluino contributions are the only ones that can lead to non-negligible effects in $C'_{7,8}$ at the leading order.

We mention that diagrams c) and f) involve a double mass-insertion along the down-squark propagators and can lead to sizable contributions that are proportional to $\mu\tan\beta$.

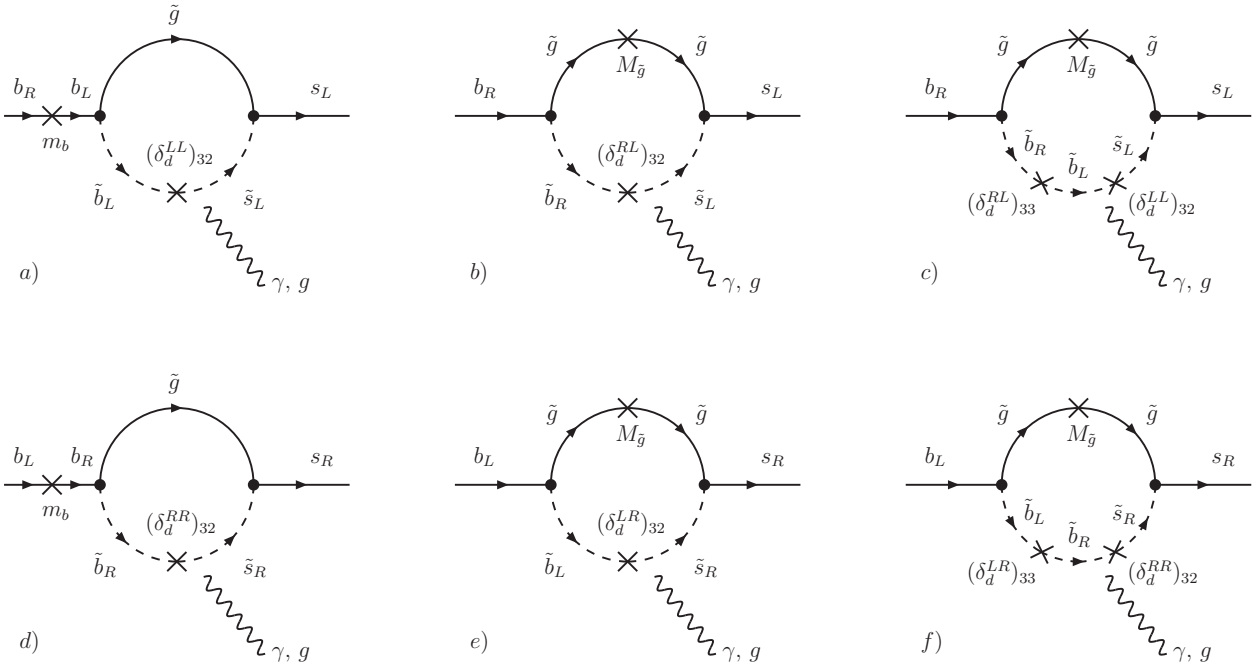

Figure 6.3: Leading order gluino contributions to the Wilson coefficients $C_{7,8}$. The photon/gluon is attached to the loop in all possible ways.

Furthermore, the terms proportional to $(\delta_d^{LR})_{32}$ and $(\delta_d^{RL})_{32}$ in (6.10) and (6.11) are chirally enhanced by a factor $M_{\tilde{g}}/m_b$ and one expects therefore strong constraints on these mass insertions coming from the experimental data on the $\mathrm{BR}(B \to X_s\gamma)$.

Finally we note that the mass insertions required for gluino contributions can also arise in MFV frameworks. In fact, $(\delta_d^{LL})_{32}$ and $(\delta_d^{RL})_{32}$ mass insertions are generated through the b_1 and b_7 coefficients in the MFV expansion of the soft masses (4.32) and, as discussed in [277, 276, 326], gluino contributions to the $b \to s\gamma$ transition can be sizable also in MFV whenever $\mu \tan\beta$ is large.

The case of large $\tan\beta$ and a flavor blind soft sector

In case of a completely flavor blind soft sector, i.e. for squark soft masses that are proportional to the identity and trilinear couplings that are proportional to the respective Yukawa couplings, there are only Higgs and Higgsino contributions to the Wilson coefficients $C_{7,8}^{\mathrm{NP}}$ at the leading order. However, for large values of $\tan\beta$ also beyond leading order corrections have to be taken into account and we refer to [295, 124] for details on the consistent treatment of these corrections. As the charged Higgs contributions are not $\tan\beta$ enhanced, we only report the chargino contributions here

$$C_{7,8}^{\tilde{\chi}^\pm} = \frac{2m_t^2}{\tilde{m}^2}\frac{\tan\beta}{1+\epsilon_0^*\tan\beta}\frac{A_t\mu}{\tilde{m}^2}\; f_{7,8}^{(5)}(x_\mu)\;. \tag{6.12}$$

The $\epsilon\tan\beta$ factor appearing in (6.12) resums the $\tan\beta$ enhanced beyond leading order corrections to all orders in perturbation theory and its analytical expressions has already been discussed in section 5.1.

Even for a completely flavor blind soft sector, there are contributions involving gluinos that arise first at the 2 loop level and that have been explicitly worked out in [124]. They can lead to non-negligible effects in particular in C_8 and read

$$C_{7,8}^{\tilde{g}} = -\frac{\alpha_s}{4\pi}\frac{\tan^2\beta}{(1+\epsilon_0^*\tan\beta)(1+\epsilon_b^*\tan\beta)}\,\frac{m_t^2}{\tilde{m}^2}\,\frac{\mu A_t}{\tilde{m}^2}\,\frac{\mu M_{\tilde{g}}}{\tilde{m}^2} f_1(x_\mu)\tilde{f}_{7,8}(x_g)\ . \tag{6.13}$$

The suppression of these contributions by $\alpha_s/4\pi \simeq 0.01$ can be compensated by the additional factor $\tan\beta$. They are consistently included in our numerical analysis using the general procedure described in [295].

Finally we mention that in principle for large $\tan\beta$ there are also neutral Higgs contributions to the Wilson coefficients $C_{7,8}$ [44, 295, 124]. However they were found to give corrections only at the percent level and therefore we will not discuss them here.

The case of large $\tan\beta$ and general flavor mixing

The large $\tan\beta$ regime with non-trivial flavor structures is the most involved case and an extensive discussion of all possible contributions to the Wilson coefficients is beyond the scope of this presentation. Instead we content ourselves with a short qualitative discussion of the most important new effects that in principle have to be taken into account. For explicit analytical expressions we refer to [297].

In addition to the contributions in the above subsection, in the case of general flavor mixing there are of course again Wino and gluino contributions at the leading order, that have to be appropriately modified by $\tan\beta$ enhanced corrections at the beyond leading order.

Furthermore, the beyond leading order corrections now are also sensitive to the additional flavor structures. In particular $(\delta_d^{RR})_{32}$ mass insertions can lead to Higgs and chargino contributions to the primed Wilson coefficients $C'_{7,8}$ beyond the leading order. As the Higgs contributions decouple with the Higgs mass and not with the SUSY scale, these effects might become important for very heavy SUSY spectrum, where the chargino and gluino contributions decouple to a large extent.

To summarize this section we stress that generically large contributions to the Wilson coefficients of the magnetic and chromomagnetic operators are expected in the MSSM. Even for a MSSM with flavor blind soft terms, there are Higgsino contributions to $C_{7,8}$ that are $\tan\beta$ enhanced and already for moderate values of $\tan\beta$ they can lead to large effects. In fact, observables that are sensitive to these Wilson coefficients are particularly well suited to probe the MSSM with minimal flavor violation. The $\mathrm{BR}(B \to X_s\gamma)$ and $\mathrm{BR}(B \to X_s\ell^+\ell^-)$ are the most important constraints, while in the presence of additional CP violating phases, in particular CP asymmetries like $A_{\mathrm{CP}}(b \to s\gamma)$, $S_{\phi K_S}$, $S_{\eta' K_S}$ and the CP asymmetries in the $B \to K^*\ell^+\ell^-$ decay are very sensitive probes of the flavor and CP violating structure of the MSSM.

6.3 Scalar Contributions to the $B_{s,d} \to \mu^+\mu^-$ Decays

While, as discussed in section 3.2.4, the contributions to the $B_s \to \mu^+\mu^-$ decay from the SM operator are strongly helicity suppressed, this suppression is absent for contributions

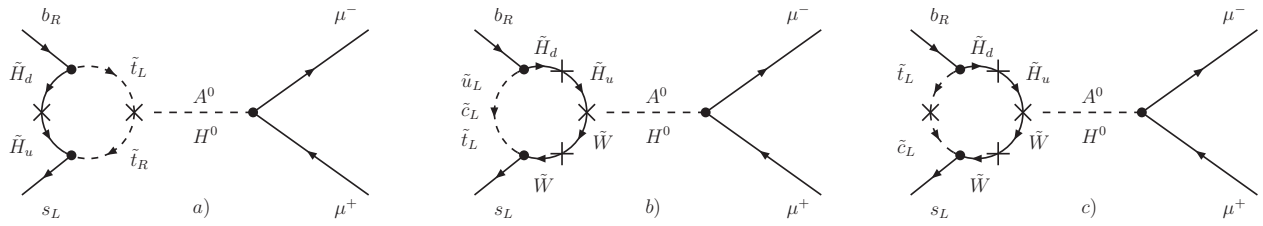

Figure 6.4: Leading order chargino contributions to the Wilson coefficients $C_{S,P}$. The neutral Higgs propagators have to be attached to the external quark legs.

coming from scalar and pseudoscalar operators. Therefore in NP models that induce scalar operators, the $\mathrm{BR}(B_s \to \mu^+\mu^-)$ can be strongly enhanced. In fact in the MSSM, Higgs penguin diagrams can lead to contributions that are proportional to $\tan^6\beta$ at the level of the branching ratio and easily lead to order of magnitude enhancements compared to the tiny SM prediction. SUSY contributions to $B_s \to \mu^+\mu^-$ have been extensively discussed in the literature. In particular, the Higgs penguin contributions have received a lot attention [327, 290, 328, 292, 329, 330, 295, 293]. A collection of the full set of 1 loop contributions can be found in [331].

Before presenting in detail the most important MSSM contributions we make some general comments. In the effective two Higgs doublet model description of the MSSM at large $\tan\beta$ as briefly described in chapter 5, the MSSM contributions to $B_s \to \mu^+\mu^-$ arise from 1 loop exchange of a charged Higgs and already at tree level from effective flavor changing $\bar{b}sH^0$ and $\bar{b}sA^0$ vertices. However, these effective vertices are induced at the 1 loop level through the exchange of SUSY particles. Therefore, following a standard loop expansion, the Wilson coefficients of the scalar and pseudoscalar $\bar{s}b\bar{\mu}\mu$ operators (see (3.75)) can be decomposed into Higgs top quark, chargino up squark, gluino down squark and neutralino down squark contributions

$$C_{S,P}^{(\prime)\,\mathrm{SUSY}} = C_{S,P}^{(\prime)\,H^\pm} + C_{S,P}^{(\prime)\,\tilde{\chi}^\pm} + C_{S,P}^{(\prime)\,\tilde{g}} + C_{S,P}^{(\prime)\,\tilde{\chi}^0} \ . \tag{6.14}$$

As usual, neutralino contributions are basically always negligible and we do not consider them here. The leading effects come from chargino and gluino diagrams that lead to contributions to the Wilson coefficients that are proportional to $\tan^3\beta$. Charged Higgs diagrams on the other hand give contributions that are only proportional to $\tan^2\beta$ [332] and also those we do not consider here.

In the following discussion of the chargino and gluino contributions we neglect the small mass difference between the heavy scalar and pseudoscalar Higgs bosons $M_H^2 \simeq M_A^2$. In that case one has

$$C_P \simeq -C_S \ , \quad C_P' \simeq C_S' \ , \tag{6.15}$$

and it is sufficient to discuss only $C_S^{(\prime)}$. Finally we remark that an fully analogous discussion applies to the $B_d \to \mu^+\mu^-$ decay.

We start with the pure Higgsino contribution to the Wilson coefficient of the scalar $\bar{s}b\bar{\mu}\mu$ operator. It is shown in diagram a) in figure 6.4 and results in

$$C_S^{\tilde{\chi}^\pm} = \frac{1}{4s_W^2}\,\frac{m_\mu}{M_A^2}\,\frac{\tan^3\beta}{(1+\epsilon_b^*\tan\beta)(1+\epsilon_0^*\tan\beta)(1+\epsilon_\ell\tan\beta)}\,\frac{m_t^2}{M_W^2}\frac{A_t\mu}{\tilde{m}^2}f_1(x_\mu) \ . \tag{6.16}$$

The $\epsilon\tan\beta$ factors appearing in the above expression resum the $\tan\beta$ enhanced beyond leading order corrections to all orders in perturbation theory and their analytical expression

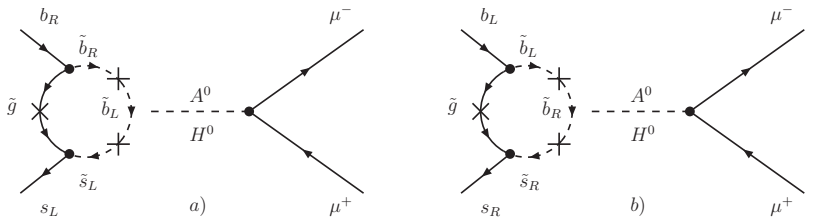

Figure 6.5: Leading order gluino contributions to the Wilson coefficients $C_{S,P}$. The neutral Higgs propagators have to be attached to the external quark legs.

is given in chapter 5. As the Higgs penguins discussed in this section are only relevant for large values of $\tan\beta$ it is of course essential to include these beyond leading order corrections. Interestingly, the Higgsino contribution (6.16) does not require any non-trivial flavor structure in the squark masses. It is also present for a completely flavor blind soft sector, proportional to $A_t\mu$ and decouples with $1/M_A^2$. The suppression of this contribution (and all the contributions discussed below) by the muon mass m_μ is more than compensated by the $\tan^3\beta$ factor. Therefore the rare flavor changing $B_s \to \mu^+\mu^-$ decay probes the large $\tan\beta$ regime of the MSSM even for a flavor blind soft sector.

In presence of a $(\delta_u^{LL})_{32}$ mass insertion or a splitting between the left handed stop and scharm masses also the Wino diagrams b) and c) in figure 6.4 contribute in addition

$$C_S^{\tilde{\chi}^\pm} = \frac{1}{2s_W^2}\,\frac{(\delta_d^{LL})_{32}}{V_{tb}V_{ts}^*}\,\frac{m_\mu}{M_A^2}\,\frac{\tan^3\beta}{(1+\epsilon_b^*\tan\beta)^2(1+\epsilon_\ell\tan\beta)}\,\frac{M_2\mu}{\tilde{m}^2}f_4(x_2,x_\mu)\ . \tag{6.17}$$

As usual, these Wino contributions vanish if the left-left *down* squark mass matrix is diagonal and typically they do not constitute the dominant effect.

Finally, for non-zero $(\delta_d^{LL})_{32}$ and $(\delta_d^{RR})_{32}$ mass insertions also gluino contributions arise as shown in figure 6.5

$$C_S^{\tilde{g}} = -\frac{1}{2s_W^2}\,\frac{8\alpha_s}{3\alpha_2}\,\frac{(\delta_d^{LL})_{32}}{V_{tb}V_{ts}^*}\,\frac{m_\mu}{M_A^2}\,\frac{\tan^3\beta}{(1+\epsilon_b^*\tan\beta)^2(1+\epsilon_\ell\tan\beta)}\,\frac{M_{\tilde{g}}\mu}{\tilde{m}^2}f_3(x_g)\ , \tag{6.18}$$

$$C_S'^{\tilde{g}} = -\frac{1}{2s_W^2}\,\frac{8\alpha_s}{3\alpha_2}\,\frac{(\delta_d^{RR})_{32}}{V_{tb}V_{ts}^*}\,\frac{m_\mu}{M_A^2}\,\frac{\tan^3\beta}{(1+\epsilon_b\tan\beta)^2(1+\epsilon_\ell^*\tan\beta)}\,\frac{M_{\tilde{g}}\mu^*}{\tilde{m}^2}f_3(x_g)\ . \tag{6.19}$$

While a $(\delta_d^{LL})_{32}$ mass insertion leads only to contributions to C_S and C_P, the only possibility to generate the primed Wilson coefficients C_S' and C_P' is in fact through gluino contributions with a $(\delta_d^{RR})_{32}$ mass insertion.

Interestingly enough, even so the scalar $\bar{s}b\bar{\mu}\mu$ operators involve a helicity flip, they are not sensitive to the helicity changing $(\delta_d^{LR})_{32}$ and $(\delta_d^{RL})_{32}$ mass insertions at the leading order. In fact, diagrams with these mass insertions correspond to *holomorphic* corrections and the corresponding Higgs vertex correction cancels at leading order with the quark field renormalization. Beyond the leading order, in principle also *non-holomorphic* corrections sensitive to $(\delta_d^{LR})_{32}$ and $(\delta_d^{RL})_{32}$ mass insertions arise. Usually these effects are subdominant and we refer to [297] for explicit expressions.

We stress that the dominant contributions to $B_s \to \mu^+\mu^-$ (and $B_d \to \mu^+\mu^-$) discussed above all arise from diagrams where the flavor change occurs in self energy corrections of the external quark lines (see figures 6.4 and 6.5). More formally speaking, they are induced

through quark field renormalization, due to *non-holomorphic* corrections to the down quark mass matrix. These *non-holomorphic* corrections can provide an additional factor of $\tan\beta$ in SUSY theories. Therefore in the MSSM, these contributions feature a $\tan^3\beta$ enhancement, which is not present in the non-supersymmetric two Higgs doublet model of type II, where the leading contributions go as $\tan^2\beta$. In fact, while in the non-supersymmetric two Higgs doublet model of type II the possible effects in $B_s \to \mu^+\mu^-$ and $B_d \to \mu^+\mu^-$ are rather limited, after the existing constraints from $\mathrm{BR}(B \to X_s\gamma)$ and $\mathrm{BR}(B^+ \to \tau^+\nu)$ are taken into account, in the MSSM still order of magnitude enhancements of these rare decays are naturally possible due to the additional $\tan\beta$ factor.

Apart from the $\tan^3\beta$ enhancement of all the contributions discussed here, another striking feature of them is, that they do not decouple with the SUSY scale but with the mass of the heavy neutral Higgs bosons. Therefore, even for very heavy squarks and gauginos beyond the LHC reach, the $B_s \to \mu^+\mu^-$ and $B_d \to \mu^+\mu^-$ decays are very sensitive probes of the squark flavor structure as long as $\tan\beta$ is large and the neutral Higgs bosons are not too heavy.

6.4 Contributions to Meson Mixing

The processes $D^0 - \bar{D}^0$, $K^0 - \bar{K}^0$, $B_d - \bar{B}_d$ and $B_s - \bar{B}_s$ mixing are described by the $\Delta F = 2$ effective Hamiltonians discussed in section 3.1.1. In a general MSSM, the Wilson coefficients of the $\Delta F = 2$ effective Hamiltonian (3.3) receive several NP contributions that can be decomposed in the following way

$$C_i^{\mathrm{SUSY}} = C_i^{H^\pm} + C_i^{\tilde{\chi}^\pm} + C_i^{\tilde{\chi}^0} + C_i^{\tilde{\chi}^0\tilde{g}} + C_i^{\tilde{g}} + C_i^{\mathrm{DP}} \ . \tag{6.20}$$

In addition to Higgs, chargino, neutralino, mixed neutralino-gluino and gluino box contributions, there are also so-called Higgs double penguin contributions that can in principle become important for $K^0 - \bar{K}^0$, $B_d - \bar{B}_d$ and $B_s - \bar{B}_s$ mixing in the large $\tan\beta$ regime. Gluino box contributions have been considered since a long time in particular in the mass insertion approximation [309] and the full set of 1 loop box contributions in the mass eigenstate basis to meson mixing in the MSSM can be found in [311, 14]. Recently also NLO corrections to the gluino boxes have been evaluated both in the mass insertion approximation [333] and working with mass eigenstates [334, 335].

Concerning the double penguins, they were first discussed in [288] in the presence of non-trivial flavor structures in the soft masses. Later the focus was mostly on MFV frameworks where these contributions were extensively studied [336, 292, 295, 337].

In the following we now discuss the main features of the most important contributions.

Box Contributions in the MFV MSSM

In MSSM frameworks with MFV the box contributions in (6.20) are generically rather limited and typically lie well within the large theoretical uncertainties associated with the SM prediction of observables like ΔM_s and ΔM_d [14]. For moderate values of $\tan\beta$ there are only contributions to the Wilson coefficient C_1. All the other Wilson coefficients involve couplings that are highly suppressed by small Yukawa couplings. The chargino and gluino

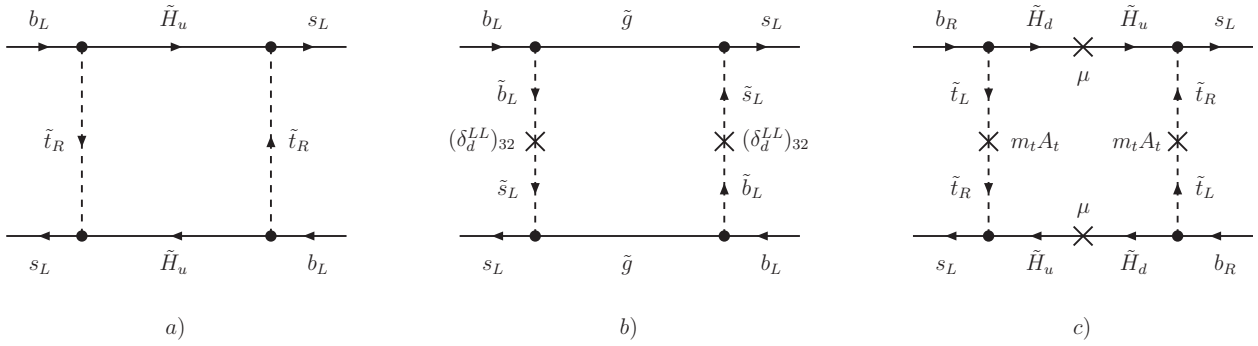

Figure 6.6: Example chargino (a,c) and gluino (b) box diagrams for $B_s - \bar{B}_s$ mixing in the MFV MSSM. Diagrams a) and b) give contributions to the Wilson coefficient C_1, while diagram c) contributes to $\tilde{C}_3$.

box contributions are the largest ones in this scenario and read in the case of $B_s - \bar{B}_s$ mixing (see figure 6.6 for example diagrams)

$$C_1^{\tilde{\chi}^\pm} \simeq \frac{\alpha_2^2}{\tilde{m}^2}(V_{tb}V_{ts}^\star)^2 \left(b_1^2 F_1^{(1)}(x_2) + \frac{m_t^4}{M_W^4} F_1^{(2)}(x_\mu) \right) , \tag{6.21}$$

$$C_1^{\tilde{g}} \simeq \frac{\alpha_s^2}{\tilde{m}^2} b_1^2 (V_{tb}V_{ts}^\star)^2 G_1(x_g) . \tag{6.22}$$

Contributions to $K^0 - \bar{K}^0$ and $B_d - \bar{B}_d$ mixing are obtained by an appropriate replacement of CKM elements. Minimal Flavor Violation contributions to $D_0 - \bar{D}_0$ mixing are always negligible. The chargino contributions (6.21) contain both Higgsino and Wino contributions. The Wino contributions are proportional to the real MFV parameter b_1 that leads to a mass splitting between the left handed stops and scharms (see (4.32)). Without such a splitting the Wino contributions would vanish due to the super-GIM mechanism. Also the gluino contributions (6.22) are proportional to b_1 that, if non-zero, introduces flavor off-diagonal entries in the left-left block of the down squark mass matrix according to (4.32). We note that all the above contributions are aligned in phase with the SM contribution. While MFV charged Higgs and chargino contributions always interfere constructively with the SM contribution (see also the model independent analysis in [338]), the gluino contributions can also have the opposite sign, if $x_g \gtrsim 2.4$. Still, once all MFV contributions are taken into account simultaneously, their sum is basically always positive [14].

None of the above contributions are sensitive to possible CP violating phases in the MFV MSSM. For large values of $\tan\beta$ additional box contributions to the Wilson coefficients might become important that are sensitive to such phases. The most important effect comes from chargino loops, that now can also contribute to the Wilson coefficient $\tilde{C}_3$ (an example diagram is shown in figure 6.6)

$$\begin{aligned} \tilde{C}_3^{\tilde{\chi}^\pm} \simeq \frac{\alpha_2^2}{\tilde{m}^2}\frac{m_b^2}{\tilde{m}^2}(V_{tb}V_{ts}^*)^2 \frac{\tan^2\beta}{(1+\epsilon_b^*\tan\beta)^2} \left(\frac{\mu^2 M_2^2}{\tilde{m}^4}(b_1 + y_b^2 b_3)^2 F_3^{(1)}(x_2, x_\mu) \right. \\ \left. + \frac{m_t^2}{M_W^2}\frac{\mu^2 A_t M_2}{\tilde{m}^4}(b_1 + y_b^2 b_3) F_3^{(2)}(x_2, x_\mu) + \frac{m_t^4}{M_W^4}\frac{\mu^2 A_t^2}{\tilde{m}^4} F_3^{(3)}(x_\mu) \right) . \end{aligned} \tag{6.23}$$

The $\epsilon \tan\beta$ factor appearing in the above expression resums $\tan\beta$ enhanced beyond leading order corrections to all orders in perturbation theory and its analytical expression has already

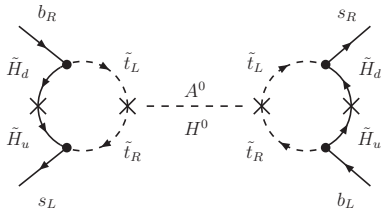

Figure 6.7: Most important double Higgs penguin contribution to $B_s - \bar{B}_s$ mixing in the MFV MSSM at large $\tan\beta$. The neutral Higgs propagator has to be attached to the external quark legs.

been discussed in section 5.1. The m_b^2 suppression in (6.23) is compensated by the $\tan^2\beta$ factor and one might expect this contribution to give non-negligible effects in the large $\tan\beta$ regime in the case of $B_s - \bar{B}_s$ and $B_d - \bar{B}_d$ mixing. In the case of $K^0 - \bar{K}^0$ mixing, these contributions are proportional to m_s^2 and always completely negligible. We note that the chargino contribution (6.23) can be complex for complex μA_t, μM_2 or b_3.

For large $\tan\beta$ there are also additional chargino and gluino box contribution to the Wilson coefficient C_1, as now also the complex parameter b_3 in (4.32) can induce flavor off-diagonal entries in the down squark mass. They are easily obtained by replacing $b_1 \to b_1 + b_3 y_b^2$ in the expressions (6.21) and (6.22).

As we will see in section 8.1, all the above potentially complex box contributions have only marginal impact on $B_s - \bar{B}_s$ and $B_d - \bar{B}_d$ mixing, once all existing constraints from other FCNC processes are taken into account.

Double Higgs Penguins in the MFV MSSM

In MFV MSSM scenarios with large $\tan\beta$ also the double Higgs penguin contributions mentioned at the beginning of this section can lead to sizable effects [336, 292, 295]. Typically considered are the diagrams with Higgsino loops shown in figure 6.7 that contribute also for a completely flavor blind soft sector. In case of $B_s - \bar{B}_s$ mixing they lead to the following contribution to the Wilson coefficient C_4

$$C_4^{\rm DP} = \frac{\alpha_2^3}{4\pi}\frac{m_b m_s}{M_W^2}\frac{\tan^4\beta}{|1+\epsilon_b\tan\beta|^2|1+\epsilon_0\tan\beta|^2}\frac{1}{M_A^2}\frac{|\mu A_t|^2}{\tilde{m}^4}\frac{m_t^4}{8M_W^4}\big(f_1(x_\mu)\big)^2\,(V_{tb}V_{ts}^*)^2\,. \quad (6.24)$$

A priori one would expect also contributions to $\tilde{C}_3$ that are proportional to m_b^2 for $B_s - \bar{B}_s$ and $B_d - \bar{B}_d$ mixing and proportional to m_s^2 for $K^0 - \bar{K}^0$. However it turns out that these contributions vanish exactly if tree level relations between neutral Higgs masses and mixing angles are employed. The most important contributions are then indeed the ones to C_4 given in (6.24) that are proportional to $m_b m_s$ in the case of $B_s - \bar{B}_s$ mixing [295, 337], while in $B_d - \bar{B}_d$ and $K^0 - \bar{K}^0$ mixing they are fully negligible. We also mention that in $D^0 - \bar{D}^0$ mixing double penguins are always negligible as they do not possess any $\tan\beta$ enhancement.

Although in a standard loop expansion the double penguins arise first at the 2 loop level they are enhanced by $\tan^4\beta$ and therefore important in the large $\tan\beta$ regime. As can be seen in (6.24), they are aligned in phase with the SM contribution and always suppress the mass difference ΔM_s compared to the SM prediction.[1] The strong $\tan^4\beta$ enhancement arises

[1] As discussed in [124, 339], for a large splitting of the third generation squark masses from the first two generations, the double penguins in principle become sensitive to flavor blind phases. This effect might become relevant for negative values of μ [124] which we do not consider here.

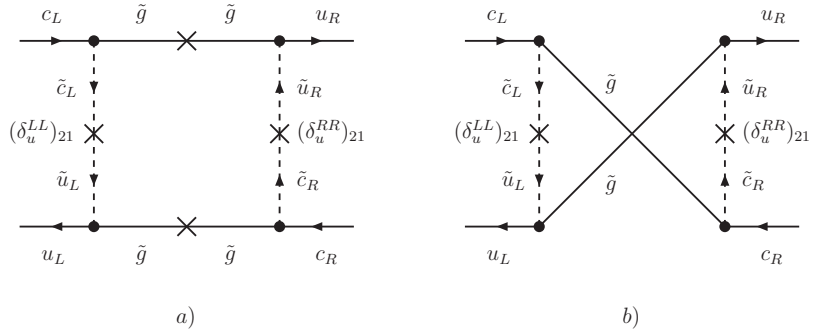

Figure 6.8: Examples of leading order gluino contributions to $D^0 - \bar{D}^0$ mixing in the presence of non-trivial flavor structures in the squark masses. The diagrams show examples of the case when both $(\delta_u^{LL})_{21}$ and $(\delta_u^{RR})_{21}$ mass insertions are present, which leads to strongly enhanced contributions to the Wilson coefficients C_4 and C_5.

from the fact that the double penguins are generated through quark field renormalization due to non-holomorphic corrections to the down quark mass matrix as it was the case in $B_s \to \mu^+\mu^-$ discussed in section 6.3. In fact, the scalar contributions to $B_s \to \mu^+\mu^-$ are strongly correlated with the double Higgs penguin contributions to $B_s - \bar{B}_s$ mixing and, apart from very fine tuned regions in parameter space, these contributions are now severely constrained by the upper bound on the branching ratio of the rare decay $B_s \to \mu^+\mu^-$ [340, 15, 337]. This statement remains true if in addition to (6.24) also MFV Wino and gluino loops are taken into account that can arise for non-zero values of the MFV parameters b_1 and b_3 and that, for complex b_3, can in principle be complex.

Gluino Box Contributions in Presence of Non-Trivial Flavor Structures

In MSSM scenarios with non-trivial flavor structures in the squark masses, the dominant contributions to the Wilson coefficients come naturally from gluino boxes. At leading order in the mass insertion approximation they read [309]

$$C_1^{\tilde{g}} = \frac{\alpha_s^2}{\tilde{m}^2}\left[(\delta_u^{LL})_{21}\right]^2 G_1(x_g)\,, \qquad \tilde{C}_1^{\tilde{g}} = \frac{\alpha_s^2}{\tilde{m}^2}\left[(\delta_u^{RR})_{21}\right]^2 G_1(x_g)\,, \tag{6.25}$$

$$C_2^{\tilde{g}} = \frac{\alpha_s^2}{\tilde{m}^2}\left[(\delta_u^{LR})_{21}\right]^2 G_2(x_g)\,, \qquad \tilde{C}_2^{\tilde{g}} = \frac{\alpha_s^2}{\tilde{m}^2}\left[(\delta_u^{RL})_{21}\right]^2 G_2(x_g)\,, \tag{6.26}$$

$$C_3^{\tilde{g}} = \frac{\alpha_s^2}{\tilde{m}^2}\left[(\delta_u^{LR})_{21}\right]^2 G_3(x_g)\,, \qquad \tilde{C}_3^{\tilde{g}} = \frac{\alpha_s^2}{\tilde{m}^2}\left[(\delta_u^{RL})_{21}\right]^2 G_3(x_g)\,, \tag{6.27}$$

$$C_4^{\tilde{g}} = \frac{\alpha_s^2}{\tilde{m}^2}\Big(\left[(\delta_u^{LL})_{21}(\delta_u^{RR})_{21}\right] G_4(x_g) + \left[(\delta_u^{LR})_{21}(\delta_u^{RL})_{21}\right]\tilde{G}_4(x_g)\Big)\,, \tag{6.28}$$

$$C_5^{\tilde{g}} = \frac{\alpha_s^2}{\tilde{m}^2}\Big(\left[(\delta_u^{LL})_{21}(\delta_u^{RR})_{21}\right] G_5(x_g) + \left[(\delta_u^{LR})_{21}(\delta_u^{RL})_{21}\right]\tilde{G}_5(x_g)\Big)\,. \tag{6.29}$$

Example diagrams that lead to these expressions are shown in figure 6.8. In (6.25) - (6.29), we restricted ourselves to the case of $D^0 - \bar{D}^0$ mixing. Contributions in the other neutral meson systems are trivially obtained by appropriate replacements of the mass insertions.

From the above expressions we observe that if both δ^{LL} and δ^{RR} mass insertions are present, the operators Q_4 and Q_5 are induced that are enhanced through QCD renormalization group effects [48, 49] and in case of $D^0 - \bar{D}^0$ and $K^0 - \bar{K}^0$ mixing also strongly chirally

enhanced. We note in addition that especially the loop function G_4 entering the Wilson coefficient $C_4^{\tilde{g}}$ is roughly a factor 30 larger than the one entering $C_1^{\tilde{g}}$ (see appendix A.1). Also if both δ^{LR} and δ^{RL} mass insertions are present, the operators Q_4 and Q_5 are generated. However the corresponding loop functions entering the Wilson coefficients $C_4^{\tilde{g}}$ and $C_5^{\tilde{g}}$ are significantly smaller with $G_4(1)/\tilde{G}_4(1) \simeq 6$. We also mention that in case of $B_s - \bar{B}_s$ mixing the contributions coming from the $(\delta_d^{LR})_{32}$ and $(\delta_d^{RL})_{32}$ mass insertions are negligible, because they are tightly constrained by $\mathrm{BR}(B \to X_s\gamma)$ (see chapter 7). In consequence, the by far largest contributions to meson mixing can be generated in frameworks where both δ^{LL} and δ^{RR} mass insertions are simultaneously non-zero.

We remark that in case of $K^0 - \bar{K}^0$ mixing also contributions might become important that are higher order in the mass insertion approximation. In particular in scenarios with very small mass insertions in the $s-d$ sector sizable effects in $K^0 - \bar{K}^0$ mixing can in principle be still generated through effective $(s \to d)$ mass insertions that are induced by a double flavor flip $(s \to b) \times (b \to d)$. Results for the Wilson coefficients with one effective $(s \to d)$ transition are obtained in the third order of the mass insertion approximation. Restricting ourselves only to δ^{LL} and δ^{RR} mass insertions, we find [21]

$$C_1^{\tilde{g}} = \frac{\alpha_s^2}{\tilde{m}^2}\left[(\delta_d^{LL})_{21}(\delta_d^{LL})_{23}(\delta_d^{LL})_{31}\right] G_1^{(2)}(x_g) \,, \tag{6.30}$$

$$\tilde{C}_1^{\tilde{g}} = \frac{\alpha_s^2}{\tilde{m}^2}\left[(\delta_d^{RR})_{21}(\delta_d^{RR})_{23}(\delta_d^{RR})_{31}\right] G_1^{(2)}(x_g) \,, \tag{6.31}$$

$$C_4^{\tilde{g}} = \frac{\alpha_s^2}{\tilde{m}^2}\frac{1}{2}\left[(\delta_d^{LL})_{21}(\delta_d^{RR})_{23}(\delta_d^{RR})_{31} + (\delta_d^{LL})_{23}(\delta_d^{LL})_{31}(\delta_d^{RR})_{21}\right] G_4^{(2)}(x_g) \,, \tag{6.32}$$

$$C_5^{\tilde{g}} = \frac{\alpha_s^2}{\tilde{m}^2}\frac{1}{2}\left[(\delta_d^{LL})_{21}(\delta_d^{RR})_{23}(\delta_d^{RR})_{31} + (\delta_d^{LL})_{23}(\delta_d^{LL})_{31}(\delta_d^{RR})_{21}\right] G_5^{(2)}(x_g) \,. \tag{6.33}$$

Finally we also have to consider the case where the $(s \to d)$ flavor transition is entirely generated by $(s \to b)$ and $(b \to d)$ transitions. We find [21]

$$C_1^{\tilde{g}} = \frac{\alpha_s^2}{\tilde{m}^2}\left[(\delta_d^{LL})_{23}(\delta_d^{LL})_{31}\right]^2 G_1^{(3)}(x_g) \,, \tag{6.34}$$

$$\tilde{C}_1^{\tilde{g}} = \frac{\alpha_s^2}{\tilde{m}^2}\left[(\delta_d^{RR})_{23}(\delta_d^{RR})_{31}\right]^2 G_1^{(3)}(x_g) \,, \tag{6.35}$$

$$C_4^{\tilde{g}} = \frac{\alpha_s^2}{\tilde{m}^2}\left[(\delta_d^{LL})_{23}(\delta_d^{LL})_{31}(\delta_d^{RR})_{23}(\delta_d^{RR})_{31}\right] G_4^{(3)}(x_g) \,, \tag{6.36}$$

$$C_5^{\tilde{g}} = \frac{\alpha_s^2}{\tilde{m}^2}\left[(\delta_d^{LL})_{23}(\delta_d^{LL})_{31}(\delta_d^{RR})_{23}(\delta_d^{RR})_{31}\right] G_5^{(3)}(x_g) \,. \tag{6.37}$$

These contributions to $K^0 - \bar{K}^0$ mixing that arise at higher order in the mass insertion approximation can be especially important in the case of hierarchical squark masses, where the first two generations of squarks are much heavier than the third one. In that case these contributions decouple with the mass of the light squarks, while the contributions involving directly $(s \to d)$ mass insertions decouple with the heavy mass. A detailed discussion of the hierarchical squark mass scenario is however beyond the scope of the present work.

Double Higgs Penguins in Presence of Non-Trivial Flavor Structures

In the large $\tan\beta$ regime of MSSM frameworks with non-trivial flavor structures in the squark masses also the double penguins can again become important. They dominantly contribute

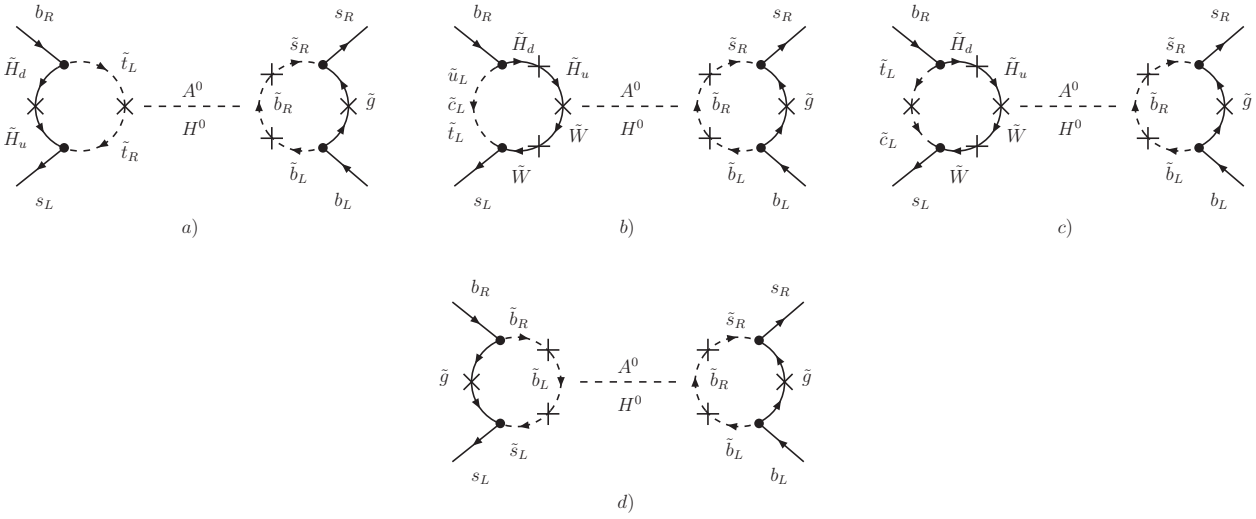

Figure 6.9: Double Higgs penguin contributions to $B_s - \bar{B}_s$ mixing in the presence of non-trivial flavor structures in the squark masses. The diagram d) shows the contribution that involves gluino loops on both sides, while in diagrams a) - c) one gluino and one chargino loop is present. The neutral Higgs propagators always have to be attached to the external quark legs.

to the Wilson coefficient C_4 and in case of $B_s - \bar{B}_s$ mixing can be approximated by

$$\begin{aligned} C_4^{\rm DP} = &\frac{\alpha_s^2\alpha_2}{4\pi}\frac{32m_b^2}{9M_W^2}\frac{\tan^4\beta}{|1+\epsilon_b\tan\beta|^4}\frac{|\mu|^2M_{\tilde{g}}^2}{M_A^2\tilde{m}^4}\ (\delta_d^{LL})_{32}(\delta_d^{RR})_{32}\ \big(f_3(x_g)\big)^2 \\ -\frac{\alpha_2^2\alpha_s}{4\pi}&\frac{2m_b^2}{3M_W^2}\frac{\tan^4\beta}{|1+\epsilon_b\tan\beta|^2(1+\epsilon_b\tan\beta)(1+\epsilon_0^*\tan\beta)}\frac{|\mu|^2A_tM_{\tilde{g}}}{M_A^2\tilde{m}^4}\frac{m_t^2}{M_W^2}(\delta_d^{RR})_{32}V_{tb}V_{ts}^*\,f_3(x_g)f_1(x_\mu) \\ &-\frac{\alpha_2^2\alpha_s}{4\pi}\frac{4m_b^2}{3M_W^2}\frac{\tan^4\beta}{|1+\epsilon_b\tan\beta|^4}\frac{|\mu|^2M_2M_{\tilde{g}}}{M_A^2\tilde{m}^4}\ (\delta_d^{LL})_{32}(\delta_d^{RR})_{32}\ f_3(x_g)f_4(x_2,x_\mu)\ . \end{aligned} \quad (6.38)$$

The first line stems from a diagram that contains two gluino loops with a $(\delta_d^{LL})_{32}$ and a $(\delta_d^{RR})_{32}$ mass insertion, respectively. The second line contains the contribution coming from a diagram with a gluino loop involving $(\delta_d^{RR})_{32}$ and a minimal flavor violating Higgsino loop. The last line finally corresponds to a diagram with the $(\delta_d^{RR})_{32}$ gluino loop and a Wino loop, induced by a $(\delta_d^{LL})_{32}$ mass insertion.

A remarkable feature of these contributions is their proportionality to m_b^2 thanks to the presence of the δ^{RR} mass insertion. This is in contrast to the MFV case where only left handed currents are present and the double Higgs penguin contributions to $B_s - \bar{B}_s$ mixing are correspondingly proportional to $m_b m_s$. Analogously to the MFV case, these double penguins are proportional to $\tan^4\beta$ and decouple with the mass of the heavy neutral Higgs bosons instead of with the SUSY scale. They are relevant both for $B_s - \bar{B}_s$ and $B_d - \bar{B}_d$ mixing and they are strongly correlated with the scalar contributions to the $B_s \to \mu^+\mu^-$ and $B_d \to \mu^+\mu^-$ decays. However, due to their enhancement of $m_b/m_{s,d}$ as compared to the MFV case, they are expected to give potentially huge contributions to $B_s - \bar{B}_s$ and $B_d - \bar{B}_d$ mixing in the large $\tan\beta$ regime.

Also in the case of $K^0 - \bar{K}^0$ mixing the double penguins can be important. Even so this might be surprising at first sight, as the contributions analogous to (6.38) are suppressed by m_s^2 in case of Kaon mixing, we note that beyond the leading order in the mass insertion

approximation this suppression can actually be circumvented. In fact if the $(s \to d)$ mass insertions are generated effectively by combined $(s \to b) \times (b \to d)$ transitions, then the most relevant effects from the neutral Higgses arise at the fourth order in the mass insertion expansion and we find the following expression

$$C_4^{\rm DP} = \frac{\alpha_s^2 \alpha_2}{4\pi} \frac{32 m_b^2}{9 M_W^2} \frac{\tan^4\beta}{|1+\epsilon_b \tan\beta|^4} \frac{|\mu|^2 M_{\tilde{g}}^2}{M_A^2 \tilde{m}^4} (\delta_d^{LL})_{23} (\delta_d^{LL})_{31} (\delta_d^{RR})_{23} (\delta_d^{RR})_{31} \big(f_5(x_g)\big)^2 \,, \qquad (6.39)$$

which can indeed induce non-negligible effects in $K^0 - \bar{K}^0$ mixing.

We summarize this section: In MSSM frameworks with MFV, box contributions to meson mixing are generically rather limited and possible effects in the mass differences lie within the associated theoretical uncertainties. This is true both for moderate and also for large values of $\tan\beta$. In the large $\tan\beta$ regime also double Higgs penguin contributions can become sizable, but only in $B_s - \bar{B}_s$ mixing, where they are proportional to $m_b m_s$. However, in most regions of parameter space, these contributions are severely constrained by the upper bound on the branching ratio of the rare decay $B_s \to \mu^+\mu^-$. While for large $\tan\beta$ the MFV contributions can in principle be complex, CP violating observables in meson mixing are found to be always SM-like as will be discussed in section 8.1.

In MSSM scenarios with a generic squark flavor structure, the dominant contributions to the Wilson coefficients come naturally from gluino boxes. Particularly large effects arise if both δ^{LL} and δ^{RR} mass insertions are present simultaneously, as the induced contributions are renormalization group enhanced, enhanced by a large loop function and in case of $D^0 - \bar{D}^0$ and $K^0 - \bar{K}^0$ mixing also strongly chirally enhanced.

If $\tan\beta$ is large, then a non-trivial squark flavor structure can also lead to important double Higgs penguin effects in $B_s - \bar{B}_s$, $B_d - \bar{B}_d$ and also in $K^0 - \bar{K}^0$ mixing. These contributions are proportional to $\tan^4\beta$ and do not decouple with SUSY scale but instead with the mass of the heavy Higgs bosons. In presence of δ^{RR} mass insertions they are proportional to m_b^2 and thus strongly enhanced compared to the MFV case. As the double penguins arise from the same mechanism as the scalar contributions to $B_{s,d} \to \mu^+\mu^-$, strong correlations between the $\Delta F = 2$ processes and $\mathrm{BR}(B_{s,d} \to \mu^+\mu^-)$ are expected in the large $\tan\beta$ regime.

In conclusion, $\Delta F = 2$ processes are particular sensitive probes of right handed flavor changing neutral currents, that in case of the MSSM arise in non-MFV frameworks in the presence of δ^{RR} mass insertions.

6.5 The $b \to s\nu\bar{\nu}$ and $s \to d\nu\bar{\nu}$ Transitions

In the MSSM there are various new contributions to the $b \to s\nu\bar{\nu}$ and $s \to d\nu\bar{\nu}$ transitions and one might expect that large effects are possible. This is indeed the case for $s \to d\nu\bar{\nu}$. However, once the existing constraints coming from other flavor changing processes are applied, the effects in $b \to s\nu\bar{\nu}$ turn out to be quite limited in the MSSM.

In the following we will discuss in detail the most important SUSY contributions to both the $b \to s\nu\bar{\nu}$ and the $s \to d\nu\bar{\nu}$ transitions.

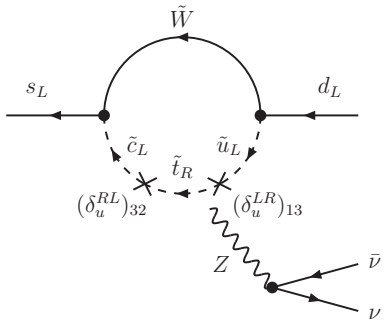

Figure 6.10: Dominant chargino contributions to the Wilson coefficient C_L^K in the presence of both $(\delta_u^{RL})_{32}$ and $(\delta_u^{LR})_{13}$ mass insertions.

The $s \to d\nu\bar{\nu}$ Transition

The $K_L \to \pi^0\nu\bar{\nu}$ and $K^+ \to \pi^+\nu\bar{\nu}$ decays that are based on the $s \to d\nu\bar{\nu}$ transition have been analyzed in the MSSM by many authors [341, 342, 343, 344, 345, 306, 275]. Sizable SUSY effects in the $s \to d\nu\bar{\nu}$ transition can be essentially generated only by two different mechanisms which both are only effective if the soft breaking terms have a non-MFV structure:

i) A non-MFV structure of the up squark trilinear couplings, in particular the simultaneous presence of $(\delta_u^{LR})_{23}$ and $(\delta_u^{RL})_{31}$ mass insertions, can lead to huge contributions to the left handed Wilson coefficient C_L^K by means of Z penguin diagrams with chargino up squark loops [343].

ii) A non-MFV structure of the down squark right-right mass matrix, in particular the simultaneous presence of $(\delta_d^{RR})_{23}$ and $(\delta_d^{RR})_{31}$ mass insertions, can lead to large contributions to the right handed Wilson coefficient C_R^K in the large $\tan\beta$ regime [306]. In that case the relevant diagrams are Z penguins with charged Higgs top quark loops, where the charged Higgs couplings receive beyond leading order corrections from gluino down squark loops.

In the first case, the relevant diagram is shown in figure 6.10 and it leads to the following contribution to the Wilson coefficient C_L^K

$$(C_L^K)^{\tilde{\chi}^\pm} = \frac{1}{s_W^2}\frac{1}{V_{td}V_{ts}^*}\left(\delta_u^{LR}\right)_{13}\left(\delta_u^{RL}\right)_{32}\frac{1}{8}f_1^\nu(x_2)\ . \tag{6.40}$$

As first pointed out in [343], a remarkable feature of the above contribution is the absence of both CKM suppression and $\mathrm{O}(M_W/M_{\mathrm{SUSY}})$ suppression. In fact the two $\mathrm{SU}(2)_L$ breaking insertions required by the Z penguin are formally provided by the left-right mixing mass insertions and therefore the $\mathrm{O}(M_W/M_{\mathrm{SUSY}})$ suppression does not appear explicitly. Furthermore, the involved mass insertions are not strongly constrained by other B and K observables. This implies that in a setup with large $(\delta_u^{LR})_{23}$ and $(\delta_u^{RL})_{31}$ mass insertions large departures from the SM expectations in both the charged and neutral $K \to \pi\nu\bar{\nu}$ decays are allowed, as confirmed by the complete analyses in [345, 275]. We remark however that the recent measurement of $D^0 - \bar{D}^0$ mixing does put constraints on the mass insertion combination $(\delta_u^{LR})_{23}(\delta_u^{RL})_{31}$ and the allowed room for NP effects in the $K \to \pi\nu\bar{\nu}$ decays should be reconsidered in the light of the new experimental results.

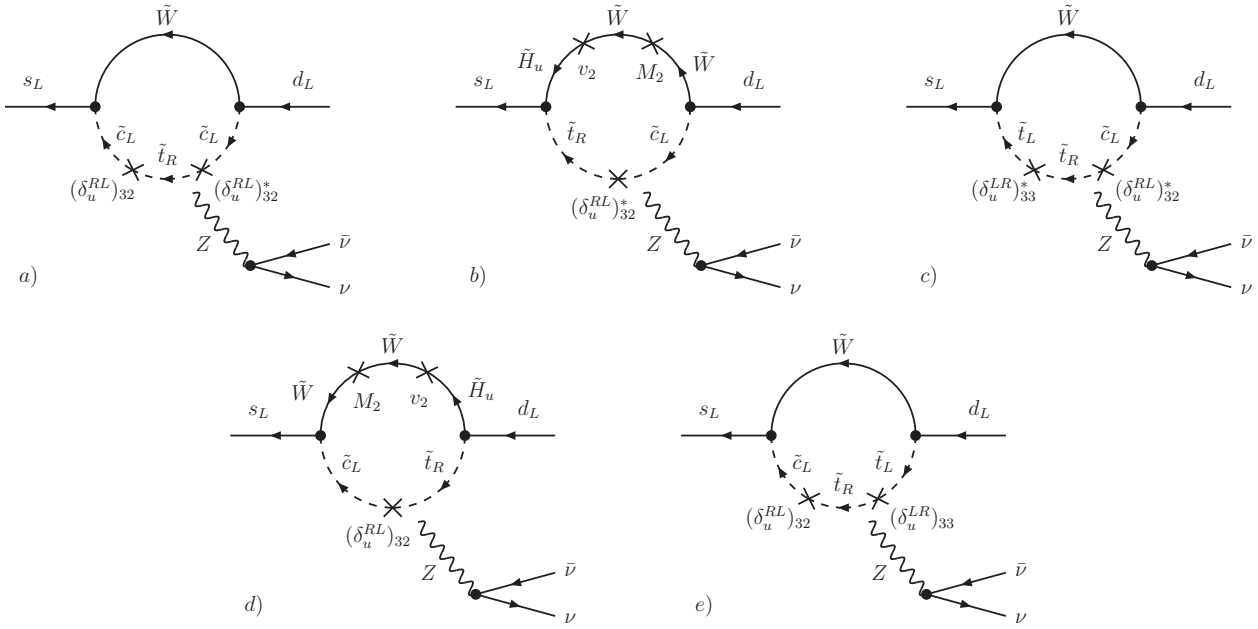

Figure 6.11: Dominant chargino contributions to the Wilson coefficient C_L^K in the presence of only a $(\delta_u^{RL})_{32}$ mass insertion.

As noted in [275], either of the mass insertions is in principle sufficient to generate large effects in the $s \to d\nu\bar{\nu}$ transition as the second mass insertion is effectively always generated through non-diagonal entries in the CKM matrix. The corresponding chargino contributions to C_L^K are then proportional to $V_{cd}V_{cs}^*|(\delta_u^{RL})_{32}|^2$ or $V_{ud}V_{us}^*|(\delta_u^{RL})_{31}|^2$, respectively, and only suppressed by one power of the Cabibbo angle λ.

The $(\delta_u^{RL})_{32}$ case has been worked out in detail by us in [20]. The relevant diagrams are shown in figure 6.11 and they lead to the following approximate expression for the Wilson coefficient C_L^K

$$\begin{aligned}(C_L^K)^{\tilde{\chi}^\pm} &= \frac{1}{s_W^2}\frac{V_{cd}V_{cs}^*}{V_{td}V_{ts}^*}|(\delta_u^{RL})_{32}|^2\frac{1}{8}f_1^\nu(x_2) \\ &\quad -\frac{1}{s_W^2}\left(\frac{V_{cs}^*}{V_{ts}^*}(\delta_u^{RL})_{32}+\frac{V_{cd}}{V_{td}}(\delta_u^{RL})^*_{32}\right)\left[\frac{m_t A_t}{8\tilde{m}^2}f_1^\nu(x_2)-\frac{m_t M_2}{4\tilde{m}^2}f_2^\nu(x_\mu,x_2)\right] \quad (6.41)\end{aligned}$$

As stated above, the leading contribution in the first line of (6.41) receives a CKM suppression only from the matrix element V_{cd} and it is shown in diagram a) of figure 6.11. It gives an almost real contribution to the combination $\lambda_t C_L^K$ and therefore dominantly leads to effects in the charged decay mode $K^+ \to \pi^+\nu\bar{\nu}$, that turn out to always suppress the branching ratio compared to the SM prediction.

The subleading contributions shown in diagrams b) to e) of figure 6.11 on the other hand involve also V_{ts} and V_{td}. In particular, they introduce sensitivity to the phase of $(\delta_u^{RL})_{32}$ and the phase of V_{td} and can therefore also affect the neutral mode $K_L \to \pi^0\nu\bar{\nu}$. However these contributions are suppressed compared to the one of diagram a) roughly by a factor λ^2 and therefore the effects in $\mathrm{BR}(K_L \to \pi^0\nu\bar{\nu})$ are generically much smaller than in $\mathrm{BR}(K^+ \to \pi^+\nu\bar{\nu})$ if only one mass insertion is present.

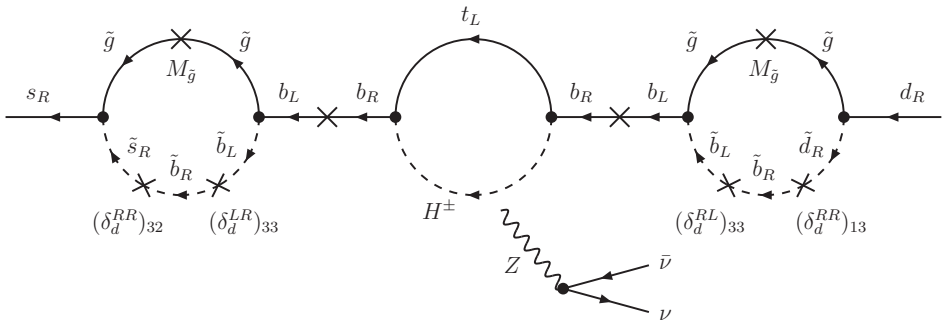

Figure 6.12: Dominant Higgs contributions to the Wilson coefficient C_R^K in the presence of both $(\delta_d^{RR})_{23}$ and $(\delta_d^{RR})_{31}$ mass insertions. Shown is the diagram in a standard loop expansion. The Z boson has to be attached to the charged Higgs top loop in all possible ways.

In the second case with a non-trivial flavor structure in the right-right down squark mass, the dominant contributions arise at the beyond leading order, through the charged Higgs diagram shown in figure 6.12. While at leading order, charged Higgs diagrams give a contribution that is suppressed by $m_d m_s/M_W^2$, beyond leading order corrections to the charged Higgs vertices can lift this suppression and lead to sizable contributions to the right handed Wilson coefficient C_R^K if $\tan\beta$ is large. One finds [306]

$$(C_R^K)^{H^\pm} = -\frac{1}{s_W^2}\frac{1}{V_{td}V_{ts}^*}\,(\delta_d^{RR})_{13}(\delta_d^{RR})_{32}\,\frac{m_b^2}{2M_W^2}\,\frac{\tan^4\beta}{|1+\epsilon_b\tan\beta|^4}\,|\epsilon_{RR}|^2\,f_3^\nu(y_t)\;, \tag{6.42}$$

where the ϵ factors have already been defined in chapter 5.

As shown in figure 6.12, this contribution appears only at the 3 loop level in a standard loop expansion, but it is largely enhanced by the $\tan^4\beta$ factor and does not contain any suppression due to light quark masses. In conclusion, this charged Higgs contribution is phenomenologically relevant only at large $\tan\beta$ and with non-MFV right-right soft breaking terms in the down sector. Interestingly, this contribution does not vanish in the limit of heavy squarks and gauginos, and has a slow decoupling with respect to the charged Higgs mass. In fact, as shown in [306], B physics constraints still allow for large non-standard effects in $K \to \pi\nu\bar{\nu}$ due to charged Higgs effects, even for flavor mixing terms of CKM size.

The $b \to s\nu\bar{\nu}$ Transition

As stated at the beginning of this section, SUSY effects in the $b \to s\nu\bar{\nu}$ transition turn out to be rather limited, once the existing constraints coming from other flavor changing processes are taken into account [346, 131, 20].

While neutralino contributions to the relevant Wilson coefficients C_L^ν and C_R^ν are generally expected to be small, gluino contributions to both C_L^ν and C_R^ν are highly constrained by the $b \to s\gamma$ decay and have only negligible impact. Charged Higgs contributions to C_L^ν scale as $1/\tan^2\beta$ and even for low values of $\tan\beta$ they play only a marginal role. Concerning the charged Higgs contributions to the right handed coefficient C_R^ν, at the leading order, they are proportional to $m_s m_b \tan^2\beta$ and therefore negligible even for large values of $\tan\beta$. On the other hand, non-holomorphic corrections to the Higgs couplings can enhance this contribution and can lead to important effects in the large $\tan\beta$ regime if flavor changing right handed currents are present. This is well known in the case of $s \to d\nu\bar{\nu}$ transitions

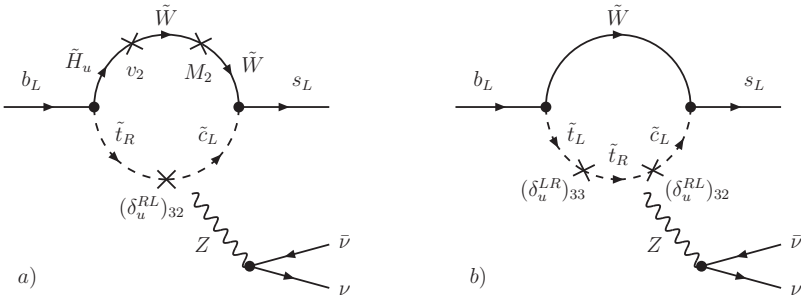

Figure 6.13: Dominant chargino contributions to the Wilson coefficient C_L^ν in the presence of a $(\delta_u^{LR})_{23}$ mass insertion.

as discussed above. In the case of $b \to s\nu\bar{\nu}$ transitions however, the upper bound on the branching ratio of the rare decay $B_s \to \mu^+\mu^-$ sets strong limits on this contribution, that then also turns out to be negligible [346, 20].

Turning to chargino contributions to the right handed coefficient C_R^ν, at the leading order they are also suppressed by $m_s m_b \tan^2\beta$, as the Higgs contributions are, and therefore negligible. One is then left with the chargino contributions to the left handed coefficient C_L^ν that are the only ones where sizable effects are still possible. Largest effects can be generated by a Z penguin with a $(\delta_u^{RL})_{32}$ mass insertion [347, 117, 106], that is not strongly constrained by existing data.

The Z penguin diagrams giving that contribution are shown in figure 6.13 and the corresponding analytical expression in the mass insertion approximation reads

$$(C_L^\nu)^{\tilde{\chi}^\pm} = -\frac{1}{s_W^2}\frac{V_{cs}^*}{V_{ts}^*}(\delta_u^{RL})_{32}\left[\frac{m_t A_t}{8\tilde{m}^2} f_1^\nu(x_2) - \frac{m_t M_2}{4\tilde{m}^2} f_2^\nu(x_\mu, x_2)\right] \ . \tag{6.43}$$

Concerning the structure of equation (6.43), we note that among the required two $\mathrm{SU}(2)_L$ breaking insertions in the Z penguin, one is formally provided by the helicity and flavor changing mass insertion $(\delta_u^{RL})_{32}$ and the other one by a Higgsino-Wino mixing (diagram a) or a flavor conserving helicity flip for the stop (diagram b), respectively.

To summarize, the contributions to C_R^ν in the MSSM turn out to be very small which implies that the longitudinal polarization fraction in the $B \to K^*\nu\bar{\nu}$ decay, F_L, is always SM-like (see section 3.2.5 for details). Non-standard effects in the branching ratios of the $B \to X_s\nu\bar{\nu}$, $B \to K\nu\bar{\nu}$ and $B \to K^*\nu\bar{\nu}$ decays can however be generated by chargino contributions to C_L^ν through a large $(\delta_u^{RL})_{32}$ mass insertion and the SM predictions of the branching ratios of these decays can be modified by up to 50% [20].

6.6 The Anomalous Magnetic Moment of the Muon

The operator that induces the anomalous magnetic moment of the muon is helicity changing which implies that the SM contributions to $(g-2)_\mu$ are necessarily proportional to the muon mass m_μ. This helicity suppression can in principle be lifted in NP scenarios. In particular in the MSSM there are Wino and Bino contributions that are enhanced by $\tan\beta$ and the induced SUSY effects in $(g-2)_\mu$ are naturally of the size of the current experimental discrepancy (3.119).

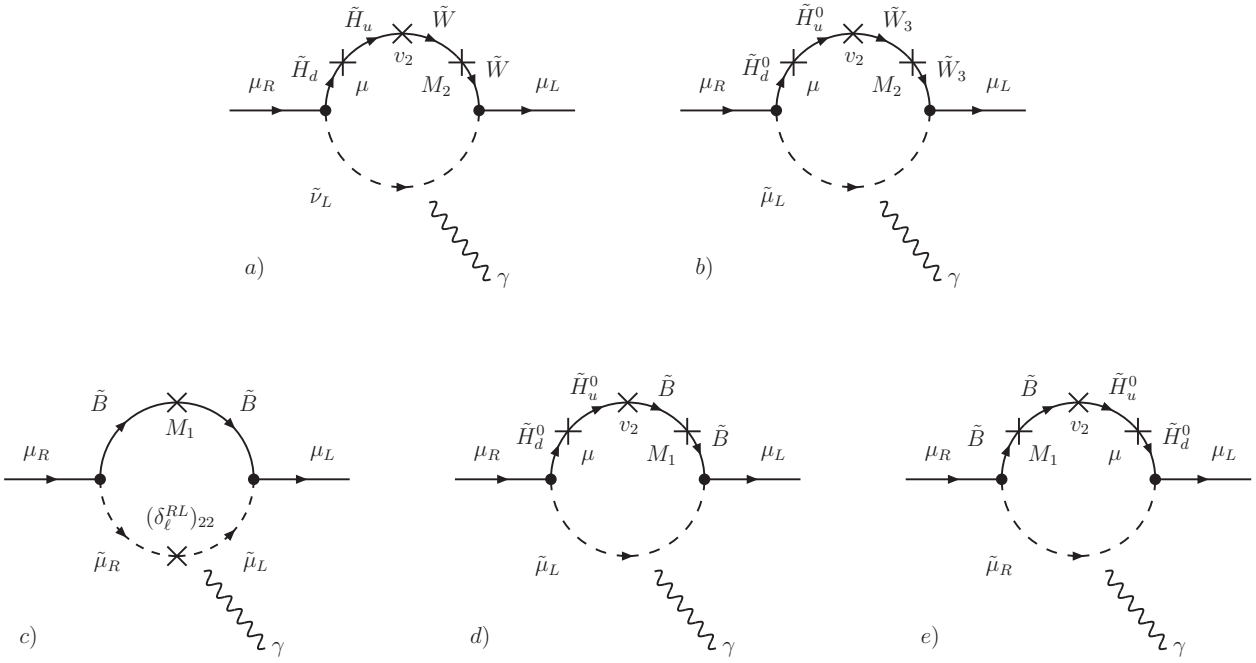

Figure 6.14: Dominant leading order SUSY contributions to the anomalous magnetic moment of the muon. The first line shows the Wino contributions, the second line the Bino contributions. The photon line is attached to the loops in all possible ways.

The full 1 loop SUSY contributions to $(g-2)_\mu$ in the general MSSM are known since long time [348] and the phenomenological implications for supersymmetric theories have been thoroughly studied, see e.g. [349, 350, 351, 352, 353]. A review on $(g-2)_\mu$ in supersymmetry and a much more complete list of references can be found in [354].

While also the most important SUSY 2 loop effects are known (see again [354] for a systematic review and a list of references), in most phenomenological studies it is usually sufficient to consider the $\tan\beta$ enhanced leading order contributions [348] supplemented by the all order resummation of beyond leading order $\tan\beta$ enhanced corrections [355]. The relevant diagrams are shown in figure 6.14 and one finds

$$\begin{aligned}\Delta a_\mu^{\rm SUSY} &= \frac{\alpha_2}{4\pi} m_\mu^2 \, \frac{\tan\beta}{1+\epsilon_\ell \tan\beta} \, \frac{\mu M_2}{\tilde{m}_\ell^4} a_1(x_2, x_\mu) \\ &+ \frac{\alpha_1}{4\pi} m_\mu^2 \, \frac{\tan\beta}{1+\epsilon_\ell \tan\beta} \, \frac{\mu M_1}{\tilde{m}_\ell^4} \left(a_2(x_1) + a_3(x_1, x_\mu)\right) \ , \end{aligned} \tag{6.44}$$

In view of the constraints on flavor diagonal phases from the EDMs discussed in section 6.7, we assumed here μ, M_1 and M_2 to be real. The Wino contributions in the first line of (6.44) are typically dominant compared to the Bino contributions that are parametrically suppressed by α_1. Only in certain corners of parameter space with very heavy left handed sleptons and light right handed sleptons also the Bino contributions can become non-negligible. In fact, if the left handed sleptons have a very large mass, then all SUSY contributions to $(g-2)_\mu$ decouple, apart from the Bino contribution, shown in diagram e) of figure 6.14.

Still, in most part of the parameter space the Wino contribution in (6.44) is the most important one, and its sign is determined by $\text{sign}(\mu M_2)$. Therefore the current data on $(g-2)_\mu$ usually excludes a relative minus sign between μ and M_2 at more than 3σ. We

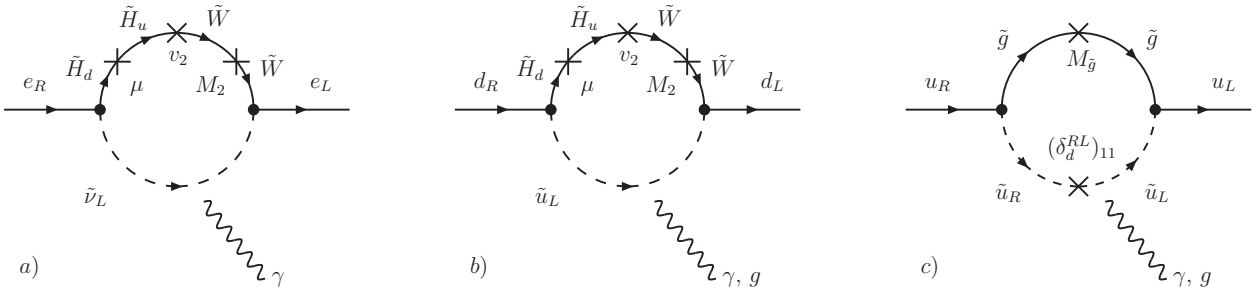

Figure 6.15: Example 1 loop contributions to the (C)EDMs in the presence of flavor diagonal phases. While diagram a) shows a Wino contribution to the electron EDM, diagrams b) and c) contribute to the down quark and up quark (C)EDMs by means of Higgsino and gluino loops, respectively. In all diagrams the photon and gluon lines are attached to the loops in all possible ways.

remind that also the sign of the dominant contribution to the resummation factor ϵ_ℓ is determined by exactly the same parameter combination (cf. section 5.1), with ϵ_ℓ *negative* for $\text{sign}(\mu M_2) = +1$. This implies that apart from fine tuned corners in parameter space, the $(g-2)_\mu$ constraint basically excludes the possibility of positive threshold corrections to lepton masses [23]. As one consequence, the $\tan\beta$ enhanced beyond leading order corrections basically always enhance the SUSY contributions to $(g-2)_\mu$ in the phenomenologically viable regions of parameter space.

Finally we also remark that within SUSY frameworks with universal gaugino masses like the CMSSM or MSUGRA scenarios, one has of course $\text{sign}(M_{\tilde{g}}) = \text{sign}(M_2) = \text{sign}(M_1)$ and $(g-2)_\mu$ basically always selects a positive sign for the μ parameter as the only phenomenologically viable option.

6.7 The Electric and Chromoelectric Dipole Moments

The SM predictions of the electric dipole moments are well below the current and future experimental sensitivities. This is in contrast to the generic contributions in NP models and in particular in the MSSM that in general contains many additional sources of CP violation to the SM CKM phase.

Within a MSSM framework, CP violating sources naturally appear through i) the phases of flavor conserving parameters as the μ parameter the gaugino masses and the flavor diagonal part of the trilinear couplings of the squarks and sleptons and ii) through complex flavor violating parameters, i.e. complex flavor off-diagonal entries in the squark and slepton masses.

The induced contributions to the EDMs coming from these sources have been analyzed in many dedicated studies in the literature [356, 357, 358, 359, 360, 90, 361, 362, 363, 195, 364, 365, 307, 366] (see also [367] for a recent review and more references). In the following we will discuss both classes of EDMs concentrating on those contributions that will be most relevant later in the analysis of concrete SUSY models in chapter 8.

Electric Dipole Moments Generated by Flavor Diagonal Phases

In figure 6.15 we show some examples of 1 loop diagrams that contribute to the (C)EDMs of the up and down quark as well as the electron. A common feature of these contributions as well as all the other 1 loop contributions coming from flavor diagonal phases is their proportionality to the light quark and lepton masses. Still, as these contributions arise already at the 1 loop level, they generically lead to predictions for the EDMs much above the experimental constraints. The source of these contributions are the imaginary parts of the parameter combinations μM_i, μA_j and $M_i A_j^*$ with $i = 1, 2, 3$ and $j = u, d, e$. Natural O(1) values for the phases of the μ term, the gaugino masses M_i and trilinear couplings A_j then lead to huge contributions to the EDMs. In fact the experimental EDM constraints (3.121) - (3.123) impose very stringent bounds on these flavor diagonal phases at the level of $10^{-3} - 10^{-2}$. This fact is often referred to as the *SUSY CP problem*.

As long as one does not assume strong cancellations between different contributions to the EDMs [358, 368], then the responsible 1 loop induced effects due to O(1) flavor diagonal phases to the (C)EDMs of the electron and the light quarks can basically only be suppressed in two ways that both require non-universal soft SUSY breaking terms at the low scale

i) Heavy first and second generation squarks [369, 370] at the level of several 10 TeV that lead to a decoupling of the effects in the EDMs of the light quarks and leptons. This solution can be compatible with the motivation of SUSY as a solution to the hierarchy problem as long as the third generation of squarks remains around the TeV scale. Given the light third squark generation, such a scenario can for example be probed through CP violating B physics observables.

ii) Hierarchical trilinear couplings [371, 372, 373]. In particular, if an approximate alignment between the phases of the μ term and the gaugino masses exists then all flavor diagonal CP violating effects arise from the trilinear couplings. Choosing the trilinear couplings of the first two generations of squarks either real or very small, the contributions to the EDMs can be kept small. Such a scenario can for example be realized in the general MFV ansatz (4.32), if $\tilde{A}_u$ is real and all CP violation arises from the coefficient b_6 [279]. Also this scenario can be probed through B physics observables, in particular those that are sensitive to complex values of the stop trilinear coupling A_t.

However, even in the above cases, additional flavor diagonal contributions to the EDMs stemming from 2 loop diagrams are unavoidable and typically large [359]. These so-called Barr-Zee type diagrams [374] shown in figure 6.16 involve the third sfermion generations and lead to the following expressions [359]

$$\frac{d_f}{e} = Q_f \frac{3\alpha_{\rm em}}{32\pi^2} \frac{R_f m_f}{M_A^2} \sum_{q=t,b} Q_q^2 y_q^2 \frac{{\rm Im}(\mu A_q)}{\tilde{m}^2} f\left(\frac{\tilde{m}^2}{M_A^2}\right) , \tag{6.45}$$

$$d_f^c = \frac{\alpha_s}{64\pi^2} \frac{R_f m_f}{M_A^2} \sum_{q=t,b} y_q^2 \frac{{\rm Im}(\mu A_q)}{\tilde{m}^2} f\left(\frac{\tilde{m}^2}{M_A^2}\right) , \tag{6.46}$$

where $f(x) = \partial F(x)$ with the 2 loop function F given in [359], and $R_f = \cot\beta$ for up-type quarks and $R_f = \tan\beta$ for down-type quarks and charged leptons. For moderate values of $\tan\beta$ the dominant effect is generated by the stop loop in diagram a) of figure 6.16. The

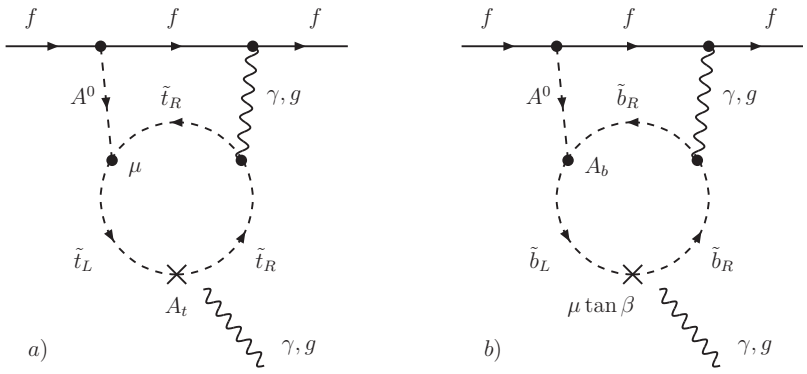

Figure 6.16: Two loop Barr-Zee type contributions to the quark and lepton (C)EDMs. Shown are the dominant diagrams involving stop and sbottom loops. The photon and gluon lines are attached to the squark loops in all possible ways.

corresponding contribution decouples with the heavier of the pseudoscalar Higgs or the stop mass. As a consequence, these contributions to the EDMs turn out to be large, provided the pseudoscalar Higgs and the 3rd generation squarks are not too heavy.

Interestingly, the diagram with the stop loop is proportional to the complex parameter combination μA_t, as the dominant contributions to the Wilson coefficients of the magnetic and chromomagnetic dipole operators C_7 and C_8 are in a flavor blind MSSM (see section 6.2). As we will analyze in section 8.1, this implies strong correlations between the EDMs and CP violating effects in observables sensitive to C_7 and C_8, as the direct CP asymmetry in $b \to s\gamma$ or the time dependent CP asymmetry $S_{\phi K_S}$ within a flavor blind MSSM scenario.

Flavored Electric Dipole Moments

Electric dipole moments cannot only be induced through flavor diagonal phases as discussed above, but also through phases of flavor violating parameters. A comprehensive analysis of these so-called *flavored* EDMs can be found in [307]. One of their most peculiar features is that they can be proportional to the heaviest fermion masses m_t, m_b and m_τ instead of the lightest ones, as it happens in the case of flavor diagonal phases. This huge enhancement factor can bring the (C)EDMs close to the current and future experimental sensitivities, providing an excellent opportunity to probe the flavor structure of the MSSM through flavor conserving observables. Such an enhancement is only possible in the presence of flavor changing right handed currents induced by δ^{RR} mass insertions. While in scenarios with only δ^{LL} mass insertions, quark and lepton EDMs can be still induced thanks to the presence of CKM matrix that allows for the required complex double flavor flip, these EDMs are proportional to the external light quark and lepton masses.

In the following we will therefore concentrate on the most important case of the *flavored* EDMs in the presence of both δ^{RR} and δ^{LL} mass insertions. The general case is discussed in detail in [307]. While *flavored* EDMs exist both in the quark and lepton sector, here we will only treat the quark case because this will be the one relevant for the analysis of concrete SUSY models in chapter 8.

The diagrams responsible for the dominant gluino contributions to the down, strange and up quark (C)EDMs in the presence of δ^{RR} and δ^{LL} mass insertions are shown in figure 6.17.

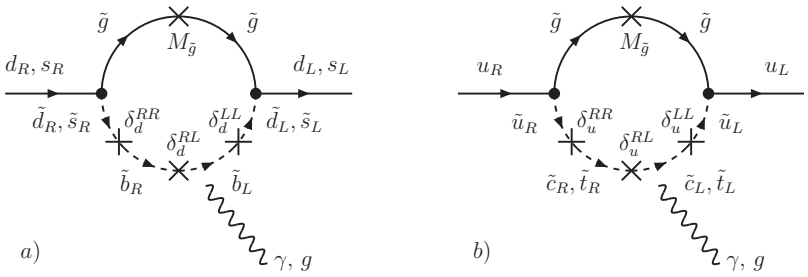

Figure 6.17: Examples of 1 loop contributions to the quark (C)EDMs in the presence of flavor off-diagonal phases. Shown are contributions to the up and down quark (C)EDMs that are induced in the presence of both δ^{LL} and δ^{RR} mass insertions. The photon and gluon lines are attached to the loops in all possible ways.

One finds the following expressions for the most important contributions

$$\left\{\frac{d_d}{e},\ d_d^c\right\}_{\tilde{g}} = -\frac{\alpha_s}{4\pi}\frac{m_b}{\tilde{m}^2}\frac{M_{\tilde{g}}\mu}{\tilde{m}^2}\frac{\tan\beta}{1+\epsilon\tan\beta}\Big\{f_{\tilde{g}}(x_g),\ f_{\tilde{g}}^c(x_g)\Big\}\mathrm{Im}\left[(\delta_d^{LL})_{13}(\delta_d^{RR})_{31}\right]\ , \quad (6.47)$$

$$\left\{\frac{d_s}{e},\ d_s^c\right\}_{\tilde{g}} = -\frac{\alpha_s}{4\pi}\frac{m_b}{\tilde{m}^2}\frac{M_{\tilde{g}}\mu}{\tilde{m}^2}\frac{\tan\beta}{1+\epsilon\tan\beta}\Big\{f_{\tilde{g}}(x_g),\ f_{\tilde{g}}^c(x_g)\Big\}\mathrm{Im}\left[(\delta_d^{LL})_{23}(\delta_d^{RR})_{32}\right]\ , \quad (6.48)$$

$$\left\{\frac{d_u}{e},\ d_u^c\right\}_{\tilde{g}} = -\frac{\alpha_s}{4\pi}\sum_{k=2,3}\frac{m_{u_k}}{\tilde{m}^2}\frac{M_{\tilde{g}}A_{u_k}}{\tilde{m}^2}\Big\{-2f_{\tilde{g}}(x_g),\ f_{\tilde{g}}^c(x_g)\Big\}\mathrm{Im}\left[(\delta_u^{LL})_{1k}(\delta_u^{RR})_{k1}\right] \quad (6.49)$$

where μ and $A_{u_2,u_3} = A_{c,t}$ are assumed to be real.

As mentioned already before, the most important feature of these expressions is the proportionality to the heavy quark masses, due to the presence of δ^{RR} mass insertions. In addition we note that the contributions to the down and strange quark (C)EDMs are enhanced by $\tan\beta$. Due to these enhancement factors, the flavored EDMs can in fact be close to the current experimental sensitivities once the existing flavor constraints on the mass insertions are imposed.

Apart from the gluino contributions, there are also chargino contributions to the flavored EDMs at leading order. However they are only sensitive to the δ^{LL} mass insertions. Consequently, they are proportional to the light quark masses and typically do not play an important role.

Going beyond leading order, both charged Higgs and chargino contributions to the down and strange quark (C)EDMs arise that are sensitive to the δ^{RR} mass insertions. Even so they are loop suppressed, it was shown in [364, 365, 307] that their effect is often non-negligible even for moderate values of $\tan\beta$ and we refer to these papers for explicit analytical expressions.

We summarize the present chapter. The rich flavor and CP violating structure of the MSSM leads to many interesting NP effects in low energy observables. Even in the MFV MSSM there can be sizable SUSY contributions to the $b \to s\gamma$ and $b \to s$ gluon transitions. For large values of $\tan\beta$ also the tree level $B \to \tau\nu$ decay and the rare $B_d \to \mu^+\mu^-$ and $B_s \to \mu^+\mu^-$ decays can be strongly modified by SUSY contributions.

New Physics effects in meson mixing on the other hand are naturally small in the MFV MSSM both for low and high $\tan\beta$. Only in the presence of non-MFV flavor off-diagonal

entries in the squark masses, sizable contributions to meson mixing naturally occur, in particular in the presence of right handed flavor changing currents induced by δ^{RR} mass insertions.

For the rare decays based on the $b \to s\nu\bar{\nu}$ and $s \to d\nu\bar{\nu}$ transitions to deviate significantly from their SM predictions, the soft SUSY breaking terms have to have a rather particular non-MFV structure. Effects in $b \to s\nu\bar{\nu}$ can only be generated by a $(\delta_u^{RL})_{32}$ mass insertion, while for large effects in the $s \to d\nu\bar{\nu}$ transition either $(\delta_u^{LR})_{23}(\delta_u^{RL})_{31}$ or $(\delta_d^{RR})_{13}(\delta_d^{RR})_{32}$ in the large $\tan\beta$ regime have to be present.

Concerning flavor conserving low energy observables, very important is the anomalous magnetic moment of the muon, $(g-2)_\mu$, that receives NP contributions proportional to $\tan\beta$. Finally, EDMs of quarks and leptons are highly sensitive probes of possible additional CP violating sources in the MSSM. EDMs can be induced both by flavor diagonal phases and through flavor effects. In particular in the presence of δ^{RR} mass insertions, large flavored EDMs can be generated, opening up the possibility to probe the MSSM flavor structure also with flavor conserving observables.

7 The SUSY Flavor Problem

If the SM is considered to be an effective theory valid up to some NP scale, one encounters the so-called *NP flavor problem*, as discussed in section 2.3. The phenomenological constraints on flavor changing dimension six operators are so strong, that for a natural NP scale of O(1 TeV) the NP flavor structure has to be highly non-generic. This general problem also manifests itself in the MSSM which will be the main topic of the present chapter. In section 7.1 we investigate the phenomenological constraints on the MSSM flavor structures. In an example MSSM scenario we impose the bounds coming from FCNCs and derive the allowed ranges for the Mass Insertions. Analyses of this type have a long tradition in the literature (see e.g. [309, 375, 376, 377, 378, 379, 380, 381, 382, 65, 383, 384, 21]) and the results presented in this chapter can be seen as a comprehensive update in view of the presently available constraints. The fact that the allowed ranges for the mass insertions seems unnaturally small for natural SUSY scales constitutes the *SUSY flavor problem*. In sections 7.2 and 7.3 we then review possible solutions to this problem. We describe different proposals that allow to fulfill the constraints from flavor phenomenology in a natural way and outline possibilities to test the proposed frameworks.

7.1 Constraining the MSSM Flavor Structures

As discussed in length in chapters 4 and 6, the soft SUSY breaking terms, i.e. the squark masses and trilinear couplings, introduce new sources of flavor violation in addition to the SM CKM matrix, resulting in large NP contributions to flavor changing processes mainly by means of gluino loops. The overall good agreement between the experimental data on FCNC observables and the corresponding SM predictions then leads to strong constraints on these MSSM flavor structures, i.e. the mass insertions.

To illustrate this point, we work out the bounds on the mass insertions in the $c-u$, $s-d$, $b-d$ and $b-s$ sectors imposing the constraints coming from the flavor observables discussed in chapter 3. In particular we consider $D^0-\bar{D}^0$ mixing, $K^0-\bar{K}^0$ mixing, $B_d-\bar{B}_d$ mixing, $B_s-\bar{B}_s$ mixing as well as the rare decays $B\to X_s\gamma$ and $B\to X_s\ell^+\ell^-$. For definiteness we chose a setup with small $\tan\beta=5$ and set all MSSM mass parameters to $M_{\rm SUSY}=500$ GeV. We chose real and positive gaugino masses, a real and positive μ parameter as well as real and positive trilinear couplings. We always switch on one mass insertion at a time and derive bounds in the single Re(δ) - Im(δ) planes. The so obtained bounds are then valid barring accidental cancellations that can in principle occur if several mass insertions are switched on simultaneously.

The bounds on the mass insertions depend of course on our choice of the SUSY scale $M_{\rm SUSY}=500$ GeV. We therefore mention that the constraints from the $\Delta F=2$ observables scale as $\delta/M_{\rm SUSY}$, and the ones coming from the $\Delta F=1$ observables as $\delta/M^2_{\rm SUSY}$. Consequently, the higher the SUSY scale is the more important are the $\Delta F=2$ constraints as

compared to the $\Delta F = 1$ constraints. For low to moderate values of $\tan\beta$, the bounds coming from the mixing observables are independent of $\tan\beta$, while the bounds from $\mathrm{BR}(B \to X_s\gamma)$ and $\mathrm{BR}(B \to X_s\ell^+\ell^-)$ on the mass insertions in the left-left and right-right sector scale as $\delta_d \tan\beta$, i.e. they become stronger with increasing $\tan\beta$.

Before presenting the results, a few comments are in order on the SUSY contributions to the FCNC processes that we include in our numerical analysis of the present section. The main SUSY contributions to the $\Delta F = 2$ processes are usually expected to come from the gluino boxes discussed in section 6.4. However, it is know that there are regions in parameter space where gluino box contributions vanish and in particular chargino contributions become non-negligible (see [385] for a recent analysis). While this does not happen in the MSSM setup described above, still, in our numerical analysis we include the full set of 1 loop box contributions as given for example in [14]. In fact we find that the mixed gluino-neutralino box contributions are not fully negligible and affect the constraints on the mass insertions at a level of 10% - 15% as compared to the situation where only gluino contributions to $\Delta F = 2$ processes are included. We mention also that we do not include the additional beyond leading order gluino contributions to $\Delta F = 2$ processes as discussed in [335]. These contributions become important in the presence of δ^{LR} and δ^{RL} mass insertions, but only if squark masses are non-degenerate, which is however not the case in our setup.

Concerning the $B \to X_s\gamma$ decay, we include the full 1 loop contributions to the Wilson coefficients of the magnetic and chromomagnetic operators as given in [319]. With the small value for $\tan\beta = 5$ and the chosen signs of the μ parameter and the trilinear couplings, the Higgs and the MFV chargino contributions cancel naturally to a large extent and the dominant effects in $B \to X_s\gamma$ arise from gluino loops. The same is true for the $B \to X_s\ell^+\ell^-$ decay that is also dominantly affected by the magnetic and chromomagnetic dipole operators. Still, even though subdominant, also the full 1 loop contributions to the semileptonic operators are included in our numerical analysis.

In the remainder of this section we now show the bounds on the mass insertions within the MSSM scenario defined above.

Bounds in the $c - u$ Sector

The mass insertions in the $c - u$ sector are strongly constrained by the recent experimental data on $D^0 - \bar{D}^0$ mixing and in figure 7.1 we present the resulting bounds on the $\left(\delta_u^{AB}\right)_{21}$.

The purple regions show the combined constraint from mass and width difference in the neutral D meson system, x_D and y_D. The green regions represent the allowed ranges once in addition also the data on CP violation in $D^0 - \bar{D}^0$ mixing is taken into account, i.e. they correspond to the combined constraint from x_D , y_D, $|q/p|$ and ϕ_D. To obtain these plots we proceed in the following way: As the SM contribution to the dispersive and absorptive parts of the mixing amplitude cannot be predicted in a relyable way, we allow them to vary freely in the ranges $-0.01\mathrm{ps}^{-1} < M_{12}^D < 0.01\mathrm{ps}^{-1}$, $-0.02\mathrm{ps}^{-1} < \Gamma_{12}^D < 0.02\mathrm{ps}^{-1}$ at the 1σ level and $-0.02\mathrm{ps}^{-1} < M_{12}^D < 0.02\mathrm{ps}^{-1}$, $-0.04\mathrm{ps}^{-1} < \Gamma_{12}^D < 0.04\mathrm{ps}^{-1}$ at the 2σ level, respectively. We then add the SUSY contributions to the mixing amplitude and require the results for x_D , y_D, $|q/p|$ and ϕ_D to lie within the ranges given in table 3.2. We make the following observations:

- The bounds from the CP conserving observables x_D and y_D are improved by roughly a factor 3 for maximal phases $\pi/4$ of the mass insertions, if also the CP violating

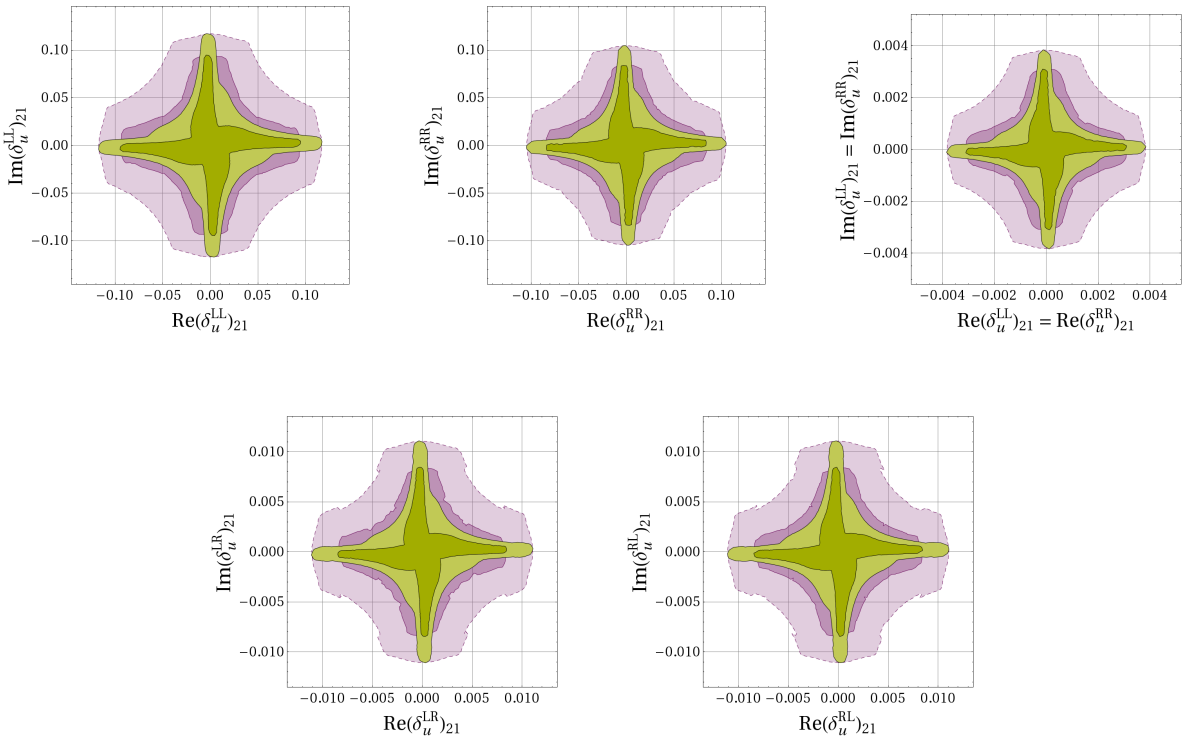

Figure 7.1: Bounds on the mass insertions $(\delta_u^{AB})_{21}$ (with $A, B = L, R$) as obtained by imposing the experimental constraints from $D^0 - \bar{D}^0$ mixing in table 3.2. The purple regions show the combined constraint from x_D and y_D while the dark (light) green areas represent the allowed ranges at the 1σ (2σ) level once all constraints (x_D, y_D, $|q/p|$ and ϕ_D) are imposed simultaneously.

observables $|q/p|$ and ϕ_D are taken into account.

- If gluino boxes were the only NP contributions to the mixing amplitude, then one would expect identical bounds in the δ^{LL} and δ^{RR} cases. The small differences at the level of 10% that are present in the plots of figure 7.1 can be traced back to the inclusion of gluino-neutralino contributions which as stated at the beginning of this section turn out to be not fully negligible.

- Particularly strong bounds at the level of 10^{-3} arise in the case $\delta^{LL} = \delta^{RR}$. In fact as discussed in section 6.4, if both left-left and right-right mass insertions are present simultaneously then left-right operators are generated that are strongly enhanced by renormalization group effects, by a large loop function and, in case of $D^0 - \bar{D}^0$ mixing, are also chirally enhanced.

- Also in the case of δ^{LR} and δ^{RL} mass insertions, left-right operators are generated. However, the involved loop function is much smaller as in the $\delta^{LL} = \delta^{RR}$ case and the corresponding bounds on the mass insertions are considerably less stringent.

We remark that for the sake of transparency we *only* imposed here the constraints from the $D^0 - \bar{D}^0$ observables. In fact, if a $(\delta_u^{LL})_{21}$ mass insertion is present, then due to the SU(2) relation (4.25) automatically also a $(\delta_d^{LL})_{21}$ mass insertion is generated, leading to NP

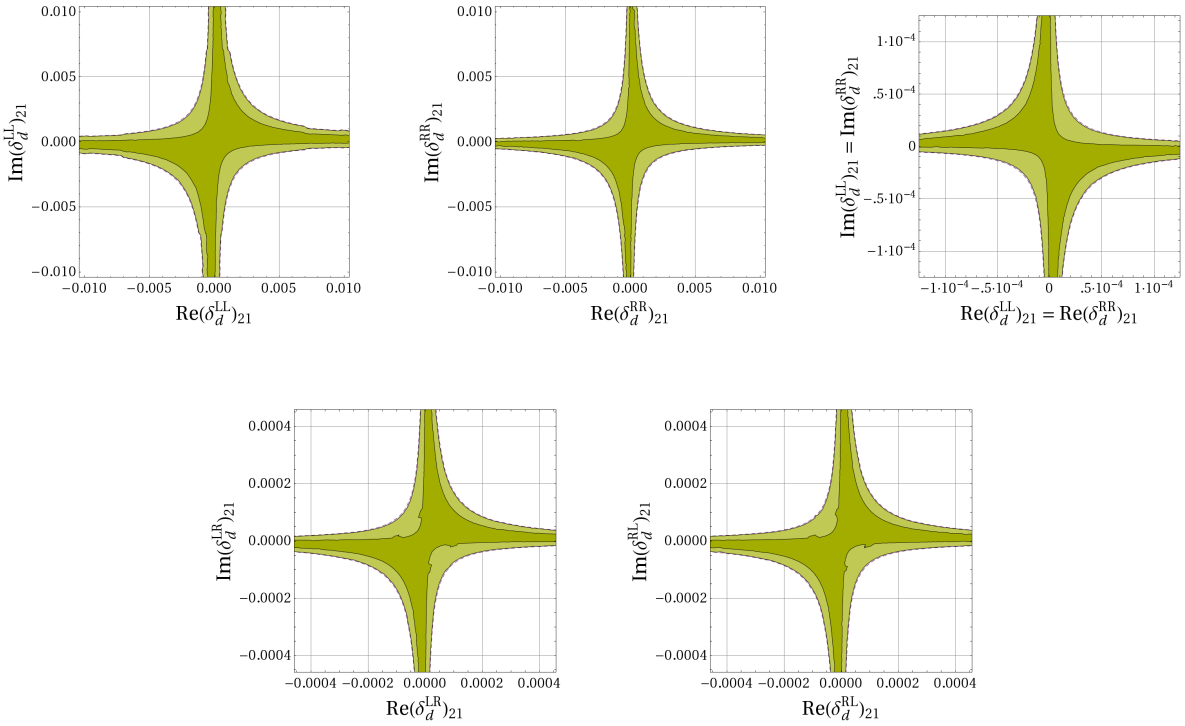

Figure 7.2: Bounds on the mass insertions $(\delta_d^{AB})_{21}$ (with $A, B = L, R$) as obtained by imposing the experimental constraints from $K^0 - \bar{K}^0$ mixing in table 3.2. The dark (light) green regions show the allowed ranges at the 1σ (2σ) level.

effects in $K^0 - \bar{K}^0$ mixing. In the δ^{LL} case discussed above, the most important constraint comes then indeed from the ϵ_K observable. As in our case $(\delta_u^{LL})_{21} \simeq (\delta_d^{LL})_{21}$ holds to a good approximation , the corresponding constraint can be directly taken from the corresponding discussion in the $s - d$ sector below. In all the other cases however, the $D^0 - \bar{D}^0$ observables of course do give the strongest constraints.

Bounds in the $s - d$ Sector

The experimental data on $K^0 - \bar{K}^0$ mixing is used to put constraints on the mass insertions $\left(\delta_d^{AB}\right)_{21}$, as shown in figure 7.2. The mass difference ΔM_K and the CP violating observable ϵ_K constrain the real and imaginary parts of the mixing amplitude M_{12}^K, respectively.

In the case of ϵ_K we directly use the bound from table 3.2. In the case of ΔM_K we proceed in the following way: given the large uncertainty coming from the unknown long distance SM contribution, we require the sum of SM and SUSY short distance contributions to lie in the ranges $[0.5\ \Delta M_K^{\text{exp}}, 1.5\ \Delta M_K^{\text{exp}}]$ and $[0, 2\ \Delta M_K^{\text{exp}}]$ at the 1σ and 2σ level, respectively. I.e. we allow for long distance contributions to ΔM_K as large as the experimental measurement. The green regions in the plots of figure 7.2 then correspond to the combined constraints at the 1σ and 2σ level. We make the following observations:

- The shown constraints are completely dominated by the bound from ϵ_K and are strongest for maximal phases of $\pi/4$. As ϵ_K is only sensitive to the imaginary part of the mixing amplitude, real and purely imaginary mass insertions actually remain

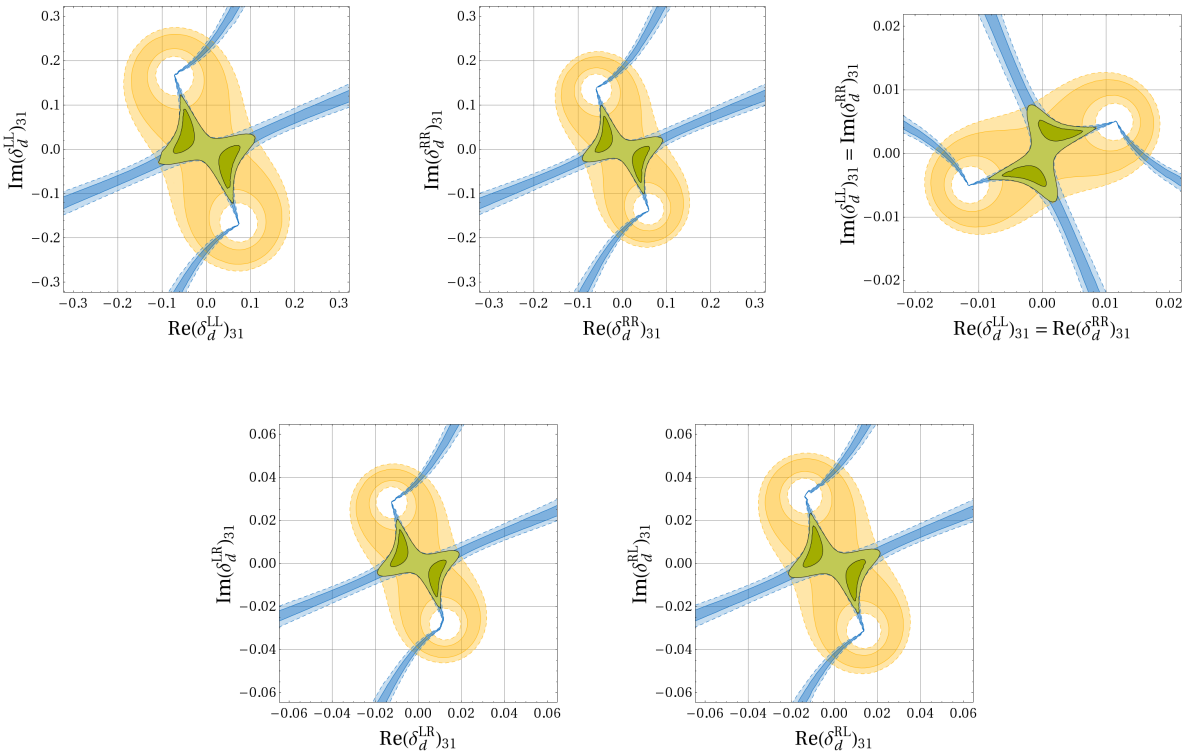

Figure 7.3: Bounds on the mass insertions $(\delta_d^{AB})_{31}$ (with $A, B = L, R$) as obtained by imposing the experimental constraints from ΔM_d and $S_{\psi K_S}$ in table 3.2. The dark (light) green regions show the allowed ranges at the 1σ (2σ) level. The blue areas show the constraint from $S_{\psi K_S}$ alone, while the yellow regions correspond to the ΔM_d constraint.

unconstrained by this observable. They are then bounded by the data on ΔM_K. These bounds lie outside the plotted regions in figure 7.2 and are at the level of 10^{-1} in the δ^{LL} and δ^{RR} cases, at the level of 10^{-3} in the $\delta^{LL} = \delta^{RR}$ case and at the level of 3×10^{-3} in the δ^{LR} and δ^{RL} cases.

- As it was the case in the $c - u$ sector, the small differences at the level of 10% between the δ^{LL} and δ^{RR} cases are due to the inclusion of the gluino-neutralino contributions.
- Also in the $s - d$ sector particularly strong bounds arise in the case $\delta^{LL} = \delta^{RR}$. The contributions to $K^0 - \bar{K}^0$ mixing of the left-right operators now feature a even stronger chiral enhancement as compared to $D^0 - \bar{D}^0$ mixing and for complex mass insertions remarkably stringent constraints at the level of 0.5×10^{-4} follow.

Finally we also mention that the measurement of ϵ'/ϵ could in principle put additional bounds on $\mathrm{Im}[(\delta_d^{LR})_{21}]$. However, given the large hadronic uncertainties in the SM calculation of ϵ'/ϵ, to be conservative, we do not use this bound here.

Bounds in the $b - d$ Sector

The measurements of ΔM_d and $S_{\psi K_S}$ constrain the modulus and the phase of the $B_d - \bar{B}_d$ mixing amplitude M_{12}^d, respectively. The resulting bounds on the various mass insertions $\left(\delta_d^{AB}\right)_{31}$ are reported in figure 7.3.

The yellow regions show the bounds coming from the mass difference ΔM_d, while the blue bands correspond to the constraints from the time dependent CP asymmetry $S_{\psi K_S}$. The green areas show the values for the mass insertions that are allowed by the combined constraint at the 1σ and 2σ level. To obtain these green areas also the constraint $\cos 2\beta > 0$ [36] is imposed, which excludes two of the four blue bands allowed by the $S_{\psi K_S}$ measurement alone. We make the following observations:

- The dark green 1σ ranges do not include the case where the mass insertions vanish, $(\delta_d^{AB})_{32} = 0$. This reflects the small tension between the rather low measurement of $S_{\psi K_S}^{\rm exp} = 0.672 \pm 0.023$ and the value for the angle β that is preferred by fits of the Unitarity Triangle. In fact, the CKM parameters that we use throughout our analysis (see appendix A.3) lead to a SM prediction $S_{\psi K_S} = 0.734 \pm 0.038$ and a small NP contribution to $B_d - \bar{B}_d$ mixing is required to get agreement with the experimental number at the 1σ level.

- As in the $c - u$ and the $s - d$ sector, there are small differences at the level of 10% - 15% between the plots of the δ^{LL} and δ^{RR} cases which are due to the inclusion of gluino-neutralino contributions. These contributions lead now also to small differences in the δ^{LR} and δ^{RL} cases.

- Also in the $b-d$ sector, particularly strong bounds arise in the $\delta^{LL} = \delta^{RR}$ case. While the generated contributions to $B_d - \bar{B}_d$ mixing from left-right operators are not chirally enhanced, the resulting constraints are still at the level of 0.5×10^{-2}.

Bounds in the $b - s$ Sector

In the $b - s$ sector a large number of experimental constraints can be used to constrain the mass insertions. Here, we concentrate on the experimental data on $B_s - \bar{B}_s$ mixing as well as the $\Delta B = 1$ processes $B \to X_s\gamma$ and $B \to X_s\ell^+\ell^-$.

In figure 7.4 we show the allowed regions for the mass insertions $(\delta_d^{AB})_{32}$. The yellow regions show the bounds coming from the mass difference ΔM_s, while the blue regions correspond to the constraint from the branching ratio of the $B \to X_s\gamma$ decay. Red areas indicate the constraint from the branching ratio of the $B \to X_s\ell^+\ell^-$ decay. The green regions finally show the values for the mass insertions that are allowed by the combined constraints at the 1σ and 2σ level. We make the following observations:

- In the δ^{LL} case, a strong constraint arises from $\mathrm{BR}(B \to X_s\gamma)$ as the related NP amplitude can interfere with the SM one. Fine tuned regions in parameter space with a large real part of $(\delta_d^{LL})_{32}$ that would be allowed by the $B \to X_s\gamma$ decay are excluded by the constraint from $\mathrm{BR}(B \to X_s\ell^+\ell^-)$. No additional constraint is provided by ΔM_s. It is interesting to note that the combined constraint is strongest for real values of the mass insertions, while much larger values for the mass insertions are allowed if they are complex.

- In the δ^{RR} case, the constraint from $\mathrm{BR}(B \to X_s\gamma)$ is less effective since the related NP amplitude (arising from right handed currents) does not interfere with the SM one. Also $\mathrm{BR}(B \to X_s\ell^+\ell^-)$ is not effective for the same reason. While ΔM_s starts to play some role in constraining the mass insertion, in the considered scenario the main

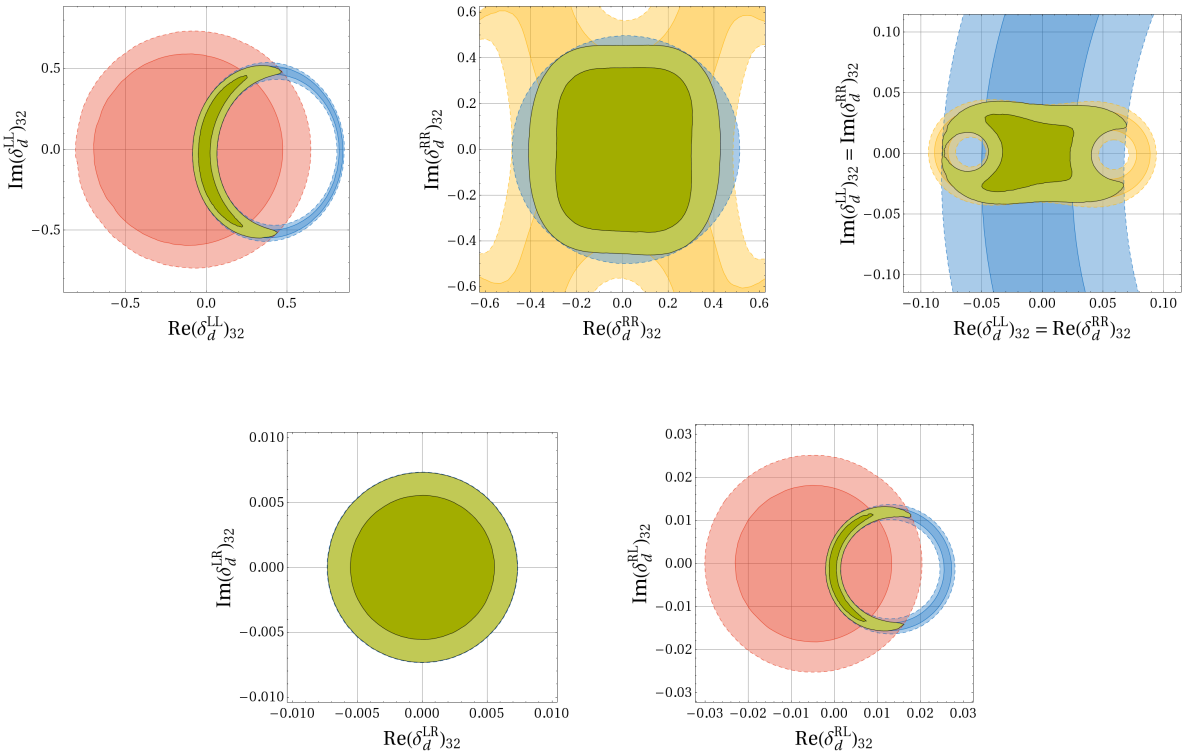

Figure 7.4: Bounds on the mass insertions $(\delta_d^{AB})_{32}$ (with $A, B = L, R$) as obtained by imposing the experimental constraints from ΔM_s as well as the $B \to X_s\gamma$ and $B \to X_s\ell^+\ell^-$ branching ratios from table 3.2. The dark (light) green regions show the allowed ranges at the 1σ (2σ) level. The blue areas show the constraint from BR($B \to X_s\gamma$) alone, while the yellow regions correspond to the ΔM_s constraint. Red regions finally indicate the ranges allowed by BR($B \to X_s\ell^+\ell^-$).

bound still arises from the $B \to X_s\gamma$ decay and is basically not sensitive to the phase of the mass insertions.

- In the $\delta^{LL} = \delta^{RR}$ case, the bound from ΔM_s is naturally the most stringent one as the left-right operators that are generated by the simultaneous presence of left-left and right-right mass insertions are strongly enhanced by renormalization group effects and a large loop function. In our setup we find a bound at the order of 5×10^{-2}.

- In the δ^{LR} and δ^{RL} cases, the BR($B \to X_s\gamma$) is by far the most important constraint as the NP amplitude realizes the necessary chirality flip for the dipole $b \to s\gamma$ transition without involving the bottom mass insertion.

- In the δ^{LR} case, the induced $b \to s\gamma$ amplitude does not interfere with the SM one and independent of the phase of the mass insertion the resulting bound, which comes entirely from the $B \to X_s\gamma$ branching ratio, is roughly 7×10^{-3}.

- In the δ^{RL} case on the other hand, the induced $b \to s\gamma$ amplitude can interfere with the SM one. The resulting bound on the mass insertion is then further strengthened by the inclusion of BR($B \to X_s\ell^+\ell^-$) that excludes large real values for $(\delta_d^{RL})_{32}$. The

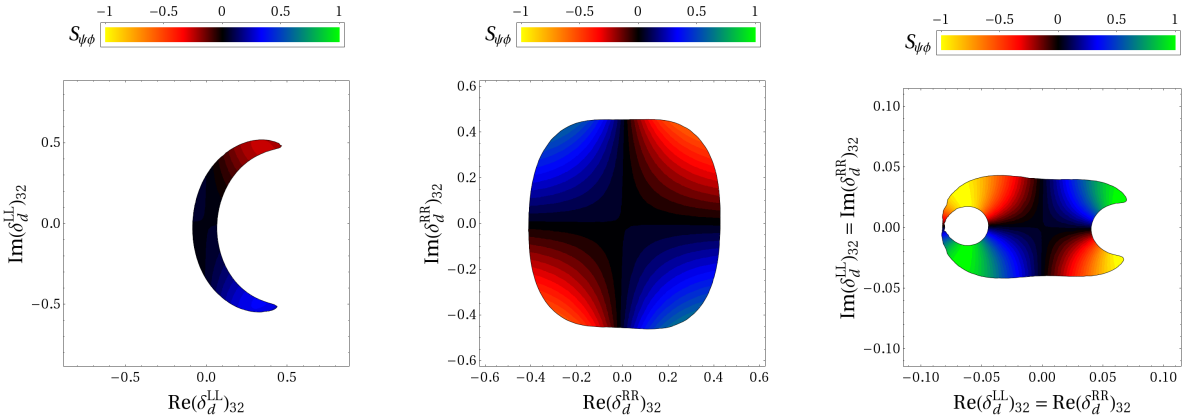

Figure 7.5: Bounds on the mass insertions $(\delta_d^{AB})_{32}$ (with $A, B = L, R$) at the 2σ level as in figure 7.4. The different colors indicate the resulting values for $S_{\psi\phi}$.

most stringent bound in the $b-s$ sector then arises in fact in the δ^{RL} case, where real mass insertions are constrained at a level of 10^{-3}.

We note that there exist various additional constraints in the $b-s$ sector, e.g. from the time-dependent CP asymmetries in $B_d \to \phi K_S$ and $B_d \to \eta' K_S$, the direct CP asymmetry in $B \to X_s\gamma$ or the time dependent CP asymmetry in $B \to K^*\gamma$. However, given the still rather large uncertainties, we did not include these additional bounds in the analysis of the present section.

Another very important observable in the $b-s$ sector is the time dependent CP asymmetry $S_{\psi\phi}$ that measures the phase of the $B_s - \bar{B}_s$ mixing amplitude. In fact, as detailed in section 3.1.5, recent data from Tevatron seems to hint at vales for $S_{\psi\phi}^{\mathrm{exp}} \simeq 0.8$ much larger than the tiny SM prediction $S_{\psi\phi}^{\mathrm{SM}} \simeq 0.038$. It is thus instructive to investigate the room left for large SUSY effects in $S_{\psi\phi}$ given the other constraints in the $b-s$ sector.

In figure 7.5 we show again the allowed 2σ ranges of the mass insertions, this time also indicating the resulting values for $S_{\psi\phi}$ with different colors. We observe that in the δ^{LL} case, where the combined constraint from $\mathrm{BR}(B \to X_s\gamma)$ and $\mathrm{BR}(B \to X_s\ell^+\ell^-)$ excludes large parts of the parameter space, possible effects in $S_{\psi\phi}$ are moderate with $-0.3 \lesssim S_{\psi\phi} \lesssim 0.3$. As the bounds from $\mathrm{BR}(B \to X_s\gamma)$ and $\mathrm{BR}(B \to X_s\ell^+\ell^-)$ are much weaker in the δ^{RR} case, the possible range for $S_{\psi\phi}$ is substantially larger. We find $-0.6 \lesssim S_{\psi\phi} \lesssim 0.6$. If both δ^{LL} and δ^{RR} mass insertions are switched on simultaneously, the constraint from ΔM_s is by far the most important one. As ΔM_s only constrains the absolute value of the $B_s - \bar{B}_s$ mixing amplitude but not its phase, $S_{\psi\phi}$ can acquire any value between -1 and 1 in this case. Finally in the δ^{LR} and δ^{RL} cases, the constraints from $\mathrm{BR}(B \to X_s\gamma)$ are so strong that they basically exclude any effects in $B_s - \bar{B}_s$ mixing, which results always in a SM-like $S_{\psi\phi}$. Consequently these cases are not shown in figure 7.5.

We mention that the precise ranges for $S_{\psi\phi}$ quoted above of course depend on the scenario considered here (all SUSY mass parameters set to 500 GeV and $\tan\beta = 5$). Also in the scenarios with only either $(\delta_d^{LL})_{32}$ or $(\delta_d^{RR})_{32}$ switched on, values for $S_{\psi\phi}$ in the full range from -1 to 1 can be generated if the other SUSY parameters are adjusted appropriately and the mass insertions are of O(1). Still, the following general statement holds: Within the MSSM with small to moderate $\tan\beta$, large values for $S_{\psi\phi}$ can be generated most naturally

if both $(\delta_d^{LL})_{32}$ and $(\delta_d^{RR})_{32}$ mass insertions are present simultaneously at the SUSY scale. In that case gluino box contributions to the $B_s - \bar{B}_s$ mixing amplitude are induced that are strongly enhanced by a large loop function and RGE effects and small, CKM-like mass insertions are sufficient to generate visible effects.

To summarize this section we stress that the strongest constraints on the SUSY flavor structures arise from data on $K^0 - \bar{K}^0$ and $D^0 - \bar{D}^0$ mixing. In particular, in certain cases the measurement of ϵ_K and the bounds on CP violation in $D^0 - \bar{D}^0$ mixing only allow for values of the corresponding mass insertions in the $s - d$ and $c - u$ sectors at the level of $\sim 10^{-4}$ and $\sim 10^{-3}$, if the SUSY scale is around 500 GeV. This immediately implies that the flavor structure of the soft SUSY breaking terms is necessarily highly non-generic for natural SUSY scales. This fact is usually referred to as the *SUSY flavor problem*.

Slightly looser bounds for the mass insertions ($\sim 10^{-2}$) arise in the $b - d$ sector from the data on $B_d - \bar{B}_d$ mixing, while in the $b - s$ sector some mass insertions are still allowed to be of O(1). Correspondingly, large non-standard effects in those $b \to s$ transitions that have not been precisely measured yet are in principle still possible. As an example, large values for the $B_s - \bar{B}_s$ mixing phase $S_{\psi\phi}$ can be accommodated for in the MSSM, in particular in a scenario where both $(\delta_d^{LL})_{32}$ and $(\delta_d^{RR})_{32}$ mass insertions are present simultaneously.

7.2 Possibilities to Address the SUSY Flavor Problem

There are various ways to keep under control dangerously large SUSY contributions to flavor observables. In the following we give a brief overview of the main possibilities and outline their most important implications for flavor physics.

Minimal Flavor Violation

One way to suppress unwanted SUSY contributions to flavor violating processes is to invoke the principle of Minimal Flavor Violation. As already described in section 4.4, the MFV hypothesis amounts to the assumption that the SM Yukawa couplings be, also in extensions of the SM, the only sources of flavor violation [44]. We recall here that the general structure of the soft terms in the MFV MSSM (4.32) leads to contributions to flavor changing processes that are governed by the same CKM factors as in the SM and therefore naturally small even for a SUSY scale at the order of 1 TeV and below. Large contributions are only expected in those flavor changing processes that are helicity suppressed in the SM and that can be enhanced by powers of $\tan\beta$ in the MSSM. Such processes are the tree level $B \to \tau\nu$ decay, the rare $B_s \to \mu^+\mu^-$ and $B_d \to \mu^+\mu^-$ decays as well as the $b \to s\gamma$ and $b \to s$ gluon transitions (see e.g. [165, 23]).

As the MFV principle in itself does not forbid the presence of additional CP violating sources, a MFV MSSM suffers, in general, from the same SUSY CP problem as the ordinary MSSM, i.e. the generic predictions for the EDMs are close to or above the current experimental bounds [278]. This problem can for example be avoided by the additional assumption that the Yukawa couplings are also the only source of CP violation [44]. In the phenomenological analysis in the following chapter we will adopt a different approach and allow for additional CP phases. We will discuss the interesting and characteristic flavor phenomenology that follows mainly from complex NP contributions to the $b \to s\gamma$ and $b \to s$

gluon amplitudes and point out correlations with NP effects in the EDMs of the neutron and electron.

Decoupling

Going beyond the MFV hypothesis, an immediate way to control the SUSY contributions to flavor and CP violating observables is decoupling. This happens for example in *Split Supersymmetry* [386, 387, 388] where the masses of sfermions are taken to be extremely heavy and only charginos and neutralinos remain relatively light. While in such a setup SUSY is not responsible anymore for a solution to the gauge hierarchy problem, Split SUSY is for example compatible with gauge coupling unification and the observed dark matter abundance. While all flavor violating observables are expected to be SM-like, visible effects can in principle occur in the EDMs through 2 loop Barr-Zee type diagrams involving the light charginos and neutralinos.

A complete decoupling of squarks obviously does not constitute a solution to the SUSY flavor problem, which requires to keep under control flavor and CP violating observables given a natural SUSY scale of O(TeV). More promising in this respect are models with a hierarchical sfermion spectrum where only the first two generations of squarks are heavy at the level of several 10 TeV, while the third generation remains at the TeV scale [369, 370]. In fact, as detailed above, the most stringent flavor and CP violation constraints involve the first two generations while the main requirement of a modest fine tuning of the electroweak scale is a light stop. The hierarchical sfermion scenario then appears to be a very "natural" MSSM framework [389], leading also to characteristic predictions for flavor phenomenology [390]. A detailed phenomenological study of such a framework is however beyond the scope of the present work.

Degeneracy

If the squark masses are degenerate to a large extent, SUSY contributions to flavor changing processes are strongly super-GIM suppressed [238]. In such a framework the soft squark masses are to a first approximation universal, i.e. proportional to the unit matrix. Deviations from universality, in particular flavor off-diagonal entries in the squark masses, appear only as small perturbations and are controlled by a small parameter. While the rotation angles that diagonalize the squark mass matrices are generally not small, the suppression of flavor violating amplitudes is due to the near degeneracy of the squark mass eigenstates.

Degeneracy in the squark masses can naturally arise in models with gauge mediated SUSY breaking – or with some other flavor blind mechanism of SUSY breaking mediation – as long as the mediation scale is not too high.[1] Another class of models with approximately degenerate squarks is given by SUSY flavor models based on non-abelian flavor symmetries to be described below.

[1] If the gauge mediation scale is high, e.g. not far below the GUT scale, large flavor violating sources can in principle be induced by gravity mediation. The resulting hybrid gauge-gravity mediation scenario has been analyzed for example in [391, 392].

Alignment

A mechanism to suppress SUSY contributions to FCNCs that is alternative to degeneracy is given by an approximate alignment of squark and quark mass matrices [393, 394], i.e. the squark and quark mass matrices are nearly simultaneously diagonal in the super-CKM basis. In contrast to models with degeneracy, the alignment mechanism does not imply almost universal squark masses. The squark masses can be widely different and SUSY contributions to flavor violating amplitudes are controlled by small squark mixing angles.

Models with alignment naturally arise in the context of SUSY flavor models based on abelian flavor symmetries.

7.3 SUSY Flavor Models

As mentioned already above, the degeneracy and alignment mechanisms can naturally be realized in so-called SUSY flavor models. Such models use flavor symmetries to explain the pattern of the SM fermion masses and mixings and simultaneously provide a sufficient suppression of FCNC and CP violating phenomena, i.e. they address both the SM and the SUSY flavor problems.

Supersymmetric models with flavor symmetries have been considered extensively in the literature. They can be divided into two classes depending on whether they are based on abelian or non-abelian flavor symmetries. They can be considered as generalizations of the Froggatt-Nielsen mechanism [47]: the flavor symmetry is spontaneously broken by vacuum expectation values of "flavon" fields Φ_i and the hierarchical patterns in the fermion mass matrices are explained by factors $(\langle\Phi_i\rangle/M)^n$, where M is the scale of the breaking of the flavor symmetry and the power n depends on the horizontal group charges of the fermions involved in the Yukawa couplings, generating the mass terms.

7.3.1 Abelian Flavor Models

There is a rich literature on models based on abelian flavor symmetries (see e.g. [395, 396, 393, 397, 398, 399, 400, 401]). Most successful models employ the flavor group $\mathrm{U}(1)_{F1} \times \mathrm{U}(1)_{F2}$ [393] which simultaneously allows to reproduce the observed hierarchies in the quark masses and mixings and to precisely align the quark and squark mass matrices.

We mention that abelian flavor symmetries do not impose any restriction on the mass splittings between squarks of different generations that are therefore expected to be non-degenerate with natural order one mass splittings.

One of the most characteristic predictions of abelian flavor models are then large NP effects in $D_0 - \bar{D}_0$ mixing. In fact, due to the SU(2) relation between the left-left blocks of the up and down squark masses, a complete alignment is only possible *either* in the up *or* in the down sector. As the strongest flavor constraints come from $K^0 - \bar{K}^0$ mixing, concrete models align the squark and quark masses in the down sector which implies a $(\delta_u^{LL})_{21}$ mass insertions of order of the Cabibbo angle. Recalling that (4.25)

$$(\delta_u^{LL})_{21} = (\delta_d^{LL})_{21} - \lambda \left(\frac{m^2_{\tilde{u}_L}}{\tilde{m}^2} - \frac{m^2_{\tilde{c}_L}}{\tilde{m}^2} \right) + O(\lambda^2) \ , \tag{7.1}$$

one observes in fact that even for $(\delta_d^{LL})_{21} = 0$, which is approximately satisfied in alignment models, there are irreducible flavor violating terms in the up squark mass as long as the left handed squarks are non-degenerate. Therefore, the recent experimental measurement of $D^0 - \bar{D}^0$ mixing leads to strong constraints on these type of models [57, 42].

We will analyze the NP effects in $D^0 - \bar{D}^0$ mixing that are generically predicted by abelian flavor models in section 8.6 focussing on CP violation in $D^0 - \bar{D}^0$ mixing. In section 8.5 we will also discuss the characteristic flavor phenomenology of a concrete abelian flavor model with a representative flavor structure in the soft sector.

7.3.2 Non-abelian Flavor Models

In contrast to abelian models, where there is a lot of freedom in fixing the charges of the SM fermions under the flavor symmetry, non-abelian models [402, 403, 404, 405, 406, 407, 408, 409, 410, 411] are quite predictive for fermion mass matrices once the pattern of symmetry breaking is specified.

Non-abelian models group two or three generations in a single multiplet of the flavor symmetry, leading to degenerate masses for the corresponding squark generations in the limit of unbroken flavor symmetry. There are many candidates for the non-abelian flavor symmetry group, each having distinct symmetry breaking patters. In general, it has to be contained in the full global $U(3)^5$ symmetry group of the SM in the limit of vanishing Yukawa couplings. In particular, a lot of attention is received by models with a U(2) symmetry motivated by the large top mass and leading to nearly degenerate squarks of the first and second generation. Consequently, in these models $s \to d$ and simultaneously also $c \to u$ transitions, that are the most constraining ones, are only induced by the small breaking of the flavor symmetry and expected to be naturally small.

Also models with a SU(3) flavor symmetry are very popular. They address the SUSY flavor problem by approximately degenerate squarks of all three generations and are additionally able to naturally predict a maximal atmospheric neutrino mixing angle $\theta_{23} \simeq 45^\circ$ and to suggest a large solar mixing angle $\theta_{12} \simeq 30^\circ$.

In sections 8.3 and 8.4 we will analyze two SU(3) models with representative flavor structures and point out their distinct predictions for low energy observables.

8 Characteristic Predictions of Specific SUSY Frameworks

In this chapter we present the main results of our numerical analyses of several specific SUSY frameworks. We start with the MSSM with minimal flavor violation where we allow for additional CP violating phases following mainly our study in [18]. While at first sight, EDMs seem to be the best probes of such a scenario, we stress that also processes that are sensitive to CP violation in $\Delta F = 1$ dipole amplitudes, like the direct CP asymmetry in $B \to X_s\gamma$ or the time dependent CP asymmetries in $B \to \phi K_S$ and $B \to \eta' K_S$ can be modified significantly and show a characteristic pattern of correlations. On the other hand, as one expects from the general discussion in section 6.4, within a MFV framework the SUSY effects in $\Delta F = 2$ processes are small. Furthermore, even allowing for additional sources of CP violation in the MFV MSSM, the leading NP contributions to $\Delta F = 2$ amplitudes are not sensitive to new CP violating phases. The SUSY effects to CP violation in meson mixing are therefore very restricted and observables like ϵ_K, $S_{\psi K_S}$ and in particular $S_{\psi\phi}$ are essentially SM-like.

To generate sizable effects in $S_{\psi\phi}$ in the MSSM, one has to go beyond the minimal ansatz of the MFV MSSM and introduce not only additional sources of CP violation, but also of flavor violation. Therefore, in addition to the MFV MSSM, we consider in the following also several representative non-MFV scenarios that are realized in concrete SUSY flavor models and characterized by

i) only CKM-like left-left mass insertions (section 8.2),

ii) comparable left-left and right-right mass insertions that are CKM-like (section 8.3),

iii) large O(1) right-right mass insertions (sections 8.4 and 8.5).

We outline the characteristic NP effects in flavor observables that arise in these frameworks, focussing in particular on the B_s mixing phase $S_{\psi\phi}$ and its correlations with the branching ratio of the rare $B_s \to \mu^+\mu^-$ decay. These sections will to a large extent be based on [21].

Finally, in the last section 8.6 we concentrate on NP effects in $D^0 - \bar{D}^0$ mixing that are generically predicted in abelian flavor models and point out an interesting correlation between CP violation in $D^0 - \bar{D}^0$ mixing and the neutron EDM that we identified in [22] within that class of models.

Throughout our numerical analyses we use the input parameter collected in appendix A.3 and impose a number of constraints. In particular, we take in to account the data on flavor physics observables in table 3.2, mass bounds from direct SUSY searches (see appendix A.3), the requirement of a neutral lightest SUSY particle and the requirement of vacuum stability and the absence of charge or color breaking minima in the scalar potential [412, 413, 414].

For the discussion of the MFV MSSM in section 8.1 we adopt a low energy approach and directly treat the MSSM parameter at the electroweak scale as free parameters. In our numerical analysis of the SUSY flavor models in sections 8.2 - 8.6 on the other hand, we follow a different approach. We assume the flavor models to be defined at the GUT scale and implement their representative flavor structures of the soft terms into a CMSSM-like spectrum at the GUT scale. We then use 2 loop renormalization group evolution [415] to run the SUSY spectrum to the electroweak scale where we evaluate the SUSY contributions to the low energy observables.

8.1 The Minimal Flavor Violating MSSM with CP Phases

As already discussed in sections 4.4 and 7.2, the principle of Minimal Flavor Violation can be implemented in the MSSM to avoid dangerously large NP contributions to flavor changing neutral current processes. The best probes of such a scenario are then observables that are helicity suppressed in the SM and can be enhanced by $\tan\beta$ factors in the MSSM (see e.g. [165, 23]). For example, as seen is section 6.3, even for a completely flavor blind soft sector there are Higgsino loop contributions to the $B_{s,d} \to \mu^+\mu^-$ decays that are strongly enhanced by $\tan^3\beta$. Similarly also the Wilson coefficients C_7 and C_8 of the magnetic and chromomagnetic dipole operators, that are responsible for the $b \to s\gamma$ and $b \to s$ gluon transitions, can receive large Higgsino loop corrections even for moderate values of $\tan\beta$ (see section 6.2).

As the symmetry based definition of MFV is fully compatible with the introduction of additional sources of CP violation, also electric dipole moments are important observables to be considered in the MFV MSSM. In order to keep under control the 1 loop NP contributions to EDMs we assume that the μ parameter as well as the gaugino masses are real and only consider a complex trilinear coupling of the stop A_t, keeping also the other trilinear couplings real. As mentioned in section 6.7, such a scenario can in fact be realized in the MFV MSSM.

In addition we will first restrict ourselves to flavor diagonal squark mass matrices. While flavor off-diagonal terms in the soft masses are of course allowed by the general MFV ansatz (4.32), leading to additional FCNC contributions by means of gluino loops, these effects can be neglected if the corresponding MFV expansion parameters b_i are small and/or if the gluino mass is significantly larger than the chargino/up-squark masses. In this respect, the contributions to FCNC processes in the scenario defined above and called Flavor Blind MSSM (FBMSSM) in [18] can be regarded as irreducible effects arising in MFV scenarios. Analyses of similar frameworks can be found e.g. in [280, 281, 282, 283, 279].

The main NP effects in flavor observables within the framework of the FBMSSM are introduced by Higgsino loop contributions to the Wilson coefficients C_7 and C_8 that are proportional to the complex parameter combination μA_t and strongly correlated effects follow in observables like the direct CP asymmetry in $B \to X_s\gamma$, the time dependent CP asymmetries in $B \to \phi K_S$ and $B \to \eta' K_S$ as well as CP asymmetries in the $B \to K^*\ell^+\ell^-$ decay. In addition also 2 loop Barr-Zee contributions to EDMs arise that are proportional to $\mathrm{Im}(\mu A_t)$ and therefore highly correlated to the NP effects in the flavor observables.

We perform our numerical analysis by scanning the free FBMSSM parameter at the SUSY scale in the following ranges

$$0 < \tilde{m}_Q^2,\ \tilde{m}_U^2,\ \tilde{m}_D^2 < 1\ \mathrm{TeV}^2\ , \qquad 0 < \tilde{A}_{u,d}^2 < 3\left(\tilde{m}_Q^2 + \tilde{m}_{U,D}^2\right)$$

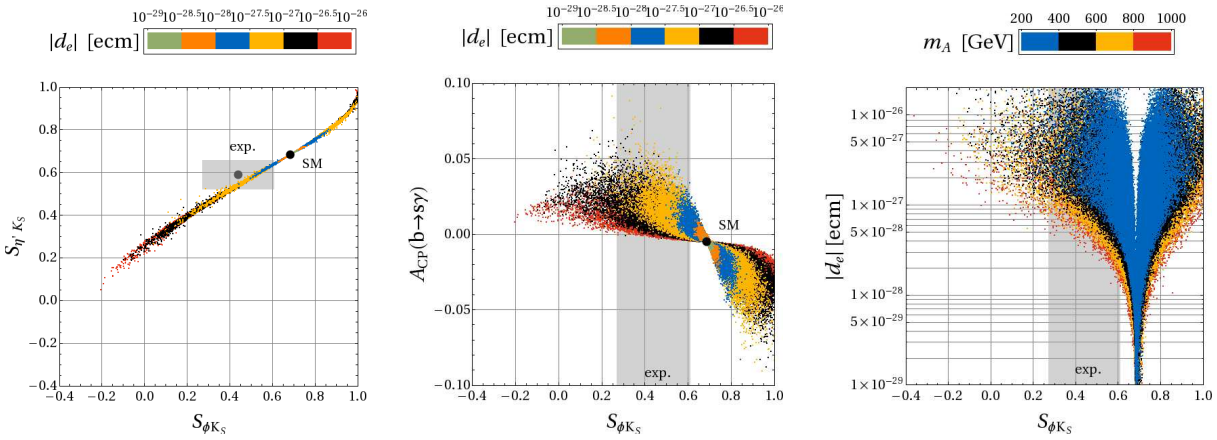

Figure 8.1: Correlations in the FBMSSM between the time dependent CP asymmetries $S_{\phi K_S}$ and $S_{\eta' K_S}$ (left), between $S_{\phi K_S}$ and the direct CP asymmetry $A_{\rm CP}(b \to s\gamma)$ (middle) as well as between $S_{\phi K_S}$ and the EDM of the electron d_e (right). The gray regions correspond to the experimental 1σ ranges for $S_{\phi K_S}$ and $S_{\eta' K_S}$. In the plots on the left and in the middle, the attained values for the electron EDM d_e are also shown through different colors. In the plot on the right, the colored bands correspond to different values for the pseudoscalar Higgs mass M_A. From [18, 416].

$$\begin{aligned} 0 < M_1,\ M_2,\ M_{\tilde{g}} < 1\ \text{TeV}\ , \qquad & 0 < \mu,\ M_A < 1\ \text{TeV}\ , \\ 3 < \tan\beta < 50\ , \qquad & 0 < \text{Arg}(A_t) < 2\pi \end{aligned} \tag{8.1}$$

and imposing all the constraints mentioned at the beginning of this chapter.

The left plot of figure 8.1 shows the correlation between $S_{\phi K_S}$ and $S_{\eta' K_S}$ in the FBMSSM framework. We emphasize that non-standard values for $S_{\phi K_S}$ are easily achieved and the present small discrepancy between the experimental value of $S_{\phi K_S}$ and its SM prediction can find a natural explanation. Moreover, the NP effects in $S_{\phi K_S}$ are larger than those in $S_{\eta' K_S}$ in agreement with the pattern observed in the data.

In the center plot of figure 8.1, we show $A_{\rm CP}(b \to s\gamma)$ as a function of $S_{\phi K_S}$. We observe that the sign of $S_{\phi K_S}$ is correlated with the sign of $A_{\rm CP}(b \to s\gamma)$. In particular, in the experimentally preferred region for $S_{\phi K_S} \simeq 0.4$, $A_{\rm CP}(b \to s\gamma)$ turns out to be unambiguously *positive* and is typically predicted to depart significantly from its tiny SM prediction $A_{\rm CP}(b \to s\gamma) \simeq -0.4\%$. Values up to $A_{\rm CP}(b \to s\gamma) \simeq +5\%$ can be reached.

In both these plots, the various colored bands show the attained values for the electron EDM d_e. In the right plot of figure 8.1, we show then also directly the prediction for the electron EDM d_e as a function of $S_{\phi K_S}$ for different values of the pseudoscalar Higgs mass M_A. We note that d_e is very sensitive to M_A, as the relevant 2 loop Barr-Zee contributions to d_e decouple with the heavier mass between M_A and the stop masses $m_{\tilde{t}_{1,2}}$, as discussed in section 6.7. One observes that large (non-standard) effects in $S_{\phi K_S}$ unambiguously imply large values for d_e. In particular, in the experimentally interesting region where $S_{\phi K_S} \simeq 0.4$, we obtain the lower bound $d_e \gtrsim 5 \times 10^{-28}\, e\,\text{cm}$. Similar results are found for the neutron EDM d_n, in which case we find the lower bound $d_n \gtrsim 8 \times 10^{-28}\, e\,\text{cm}$.

However, we observe that while $S_{\phi K_S}$, $S_{\eta' K_S}$ and $A_{\rm CP}(b \to s\gamma)$ are not directly sensitive to M_A (they feel M_A mainly through the indirect $\text{BR}(b \to s\gamma)$ constraint), in contrast, the EDMs d_e and d_n go to zero when M_A decouples. In particular, if we enlarge the allowed values for M_A up to $M_A < 3$ TeV while varying all the other SUSY parameters in the

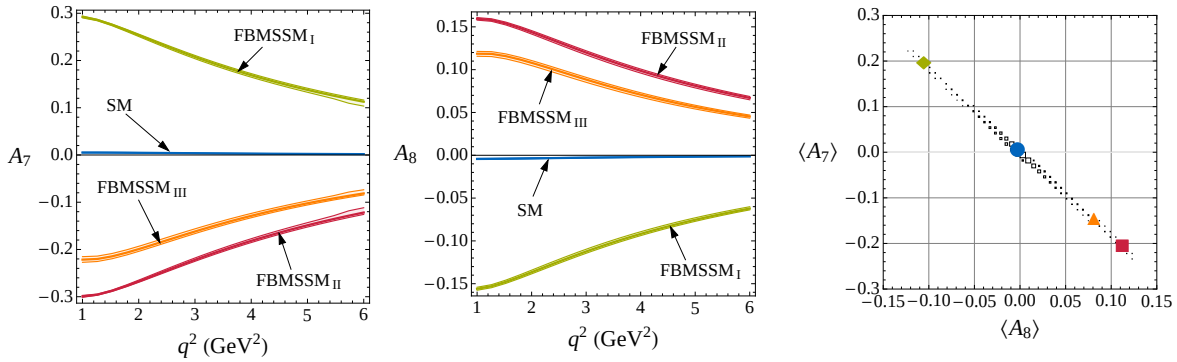

Figure 8.2: Left and center plot: The q^2 dependence of the CP asymmetries A_7 and A_8 in $B \to K^* \ell^+ \ell^-$ in the SM (blue band) and three example FBMSSM scenarios as described in the text. Right plot: correlation between the integrated asymmetries $\langle A_7 \rangle$ and $\langle A_8 \rangle$ in the FBMSSM. Blue circle: SM, green diamond: FBMSSM$_{\rm I}$, red square: FBMSSM$_{\rm II}$, orange triangle: FBMSSM$_{\rm III}$. From [19].

same range as in (8.1), the requirement of $S_{\phi K_S} \simeq 0.4$ would imply the lower bound $d_e \gtrsim (5,\ 3,\ 2,\ 1,\ 0.5) \times 10^{-28}\, e\,\text{cm}$ for $M_A < (1,\ 1.5,\ 2,\ 2.5,\ 3)$ TeV, respectively.

We also find large effects in several observables accessible in the $B \to K^* \ell^+ \ell^-$ decay that are induced by the large complex NP contributions to the Wilson coefficient C_7 in the FBMSSM.

As expected from the model independent discussion in section 3.2.2, in such a situation, the most pronounced effects arise in the CP asymmetries A_7 and A_8 and these are shown in the left and center plot of figure 8.2. The plot contains three example FBMSSM scenarios characterized by a large positive imaginary part of C_7 (FBMSSM$_{\rm I}$, green), a large negative imaginary part of C_7 (FBMSSM$_{\rm II}$, red) and a large negative imaginary part of C_7 such that $S_{\phi K_S}$ agrees with the central experimental value $S_{\phi K_S} \simeq 0.4$ (FBMSSM$_{\rm III}$, orange). The input parameter for the three scenarios can be found in [19]. The effects in figure 8.2 follow exactly the model independent pattern shown in figure 3.3, i.e. positive values for A_7 imply negative ones for A_8 and vice versa. This is then also displayed in the right plot of figure 8.2, where we show the correlation between the integrated asymmetries $\langle A_7 \rangle$ and $\langle A_8 \rangle$ that is in complete analogy to the model independent situation shown in the left plot of figure 3.4.

Also in the CP averaged angular coefficients we find visible departures from the SM. For S_4, S_5 and the forward–backward asymmetry S_s^6 we find significant shifts in their zero crossings towards values of q^2 lower than the SM prediction. The reason for these large shifts are the large values of $\text{Im}(C_7)$ in the scenarios considered, as discussed in section 3.2.2.

In view of the start of the LHC experiments it is also interesting to investigate the implications of sizable effects in the above discussed flavor observables on the SUSY spectrum. The left plot of figure 8.3 shows the dependence of $S_{\phi K_S}$ on the lightest stop mass $m_{\tilde{t}_1}$ for different values of the μ parameter while the right plot shows the dependence of $A_{\rm CP}(b \to s\gamma)$ on the Higgsino mass μ for different values of the lightest stop mass $m_{\tilde{t}_1}$. One observes that large (non-standard) effects for both observables, $S_{\phi K_S}$ and $A_{\rm CP}(b \to s\gamma)$, can be expected as long as the SUSY spectrum is not extremely heavy. For example, values for the direct CP asymmetry in $B \to X_s\gamma$, $|A_{\rm CP}(b \to s\gamma)| > 2\%$, arise only if Higgsinos and stops are below the TeV scale $\mu \lesssim 600$ GeV and $m_{\tilde{t}_1} \lesssim 800$ GeV, i.e. well within the LHC reach.

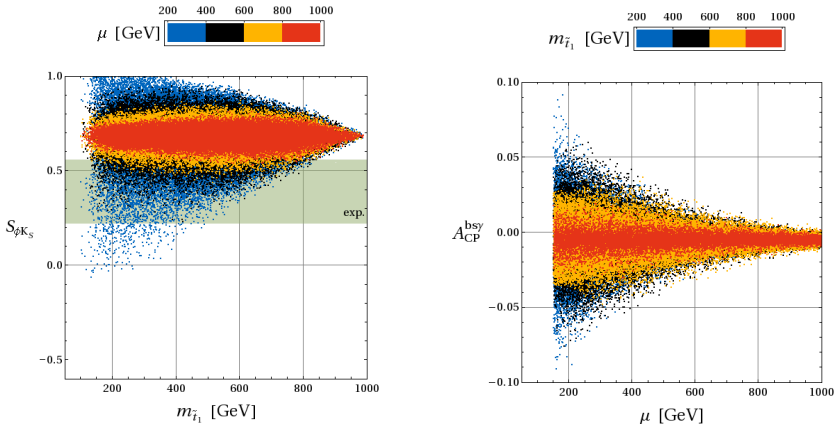

Figure 8.3: Dependence of the time dependent CP asymmetry $S_{\phi K_S}$ on the lightest stop mass $m_{\tilde{t}_1}$ (left) and of the direct CP asymmetry $A_{\rm CP}(b \to s\gamma)$ on the Higgsino mass parameter μ (right). The dependence of $S_{\phi K_S}$ ($A_{\rm CP}(b \to s\gamma)$) on the μ parameter (lightest stop mass $m_{\tilde{t}_1}$) is also shown through different colored bands. From [18].

While large NP effects are indeed possible in the MFV MSSM in $\Delta F = 0$ and $\Delta F = 1$ dipole transitions as detailed above, the same is not true for $\Delta F = 2$ amplitudes. SUSY box contributions to the mixing amplitudes are naturally small in the MFV MSSM. In addition, the leading NP contributions are real, even in the presence of CP violating phases. Complex contributions from flavor diagonal phases arise only at the subleading level through chargino loops in the Wilson coefficient $\tilde{C}_3$ (see (6.23)) in the large $\tan\beta$ regime. For large $\tan\beta$ also double penguins can become relevant for $B_s - \bar{B}_s$ mixing. However, also they are real at leading order, and beyond leading order corrections can only lead to small imaginary parts if the squark masses are non-degenerate [124, 339] and if μ is negative [124], which is strongly disfavored by the $(g-2)_\mu$ constraint. One might then hope that flavored CP phases in the general MFV ansatz (4.32) can still lead to visible CP violation in meson mixing in particular in $S_{\psi\phi}$, the B_s mixing phase. As discussed in section 6.4, a complex b_3 coefficient results in complex gluino box contributions to the Wilson coefficient C_1 but only for large values of $\tan\beta$.

In figure 8.4, we show the predictions for $S_{\psi\phi}$ as a function of $\tan\beta$ in a MFV MSSM scenario taking into account all possible complex SUSY contributions to the $B_s - \bar{B}_s$ mixing amplitude mentioned above. As expected, potentially sizable effects to $S_{\psi\phi}$ are only possible in the very large $\tan\beta$ regime (light blue points). However, in this case the constraints from both $\mathrm{BR}(B_s \to \mu^+\mu^-)$ and $\mathrm{BR}(B \to X_s\gamma)$ become very powerful and prevent any visible effect in $S_{\psi\phi}$ (black points).

To summarize this section we stress that in a MFV MSSM, sizable non-standard effects in low energy observables are possible. In particular, allowing for additional CP phases in the soft SUSY breaking sector, CP violating $\Delta F = 0$ and $\Delta F = 1$ dipole amplitudes can receive large complex NP contributions, leading to highly correlated modifications of the SM predictions of the EDMs, $S_{\phi K_S}$, $S_{\eta' K_S}$, $A_{\rm CP}(b \to s\gamma)$ and CP asymmetries in $B \to K^* \mu^+ \mu^-$. CP violation in $\Delta F = 2$ amplitudes however remains SM-like, i.e. one gets only small effects in ϵ_K, $S_{\psi K_S}$ and especially in $S_{\psi\phi}$. We conclude that the combined study of the above considered observables and especially the characteristic pattern of correlations among them

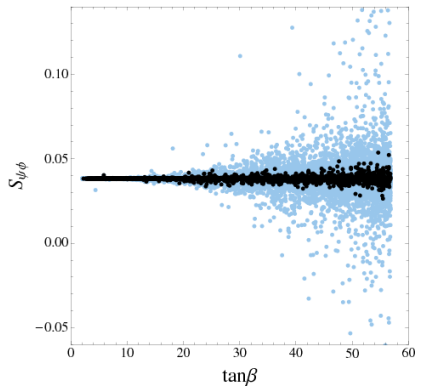

Figure 8.4: The B_s mixing phase $S_{\psi\phi}$ in the MFV MSSM as function of $\tan\beta$. Black points fulfill the constraints from $\mathrm{BR}(B \to X_s\gamma)$ and $\mathrm{BR}(B_s \to \mu^+\mu^-)$, light blue points do not. From [21].

constitutes a very powerfull test of this framework.

We also conclude that large CP violating effects in $\Delta F = 2$ amplitudes require additional flavor structures in the soft SUSY breaking terms: Only in the presence of additional sources of *flavor violation*, sizable New Physics effects to *CP violation* in meson mixing can occur.

8.2 Flavor Models with only CKM-like Left-Left Mass Insertions

As a first step we introduce new sources of flavor violation of CKM size only in the m_Q^2 squark soft mass. As it will turn out, models based on a flavor structure with only left handed CKM-like flavor changing currents share many similarities with the MFV MSSM. Correlations among the studied CP violating B physics observables are often very similar in these scenarios and also the size of the effects are comparable. In particular also in this class of models, effects in $\Delta F = 2$ processes are rather limited and especially $S_{\psi\phi}$ turns out to be almost SM-like. This can be easily understood by recalling that if only left-left mass insertions are present, they have to be of O(1) to induce sizable effects in $B_s - \bar{B}_s$ mixing (see discussion in section 7.1).

Concretely we analyze now a framework based on the following left-left mass insertions

$$(\delta_d^{LL}) \simeq \begin{pmatrix} 0 & \lambda^5 & \lambda^3 \\ \lambda^5 & 0 & \lambda^2 e^{i\phi_L} \\ \lambda^3 & \lambda^2 e^{-i\phi_L} & 0 \end{pmatrix} . \tag{8.2}$$

While (8.2) determines the main structure in the mass insertions, we allow for O(1) prefactors in all the entries and scan them randomly in the range $\pm[0.5, 2]$. The phase ϕ_L we allow to vary between 0 and 2π. As mentioned at the beginning of the chapter, we assume that (8.2) holds at the GUT scale $\sim 10^{16}$ GeV and implement the flavor structures on top of a CMSSM spectrum. We scan the CMSSM parameter in the following ranges

$$\begin{aligned} 0 < m_0 < 2 \text{ TeV} , \qquad & -3m_0 < A_0 < 3m_0 , \\ 0 < M_{1/2} < 1 \text{ TeV} , \qquad & 5 < \tan\beta < 55 , \end{aligned} \tag{8.3}$$

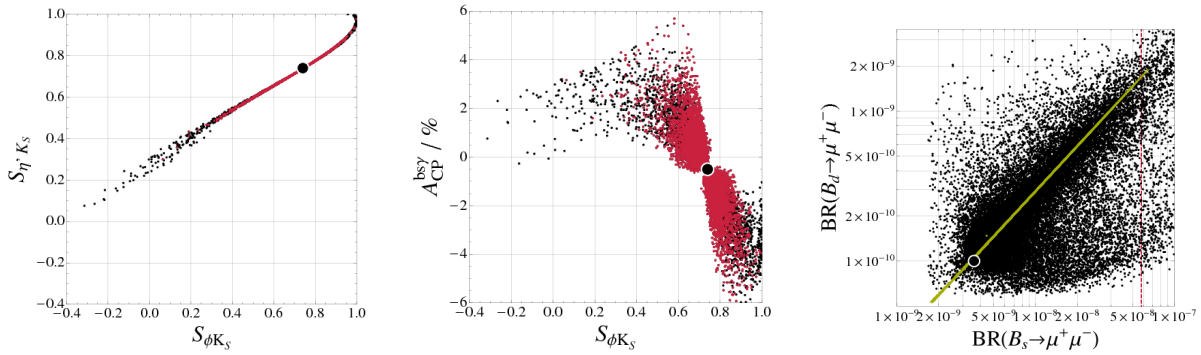

Figure 8.5: Correlations in models with only CKM-like, left-left mass insertions between the time dependent CP asymmetries $S_{\phi K_S}$ and $S_{\eta' K_S}$ (left), between $S_{\phi K_S}$ and the direct CP asymmetry $A_{\rm CP}(b \to s\gamma)$ (middle) as well as between $\mathrm{BR}(B_s \to \mu^+\mu^-)$ and $\mathrm{BR}(B_d \to \mu^+\mu^-)$ (right). Red points satisfy $\mathrm{BR}(B_s \to \mu^+\mu^-) < 6 \times 10^{-9}$. The green points in the plot of $\mathrm{BR}(B_s \to \mu^+\mu^-)$ vs. $\mathrm{BR}(B_d \to \mu^+\mu^-)$ show the correlation of these observables in the MFV MSSM. From [21].

and assume the μ term to be positive, in agreement with the data on the anomalous magnetic moment of the muon.

The left and the center plot of figure 8.5 show $S_{\phi K_S}$ as a function of $S_{\eta' K_S}$ and $A_{\rm CP}(b \to s\gamma)$, respectively. Indeed, the emerging correlations share great similarity with the situation in the FBMSSM discussed in the previous section (see figure 8.1). While in case of $S_{\phi K_S}$ vs. $S_{\eta' K_S}$, this is due to the dominance of left handed flavor changing currents, the sign of the correlation between $S_{\phi K_S}$ and $A_{\rm CP}(b \to s\gamma)$ can be understood in the following way: While the NP contributions to $S_{\phi K_S}$ arise dominantly from the Wilson coefficient C_8, the CP asymmetry $A_{\rm CP}(b \to s\gamma)$ crucially depends on the relative size of the imaginary parts of C_7 and C_8, see (3.51). In the considered model, gluino loops typically give $C_7^{\tilde{g}} < C_8^{\tilde{g}}$ (6.10), while Wino loops lead to the opposite situation, i.e. $C_7^{\tilde{W}} < C_8^{\tilde{W}}$ (6.9). In fact the correlation that we find corresponds to the latter case, implying that Wino contributions dominate over gluino ones in large parts of the parameter space, since Winos are typically a factor 3 lighter than gluinos in a CMSSM spectrum.

In addition we also find that the observables in the $B \to K^* \ell^+ \ell^-$ decay show the same pattern of effects as in the FBMSSM case that is model independently dictated by the dominance of left handed flavor changing currents. Also the implications for the SUSY spectrum are similar: Visible non-standard effects in the above mentioned observables imply necessarily SUSY particles within the reach of LHC.

An important way to distinguish these two scenarios is given by the correlation between the $B_s \to \mu^+\mu^-$ and $B_d \to \mu^+\mu^-$ decays as shown in the right plot of figure 8.5. In fact in MFV frameworks, flavor violation is determined purely by the CKM matrix and the branching ratios of these two decays are strongly correlated [126] leading to the green line in the plot. The non-MFV structures in the considered scenario however are not universal in the $b-d$ and $b-s$ sectors and lead to potentially large deviations from the MFV prediction.

Another major difference discriminating these scenarios regards their predictions for the leptonic and hadronic EDMs. Within the FBMSSM, we predicted $d_{e,n} \gtrsim 10^{28} e\,\mathrm{cm}$ for $S_{\phi K_S} \simeq 0.4$. Within the general class of models with pure left handed CKM-like flavor changing currents however, such a lower bound is significantly relaxed. In fact, in this latter case, the

source of CP violation is assumed to come from flavor effects and the resulting EDMs are suppressed by small flavor mixing angles. Hence, a potential discovery of some of the above CP asymmetries with the identified peculiar correlations without any NP signal in EDMs at the level of $d_{e,n} \simeq 10^{28} e\,\text{cm}$ would most likely rule out the FBMSSM and favor non-MFV models with purely left handed currents.

8.3 A Non-Abelian Flavor Model with CKM-like Right-Right Mass Insertions

Next, we also allow for non-trivial flavor structures in the right-right sector that are CKM-like. For definiteness we consider a concrete non-abelian SU(3) flavor model analyzed by Antusch et al. [411] to which we refer to as AKM model. The down squark flavor structure in the right-right soft sector of the AKM model, and the flavor off-diagonal entries in the left-right sector that are induced by the trilinear couplings read [411]

$$\delta_d^{RR} \simeq \begin{pmatrix} \bar{\varepsilon}^4 & \bar{\varepsilon}^3 & \bar{\varepsilon}^3 \\ \bar{\varepsilon}^3 & \bar{\varepsilon}^2 & \bar{\varepsilon}^2 e^{i\Psi_d} \\ \bar{\varepsilon}^3 & \bar{\varepsilon}^2 e^{-i\Psi_d} & \bar{\varepsilon}_3^2 \end{pmatrix} \quad , \quad \delta_d^{LR} \simeq \begin{pmatrix} \star & \bar{\varepsilon}^3 & \bar{\varepsilon}^3 \\ \bar{\varepsilon}^3 & \star & \bar{\varepsilon}^2 \\ \bar{\varepsilon}^3 & \bar{\varepsilon}^2 & \star \end{pmatrix} \frac{A_0 v}{m_0^2 \tan\beta} \ , \tag{8.4}$$

where $\bar{\varepsilon} \simeq 0.15$ and $\bar{\varepsilon}_3 \simeq 0.5$ and we suppressed O(1) coefficients in the various entries. As an interesting feature of the AKM model we observe the presence of a leading O(1) CP violating phase, Ψ_d, in the $b-s$ right-right sector but not in the $b-d$ and $s-d$ sectors.

The flavor structures in the up sector are strongly suppressed and can be safely neglected in our analysis. Furthermore, in the AKM model there is the freedom to suppress arbitrarily the flavor changing soft terms in the left-left sector and we chose to work in the limit where $(\delta_d^{LL})_{ij} = 0$. Therefore, our results have to be regarded as irreducible predictions of the AKM model, barring accidental cancellations among different contributions to physical observables. We remind here that we again implement these flavor structures at the high scale. In the running down to the electroweak scale δ_d^{LL} mass insertions are always generated radiatively that are proportional to the corresponding combinations of CKM matrix elements. The AKM model therefore predicts CKM-like mass insertions both in the left-left and in the right-right down squark mass matrices and according to the discussions in section 7.1 interesting effects in meson mixing observables can be expected. In particular, due to the predicted O(1) CP phase in $(\delta_d^{RR})_{32}$, the B_s mixing phase might receive sizable NP effects in this model.

We perform our numerical analysis analogous to the previous section. We scan the free O(1) parameter in the range $\pm[0.5, 2]$, allow the phase Ψ_d to vary between 0 and 2π, scan the parameter of the underlying CMSSM spectrum in the intervals given in (8.3) and impose all constraints as listed at the beginning of this chapter.

The left plot of figure 8.6 shows the model independent correlation between the B_s mixing phase $S_{\psi\phi}$ and the semileptonic asymmetry A_{SL}^s in the AKM model. We observe that B_s mixing phase lies in the range $-0.3 \lesssim S_{\psi\phi} \lesssim 0.3$ while being compatible with all the constraints.

Large non-standard values for $S_{\psi\phi}$ unambiguously imply a strong enhancement of the branching ratio of the rare $B_s \to \mu^+\mu^-$ decay as can be seen from the center plot in figure 8.6. In fact, we find that the effects in $B_s - \bar{B}_s$ mixing in the AKM model are dominantly generated by the double Higgs penguin diagrams discussed in section 6.4 that are strongly

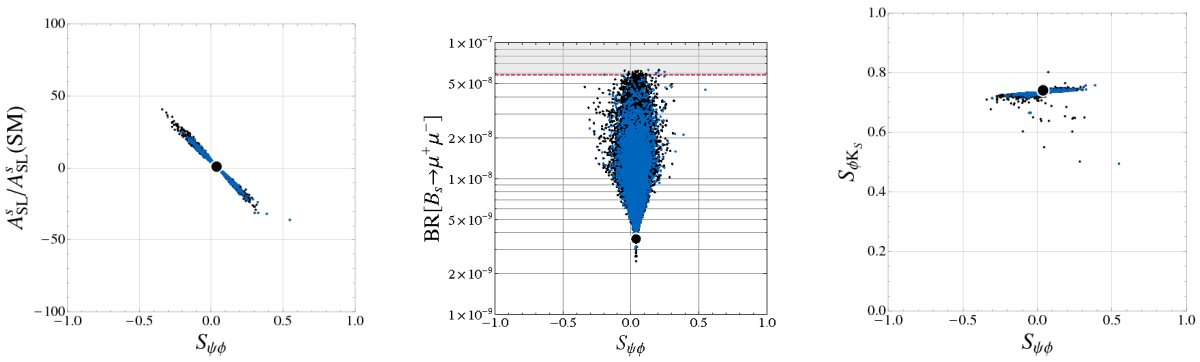

Figure 8.6: Correlations in the AKM model between the B_s mixing phase $S_{\psi\phi}$ and the semileptonic asymmetry $A^s_{\rm SL}$ (left), between $S_{\psi\phi}$ and BR$(B_s \to \mu^+\mu^-)$ (middle) as well as between $S_{\psi\phi}$ and $S_{\phi K_S}$ (right). The blue points correspond to positive NP effects in $|\epsilon_K|$ such that $1.2 < |\epsilon_K|/|\epsilon_K|_{\rm SM} < 1.3$. From [21].

correlated with Higgs contributions to $B_s \to \mu^+\mu^-$ and $|S_{\psi\phi}| \gtrsim 0.2$ implies for example BR$(B_s \to \mu^+\mu^-) \gtrsim 10^{-8}$.

Large effects also arise in $K^0 - \bar{K}^0$ mixing. Together with the radiatively induced, complex $(\delta_d^{LL})_{21} \sim V_{td}V_{ts}^*$, the rather large $(\delta_d^{RR})_{21} \sim \bar{\varepsilon}^3$ mass insertions generates left-right operators that lead to strongly enhanced NP contributions in particular in ϵ_K that turns out to be the most important constraint of this model in the quark sector. In fact, the small tension in the determination of the unitarity triangle mentioned in section 2.1 can be easily addressed in that model by means of NP contributions to ϵ_K at the level of $20 - 30\%$ as shown by the blue points in the plots of figure 8.6.

The right plot of figure 8.6 shows the correlation between $S_{\psi\phi}$ and $S_{\phi K_S}$ and we observe that $S_{\phi K_S}$ basically remains SM-like, once all constraints are taken into account.

Due to the presence non-MFV structures, the model does not follow the correlation between ΔM_s and BR$(B_s \to \mu^+\mu^-)$ predicted within MFV frameworks and shown as green points in the left plot of figure 8.7. The same is true for the MFV correlation between BR$(B_s \to \mu^+\mu^-)$ and BR$(B_d \to \mu^+\mu^-)$. Still, the deviations from the green line shown in the center plot of figure 8.7 are moderate due to the fact that MFV Higgsino loops still give very important contributions to the $B_s \to \mu^+\mu^-$ and $B_d \to \mu^+\mu^-$ decays.

The SU(3) flavor symmetry of the AKM model links the flavor structures in the quark and lepton sector, and we find indeed that large effects in $S_{\psi\phi}$ are also correlated with NP effects in lepton flavor violating processes as for example the radiative $\mu \to e\gamma$ decay. In the right plot of figure 8.7 we show the emerging correlation between these two observables. Large values for $S_{\psi\phi}$ imply also large values for BR$(\mu \to e\gamma)$ close to the current experimental bound of $\sim 10^{-11}$ [417] and within reach of the MEG experiment that has an expected sensitivity down to a level of $\sim 10^{-13}$.

Finally, concerning the predictions for EDMs in the AKM model, we note that the NP effects in the electron EDM are rather restricted with $d_e \lesssim 10^{-29} e\,$cm once the experimental constraint from BR$(\mu \to e\gamma)$ is imposed. Similarly also quark EDMs are well under control. The down quark (C)EDM can be generated through flavor effects by means of the CKM phase contained in $(\delta_d^{LL})_{31} \sim V_{tb}V_{td}^*$ in the presence of the real $(\delta_d^{RR})_{31}$ mass insertion (see (6.47)) and can only reach values up to $10^{-28} e\,$cm. However, for large CP violating effects in the

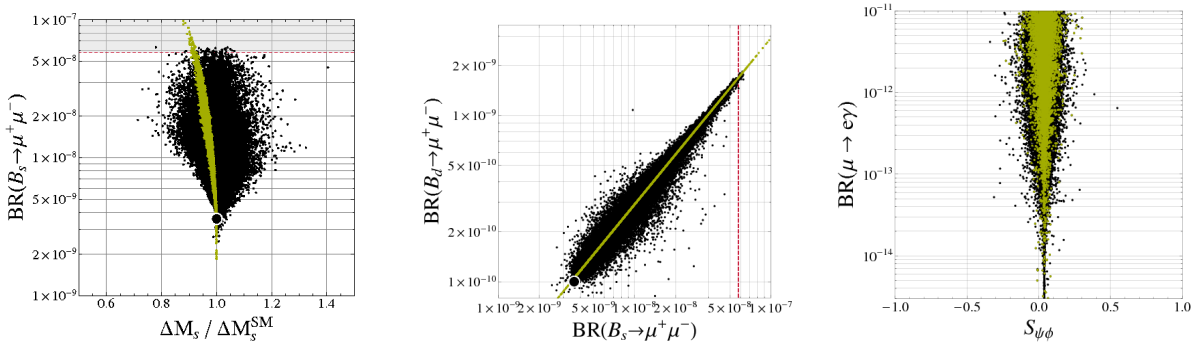

Figure 8.7: Correlations in the AKM model between the B_s mass difference ΔM_s and BR($B_s \to \mu^+\mu^-$) (left), between BR($B_s \to \mu^+\mu^-$) and BR($B_d \to \mu^+\mu^-$) (middle) as well as between $S_{\psi\phi}$ and BR($\mu \to e\gamma$) (right). The green points in the left and center plots show the correlation of the corresponding observables in the MFV MSSM. The green points in the right plot explain the $(g-2)_\mu$ anomaly at the 95% C.L., i.e. $\Delta a_\mu > 1 \times 10^{-9}$. From [21].

B_s system also the strange quark (C)EDM is induced by the analogous mechanism and enhanced compared to d_d by a factor $\bar{\varepsilon}^{-2} \simeq 50$. It would be crucial to know how the strange (C)EDM enters the prediction of hadronic EDMs in order to be sure that the possible size of the B_s mixing phase in this model is not excluded by EDM constraints.

In figure 8.8 we show the planes of the lightest stop mass, $m_{\tilde{t}_1}$ vs. the lightest chargino mass, $M_{\tilde{\chi}_1^\pm}$ and of the charged Higgs mass, $M_{H^\pm}$ vs. $\tan\beta$ in the AKM model, indicating the possible values for $S_{\psi\phi}$ with different colors. Large values for $S_{\psi\phi}$ obviously do not require a light SUSY spectrum. This is due to the fact that the NP effects in B_s mixing are induced by double Higgs penguins that do not decouple with the SUSY spectrum. The double penguins scale with $\tan^4\beta$ and as is clearly shown in the $M_{H^\pm}$ - $\tan\beta$ plane, the large values of $S_{\psi\phi}$ are only possible for very large values of $\tan\beta \gtrsim 50$.

For such high $\tan\beta$, the $B^+ \to \tau^+\nu$ decay gets potentially large NP contributions leading to a strong suppression of the branching ratio. The experimental constraint from this decay excludes then charged Higgs masses below roughly 500 GeV and also restricts to some extend the possible values for $S_{\psi\phi}$ that can be obtained in the AKM model.

To summarize: The presence of right-right mass insertions, even if only CKM-like in size, has profound impact on the flavor phenomenology of the considered model. In contrast to the MFV MSSM and the model with only left-left mass insertions, now also sizable effects in $\Delta F = 2$ observables are possible. In the concrete model that we consider, ϵ_K turns out to be the main constraint in the quark sector. Also the B_s mixing phase can receive visible NP effects up to values of $|S_{\psi\phi}| \lesssim 0.3$ that arise in the large $\tan\beta$ regime and are strongly correlated with enhancements of the BR($B_s \to \mu^+\mu^-$). Interestingly, the effects in $S_{\psi\phi}$ and BR($B_s \to \mu^+\mu^-$) do not decouple with the SUSY scale and are also present for a SUSY spectrum beyond the LHC reach.

The characteristic flavor phenomenology of this model is thus quite different from the MFV MSSM and in general from models with only left handed flavor changing currents and allows a clear distinction from such scenarios.

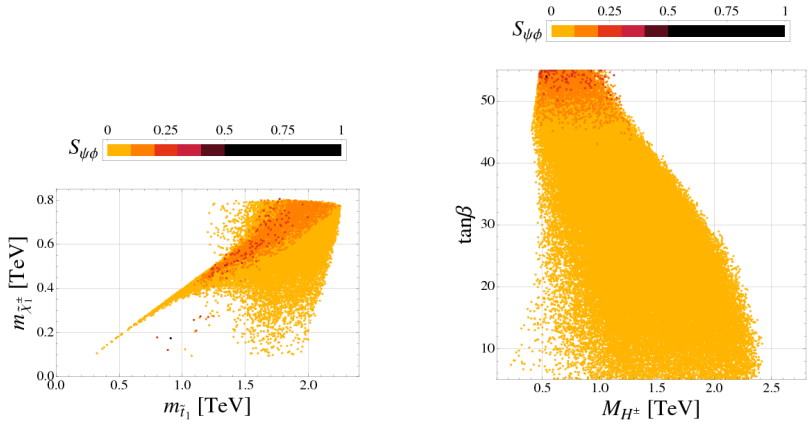

Figure 8.8: Planes of the lightest stop mass $m_{\tilde{t}_1}$ vs. the lightest chargino mass $M_{\tilde{\chi}_1^\pm}$ (left) and of the charged Higgs mass $M_{H^\pm}$ vs. $\tan\beta$ (right) in the AKM model. The different colors show the possible values for $S_{\psi\phi}$. From [21].

8.4 A Non-Abelian Flavor Model with Large Right-Right Mass Insertions

After the analysis of the AKM model in the previous section that featured at the electroweak scale small CKM-like mass insertions both in the left-left and in the right-right sector, in this section we now discuss a framework with large right-right mass insertions. We again choose to analyze an explicit realization of such a scenario, namely a non-abelian SU(3) flavor model based on the work by Ross et al. [410] and analyzed in [418, 419]. In the following we will refer to it as the RVV2 model.

At the GUT scale, again suppressing the O(1) coefficients, the expressions for the flavor off-diagonal entries in the super-CKM basis read [419][1]

$$\delta_d^{RR} \simeq \begin{pmatrix} \bar{\varepsilon}^2 y_b & -\bar{\varepsilon}^3 e^{i\omega_{us}} & -\bar{\varepsilon}^2 y_b^{0.5} e^{i(\omega_{us}-\chi+\beta_3)} \\ -\bar{\varepsilon}^3 e^{-i\omega_{us}} & \bar{\varepsilon}^2 & \bar{\varepsilon} y_b^{0.5} e^{-i(\chi-\beta_3)} \\ -\bar{\varepsilon}^2 y_b^{0.5} e^{-i(\omega_{us}-\chi+\beta_3)} & \bar{\varepsilon} y_b^{0.5} e^{i(\chi-\beta_3)} & y_b \end{pmatrix} , \tag{8.5}$$

$$\delta_d^{LL} \simeq \begin{pmatrix} \varepsilon^2 y_t & -\varepsilon^2 \bar{\varepsilon} e^{i\omega_{us}} & \varepsilon\bar{\varepsilon} y_t^{0.5} e^{i(\omega_{us}-2\chi+\beta_3)} \\ -\varepsilon^2 \bar{\varepsilon} e^{-i\omega_{us}} & \varepsilon^2 & \varepsilon y_t^{0.5} e^{-i(2\chi-\beta_3)} \\ \varepsilon\bar{\varepsilon} y_t^{0.5} e^{-i(\omega_{us}-2\chi+\beta_3)} & \varepsilon y_t^{0.5} e^{i(2\chi-\beta_3)} & y_t \end{pmatrix} , \tag{8.6}$$

with the parameters $\varepsilon \simeq 0.05$ and $\bar{\varepsilon} \simeq 0.15$. The phases ω_{us}, χ and β_3 are set, to a large extent, by the requirement of reproducing the CKM phase. In particular, it turns out that $\omega_{us} \simeq -\lambda$ and $(\chi, \beta_3) \simeq (20°, -20°)$ (or any other values obtained by adding 180° to each) [419].

In the SCKM basis, the trilinear couplings of the RVV2 model lead to the following flavor

[1] In order to avoid accidental cancellations among different phases in the expressions (8.5) and (8.5), we have set to zero an extra CP violating phase, β_2', that is not constrained by the requirement of reproducing a correct CKM matrix [419].

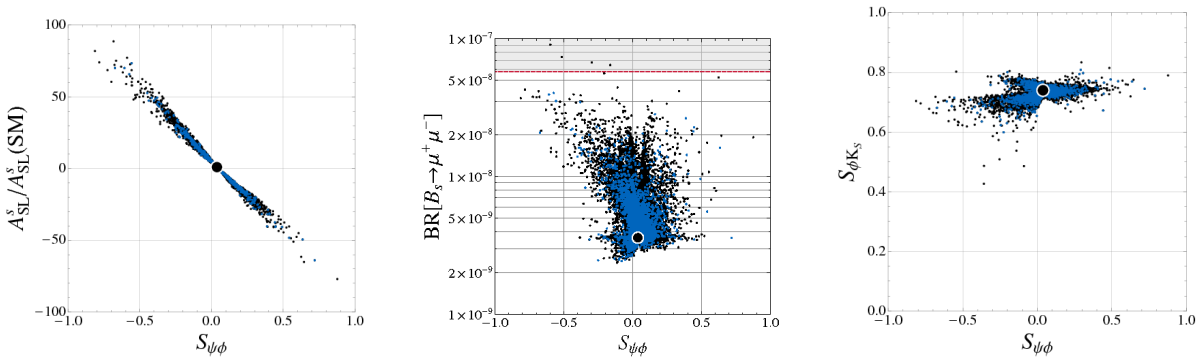

Figure 8.9: Correlations in the RVV2 model between the B_s mixing phase $S_{\psi\phi}$ and the semileptonic asymmetry $A^s_{\rm SL}$ (left), between $S_{\psi\phi}$ and BR$(B_s \to \mu^+\mu^-)$ (middle) as well as between $S_{\psi\phi}$ and $S_{\phi K_S}$ (right). The blue points correspond to positive NP effects in $|\epsilon_K|$ such that $1.2 < |\epsilon_K|/|\epsilon_K|_{\rm SM} < 1.3$. From [21].

off-diagonal left-right mass insertions [419]

$$\delta_d^{LR} \simeq \begin{pmatrix} \star & \bar{\varepsilon}^3 e^{-i\omega_{us}} & \bar{\varepsilon}^3 e^{-i\omega_{us}} \\ \bar{\varepsilon}^3 e^{-i\omega_{us}} & \star & \bar{\varepsilon}^2 \\ \bar{\varepsilon}^3 e^{i(\omega_{us}+2\beta_3-2\chi)} & \bar{\varepsilon}^2 e^{2i(\beta_3-\chi)} & \star \end{pmatrix} \frac{A_0}{m_0^2} m_b \ . \tag{8.7}$$

Additionally it is found that the mass insertions in the up sector are strongly suppressed and we can neglect them in our analysis.

We observe that the RVV2 model contains complex $b-s$ mass insertions both in the left-left sector, $(\delta_d^{LL})_{32} \sim \varepsilon y_t^{0.5}$ and in the right-right sector $(\delta_d^{RR})_{32} \sim \bar{\varepsilon} y_b^{0.5}$. In particular $(\delta_d^{RR})_{32}$ is considerably larger than in the previously considered AKM model and sizable NP effects are expected in $b \to s$ transitions.

We perform our numerical analysis analogous to the previous sections. We scan the free O(1) parameter in the range $\pm[0.5, 2]$, and vary the parameter of the underlying CMSSM spectrum in the intervals given in (8.3) and impose all constraints as listed at the beginning of this chapter.

In analogy to the discussion of the flavor phenomenology in the AKM model, we show the main predictions for flavor observables in the RVV2 model in figures 8.9 and 8.10. We find that values up to $-0.7 \lesssim S_{\psi\phi} \lesssim 0.7$ are possible in the RVV2 model while being compatible with all the constraints. In contrast to the AKM model, the correlation between $S_{\psi\phi}$ and the BR$(B_s \to \mu^+\mu^-)$ is lost to a large extent. In fact, in the RVV2 model not only double Higgs penguins contribute significantly to $B_s - \bar{B}_s$ mixing, but also gluino box contributions play an important role and wash out the correlation with the $B_s \to \mu^+\mu^-$ decay.

Similarly to the AKM model, the ϵ_K observable constitutes a very important constraint of the model as it can be modified significantly by NP effects. Large effects in ϵ_K at the level of $20\% - 30\%$ are obtained without problems and the small tension in the unitarity triangle can be easily solved.

In $S_{\phi K_S}$, slightly larger effects than in the AKM model are possible due to the larger mass insertions in the $b-s$ sector. Still, once all constraints are imposed, $S_{\phi K_S}$ essentially stays SM-like, with $0.6 \lesssim S_{\phi K_S} \lesssim 0.8$.

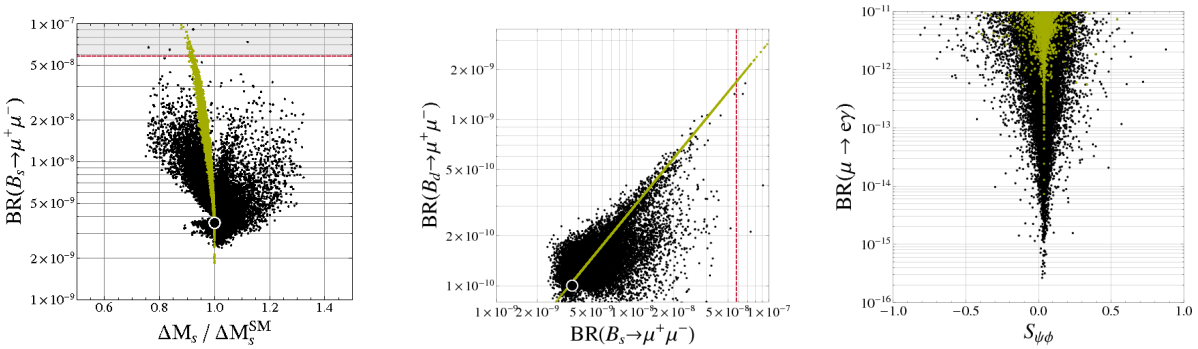

Figure 8.10: Correlations in the RVV2 model between the B_s mass difference ΔM_s and BR($B_s \to \mu^+\mu^-$) (left), between BR($B_s \to \mu^+\mu^-$) and BR($B_d \to \mu^+\mu^-$) (middle) as well as between $S_{\psi\phi}$ and BR($\mu \to e\gamma$) (right). The green points in the left and center plots show the correlation of the corresponding observables in the MFV MSSM. The green points in the right plot explain the $(g-2)_\mu$ anomaly at the 95% C.L., i.e. $\Delta a_\mu > 1 \times 10^{-9}$. From [21].

The correlation between ΔM_s and BR($B_s \to \mu^+\mu^-$) as well as between BR($B_s \to \mu^+\mu^-$) and BR($B_d \to \mu^+\mu^-$) clearly show the non-MFV nature of the considered model.

Finally, as the RVV2 model is embedded in a SO(10) SUSY GUT, also there correlations between observables in the quark and lepton sector exist. In the right plot of figure 8.10 we show again the correlation between $S_{\psi\phi}$ and the branching ratio of the $\mu \to e\gamma$ decay. In fact, large $|S_{\psi\phi}| > 0.3$ automatically also implies BR($\mu \to e\gamma$) $\gtrsim 10^{-13}$ within the reach of the MEG experiment. It is interesting to note, that an explanation of the $(g-2)_\mu$ anomaly (green points in the plot) and simultaneously sizable effects in $S_{\psi\phi}$ even requires a BR($\mu \to e\gamma$) very close to the present experimental bound of $\simeq 10^{-11}$.

The main characteristics of the SUSY spectrum of the RVV2 model are shown in the plots of figure 8.11. As can be seen from the left plot, the large effects in $S_{\psi\phi}$ that are possible, do not necessarily imply a SUSY spectrum in the LHC reach but are possible over broad regions of parameter space.

In conclusion, the RVV2 and the AKM model share many similarities. They are both non-abelian flavor models based on a SU(3) flavor symmetry and feature non-trivial flavor structures in the right-right down squark mass matrix. Correspondingly, ϵ_K turns out to be a strong constraint in both models. The main difference of the two models concerning the flavor phenomenology in the quark sector is that in the RVV2 model larger values for the B_s mixing phase, up to $-0.7 \lesssim S_{\psi\phi} \lesssim 0.7$, are possible due to the significantly larger $(\delta_d^{RR})_{32}$ mass insertion. In contrast to the AKM model, the NP effects in $S_{\psi\phi}$ are not correlated with an enhancement of BR($B_s \to \mu^+\mu^-$) as also gluino boxes lead to sizable contributions to the $B_s - \bar{B}_s$ mixing amplitude.

8.5 An Abelian Flavor Model with Large Right-Right Mass Insertions

Finally we also discuss the characteristic predictions of an abelian flavor model that predicts O(1) mass insertions for $b \to s$ transitions in the right-right sector. Concretely we analyze a

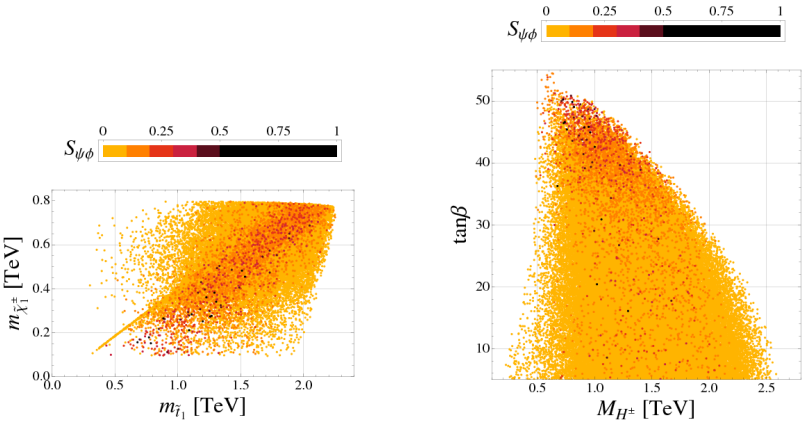

Figure 8.11: Planes of the lightest stop mass $m_{\tilde{t}_1}$ vs. the lightest chargino mass $M_{\tilde{\chi}_1^\pm}$ (left) and of the charged Higgs mass $M_{H^\pm}$ vs. $\tan\beta$ (right) in the RVV2 model. The different colors show the possible values for $S_{\psi\phi}$. From [21].

flavor model by Agashe, Carone (AC) [401] that is based on a single horizontal U(1) flavor symmetry. While flavor models with a single U(1) are typically disfavored by the ϵ_K and ΔM_K constraints [393, 398], the AC model realizes a high degree of quark-squark alignment by means of a non-trivial extra-dimensional topography, suppressing unwanted FCNC effects.

The pattern of the relevant mass insertions at the GUT scale, given in powers of the Cabibbo angle λ, is given by

$$\delta_d^{LL} \simeq \begin{pmatrix} 1 & 0 & 0 \\ 0 & 1 & \lambda^2 \\ 0 & \lambda^2 & 1 \end{pmatrix} , \quad \delta_d^{RR} \simeq \begin{pmatrix} 1 & 0 & 0 \\ 0 & 1 & e^{i\phi_R} \\ 0 & e^{-i\phi_R} & 1 \end{pmatrix} , \quad (\delta_u^{LL})_{12} \simeq \lambda , \quad (\delta_u^{RR})_{12} \simeq \lambda^3 e^{i\phi_u} , \tag{8.8}$$

where we have suppressed unknown O(1) coefficients which multiply the individual elements of the matrices. As already remarked in [401] the "model yields a remarkable level of quark squark alignment" in the $s-d$ and also in the $b-d$ sector, and tiny NP effects are in particular expected in $K^0 - \bar{K}^0$ as well as in $B_d - \bar{B}_d$ mixing. On the other hand the model predicts a $(\delta_d^{RR})_{32}$ of order one with a CP violating phase and also a $(\delta_d^{LL})_{32}$ that is CKM-like in size. Correspondingly, among the considered scenarios in this chapter, the largest NP effects in $b \to s$ transitions are expected in the AC model. Large effects are also expected in $D^0 - \bar{D}^0$ mixing, due to the presence of the $(\delta_u^{LL})_{21}$ mass insertion of the order of the Cabibbo angle, as it naturally happens in abelian flavor models that realize the alignment mechanism (see discussion in section 7.3).

As in the previous sections, we implement the above flavor structures at the GUT scale into a CMSSM spectrum. We scan the CMSSM parameter in the intervals given in (8.3) and vary the free O(1) parameter in front of the off-diagonal entries in the range $\pm[0.5, 2]$. Concerning the diagonal masses we impose a large splitting between the first and second generation of left handed squarks such that $m_{\tilde{u}_L} = 2m_{\tilde{c}_L} = 2m_0$. This splitting leads to the $(\delta_u^{LL})_{21} \simeq \lambda$ at the GUT scale, characteristic for abelian flavor models as explained in section 7.3 and leading to large NP effects in $D^0 - \bar{D}^0$ mixing.

However, in the running from the GUT scale down to the low scale where we evaluate the SUSY contributions to observables, the $(\delta_u^{LL})_{21}$ mass insertion can get significantly reduced.

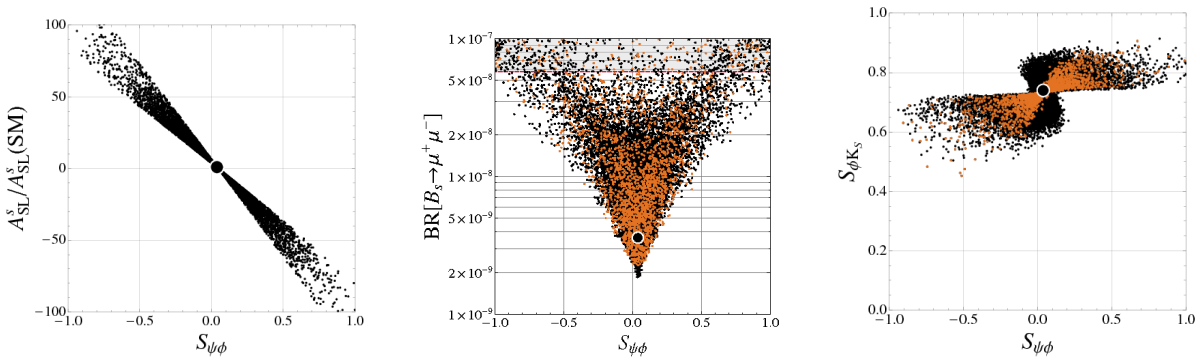

Figure 8.12: Correlations in the AC model between the B_s mixing phase $S_{\psi\phi}$ and the semileptonic asymmetry $A^s_{\rm SL}$ (left), between $S_{\psi\phi}$ and BR$(B_s \to \mu^+\mu^-)$ (middle) as well as between $S_{\psi\phi}$ and $S_{\phi K_S}$ (right). The orange points correspond to negative NP contributions in $\Delta M_d/\Delta M_s$ at the level of $15\% - 25\%$. From [21].

In fact, there is a degeneracy mechanism triggered mainly by the flavor blind SU(3) interactions that restores a partial degeneracy between the first and second generation squark masses [394]. The diagonal masses get strongly renormalized by SU(3) interactions and their GUT scale values $m^2_{\tilde{u}_L}(M_{\rm GUT}) = 4m_0^2$ and $m^2_{\tilde{c}_L}(M_{\rm GUT}) = m_0^2$ become at the low scale $m^2_{\tilde{u}_L}(M_W) \simeq 4m_0^2 + 6M^2_{1/2}$ and $m_{\tilde{c}_L}(M_W) \simeq m_0^2 + 6M^2_{1/2}$. As a result, the GUT mass insertion $(\delta_u^{LL})_{21} \sim \lambda$ can be easily reduced by one order of magnitude at the low scale and the constraints from $D^0 - \bar{D}^0$ mixing can in principle be satisfied also for squark masses below the TeV scale. This is in contrast with the results of a low energy approach were $(\delta_u^{LL})_{21} \sim \lambda$ holds at the low scale implying a lower bound on the squark masses of around 2 TeV [65, 55].

Still, in contrast to the AKM and RVV2 models, the $D^0 - \bar{D}^0$ mixing observables are the most important constraints now, while ϵ_K is always SM-like. In figures 8.12 and 8.13 we show the most important results for flavor observables that are predicted by the AC model, once all constraints mentioned at the beginning of the chapter have been imposed.

As expected, due to the O(1) $(\delta_d^{RR})_{32}$ mass insertion, huge effects both in $\Delta F = 1$ and $\Delta F = 2$ $b \to s$ transitions can arise in this model. In particular large values for $S_{\psi\phi}$ in the full range $-1 \lesssim S_{\psi\phi} \lesssim +1$ are allowed and are strongly correlated with enhancements of the $B_s \to \mu^+\mu^-$ branching ratio. We predict a lower bound on BR$(B_s \to \mu^+\mu^-)$ at the level of BR$(B_s \to \mu^+\mu^-) \gtrsim 10^{-8}$ for $|S_{\psi\phi}| \gtrsim 0.3$. In fact, as in the AKM model, the double Higgs penguins give the dominant contribution to $B_s - \bar{B}_s$ mixing. Contributions from gluino boxes that would wash out the correlation between $S_{\psi\phi}$ and BR$(B_s \to \mu^+\mu^-)$ turn out to be strongly constrained by the $D^0 - \bar{D}^0$ constraints.

The right plot in figure 8.12 shows the correlation between $S_{\psi\phi}$ and $S_{\phi K_S}$ indicating that both asymmetries can simultaneously depart significantly from the SM expectations. However, a suppression of $S_{\phi K_S}$ below its SM prediction as indicated by experiment implies negative values for $S_{\psi\phi}$, in contrast with the present data. The shape of the correlation between $S_{\psi\phi}$ and $S_{\phi K_S}$, i.e. the fact that a positive (negative) $S_{\psi\phi}$ implies an enhancement (suppression) of $S_{\phi K_S}$ can also be understood analytically. In the considered model, the NP effects in $S_{\phi K_S}$ are dominantly induced by the Wilson coefficient $\tilde{C}_8$ given in (6.11). As we consider only the case of a real and positive μ parameter, the sign and phase of $\tilde{C}_8$ and therefore also of the NP contribution to $S_{\phi K_S}$ is fixed by $(\delta_d^{RR})_{32}$. Concerning $S_{\psi\phi}$, the

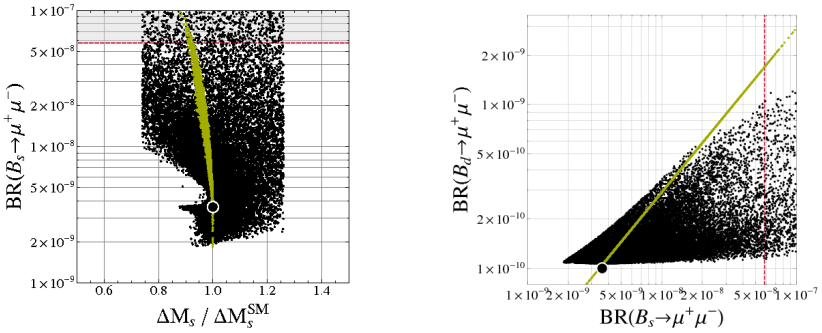

Figure 8.13: Correlations in the AC model between the B_s mass difference ΔM_s and BR($B_s \to \mu^+\mu^-$) (left) and between BR($B_s \to \mu^+\mu^-$) and BR($B_d \to \mu^+\mu^-$) (right). The green points show the correlation of the corresponding observables in the MFV MSSM. From [21].

dominant NP contribution to the B_s mixing amplitude M_{12}^s is induced by the double Higgs penguin contribution. In particular, we find that in most parts of the parameter space the largest contribution comes from a double penguin with one gluino and one Higgsino loop (see diagram a) in figure 6.9) with the corresponding analytical expression stated in the second line of (6.38). As both the trilinear coupling A_t and the loop functions f_1 and f_3 have a fixed sign in almost the entire parameter space considered by us, the sign and phase of the NP contribution to M_{12}^s and hence to $S_{\psi\phi}$ is again determined by $\left(\delta_d^{RR}\right)_{32}$ and the correlation in the right plot of figure 8.12 emerges.[2]

Similar to $S_{\psi\phi}$, also the mass difference in the B_s system, ΔM_s, receives large NP contributions in the AC model. On the other hand neither ϵ_K nor $S_{\psi K_S}$ deviate significantly from their SM predictions. Consequently the small tension in the unitarity triangle can only be addressed by an enhancement of ΔM_s leading to the required suppression of $\Delta M_d/\Delta M_s$ by approximately 20% (see section 2.1). Such a situation appears naturally in the AC model and is shown by the orange points in the plots of figure 8.12.

The effects in ΔM_s do not follow the MFV correlation with BR($B_s \to \mu^+\mu^-$), showing clearly that non-MFV sources of flavor violation are present in the model. Also the correlation between BR($B_s \to \mu^+\mu^-$) and BR($B_d \to \mu^+\mu^-$) can deviate significantly from the MFV prediction as shown in figure 8.13.

Concerning the predictions for EDMs in the AC model, we note that the large CP violating effects in B_s mixing unambiguously imply a very large flavored strange quark (C)EDM (see (6.48)) at the level of $d_s^{(c)} \sim 10^{-24} - 10^{-23} e\,\text{cm}$. Hence, the current experimental bounds on d_n imply that either the strange quark contributions to d_n have to be very small, with a proportionality coefficient smaller than 10^{-3}, or that O(1) CP violating phases for the product $(\delta_d^{LL})_{23}(\delta_d^{RR})_{32}$ are not allowed (unless $\text{Arg}(\delta_d^{LL})_{32} = \text{Arg}(\delta_d^{RR})_{32}$). In this respect, a reliable knowledge of the order of magnitude of the strange quark contributions to d_n would be of utmost importance to probe or to falsify abelian flavor models embedded in a SUSY framework.

Furthermore, we also remark that a large flavored up quark (C)EDM at the level of

[2] We note that if the dominant contribution to M_{12}^s came from gluino boxes (6.28) or from double penguins with two gluino loops (first line of (6.38)), with $(\delta_d^{LL})_{32}$ induced radiatively through renormalization group effects, the correlation between $S_{\psi\phi}$ and $S_{\phi K_S}$ would have the opposite sign.

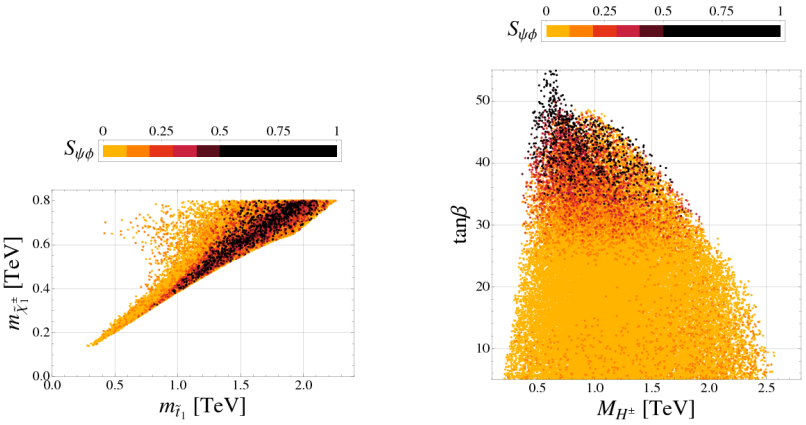

Figure 8.14: Planes of the lightest stop mass $m_{\tilde{t}_1}$ vs. the lightest chargino mass $M_{\tilde{\chi}_1^\pm}$ (left) and of the charged Higgs mass $M_{H^\pm}$ vs. $\tan\beta$ (right) in the AC model. The different colors show the possible values for $S_{\psi\phi}$. From [21].

$d_u^{(c)} \sim 10^{-27} - 10^{-26} e\,\text{cm}$ is induced in the AC model through the large complex combination of mass insertions in the up sector, $(\delta_u^{RR})_{12}(\delta_u^{LL})_{21}$. A large up quark (C)EDM is in fact a generic prediction of abelian flavor models as we will detail in the following section.

Finally, concerning the SUSY spectrum of the AC model, we observe from the left plot in figure 8.14 that significant deviations of $S_{\psi\phi}$ from its SM prediction are possible also a SUSY spectrum beyond the LHC reach and even seem to favor a heavy spectrum. In fact for heavy SUSY particles, the constraints from $D^0 - \bar{D}^0$ and e.g. also BR($B \to X_s\gamma$) can be more easily fulfilled while the non-decoupling properties of the double Higgs penguins ensure that large effects in $S_{\psi\phi}$ are still possible. As seen in the right plot of figure 8.14, large effects in $|S_{\psi\phi} > 0.3|$ require values for $\tan\beta \gtrsim 30$.

To summarize we stress that due to the O(1) $(\delta_d^{RR})_{32}$ mass insertion huge effects in $b \to s$ transitions are possible in the AC model. In particular the B_s mixing phase can reach all possible values in the full interval $-1 \lesssim S_{\psi\phi} \lesssim 1$. The effects in $B_s - \bar{B}_s$ mixing are generated by double Higgs penguins and large values of $S_{\psi\phi}$ are correlated with a significant enhancement of BR($B_s \to \mu^+\mu^-$) over its SM prediction. In contrast to the non-abelian AKM and RVV2 models, effects in ϵ_K are basically absent by construction. On the other hand large NP effects arise in $D^0 - \bar{D}^0$ mixing, which is a general feature of abelian flavor models.

8.6 A Generic Prediction of Abelian Flavor Models

As discussed in general terms in section 7.3 and also in the context of a concrete abelian flavor model in the previous section 8.5, $D^0 - \bar{D}^0$ mixing observables provide a crucial tool to probe models with alignment. On general grounds, as also discussed already in section 3.1.2, in particular CP violation in $D^0 - \bar{D}^0$ mixing offers excellent possibilities to discover NP effects. As CP violation in $D^0 - \bar{D}^0$ mixing is expected below the level of 10^{-3} in the SM, any experimental signal above the per mill level would necessarily imply the presence of NP.

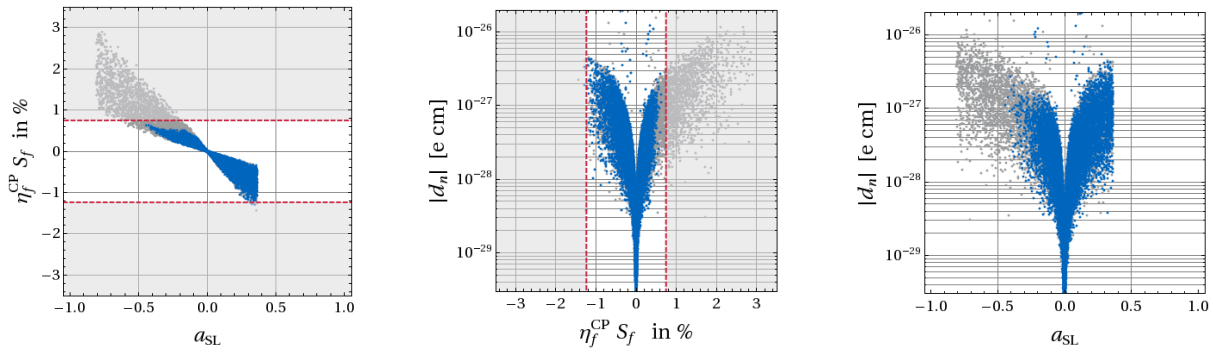

Figure 8.15: Correlations between $a_{\rm SL}^D$ and S_f^D (left), d_n and S_f^D (middle) and d_n and $a_{\rm SL}^D$ (right) in SUSY alignment models. Gray points satisfy the constraints from x_d, y_D and $|q/p|$, while blue points further satisfy the constraint from ϕ_D as given in table 3.2. Dashed lines stand for the allowed range (3.17) for S_f^D. From [22].

As shown in [394] it is possible to derive both lower and upper bounds for mass insertions for a broad class of abelian flavor models that realize the alignment mechanism. While mass insertions in the $b-s$, $b-d$ and $s-d$ can be suppressed to a large extent in these models, the most important prediction is the inevitable appearance of a large *real* mass insertion $(\delta_u^{LL})_{21} \sim \lambda$ as long as the left handed squarks are split in mass. In addition also a non-negligible mass insertion in the right-right sector $(\delta_u^{RR})_{21} \sim \lambda^4 - \lambda^2$ that is potentially complex is predicted. Correspondingly, large NP effects in $D^0 - \bar{D}^0$ mixing are expected in these models that are generated by gluino box contributions to the Wilson coefficient C_4 (6.28). In particular, if the mass insertion in the right-right sector features a large CP phase, CP violating effects in $D^0 - \bar{D}^0$ mixing should be caused by the imaginary part of the mixing amplitude $\text{Im}M_{12}^D \sim \text{Im}\left[(\delta_u^{LL})_{21}(\delta_u^{RR})_{21}\right]$, and CP violating observables like the semileptonic asymmetry $a_{\rm SL}^D$ or the time dependent asymmetry S_f^D, discussed in section 3.1.2, could be close to the present experimental bounds.

Simultaneously, the same mass insertions also induce a sizable flavored up quark (C)EDM. As seen in section 6.7, flavor effects even lead to an enhancement factor m_c/m_u in the up quark (C)EDM that is proportional to $d_u^{(c)} \sim \text{Im}\left[(\delta_u^{LL})_{12}(\delta_u^{RR})_{21}\right]$. Therefore also hadronic EDMs, as the mercury and neutron EDMs, $d_{\rm Hg}$ and d_n, that are induced by the up quark (C)EDM, provide equally important probes of the flavor structure of abelian flavor models.

Recent experimental results on the mercury EDM [186] lead to a considerably improved bound on $d_{\rm Hg}$ (3.122), which makes the mercury EDM very sensitive to NP effects. Still, given the large theoretical uncertainties affecting its theoretical prediction (3.128), we focus in the following only on the neutron EDM to be conservative.

To numerically establish the expected correlation between CP violation in $D^0 - \bar{D}^0$ mixing and the neutron EDM, we follow the same the procedure as in the previous sections. We assume a CMSSM spectrum with the corresponding parameter in the ranges given in (8.3). We set at the GUT scale $(\delta_u^{RR})_{21} = \lambda^3 e^{i\phi_u}$ and scan the phase in the range $0 < \phi_u < 2\pi$. Finally, we also set the mass splitting between the first and second squark generation masses as $m_{\tilde{u}_L} = 2m_{\tilde{c}_L} = 2m_0$ inducing a $(\delta_u^{LL})_{21}$ mass insertion of the order of the Cabibbo angle at the GUT scale.

In the plot on the left of figure 8.15 we show the correlation between S_f^D and $a_{\rm SL}^D$, as

expected by the model independent relation in (3.19). We observe that within alignment models, it is possible to saturate the model independent values for S_f^D and $a_{\rm SL}^D$ shown in figure 3.1.

In the center and right plots of figure 8.15, we show the correlation between d_n and S_f^D as well as between d_n and $a_{\rm SL}^D$. Even so the CP violating source is the same, d_n cannot be exactly correlated with S_f^D and $a_{\rm SL}^D$. In particular, while $d_u^{(c)}$ is directly proportional to the scharm trilinear coupling A_c (see (6.49)), ${\rm Im}M_{12}^D$ is not. While the natural value for A_c is $A_c \sim M_{\tilde{g}}, \tilde{m}$, there are corners in the SUSY parameter space where $A_c \ll M_{\tilde{g}}, \tilde{m}$ as in the CMSSM-like spectrum, which we assume, $A_c \simeq 0.65\ A_0 - 2.8\ M_{1/2}$ at the low scale.

Still, interestingly enough, large values for S_f^D and $a_{\rm SL}^D$ necessarily imply a lower bound for the neutron EDM $d_n \gtrsim 10^{-(28-29)} e$ cm, that is an interesting level for the expected future experimental resolutions. Similarly, according to (3.128), it turns out that the corresponding lower bound for $d_{\rm Hg}$ is $d_{\rm Hg} \gtrsim 10^{-(30-31)} e$ cm.

In summary, the most peculiar predictions of the broad class of supersymmetric abelian flavor models considered in [394] are:

- Natural solution of the SUSY flavor problem thanks to small (most probably undetectable) effects in the down quark sector, i.e. in $K^0 - \bar{K}^0$, $B^0 - \bar{B}^0$ and $B_s^0 - \bar{B}_s^0$ mixings.[3]

- Experimentally visible CP violating effects in $D^0 - \bar{D}^0$ mixing, as the time dependent CP asymmetry in decays to CP eigenstates S_f^D and the semileptonic asymmetry $a_{\rm SL}^D$.

- Large values for the hadronic EDMs (like the neutron EDM and the mercury EDM), in the reach of the future experimental sensitivities, generated by the up-quark (C)EDM. A correlated study of several hadronic EDMs, with different sensitivity to the up-quark (C)EDM would therefore provide a crucial tool to probe SUSY alignment models.

- A lower bound for the hadronic EDMs in the reach of future experimental sensitivities, for given large (non-standard) values of S_f^D and $a_{\rm SL}^D$.

As is clear from the discussions in this chapter, the patterns of NP effects in low energy observables found in the various supersymmetric extensions of the SM are characteristic for a given model. This is summarized also in table 8.1, where we show a "flavor DNA" of the models considered in this section, i.e. the possible size of NP effects in a selection of important low energy observables. Three stars signal large effects that could be clearly distinguished from the SM prediction with the sensitivity of upcoming experiments. Two stars correspond to moderate but probably still visible effects and one star implies that the given model cannot significantly modify a given observable. Of particular importance to distinguish the various models are also their characteristic correlations among the observables as extensively discussed in the above sections.

Consequently, precise measurements of low energy observables allow to draw conclusions about the possible NP flavor structure and allow in principle to distinguish the considered models based on their distinct predictions in the flavor sector.

[3] An exception to these findings arises in the AC model that does not belong to the class of the abelian flavor models considered in [394]. As thoroughly discussed in section 8.5, the AC model predicts, in addition to large NP effects in $D^0 - \bar{D}^0$ mixing, also large NP effects for $b \to s$ transitions.

	MFV	δLL	AKM	RVV2	AC	GMSSM
S_f^D	★	★	★	★	★★★	★★★
$a_{\rm SL}^D$	★	★	★	★	★★★	★★★
$S_{\psi\phi}$	★	★	★★	★★★	★★★	★★★
$S_{\phi K_S}$, $S_{\eta' K_S}$	★★★	★★★	★	★	★★	★★★
$A_{\rm CP}(b\to s\gamma)$	★★★	★★★	★	★	★	★★★
$S_3(B\to K^*\mu^+\mu^-)$	★	★	★	★	★	★★★
$S_{4,5}(B\to K^*\mu^+\mu^-)$	★★★	★★★	★	★	★	★★★
$S_6^s(B\to K^*\mu^+\mu^-)$	★★★	★★★	★	★	★	★★★
$A_{7,8}(B\to K^*\mu^+\mu^-)$	★★★	★★★	★	★	★	★★★
$A_9(B\to K^*\mu^+\mu^-)$	★	★	★	★	★	★★★
${\rm BR}(B_s\to\mu^+\mu^-)$	★★★	★★★	★★★	★★★	★★★	★★★
${\rm BR}(B_d\to\mu^+\mu^-)$	★★★	★★★	★★★	★★★	★★★	★★★
${\rm BR}(K^+\to\pi^+\nu\bar\nu)$	★	★	★	★	★	★★★
${\rm BR}(K_L\to\pi^0\nu\bar\nu)$	★	★	★	★	★	★★★
${\rm BR}(B^+\to K^+\nu\bar\nu)$	★	★	★	★	★	★★
${\rm BR}(B\to K^*\nu\bar\nu)$	★	★	★	★	★	★★
$F_L(B\to K^*\nu\bar\nu)$	★	★	★	★	★	★
d_n	★★★	★★	★★★	★★★	★★★	★★★
d_e	★★★	★	★★	★★★	★★★	★★★

Table 8.1: The "flavor DNA" of the SUSY models analyzed in chapter 8. Shown is the possible size of NP effects in a selection of important low energy observables. ★★★ signals large effects that could be clearly distinguished from the SM prediction with the sensitivity of upcoming experiments. ★★ corresponds to moderate but probably still visible effects and ★ implies that the given model cannot significantly modify a given observable. For comparison, the last column shows possible effects in the MSSM with completely generic flavor structure.

9 Summary and Outlook

In the coming years the LHC will for the first time directly explore the TeV scale in order to clarify the mechanism of electroweak symmetry breaking and to hopefully discover new degrees of freedom at the TeV scale. Parallel to this seminal advance at the *high energy frontier*, important results are also expected at the *high precision frontier* in particular through the B_s physics programs at the Tevatron and of course at LHCb. In addition, the planned superB factory at Frascati and the Belle II experiment at KEK as well as coming experiments looking for the very rare $K \to \pi\nu\bar{\nu}$ decays, as the NA62 experiment at CERN and the K0TO experiment at J-PARC, will provide invaluable insights in the flavor structure of possible NP models.

The main goal of the high p_T program at the LHC is the direct production of e.g. the Higgs boson or other new particles and to determine their masses. On the other hand, flavor physics aims at searching for the footprints of these new particles in low energy processes through quantum effects. While the latter exploration of very short distance scales is indirect, the measurements of a large number of low energy observables and the study of correlations between them in a given extension of the SM allows in principle to identify the flavor structure of the new degrees of freedom.

In this work, we performed an extensive analysis of low energy processes in the framework of the Minimal Supersymmetric Standard Model. We discussed observables in the $\Delta F = 2$ sector, i.e. in $D^0 - \bar{D}^0$, $K^0 - \bar{K}^0$, $B_d - \bar{B}_d$ and $B_s - \bar{B}_s$ mixing. While the well measured observables in meson mixing lead to strong constraints on the NP flavor structure, there are also observables where experimental data is still poor and large NP effects are still possible. Of particular interest in this respect are CP violating observables in $D^0 - \bar{D}^0$ mixing as well as the observable $S_{\psi\phi}$, the phase of B_s mixing, where recent data from Tevatron might be interpreted as a hint for the presence of New Physics.

In the $\Delta F = 1$ sector we investigated processes sensitive to NP effects in flavor changing dipole operators, including the radiative $b \to s\gamma$ decay as well as the semileptonic $B \to K^*\ell^+\ell^-$ and the non-leptonic $B \to \phi K_s$ and $B \to \eta' K_S$ decay modes. Apart from the extremely important $B \to X_s\gamma$ branching ratio, our focus was in particular on observables that are theoretically clean as e.g. CP asymmetries. We also discussed the purely leptonic $B_s \to \mu^+\mu^-$ and $B_d \to \mu^+\mu^-$ decays that, as well as the tree level $B^+ \to \tau^+\nu$ decay, are especially sensitive probes of the large $\tan\beta$ regime of the MSSM. In addition, we considered rare B and K decays with two neutrinos in the final state, i.e. $B \to X_s\nu\bar{\nu}$, $B \to K^{(*)}\nu\bar{\nu}$, $K^+ \to \pi^+\nu\bar{\nu}$ and $K_L \to \pi^0\nu\bar{\nu}$. They are among the theoretically cleanest FCNC processes and we emphasized the peculiar flavor structures that are necessary in the MSSM to generate sizeable non-standard effects in these decays.

Finally we also considered $\Delta F = 0$ observables, i.e. observables that do not require any source of flavor violation. In particular we discussed the anomalous magnetic moment of the muon, $(g-2)_\mu$, and electric dipole moments. The EDMs are particular interesting

observables as the corresponding SM predictions are extremely small and any experimental evidence would be a clear signal of New Physics.

The soft breaking terms in the MSSM contain many sources of flavor and CP violation in addition to the SM CKM matrix. These sources lead to potentially large SUSY contributions to flavor and CP violating processes at the loop level. In fact, if SUSY particles are assumed to have masses of the order of the natural TeV scale, the existing measurements of flavor observables lead to strong constraints on the MSSM flavor structures. As detailed in section 7.1, the bounds on the flavor off-diagonal entries of the squark masses coming in particular from $D^0 - \bar{D}^0$ and $K^0 - \bar{K}^0$ mixing are extremely tight and the allowed ranges for the mass insertions are highly non-generic and seem unnatural. This is the so-called *SUSY flavor problem*.

One way to address the SUSY flavor problem is to invoke the principle of Minimal Flavor Violation, which states that the only source of flavor violation are the SM Yukawa couplings. The NP contributions to FCNC processes are then suppressed by the same CKM elements as in the SM and NP effects to many observables are naturally small. Still, large effects can be expected in helicity suppressed processes as $B_{s,d} \to \mu^+\mu^-$ and $B \to \tau\nu$ and particular in observables sensitive to NP effects in the $b \to s\gamma$ and $b \to s$ gluon transitions.

While the MFV principle forbids any flavor violating structures apart from the CKM matrix, in general it does not forbid the presence of additional sources of CP violation. As discussed in detail in section 8.1, the characteristic phenomenology of CP violation in the MFV MSSM consists of large and highly correlated NP effects in observables sensitive to CP violation in $\Delta F = 0$ and $\Delta F = 1$ dipole amplitudes, as the EDMs of the electron and the neutron and e.g. the time dependent CP asymmetries in the $B \to \phi K_S$ and $B \to \eta' K_S$ decays as well as the direct CP asymmetry in $B \to X_s\gamma$ and the CP asymmetries in the $B \to K^*\ell^+\ell^-$ decay. In particular, sizable effects in the CP asymmetries in the B meson decays unambiguously imply lower bounds on the electric dipole moments at the level of $10^{-28} e\,\mathrm{cm}$, which is not far below the current experimental constraints and in the reach of future experiments.

Possible NP effects in $\Delta F = 2$ processes are however found to be small in the MFV MSSM. In particular, CP violation in the meson mixing amplitudes remains basically SM-like in this framework, resulting e.g. in a SM-like $S_{\psi\phi}$. We can conclude that within the MSSM only in the presence of new sources of *flavor violation*, sizeable NP contributions to *CP violation* in meson mixing can occur.

Well motivated SUSY theories that contain non-minimal sources of flavor violation are for example SUSY flavor models that try to explain the hierarchies in the masses and mixings of the SM fermions using flavor symmetries and simultaneously suppress FCNC and CP violating processes by means of the degeneracy or alignment mechanisms. In our extensive comparative analysis of SUSY flavor models based both on abelian and non-abelian flavor symmetries that show representative flavor structures in the soft SUSY breaking terms (see sections 8.2 - 8.5), we showed the distinct patterns of NP effects in flavor observables in these models.

Flavor models that predict only CKM-like left-left mass insertions share many similarities with the MFV MSSM. In particular, NP effects in meson mixing observables are naturally small implying in particular a SM-like $S_{\psi\phi}$ also in these frameworks. Large effects arise

on the other hand in the $b \to s\gamma$ and $b \to s$ gluon transitions, as well as in the $B \to \tau\nu$, $B_s \to \mu^+\mu^-$ and $B_d \to \mu^+\mu^-$ decays for large values of $\tan\beta$. In contrast to the MFV MSSM however, models with only left-left mass insertions do not predict a correlation between the branching ratios of the $B_s \to \mu^+\mu^-$ and $B_d \to \mu^+\mu^-$ decays. In addition sizable effects in CP asymmetries in B decays do not necessarily imply large enhancements of EDMs.

Once right-right mass insertions are present, $\Delta F = 2$ observables are particularly well suited to probe the MSSM flavor and CP structure. In fact, the most natural way to generate large effects in meson mixing is through simultaneous δ^{LL} and δ^{RR} mass insertions. As left-left mass insertions are always introduced radiatively through renormalization group running, models that predict sizable $(\delta^{RR})_{32}$ mass insertions are the most natural frameworks to obtain large values for the B_s mixing phase $S_{\psi\phi}$. This is indeed verified in our numerical study of the SUSY flavor models in sections 8.3, 8.4 and 8.5 that all contain a non-vanishing $(\delta^{RR})_{32}$. Interestingly, in the non-abelian AKM model and the abelian AC model discussed in sections 8.3 and 8.5, respectively, sizable effects in $S_{\psi\phi}$ are strongly correlated with strong enhancements of the $\mathrm{BR}(B_s \to \mu^+\mu^-)$ as both processes are generated in the large $\tan\beta$ regime of these models by neutral Higgs exchange with loop induced effective flavor changing vertices.

Another very interesting observation concerns NP effects in $D^0 - \bar{D}^0$ mixing in the framework of abelian flavor models. As discussed in sections 7.3, 8.5 and 8.6, abelian flavor models that implement the alignment mechanism generically lead to large NP contributions to $D^0 - \bar{D}^0$ mixing. While this is a well know fact, we identified an interesting correlation between CP violation in $D^0 - \bar{D}^0$ mixing and hadronic EDMs that are induced by flavor effects within that class of models. As explained in section 8.6, visible effects in the time dependent CP asymmetry of the decays of D^0 and $\bar{D}^0$ into CP eigenstates, S_f^D, or in the semileptonic asymmetry a_{SL}^D imply a lower bound e.g. on the neutron EDM at the level of $d_n \gtrsim 10^{-(28-29)} e$ cm, which is within the expected future experimental resolutions.

This discussion shows that there exist clear patterns of NP effects in many low energy processes that are characteristic for a given model. These characteristic patterns of deviations from the SM predictions allow in principle to distinguish between the different SUSY frameworks once additional data will become available. In addition, our analysis also offers the possibility to distinguish the considered SUSY scenarios from models with warped extra dimensions or little Higgs models based on their distinctive predictions for low energy observables.

Given the start of LHC, an essential issue to address is the complementarity and synergy of flavor and collider physics in searching for NP. Which predictions can one make for the NP mass spectrum in case non-standard effects will be observed in low energy observables? And, conversely, at which level does one expect NP contributions to flavor observables if new degrees of freedom will be discovered at the LHC?

In fact, as seen throughout chapter 8, large non-standard effects in flavor observables often imply a SUSY spectrum within the LHC reach. Hence, combining the information on the spectrum from the LHC with the information from the low energy flavor processes, will to some extent offer the possibility to measure mixing angles regulating flavor transitions between SUSY particles. Such an achievement would represent a crucial step forward towards the reconstruction of the underlying SUSY flavor structure. On the other hand we also saw that there exist regions of the SUSY parameter space at the border or even beyond the

LHC reach where one can still expect clear non-standard signals in flavor processes. In these regions, flavor phenomena, and thus the indirect search, would represent the most powerful tool to shed light on the SUSY degrees of freedom.

The start of the LHC will lead to tremendous progress in the field of high energy physics in the coming years. Combining the results from both high and low energy observables will hopefully lead to fundamental insights to the mechanism of electroweak symmetry breaking and the structure of the New Physics that might be awaiting us at the TeV scale.

A Appendix

In appendix A.1 we list all the 1 loop functions that appear in chapters 5 and 6. We give both analytical expressions for these functions, as well as their values in the limiting case of a common mass for all the particles in the loop.

In appendix A.2 we give a translation table between the conventions for SUSY parameters used in the present work, the "SUSY Les Houches Accord" (SLHA) conventions [256, 257] and the conventions adopted in [254, 255].

In appendix A.3 finally, we collect all the input parameter that are used in our numerical analyses.

A.1 Compendium of Loop Functions

Loop Functions for the Threshold Corrections and $B_s \to \mu^+\mu^-$

$$f_1(x) = \frac{1}{1-x} + \frac{x}{(1-x)^2}\log x \ , \qquad f_1(1) = \frac{1}{2} \ , \tag{A.1}$$

$$f_2(x,y) = \frac{x\log x}{(1-x)(y-x)} + \frac{y\log y}{(1-y)(x-y)} \ , \qquad f_2(1,1) = \frac{1}{2} \ , \tag{A.2}$$

$$f_3(x) = -\frac{1+x}{2(1-x)^2} - \frac{x}{(1-x)^3}\log x \ , \qquad f_3(1) = -\frac{1}{6} \ , \tag{A.3}$$

$$f_4(x,y) = -\frac{x\log x}{(1-x)^2(y-x)} - \frac{y\log y}{(1-y)^2(x-y)} + \frac{1}{(1-x)(1-y)} \ , \quad f_4(1,1) = -\frac{1}{6} \ , \tag{A.4}$$

$$f_5(x) = \frac{2+5x-x^2}{6(1-x)^3} + \frac{x}{(1-x)^4}\log x \ , \qquad f_5(1) = \frac{1}{12} \ . \tag{A.5}$$

Loop Functions for $b \to s\gamma$

$$h_7(x) = -\frac{5x^2-3x}{12(1-x)^2} - \frac{3x^2-2x}{6(1-x)^3}\log x \ , \qquad h_7(1) = -\frac{7}{36} \ , \tag{A.6}$$

$$h_8(x) = -\frac{x^2-3x}{4(1-x)^2} + \frac{x}{2(1-x)^3}\log x \ , \qquad h_8(1) = -\frac{1}{6} \ , \tag{A.7}$$

$$f_7^{(1)}(x) = -\frac{2+11x-7x^2}{18(1-x)^4} - \frac{x(3-x^2)}{6(1-x)^5}\log x \ , \qquad f_7^{(1)}(1) = -\frac{1}{60} \ , \tag{A.8}$$

$$f_7^{(4)}(x) = \frac{8+5x-7x^2}{144(1-x)^3} + \frac{x(3-2x)}{24(1-x)^4}\log x \ , \qquad f_7^{(4)}(1) = , \frac{5}{288} \tag{A.9}$$

$$f_7^{(5)}(x) = -\frac{13-7x}{24(1-x)^3} - \frac{3+2x-2x^2}{12(1-x)^4}\log x \ , \qquad f_7^{(5)}(1) = , \frac{5}{144} \tag{A.10}$$

$$f_8^{(1)}(x) = -\frac{1-8x-17x^2}{24(1-x)^4} + \frac{x^2(3+x)}{4(1-x)^5}\log x \ , \qquad f_8^{(1)}(1) = -\frac{1}{80} \ , \tag{A.11}$$

$$f_8^{(4)}(x) = \frac{1-5x-2x^2}{48(1-x)^3} - \frac{x^2}{8(1-x)^4}\log x \ , \qquad f_8^{(4)}(1) = \frac{1}{96} \ , \tag{A.12}$$

$$f_8^{(5)}(x) = \frac{1+5x}{8(1-x)^3} + \frac{x(2+x)}{4(1-x)^4}\log x \ , \qquad f_8^{(5)}(1) = \frac{1}{48} \ , \tag{A.13}$$

$$f_{7,8}^{(2)}(x,y) = \frac{2}{x-y}\left(x f_{7,8}^{(5)}(x) - y f_{7,8}^{(5)}(y)\right) \ , \qquad f_{7,8}^{(2)}(1,1) = -\frac{1}{360}, \ \frac{1}{120} \ , \tag{A.14}$$

$$f_{7,8}^{(3)}(x,y) = \frac{2}{x-y}\left(f_{7,8}^{(5)}(x) - f_{7,8}^{(5)}(y)\right) \ , \qquad f_{7,8}^{(3)}(1,1) = -\frac{13}{180}, \ -\frac{1}{30} \ , \tag{A.15}$$

$$g_7^{(1)}(x) = \frac{1-8x-17x^2}{27(1-x)^4} - \frac{2x^2(3+x)}{9(1-x)^5}\log x \ , \qquad g_7^{(1)}(1) = \frac{1}{90} \ , \tag{A.16}$$

$$g_7^{(2)}(x) = -\frac{2(1+5x)}{9(1-x)^3} - \frac{4x(2+x)}{9(1-x)^4}\log x \ , \qquad g_7^{(2)}(1) = -\frac{1}{27} \ , \tag{A.17}$$

$$g_7^{(3)}(x) = -\frac{2(1+10x+x^2)}{9(1-x)^4} - \frac{4x(1+x)}{3(1-x)^5}\log x \ , \qquad g_7^{(3)}(1) = -\frac{1}{45} \ , \tag{A.18}$$

$$g_8^{(1)}(x) = \frac{19+172x+x^2}{72(1-x)^4} + \frac{x(18+15x-x^2)}{12(1-x)^5}\log x \ , \qquad g_8^{(1)}(1) = \frac{7}{240} \ , \tag{A.19}$$

$$g_8^{(2)}(x) = \frac{11+x}{3(1-x)^3} + \frac{9+16x-x^2}{6(1-x)^4}\log x \ , \qquad g_8^{(2)}(1) = -\frac{5}{36} \ , \tag{A.20}$$

$$g_8^{(3)}(x) = \frac{53+44x-x^2}{12(1-x)^4} + \frac{3+11x+2x^2}{2(1-x)^5}\log x \ , \qquad g_8^{(3)}(1) = -\frac{7}{120} \ , \tag{A.21}$$

$$\tilde{g}_7(x) = \frac{4(1+5x)}{18(1-x)^3} + \frac{4x(2+x)}{9(1-x)^4}\log x \ , \qquad \tilde{g}_7(1) = \frac{1}{27} \ , \tag{A.22}$$

$$\tilde{g}_8(x) = -\frac{11+x}{3(1-x)^3} - \frac{9+16x-x^2}{6(1-x)^4}\log x \ , \qquad \tilde{g}_8(1) = \frac{5}{36} \ . \tag{A.23}$$

Loop Functions for Meson Mixing

$$F_1^{(1)}(x) = -\frac{x^2+10x+1}{24(1-x)^4} - \frac{x(x+1)}{4(1-x)^5}\log x \ , \qquad F_1^{(1)}(1) = \frac{1}{240} \ , \tag{A.24}$$

$$F_1^{(2)}(x) = -\frac{x+1}{32(1-x)^2} - \frac{x}{16(1-x)^3}\log x \ , \qquad F_1^{(2)}(1) = -\frac{1}{96} \ , \tag{A.25}$$

$$\begin{aligned} F_3^{(1)}(x,y) &= \frac{5x^2-3xy-x-y}{2(1-x)^5(y-x)^3}\log x + \frac{5y^2-3xy-x-y}{2(1-y)^5(x-y)^3}\log y \\ &\quad -\frac{2}{(1-y)^4(1-x)^2} - \frac{x+5}{2(1-y)^3(1-x)^3} - \frac{1}{(y-x)^2(1-x)^4} \\ &\quad +\frac{(x-8)x-29}{12(1-y)^2(1-x)^4} - \frac{2}{(1-y)(1-x)^5} - \frac{2}{(y-x)(1-x)^5} \ , \end{aligned} \tag{A.26}$$

$$\begin{aligned} F_3^{(2)}(x,y) &= -\frac{4x^2-3xy-y}{2(1-x)^5(y-x)^2}\log x - \frac{y}{2(1-y)^4(x-y)^2}\log y \\ &\quad -\frac{1}{2(1-y)^3(1-x)^2} - \frac{x+3}{4(1-y)^2(1-x)^3} - \frac{11-(x-8)x}{12(1-x)^4(1-y)} \\ &\quad +\frac{1}{(y-x)(1-x)^4} \ , \end{aligned} \tag{A.27}$$

$$F_3^{(3)}(x) = \frac{x^2-8x-17}{6(1-x)^4} - \frac{3x+1}{(1-x)^5}\log x \ , \tag{A.28}$$

$$F_3^{(1)}(1,1) = \frac{1}{84} \ , \quad F_3^{(2)}(1,1) = -\frac{1}{60} \ , \quad F_3^{(3)}(1) = \frac{1}{160} \ , \tag{A.29}$$

$$G_1(x) = -\frac{11+144x+27x^2-2x^3}{108(1-x)^4} - \frac{x(13+17x)}{18(1-x)^5}\log x \ , \qquad G_1(1) = -\frac{1}{216} \ , \tag{A.30}$$

$$G_2(x) = \frac{17x(x^2-8x-17)}{108(1-x)^4} - \frac{17x(3x+1)}{18(1-x)^5}\log x \ , \qquad G_2(1) = \frac{17}{360} \ , \tag{A.31}$$

$$G_3(x) = -\frac{3}{17}G_2(x) \ , \qquad G_3(1) = -\frac{1}{120} \ , \tag{A.32}$$

$$G_4(x) = \frac{2-99x-54x^2+7x^3}{18(1-x)^4} - \frac{x(5+19x)}{3(1-x)^5}\log x \ , \qquad G_4(1) = \frac{23}{180} \ , \tag{A.33}$$

$$\tilde{G}_4(x) = \frac{11(x^2+10x+1)}{54(1-x)^4} + \frac{11x(x+1)}{9(1-x)^5}\log x \ , \qquad \tilde{G}_4(1) = \frac{11}{540} \ , \tag{A.34}$$

$$G_5(x) = -\frac{10+117x+18x^2-x^3}{54(1-x)^4} - \frac{x(11+13x)}{9(1-x)^5}\log x \ , \qquad G_5(1) = -\frac{7}{540} \ , \tag{A.35}$$

$$\tilde{G}_5(x) = \frac{15}{11}\tilde{G}_4(x) \ , \qquad \tilde{G}_5(1) = \frac{1}{36} \ , \tag{A.36}$$

$$G_1^{(2)}(x) = \frac{33 + 665x + 237x^2 - 39x^3 + 4x^4}{216(1-x)^5} + \frac{x(26+49x)}{18(1-x)^6}\log x \ , \tag{A.37}$$

$$G_4^{(2)}(x) = -\frac{3 - 212x - 192x^2 + 48x^3 - 7x^4}{18(1-x)^5} + \frac{10x(1+5x)}{3(1-x)^6}\log x \ , \tag{A.38}$$

$$G_5^{(2)}(x) = \frac{15 + 272x + 84x^2 - 12x^3 + x^4}{54(1-x)^5} + \frac{2x(11+19x)}{9(1-x)^6}\log x \ , \tag{A.39}$$

$$G_1^{(2)}(1) = \frac{1}{360} \ , \quad G_4^{(2)}(1) = -\frac{1}{6} \ , \quad G_5^{(2)}(1) = \frac{1}{90} \ , \tag{A.40}$$

$$G_1^{(3)}(x) = -\frac{66 + 1835x + 1005x^2 - 255x^3 + 55x^4 - 6x^5}{1080(1-x)^6} - \frac{x(13+32x)}{18(1-x)^7}\log x \ , \tag{A.41}$$

$$G_4^{(3)}(x) = \frac{12 - 1117x - 1452x^2 + 528x^3 - 152x^4 + 21x^5}{180(1-x)^6} - \frac{x(5+31x)}{3(1-x)^7}\log x \ , \tag{A.42}$$

$$G_5^{(3)}(x) = -\frac{60 + 1507x + 732x^2 - 168x^3 + 32x^4 - 3x^5}{540(1-x)^6} - \frac{x(11+25x)}{9(1-x)^7}\log x \ , \tag{A.43}$$

$$G_1^{(3)}(1) = -\frac{1}{3780} \ , \quad G_4^{(3)}(1) = \frac{37}{630} \ , \quad G_5^{(3)}(1) = -\frac{1}{378} \ . \tag{A.44}$$

Loop Functions for $s \longrightarrow d\nu\bar{\nu}$ and $b \longrightarrow s\nu\bar{\nu}$

$$f_1^\nu(x) = \frac{1 - 5x - 2x^2}{6(1-x)^3} - \frac{x^2}{(1-x)^4}\log x \ , \tag{A.45}$$

$$\begin{aligned} f_2^\nu(x,y) = & -\frac{x(2x^2 - x(y+3) + 2y)}{2(1-x)^3(y-x)^2}\log x - \frac{2x^2(y+1) - 5xy^2 + y^2(2y-1)}{2(1-y)^3(x-y)^2}\log y \\ & + \frac{8x^3 - x^2(7y+11) + x(y(y+10)+1) - y(3y-1)}{4(1-x)^2(1-y)^2(y-x)} \ , \end{aligned} \tag{A.46}$$

$$f_3^\nu(x) = \frac{x}{4(1-x)} + \frac{x}{4(1-x)^2}\log x \ , \tag{A.47}$$

$$f_1^\nu(1) = \frac{1}{12} \ , \quad f_2^\nu(1,1) = 0 \ , \quad f_3^\nu(1) = -\frac{1}{8} \ . \tag{A.48}$$

Loop Functions for $(g-2)_\mu$

$$a_1(x,y) = \frac{8-25y+11y^2-3x^2(1+y)+x(1+16y-5y^2)}{2(1-x)^2(1-y)^2(x-y)} + \frac{7x^2-4x^3-4y+xy}{(1-x)^3(y-x)^2}\log x + \frac{(4-3x-5y+4y^2)y}{(1-y)^3(x-y)^2}\log y \ , \tag{A.49}$$

$$a_2(x) = \frac{1+5x^3}{1-x} + \frac{2x(2+x)}{(1-x)^4}\log x \ , \tag{A.50}$$

$$a_3(x,y) = -\frac{x-3x^2+y+xy}{2(1-x)^2(x-y)^2} - \frac{x(x^3+y-3xy+y^2)}{(1-x)(y-x)^3}\log x - \frac{xy}{(1-y)(x-y)^3}\log y \ , \tag{A.51}$$

$$a_1(1,1) = \frac{5}{12} \ , \quad a_2(1) = \frac{1}{6} \ , \quad a_3(1,1) = -\frac{1}{12} \ . \tag{A.52}$$

Loop Functions for the EDMs

$$f_{\tilde g}(x) = -\frac{4(x^3-11x^2-47x-3)}{27(1-x)^5} + \frac{16x(3x+2)}{9(1-x)^6}\log x \ , \qquad f_{\tilde g}(1) = \frac{4}{135} \ , \tag{A.53}$$

$$f^c_{\tilde g}(x) = -\frac{x^3+7x^2+295x+177}{18(1-x)^5} - \frac{21x^2+50x+9}{3(1-x)^6}\log x \ , \qquad f^c_{\tilde g}(1) = \frac{11}{180} \ . \tag{A.54}$$

A.2 Conventions for the MSSM Parameters

this work	SLHA [256, 257]	[254, 255]
$\hat y_u, \hat y_d, \hat y_\ell$	$\hat Y_U, \hat Y_D, \hat Y_E$	$+y_u, -y_d, -y_l$
$\hat A_u, \hat A_d, \hat A_\ell$	$-\hat T_U^{\mathrm T}, -\hat T_D^{\mathrm T}, -\hat T_E^{\mathrm T}$	$+A_u, -A_d, -A_l$
m^2_Q, m^2_L	$\hat m^2_{\tilde Q}, \hat m^2_{\tilde L}$	m^2_Q, m^2_L
m^2_U, m^2_D, m^2_E	$(\hat m^2_{\tilde u})^{\mathrm T}, (\hat m^2_{\tilde d})^{\mathrm T}, (\hat m^2_{\tilde e})^{\mathrm T}$	m^2_U, m^2_D, m^2_R
$\mathcal{M}^2_u, \mathcal{M}^2_d$	$(\mathcal{M}^2_{\tilde u})^{\mathrm T}, (\mathcal{M}^2_{\tilde d})^{\mathrm T}$	$\mathcal{M}^2_U, \mathcal{M}^2_D$

Table A.1: Dictionary between the SUSY conventions adopted the present work, the SLHA conventions [256, 257] and the conventions of [254, 255].

A.3 Numerical Input

parameter	value	ref.	parameter	value	ref.
G_F	1.16637×10^{-5} GeV^{-2}	[73]	$\alpha_s(M_Z)$	0.1184(7)	[420]
v	246 GeV	[73]	$\alpha_{\text{em}}(M_Z)$	1/127.918	[73]
			$\sin^2\theta_W$	0.23119	[73]

Table A.2: Fermi constant, vacuum expectation value, gauge couplings and Weinberg angle.

parameter	value	ref.	parameter	value	ref.
m_e	511 keV	[73]	M_W	80.398(25) GeV	[73]
m_μ	105.66 MeV	[73]	M_Z	91.1876(21) GeV	[73]
m_τ	1.777 GeV	[73]	M_K	0.497614(24) GeV	[73]
$m_d(2\text{ GeV})$	$5.04^{+0.96}_{-1.54}$ MeV	[73]	M_D	1.86484(17) GeV	[73]
$m_s(2\text{ GeV})$	$105^{+0.25}_{-0.35}$ MeV	[73]	$M_{B^\pm}$	5.27917(29) GeV	[73]
$m_b(m_b)$	$4.20^{+0.17}_{-0.07}$ GeV	[73]	M_{B_d}	5.2795(3) GeV	[73]
$m_u(2\text{ GeV})$	$2.55^{+0.75}_{-1.05}$ MeV	[73]	M_{B_s}	5.3663(6) GeV	[73]
$m_c(m_c)$	1.270 ± 0.017 GeV	[73]	τ_D	$0.4101(15)\,\text{ps}^{-1}$	[73]
$m_t(m_t)$	163.5 ± 1.7 GeV	[421, 422]	$\tau_{B^\pm}$	$1.638(11)\,\text{ps}^{-1}$	[73]
m_t^{pole}	173.1 ± 1.7 GeV	[421]	τ_{B_d}	$1.525(9)\,\text{ps}^{-1}$	[73]
			τ_{B_s}	$1.425(41)\,\text{ps}^{-1}$	[73]

Table A.3: Particle masses and life times. The lepton masses are pole masses, while the quark masses refer to running $\overline{\text{MS}}$ masses at the indicated scales.

parameter	value	ref.
F_D	(205.8 ± 0.9) MeV	[423]
F_K	(155.8 ± 1.7) MeV	[34]
F_{B_d}	(200 ± 20) MeV	[424]
F_{B_s}	(245 ± 25) MeV	[424]
$\hat{B}_K$	0.724 ± 0.036	[425]
$\hat{B}_d$	1.22 ± 0.12	[424]
$\hat{B}_s$	1.22 ± 0.12	[424]

parameter	value	ref.
$\sqrt{F_{B_d}^2 \hat{B}_d}$	(225 ± 25) MeV	[424]
$\sqrt{F_{B_s}^2 \hat{B}_s}$	(270 ± 30) GeV	[424]
ξ	1.21 ± 0.04	[424]
η_{cc}	1.48 ± 0.36	[426]
η_{tt}	0.57 ± 0.01	[426]
η_{ct}	0.47 ± 0.05	[426]
η_B	0.55 ± 0.01	[69]
κ_ϵ	0.94 ± 0.02	[67]

Table A.4: Decay constants, SM Bag parameter and RGE parameter. The hadronic parameters are mainly taken from [424]. Updated lattice results for decay constants and Bag parameter with considerably smaller uncertainties have recently been given in [34]. To be conservative we still used the values from [424] in this work.

parameter	value	ref.
λ	0.2254 ± 0.0006	[174]
A	0.808 ± 0.013	[28]
$\bar{\varrho}$	0.177 ± 0.044	[28]
$\bar{\eta}$	0.360 ± 0.031	[28]

parameter	value	ref.
$\lvert V_{cb}\rvert$	$(4.12 \pm 0.11) \times 10^{-2}$	[73]
$\lvert V_{ub}\rvert$	$(3.95 \pm 0.35) \times 10^{-3}$	[73]

Table A.5: CKM parameter. The Wolfenstein parameter are taken from the NP fit of the Unitarity Triangle [28] and used throughout the numerical analysis in chapter 8. The PDG values for $|V_{cb}|$ and $|V_{ub}|$ are used in the SM predictions for ϵ_K and $\mathrm{BR}(B \to \tau\nu)$.

parameter	value	ref.	parameter	value	ref.
B_1^D	0.87 ± 0.09	[424]	B_1^d	$0.87^{+0.06}_{-0.06}$	[428]
B_2^D	0.92 ± 0.09	[424]	B_2^d	$0.79^{+0.04}_{-0.04}$	[428]
B_2^D	1.13 ± 0.12	[424]	B_2^d	$0.92^{+0.10}_{-0.10}$	[428]
B_4^D	1.34 ± 0.11	[424]	B_4^d	$1.15^{+0.06}_{-0.08}$	[428]
B_5^D	1.57 ± 0.14	[424]	B_5^d	$1.72^{+0.20}_{-0.07}$	[428]
B_1^K	0.70 ± 0.21	[427]	B_1^s	$0.87^{+0.05}_{-0.04}$	[428]
B_2^K	0.75 ± 0.04	[427]	B_2^s	$0.80^{+0.04}_{-0.04}$	[428]
B_2^K	1.12 ± 0.12	[427]	B_2^s	$0.93^{+0.09}_{-0.09}$	[428]
B_4^K	1.29 ± 0.06	[427]	B_4^s	$1.16^{+0.05}_{-0.07}$	[428]
B_5^K	0.96 ± 0.10	[427]	B_5^s	$1.75^{+0.21}_{-0.07}$	[428]

Table A.6: Bag parameter for the full set of $\Delta F = 2$ operators. The corresponding scales where these parameters are evaluated are $\mu = 2$ GeV for $K^0 - \bar{K}^0$, $\mu = 2.8$ GeV for $D^0 - \bar{D}^0$ and $\mu = 4.6$ GeV for $B_{d,s} - \bar{B}_{d,s}$, respectively. In [424] and [427], the $D^0 - \bar{D}^0$ and $K^0 - \bar{K}^0$ Bag parameters are given in RI-MOM scheme. We converted them into the $\overline{\text{MS}}$ scheme following [49, 50]. Updated values for the B_i^K have been given in [429] and they agree with the ones found in [427] and used in this work.

parameter	bound	parameter	bound	parameter	bound
$m_{\tilde{t}_1}$	95.7 GeV	$M_{\tilde{\chi}_1^0}$	46 GeV	M_h	114.4 GeV
$m_{\tilde{b}_1}$	89 GeV	$M_{\tilde{\chi}_1^\pm}$	94 GeV	M_H	92.8 GeV
$m_{\tilde{\tau}_1}$	81.9 GeV	$M_{\tilde{g}}$	308 GeV	M_A	93.4 GeV
				$M_{H^\pm}$	79.3 GeV

Table A.7: Mass bounds of SUSY particles and Higgs bosons. From [73].

Bibliography

[1] G. F. Giudice, "Naturally Speaking: The Naturalness Criterion and Physics at the LHC," arXiv:0801.2562 [hep-ph].

[2] J. Wess and B. Zumino, "A Lagrangian Model Invariant Under Supergauge Transformations," *Phys. Lett.* **B49** (1974) 52.

[3] H. P. Nilles, "Supersymmetry, Supergravity and Particle Physics," *Phys. Rept.* **110** (1984) 1–162.

[4] L. Susskind, "Dynamics of Spontaneous Symmetry Breaking in the Weinberg-Salam Theory," *Phys. Rev.* **D20** (1979) 2619–2625.

[5] E. Farhi and L. Susskind, "Technicolor," *Phys. Rept.* **74** (1981) 277.

[6] N. Arkani-Hamed, S. Dimopoulos, and G. R. Dvali, "The hierarchy problem and new dimensions at a millimeter," *Phys. Lett.* **B429** (1998) 263–272, arXiv:hep-ph/9803315.

[7] N. Arkani-Hamed, S. Dimopoulos, and G. R. Dvali, "Phenomenology, astrophysics and cosmology of theories with sub-millimeter dimensions and TeV scale quantum gravity," *Phys. Rev.* **D59** (1999) 086004, arXiv:hep-ph/9807344.

[8] I. Antoniadis, N. Arkani-Hamed, S. Dimopoulos, and G. R. Dvali, "New dimensions at a millimeter to a Fermi and superstrings at a TeV," *Phys. Lett.* **B436** (1998) 257–263, arXiv:hep-ph/9804398.

[9] L. Randall and R. Sundrum, "A large mass hierarchy from a small extra dimension," *Phys. Rev. Lett.* **83** (1999) 3370–3373, arXiv:hep-ph/9905221.

[10] N. Arkani-Hamed, A. G. Cohen, and H. Georgi, "Electroweak symmetry breaking from dimensional deconstruction," *Phys. Lett.* **B513** (2001) 232–240, arXiv:hep-ph/0105239.

[11] N. Arkani-Hamed, A. G. Cohen, E. Katz, and A. E. Nelson, "The littlest Higgs," *JHEP* **07** (2002) 034, arXiv:hep-ph/0206021.

[12] M. Schmaltz and D. Tucker-Smith, "Little Higgs Review," *Ann. Rev. Nucl. Part. Sci.* **55** (2005) 229–270, arXiv:hep-ph/0502182.

[13] S. L. Glashow, J. Iliopoulos, and L. Maiani, "Weak Interactions with Lepton-Hadron Symmetry," *Phys. Rev.* **D2** (1970) 1285–1292.

[14] W. Altmannshofer, A. J. Buras, and D. Guadagnoli, "The MFV limit of the MSSM for low tan β : Meson mixings revisited," *JHEP* **11** (2007) 065, arXiv:hep-ph/0703200.

[15] W. Altmannshofer, A. J. Buras, D. Guadagnoli, and M. Wick, "Large $|V_{ub}|$: A Challenge for the minimal flavour violating MSSM," *JHEP* **12** (2007) 096, arXiv:0706.3845 [hep-ph].

[16] M. Albrecht, W. Altmannshofer, A. J. Buras, D. Guadagnoli, and D. M. Straub, "Challenging SO(10) SUSY GUTs with family symmetries through FCNC processes," *JHEP* **10** (2007) 055, arXiv:0707.3954 [hep-ph].

[17] W. Altmannshofer, D. Guadagnoli, S. Raby, and D. M. Straub, "SUSY GUTs with Yukawa unification: A Go/no-go study using FCNC processes," *Phys. Lett.* **B668** (2008) 385–391, arXiv:0801.4363 [hep-ph].

[18] W. Altmannshofer, A. J. Buras, and P. Paradisi, "Low Energy Probes of CP Violation in a Flavor Blind MSSM," *Phys. Lett.* **B669** (2008) 239–245, arXiv:0808.0707 [hep-ph].

[19] W. Altmannshofer *et al.*, "Symmetries and Asymmetries of $B \to K^* \mu^+ \mu^-$ Decays in the Standard Model and Beyond," *JHEP* **01** (2009) 019, arXiv:0811.1214 [hep-ph].

[20] W. Altmannshofer, A. J. Buras, D. M. Straub, and M. Wick, "New strategies for New Physics search in $B \to K^* \nu\bar{\nu}$, $B \to K \nu\bar{\nu}$ and $B \to X_s \nu\bar{\nu}$ decays," *JHEP* **04** (2009) 022, arXiv:0902.0160 [hep-ph].

[21] W. Altmannshofer, A. J. Buras, S. Gori, P. Paradisi, and D. M. Straub, "Anatomy and Phenomenology of FCNC and CPV Effects in SUSY Theories," *Nucl. Phys.* **B830** (2010) 17–94, arXiv:0909.1333 [hep-ph].

[22] W. Altmannshofer, A. J. Buras, and P. Paradisi, "A Lower Bound on hadronic EDMs from CP Violation in $D^0 - \bar{D}^0$ mixing in SUSY Alignment Models," *Phys. Lett.* **B688** (2010) 202–207, arXiv:1001.3835 [hep-ph].

[23] W. Altmannshofer and D. M. Straub, "Viability of MSSM scenarios at very large $\tan\beta$," arXiv:1004.1993 [hep-ph].

[24] N. Cabibbo, "Unitary Symmetry and Leptonic Decays," *Phys. Rev. Lett.* **10** (1963) 531–533.

[25] M. Kobayashi and T. Maskawa, "CP Violation in the Renormalizable Theory of Weak Interaction," *Prog. Theor. Phys.* **49** (1973) 652–657.

[26] L. Wolfenstein, "Parametrization of the Kobayashi-Maskawa Matrix," *Phys. Rev. Lett.* **51** (1983) 1945.

[27] **CKMfitter Group** Collaboration, J. Charles *et al.*, "CP violation and the CKM matrix: Assessing the impact of the asymmetric B factories," *Eur. Phys. J.* **C41** (2005) 1–131, arXiv:hep-ph/0406184. Online update at http://ckmfitter.in2p3.fr/.

[28] **UTfit** Collaboration, M. Bona *et al.*, "The 2004 UTfit Collaboration report on the status of the unitarity triangle in the standard model," *JHEP* **07** (2005) 028, arXiv:hep-ph/0501199. Online update at http://www.utfit.org/.

[29] Y. Nir, "CP violation: The CKM matrix and new physics," *Nucl. Phys. Proc. Suppl.* **117** (2003) 111–126, arXiv:hep-ph/0208080.

[30] E. Lunghi and A. Soni, "Possible Indications of New Physics in B_d mixing and in $\sin 2\beta$ Determinations," *Phys. Lett.* **B666** (2008) 162–165, arXiv:0803.4340 [hep-ph].

[31] A. J. Buras and D. Guadagnoli, "Correlations among new CP violating effects in $\Delta F = 2$ observables," *Phys. Rev.* **D78** (2008) 033005, arXiv:0805.3887 [hep-ph].

[32] A. J. Buras and D. Guadagnoli, "On the consistency between the observed amount of CP violation in the K- and B_d-systems within minimal flavor violation," *Phys. Rev.* **D79** (2009) 053010, arXiv:0901.2056 [hep-ph].

[33] E. Lunghi and A. Soni, "Hints for the scale of new CP-violating physics from B CP anomalies," *JHEP* **08** (2009) 051, arXiv:0903.5059 [hep-ph].

[34] J. Laiho, E. Lunghi, and R. S. Van de Water, "Lattice QCD inputs to the CKM unitarity triangle analysis," *Phys. Rev.* **D81** (2010) 034503, arXiv:0910.2928 [hep-ph].

[35] A. J. Buras, F. Parodi, and A. Stocchi, "The CKM matrix and the unitarity triangle: Another look," *JHEP* **01** (2003) 029, arXiv:hep-ph/0207101.

[36] **Heavy Flavor Averaging Group** Collaboration, E. Barberio *et al.*, "Averages of $b-$hadron and $c-$hadron Properties at the End of 2007," arXiv:0808.1297 [hep-ex]. Online update at http://www.slac.stanford.edu/xorg/hfag/.

[37] M. Bona *et al.*, "SuperB: A High-Luminosity Asymmetric e^+e^- Super Flavor Factory. Conceptual Design Report," arXiv:0709.0451 [hep-ex].

[38] T. E. Browder, T. Gershon, D. Pirjol, A. Soni, and J. Zupan, "New Physics at a Super Flavor Factory," arXiv:0802.3201 [hep-ph].

[39] T. Aushev *et al.*, "Physics at Super B Factory," arXiv:1002.5012 [hep-ex].

[40] G. Isidori, Y. Nir, and G. Perez, "Flavor Physics Constraints for Physics Beyond the Standard Model," arXiv:1002.0900 [hep-ph].

[41] **UTfit** Collaboration, M. Bona *et al.*, "Model-independent constraints on $\Delta F = 2$ operators and the scale of new physics," *JHEP* **03** (2008) 049, arXiv:0707.0636 [hep-ph].

[42] K. Blum, Y. Grossman, Y. Nir, and G. Perez, "Combining $K - \bar{K}$ mixing and $D - \bar{D}$ mixing to constrain the flavor structure of new physics," *Phys. Rev. Lett.* **102** (2009) 211802, arXiv:0903.2118 [hep-ph].

[43] A. J. Buras, P. Gambino, M. Gorbahn, S. Jager, and L. Silvestrini, "Universal unitarity triangle and physics beyond the standard model," *Phys. Lett.* **B500** (2001) 161–167, arXiv:hep-ph/0007085.

[44] G. D'Ambrosio, G. F. Giudice, G. Isidori, and A. Strumia, "Minimal flavour violation: An effective field theory approach," *Nucl. Phys.* **B645** (2002) 155–187, arXiv:hep-ph/0207036.

[45] T. Feldmann and T. Mannel, "Minimal Flavour Violation and Beyond," *JHEP* **02** (2007) 067, arXiv:hep-ph/0611095.

[46] T. Hurth, G. Isidori, J. F. Kamenik, and F. Mescia, "Constraints on New Physics in MFV models: A Model- independent analysis of $\Delta F = 1$ processes," *Nucl. Phys.* **B808** (2009) 326–346, arXiv:0807.5039 [hep-ph].

[47] C. D. Froggatt and H. B. Nielsen, "Hierarchy of Quark Masses, Cabibbo Angles and CP Violation," *Nucl. Phys.* **B147** (1979) 277.

[48] M. Ciuchini *et al.*, "Next-to-leading order QCD corrections to $\Delta F = 2$ effective Hamiltonians," *Nucl. Phys.* **B523** (1998) 501–525, arXiv:hep-ph/9711402.

[49] A. J. Buras, M. Misiak, and J. Urban, "Two-loop QCD anomalous dimensions of flavour-changing four-quark operators within and beyond the standard model," *Nucl. Phys.* **B586** (2000) 397–426, arXiv:hep-ph/0005183.

[50] A. J. Buras, S. Jager, and J. Urban, "Master formulae for $\Delta F = 2$ NLO-QCD factors in the standard model and beyond," *Nucl. Phys.* **B605** (2001) 600–624, arXiv:hep-ph/0102316.

[51] A. J. Schwartz, "$D^0 - \bar{D}^0$ Mixing and CP Violation: HFAG Combination of Parameters," arXiv:0911.1464 [hep-ex].

[52] A. F. Falk, Y. Grossman, Z. Ligeti, and A. A. Petrov, "SU(3) breaking and $D^0 - \bar{D}^0$ mixing," *Phys. Rev.* **D65** (2002) 054034, arXiv:hep-ph/0110317.

[53] A. F. Falk, Y. Grossman, Z. Ligeti, Y. Nir, and A. A. Petrov, "The $D^0 - \bar{D}^0$ mass difference from a dispersion relation," *Phys. Rev.* **D69** (2004) 114021, arXiv:hep-ph/0402204.

[54] S. Bergmann, Y. Grossman, Z. Ligeti, Y. Nir, and A. A. Petrov, "Lessons from CLEO and FOCUS Measurements of $D^0 - \bar{D}^0$ Mixing Parameters," *Phys. Lett.* **B486** (2000) 418–425, arXiv:hep-ph/0005181.

[55] Y. Nir, "Lessons from BaBar and Belle measurements of $D - \bar{D}$ mixing parameters," *JHEP* **05** (2007) 102, arXiv:hep-ph/0703235.

[56] E. Golowich, J. Hewett, S. Pakvasa, and A. A. Petrov, "Implications of $D^0 - \bar{D}^0$ Mixing for New Physics," *Phys. Rev.* **D76** (2007) 095009, arXiv:0705.3650 [hep-ph].

[57] O. Gedalia, Y. Grossman, Y. Nir, and G. Perez, "Lessons from Recent Measurements of $D - \bar{D}$ Mixing," *Phys. Rev.* **D80** (2009) 055024, arXiv:0906.1879 [hep-ph].

[58] M. Bobrowski, A. Lenz, J. Riedl, and J. Rohrwild, "How large can the SM contribution to CP violation in $D^0 - \bar{D}^0$ mixing be?," *JHEP* **03** (2010) 009, arXiv:1002.4794 [hep-ph].

[59] G. Blaylock, A. Seiden, and Y. Nir, "The Role of CP violation in $D^0 - \bar{D}^0$ mixing," *Phys. Lett.* **B355** (1995) 555–560, arXiv:hep-ph/9504306.

[60] S. Bianco, F. L. Fabbri, D. Benson, and I. Bigi, "A Cicerone for the physics of charm," *Riv. Nuovo Cim.* **26N7** (2003) 1–200, arXiv:hep-ex/0309021.

[61] Y. Nir, "CP violation in meson decays," arXiv:hep-ph/0510413.

[62] Y. Grossman, A. L. Kagan, and Y. Nir, "New physics and CP violation in singly Cabibbo suppressed D decays," *Phys. Rev.* **D75** (2007) 036008, arXiv:hep-ph/0609178.

[63] A. L. Kagan and M. D. Sokoloff, "On Indirect CP Violation and Implications for $D^0 - \bar{D}^0$ and $B_s - \bar{B}_s$ mixing," *Phys. Rev.* **D80** (2009) 076008, arXiv:0907.3917 [hep-ph].

[64] I. I. Bigi, M. Blanke, A. J. Buras, and S. Recksiegel, "CP Violation in $D_0 - \bar{D}_0$ Oscillations: General Considerations and Applications to the Littlest Higgs Model with T-Parity," *JHEP* **07** (2009) 097, arXiv:0904.1545 [hep-ph].

[65] M. Ciuchini *et al.*, "$D - \bar{D}$ mixing and new physics: General considerations and constraints on the MSSM," *Phys. Lett.* **B655** (2007) 162–166, arXiv:hep-ph/0703204.

[66] Y. Grossman, Y. Nir, and G. Perez, "Testing New Indirect CP Violation," *Phys. Rev. Lett.* **103** (2009) 071602, arXiv:0904.0305 [hep-ph].

[67] A. J. Buras, D. Guadagnoli, and G. Isidori, "On ϵ_K beyond lowest order in the Operator Product Expansion," *Phys. Lett.* **B688** (2010) 309–313, arXiv:1002.3612 [hep-ph].

[68] G. Buchalla, A. J. Buras, and M. E. Lautenbacher, "Weak decays beyond leading logarithms," *Rev. Mod. Phys.* **68** (1996) 1125–1144, arXiv:hep-ph/9512380.

[69] A. J. Buras, M. Jamin, and P. H. Weisz, "Leading and next-to-leading QCD corrections to ϵ parameter and $B^0 - \bar{B}^0$ mixing in the presence of a heavy top quark," *Nucl. Phys.* **B347** (1990) 491–536.

[70] S. Herrlich and U. Nierste, "Enhancement of the $K_L - K_S$ mass difference by short distance QCD corrections beyond leading logarithms," *Nucl. Phys.* **B419** (1994) 292–322, arXiv:hep-ph/9310311.

[71] S. Herrlich and U. Nierste, "Indirect CP violation in the neutral kaon system beyond leading logarithms," *Phys. Rev.* **D52** (1995) 6505–6518, arXiv:hep-ph/9507262.

[72] S. Herrlich and U. Nierste, "The Complete $|\Delta S| = 2$ Hamiltonian in the Next-To-Leading Order," *Nucl. Phys.* **B476** (1996) 27–88, arXiv:hep-ph/9604330.

[73] **Particle Data Group** Collaboration, C. Amsler *et al.*, "Review of particle physics," *Phys. Lett.* **B667** (2008) 1. See also http://pdg.lbl.gov/.

[74] Z. Ligeti, M. Papucci, and G. Perez, "Implications of the measurement of the $B_s^0 - \bar{B}_s^0$ mass difference," *Phys. Rev. Lett* **97** (2006) 101801, arXiv:hep-ph/0604112.

[75] A. Lenz and U. Nierste, "Theoretical update of $B_s - \bar{B}_s$ mixing," *JHEP* **06** (2007) 072, arXiv:hep-ph/0612167.

[76] **CDF** Collaboration, A. Abulencia *et al.*, "Observation of B_s^0 - $\bar{B}_s^0$ oscillations," *Phys. Rev. Lett.* **97** (2006) 242003, arXiv:hep-ex/0609040.

[77] **CDF** Collaboration, T. Aaltonen *et al.*, "First Flavor-Tagged Determination of Bounds on Mixing-Induced CP Violation in $B_s^0 \to J/\psi\phi$ Decays," *Phys. Rev. Lett.* **100** (2008) 161802, arXiv:0712.2397 [hep-ex].

[78] **D0** Collaboration, V. M. Abazov *et al.*, "Measurement of B_s^0 mixing parameters from the flavor-tagged decay $B_s^0 \to J/\psi\phi$," *Phys. Rev. Lett.* **101** (2008) 241801, arXiv:0802.2255 [hep-ex].

[79] **UTfit** Collaboration, M. Bona *et al.*, "First Evidence of New Physics in $b \to s$ Transitions," *PMC Phys.* **A3** (2009) 6, arXiv:0803.0659 [hep-ph].

[80] V. Tisserand, "CKM fits as of winter 2009 and sensitivity to New Physics," arXiv:0905.1572 [hep-ph].

[81] **The D0** Collaboration, V. M. Abazov *et al.*, "Evidence for an anomalous like-sign dimuon charge asymmetry," arXiv:1005.2757 [hep-ex].

[82] Talk by Louise Oakes at the Flavor Physics and CP Violation Conference (FPCP 2010) in Turin, May 25-29, 2010.

[83] M. Artuso *et al.*, "B, D and K decays," *Eur. Phys. J.* **C57** (2008) 309–492, arXiv:0801.1833 [hep-ph].

[84] M. Misiak *et al.*, "The first estimate of $\mathrm{B}(\bar{B} \to X_s\gamma)$ at $\mathrm{O}(\alpha_s^2)$," *Phys. Rev. Lett.* **98** (2007) 022002, arXiv:hep-ph/0609232.

[85] U. Haisch, "$\bar{B} \to X_s\gamma$: Standard Model and Beyond," arXiv:0805.2141 [hep-ph].

[86] K. G. Chetyrkin, M. Misiak, and M. Munz, "Weak radiative B meson decay beyond leading logarithms," *Phys. Lett.* **B400** (1997) 206–219, arXiv:hep-ph/9612313.

[87] A. L. Kagan and M. Neubert, "QCD anatomy of $B \to X_s\gamma$ decays," *Eur. Phys. J.* **C7** (1999) 5–27, arXiv:hep-ph/9805303.

[88] E. Lunghi and J. Matias, "Huge right-handed current effects in $B \to K^*(K\pi)\ell^+\ell^-$ in supersymmetry," *JHEP* **04** (2007) 058, arXiv:hep-ph/0612166.

[89] K.-i. Okumura and L. Roszkowski, "Large beyond-leading-order effects in $b \to s\gamma$ in supersymmetry with general flavor mixing," *JHEP* **10** (2003) 024, arXiv:hep-ph/0308102.

[90] S. Pokorski, J. Rosiek, and C. A. Savoy, "Constraints on phases of supersymmetric flavour conserving couplings," *Nucl. Phys.* **B570** (2000) 81–116, arXiv:hep-ph/9906206.

[91] J. M. Soares, "CP violation in radiative B decays," *Nucl. Phys.* **B367** (1991) 575–590.

[92] A. L. Kagan and M. Neubert, "Direct CP violation in $B \to X_s\gamma$ decays as a signature of new physics," *Phys. Rev.* **D58** (1998) 094012, arXiv:hep-ph/9803368.

[93] T. Hurth, E. Lunghi, and W. Porod, "Untagged $B \to X_{s+d}\gamma$ CP asymmetry as a probe for new physics," *Nucl. Phys.* **B704** (2005) 56–74, arXiv:hep-ph/0312260.

[94] **BELLE** Collaboration, S. Nishida *et al.*, "Measurement of the CP asymmetry in $B \to X_s\gamma$," *Phys. Rev. Lett.* **93** (2004) 031803, arXiv:hep-ex/0308038.

[95] **BABAR** Collaboration, B. Aubert *et al.*, "Measurement of the direct CP asymmetry in $b \to s\gamma$ decays," *Phys. Rev. Lett.* **93** (2004) 021804, arXiv:hep-ex/0403035.

[96] **BABAR** Collaboration, B. Aubert *et al.*, "A Measurement of CP Asymmetry in $b \to s\gamma$ using a Sum of Exclusive Final States," *Phys. Rev. Lett.* **101** (2008) 171804, arXiv:0805.4796 [hep-ex].

[97] D. Atwood, M. Gronau, and A. Soni, "Mixing-induced CP asymmetries in radiative B decays in and beyond the standard model," *Phys. Rev. Lett.* **79** (1997) 185–188, arXiv:hep-ph/9704272.

[98] P. Ball and R. Zwicky, "Time-dependent CP asymmetry in $B \to K^*\gamma$ as a (quasi) null test of the standard model," *Phys. Lett.* **B642** (2006) 478–486, arXiv:hep-ph/0609037.

[99] **Belle** Collaboration, Y. Ushiroda *et al.*, "Time-dependent CP asymmetries in $B^0 \to K^0_S\pi^0\gamma$ transitions," *Phys. Rev.* **D74** (2006) 111104, arXiv:hep-ex/0608017.

[100] **BABAR** Collaboration, B. Aubert *et al.*, "Measurement of Time-Dependent CP Asymmetry in $B^0 \to K^0_S\pi^0\gamma$ Decays," *Phys. Rev.* **D78** (2008) 071102, arXiv:0807.3103 [hep-ex].

[101] G. Burdman, "Testing the standard model in $B \to K^{(*)}\ell^+\ell^-$," *Phys. Rev.* **D52** (1995) 6400–6410, arXiv:hep-ph/9505352.

[102] D. Melikhov, N. Nikitin, and S. Simula, "Probing right-handed currents in $B \to K^*\ell^+\ell^-$ transitions," *Phys. Lett.* **B442** (1998) 381–389, arXiv:hep-ph/9807464.

[103] F. Kruger, L. M. Sehgal, N. Sinha, and R. Sinha, "Angular distribution and CP asymmetries in the decays $\bar{B} \to K^-\pi^+e^-e^+$ and $\bar{B} \to \pi^-\pi^+e^-e^+$," *Phys. Rev.* **D61** (2000) 114028, arXiv:hep-ph/9907386.

[104] A. Ali, P. Ball, L. T. Handoko, and G. Hiller, "A Comparative study of the decays $B \to (K, K^*)\ell^+\ell^-$ in standard model and supersymmetric theories," *Phys. Rev.* **D61** (2000) 074024, arXiv:hep-ph/9910221.

[105] C. S. Kim, Y. G. Kim, C.-D. Lu, and T. Morozumi, "Azimuthal angle distribution in $B \to K^*(\to K\pi)\ell^+\ell^-$ at low invariant $m_{\ell^+\ell^-}$ region," *Phys. Rev.* **D62** (2000) 034013, arXiv:hep-ph/0001151.

[106] A. Ali, E. Lunghi, C. Greub, and G. Hiller, "Improved model independent analysis of semileptonic and radiative rare B decays," *Phys. Rev.* **D66** (2002) 034002, arXiv:hep-ph/0112300.

[107] F. Kruger and J. Matias, "Probing new physics via the transverse amplitudes of $B^0 \to K^{*0}(\to K^-\pi^+)\ell^+\ell^-$ at large recoil," *Phys. Rev.* **D71** (2005) 094009, arXiv:hep-ph/0502060.

[108] C. Bobeth, G. Hiller, and G. Piranishvili, "Angular Distributions of $B \to K\ell^+\ell^-$ Decays," *JHEP* **12** (2007) 040, arXiv:0709.4174 [hep-ph].

[109] C. Bobeth, G. Hiller, and G. Piranishvili, "CP Asymmetries in $\bar{B} \to \bar{K}^*(\to \bar{K}\pi)\bar{\ell}\ell$ and Untagged $\bar{B}_s$, $B_s \to \phi(\to K^+K^-)\bar{\ell}\ell$ Decays at NLO," *JHEP* **07** (2008) 106, arXiv:0805.2525 [hep-ph].

[110] U. Egede, T. Hurth, J. Matias, M. Ramon, and W. Reece, "New observables in the decay mode $\bar{B} \to \bar{K}^*_0\ell^+\ell^-$," *JHEP* **11** (2008) 032, arXiv:0807.2589 [hep-ph].

[111] P. Ball and V. M. Braun, "Exclusive semileptonic and rare B meson decays in QCD," *Phys. Rev.* **D58** (1998) 094016, arXiv:hep-ph/9805422.

[112] P. Ball and R. Zwicky, "$B_{d,s} \to \rho, \omega, K^*, \phi$ Decay Form Factors from Light-Cone Sum Rules Revisited," *Phys. Rev.* **D71** (2005) 014029, arXiv:hep-ph/0412079.

[113] M. Beneke, T. Feldmann, and D. Seidel, "Systematic approach to exclusive $B \to V\ell^+\ell^-$, $V\gamma$ decays," *Nucl. Phys.* **B612** (2001) 25–58, arXiv:hep-ph/0106067.

[114] M. Beneke, T. Feldmann, and D. Seidel, "Exclusive radiative and electroweak $b \to d$ and $b \to s$ penguin decays at NLO," *Eur. Phys. J.* **C41** (2005) 173–188, arXiv:hep-ph/0412400.

[115] A. Bharucha and W. Reece, "Constraining new physics with $B \to K^*\mu^+\mu^-$ in the early LHC era," arXiv:1002.4310 [hep-ph].

[116] A. Ali, T. Mannel, and T. Morozumi, "Forward backward asymmetry of dilepton angular distribution in the decay $b \to s\ell^+\ell^-$," *Phys. Lett.* **B273** (1991) 505–512.

[117] G. Buchalla, G. Hiller, and G. Isidori, "Phenomenology of nonstandard Z couplings in exclusive semileptonic $b \to s$ transitions," *Phys. Rev.* **D63** (2000) 014015, arXiv:hep-ph/0006136.

[118] G. Burdman, "Short distance coefficients and the vanishing of the lepton asymmetry in $B \to V\ell^+\ell^-$," *Phys. Rev.* **D57** (1998) 4254–4257, arXiv:hep-ph/9710550.

[119] Y. Grossman, G. Isidori, and M. P. Worah, "CP asymmetry in $B_d \to \phi K_S$: Standard model pollution," *Phys. Rev.* **D58** (1998) 057504, arXiv:hep-ph/9708305.

[120] G. Buchalla, G. Hiller, Y. Nir, and G. Raz, "The pattern of CP asymmetries in $b \to s$ transitions," *JHEP* **09** (2005) 074, arXiv:hep-ph/0503151.

[121] M. Beneke, "Corrections to $\sin 2\beta$ from CP asymmetries in $B^0 \to (\pi^0, \rho^0, \eta, \eta', \omega, \Phi)K_S$ decays," *Phys. Lett.* **B620** (2005) 143–150, arXiv:hep-ph/0505075.

[122] Y. Grossman and M. P. Worah, "CP asymmetries in B decays with new physics in decay amplitudes," *Phys. Lett.* **B395** (1997) 241–249, arXiv:hep-ph/9612269.

[123] D. London and A. Soni, "Measuring the CP angle β in hadronic $b \to s$ penguin decays," *Phys. Lett.* **B407** (1997) 61–65, arXiv:hep-ph/9704277.

[124] L. Hofer, U. Nierste, and D. Scherer, "Resummation of $\tan\beta$ enhanced supersymmetric loop corrections beyond the decoupling limit," *JHEP* **10** (2009) 081, arXiv:0907.5408 [hep-ph].

[125] E. Gabrielli, K. Huitu, and S. Khalil, "Comparative study of CP asymmetries in supersymmetric models," *Nucl. Phys.* **B710** (2005) 139–188, arXiv:hep-ph/0407291.

[126] A. J. Buras, "Relations between $\Delta M_{s,d}$ and $B_{s,d} \to \mu\bar{\mu}$ in models with minimal flavor violation," *Phys. Lett.* **B566** (2003) 115–119, arXiv:hep-ph/0303060.

[127] **CDF** Collaboration, T. Aaltonen *et al.*, "Search for $B_s^0 \to \mu^+\mu^-$ and $B_d^0 \to \mu^+\mu^-$ decays with $2fb^{-1}$ of $p\bar{p}$ collisions," *Phys. Rev. Lett.* **100** (2008) 101802, arXiv:0712.1708 [hep-ex].

[128] **D0** Collaboration, V. M. Abazov *et al.*, "Search for $B_s \to \mu^+\mu^-$ at D0," *Phys. Rev.* **D76** (2007) 092001, arXiv:0707.3997 [hep-ex].

[129] **CDF** Collaboration, "Search for $B_s^0 \to \mu^+\mu^-$ and $B_s^0 \to \mu^+\mu^-$ Decays in 3.7 fb^{-1} of $p\bar{p}$ Collisions with CDF II,". CDF public note 9892.

[130] D. Martinez, J. A. Hernando, and F. Teubert, "LHCb potential to measure / exclude the branching ratio of the decay $B_s \to \mu^+\mu^-$,". CERN-LHCB-2007-033.

[131] Y. Grossman, Z. Ligeti, and E. Nardi, "New limit on inclusive $B \to X_s\bar{\nu}\nu$ decay and constraints on new physics," *Nucl. Phys.* **B465** (1996) 369–398, arXiv:hep-ph/9510378.

[132] P. Colangelo, F. De Fazio, P. Santorelli, and E. Scrimieri, "Rare $B \to K^{(*)}\nu\bar{\nu}$ decays at B factories," *Phys. Lett.* **B395** (1997) 339–344, arXiv:hep-ph/9610297.

[133] D. Melikhov, N. Nikitin, and S. Simula, "Right-handed currents in rare exclusive $B \to (K, K^*)\nu\bar{\nu}$ decays," *Phys. Lett.* **B428** (1998) 171–178, arXiv:hep-ph/9803269.

[134] C. S. Kim, Y. G. Kim, and T. Morozumi, "New physics effects in $B \to K^{(*)}\nu\bar{\nu}$ decays," *Phys. Rev.* **D60** (1999) 094007, arXiv:hep-ph/9905528.

[135] M. Misiak and J. Urban, "QCD corrections to FCNC decays mediated by Z-penguins and W-boxes," *Phys. Lett.* **B451** (1999) 161–169, arXiv:hep-ph/9901278.

[136] G. Buchalla and A. J. Buras, "The rare decays $K \to \pi\nu\bar{\nu}$, $B \to X\nu\bar{\nu}$ and $B \to \ell^+\ell^-$: An update," *Nucl. Phys.* **B548** (1999) 309–327, arXiv:hep-ph/9901288.

[137] P. Ball and R. Zwicky, "New Results on $B \to \pi, K, \eta$ Decay Formfactors from Light- Cone Sum Rules," *Phys. Rev.* **D71** (2005) 014015, arXiv:hep-ph/0406232.

[138] A. Bharucha, T. Feldmann, and M. Wick, "Theoretical and Phenomenological Constraints on Form Factors for Radiative and Semi-Leptonic B-Meson Decays," arXiv:1004.3249 [hep-ph].

[139] J. F. Kamenik and C. Smith, "Tree-level contributions to the rare decays $B^+ \to \pi^+\nu\bar{\nu}$, $B^+ \to K^+\nu\bar{\nu}$ and $B^+ \to K^{*+}\nu\bar{\nu}$ in the Standard Model," *Phys. Lett.* **B680** (2009) 471–475, arXiv:0908.1174 [hep-ph].

[140] M. Bartsch, M. Beylich, G. Buchalla, and D. N. Gao, "Precision Flavour Physics with $B \to K\nu\bar{\nu}$ and $B \to K\ell^+\ell^-$," *JHEP* **11** (2009) 011, arXiv:0909.1512 [hep-ph].

[141] **ALEPH** Collaboration, R. Barate *et al.*, "Measurements of BR($b \to \tau^-\bar{\nu}_\tau X$) and BR($b \to \tau^-\bar{\nu}_\tau D^{*\pm} X$) and upper limits on BR($B^- \to \tau^-\bar{\nu}_\tau$) and BR($b \to s\nu\bar{\nu}$)," *Eur. Phys. J.* **C19** (2001) 213–227, arXiv:hep-ex/0010022.

[142] **BELLE** Collaboration, K. F. Chen *et al.*, "Search for $B \to h^{(*)}\nu\bar{\nu}$ Decays at Belle," *Phys. Rev. Lett.* **99** (2007) 221802, arXiv:0707.0138 [hep-ex].

[143] **BABAR** Collaboration, B. Aubert *et al.*, "Search for $B \to K^*\nu\bar{\nu}$ decays," *Phys. Rev.* **D78** (2008) 072007, arXiv:0808.1338 [hep-ex].

[144] "Recoil analysis and $B \to K^*\nu\bar{\nu}$ at SuperB,". Talk given by Francesco Renga at SuperB Physics Physics Workshop, Warwick, April 14-17, 2009.

[145] M. Wick, "Probing New Physics with $b \to s\ell^+\ell^-$ and $b \to s\nu\bar{\nu}$ transitions," *AIP Conf. Proc.* **1200** (2010) 835–838, arXiv:0911.0297 [hep-ph].

[146] A. J. Buras, F. Schwab, and S. Uhlig, "Waiting for precise measurements of $K^+ \to \pi^+\nu\bar{\nu}$ and $K_L \to \pi^0\nu\bar{\nu}$," *Rev. Mod. Phys.* **80** (2008) 965–1007, arXiv:hep-ph/0405132.

[147] J. Brod and M. Gorbahn, "Electroweak Corrections to the Charm Quark Contribution to $K^+ \to \pi^+\nu\bar{\nu}$," *Phys. Rev.* **D78** (2008) 034006, arXiv:0805.4119 [hep-ph].

[148] F. Mescia and C. Smith, "Improved estimates of rare K decay matrix-elements from K_{l3} decays," *Phys. Rev.* **D76** (2007) 034017, arXiv:0705.2025 [hep-ph].

[149] **E391a** Collaboration, J. K. Ahn *et al.*, "Experimental study of the decay $K_L^0 \to \pi^0\nu\bar{\nu}$," *Phys. Rev.* **D81** (2010) 072004, arXiv:0911.4789 [hep-ex].

[150] **E949** Collaboration, A. V. Artamonov *et al.*, "New measurement of the $K^+ \to \pi^+\nu\bar{\nu}$ branching ratio," *Phys. Rev. Lett.* **101** (2008) 191802, arXiv:0808.2459 [hep-ex].

[151] G. Anelli *et al.*, "Proposal to measure the rare decay $K^+ \to \pi^+\nu\bar{\nu}$ at the CERN SPS,". CERN-SPSC-2005-013.

[152] H. Nanjo, "J-PARC E14 K0TO experiment for $K_L \to \pi^0\nu\bar{\nu}$," *PoS* **KAON09** (2009) 047.

[153] Y. Grossman and Y. Nir, "$K_L \to \pi^0\nu\bar{\nu}$ beyond the standard model," *Phys. Lett.* **B398** (1997) 163–168, arXiv:hep-ph/9701313.

[154] G. D'Ambrosio and G. Isidori, "$K^+ \to \pi^+\nu\bar{\nu}$: A rising star on the stage of flavour physics," *Phys. Lett.* **B530** (2002) 108–116, arXiv:hep-ph/0112135.

[155] D. Bryman, A. J. Buras, G. Isidori, and L. Littenberg, "$K_L \to \pi^0\nu\bar{\nu}$ as a probe of new physics," *Int. J. Mod. Phys.* **A21** (2006) 487–504, arXiv:hep-ph/0505171.

[156] G. Isidori, F. Mescia, and C. Smith, "Light-quark loops in $K \to \pi\nu\bar{\nu}$," *Nucl. Phys.* **B718** (2005) 319–338, arXiv:hep-ph/0503107.

[157] A. J. Buras, M. Gorbahn, U. Haisch, and U. Nierste, "The rare decay $K^+ \to \pi^+\nu\bar{\nu}$ at the next-to-next- to-leading order in QCD," *Phys. Rev. Lett.* **95** (2005) 261805, arXiv:hep-ph/0508165.

[158] A. J. Buras, M. Gorbahn, U. Haisch, and U. Nierste, "Charm quark contribution to $K^+ \to \pi^+\nu\bar{\nu}$ at next-to-next-to-leading order," *JHEP* **11** (2006) 002, arXiv:hep-ph/0603079.

[159] **BABAR** Collaboration, B. Aubert *et al.*, "A Search for $B^+ \to \tau^+\nu$ with Hadronic B tags," *Phys. Rev.* **D77** (2008) 011107, arXiv:0708.2260 [hep-ex].

[160] **BABAR** Collaboration, B. Aubert *et al.*, "A Search for $B^+ \to \ell^+\nu_\ell$ Recoiling Against $B^- \to D^0\ell^-\bar{\nu}X$," *Phys. Rev.* **D81** (2010) 051101, arXiv:0809.4027 [hep-ex].

[161] K. Ikado *et al.*, "Evidence of the purely leptonic decay $B^- \to \tau^-\bar{\nu}_\tau$," *Phys. Rev. Lett.* **97** (2006) 251802, arXiv:hep-ex/0604018.

[162] **Belle** Collaboration, I. Adachi *et al.*, "Measurement of $B^- \to \tau^-\nu_{\bar{\tau}}$ Decay With a Semileptonic Tagging Method," arXiv:0809.3834 [hep-ex].

[163] W.-S. Hou, "Enhanced charged Higgs boson effects in $B \to \tau\bar{\nu}$, $\mu\bar{\nu}$ and $b \to \tau\nu + X$," *Phys. Rev.* **D48** (1993) 2342–2344.

[164] A. G. Akeroyd and S. Recksiegel, "The effect of $H^\pm$ on $B^\pm \to \tau^\pm nu_\tau$ and $B^\pm \to \mu^\pm\nu_\mu$," *J. Phys.* **G29** (2003) 2311–2317, arXiv:hep-ph/0306037.

[165] G. Isidori and P. Paradisi, "Hints of large $\tan\beta$ in flavour physics," *Phys. Lett.* **B639** (2006) 499–507, arXiv:hep-ph/0605012.

[166] Talk by Koji Ikado at the Flavor Physics and CP Violation Conference (FPCP 2006) in Vancouver, April 9-12, 2006.

[167] **UTfit** Collaboration, M. Bona *et al.*, "An Improved Standard Model Prediction Of BR($B \to \tau\nu$) And Its Implications For New Physics," *Phys. Lett.* **B687** (2010) 61–69, arXiv:0908.3470 [hep-ph].

[168] B. Grzadkowski and W.-S. Hou, "Searching for $B \to D\tau\bar{\nu}_\tau$ at the 10% level," *Phys. Lett.* **B283** (1992) 427–433.

[169] K. Kiers and A. Soni, "Improving constraints on $\tan\beta/M_H$ using $B \to D\tau\bar{\nu}$," *Phys. Rev.* **D56** (1997) 5786–5793, arXiv:hep-ph/9706337.

[170] U. Nierste, S. Trine, and S. Westhoff, "Charged-Higgs effects in a new $B \to D\tau\nu$ differential decay distribution," *Phys. Rev.* **D78** (2008) 015006, arXiv:0801.4938 [hep-ph].

[171] J. F. Kamenik and F. Mescia, "$B \to D\tau\nu$ Branching Ratios: Opportunity for Lattice QCD and Hadron Colliders," *Phys. Rev.* **D78** (2008) 014003, arXiv:0802.3790 [hep-ph].

[172] **BABAR** Collaboration, B. Aubert *et al.*, "Measurement of the Semileptonic Decays $B \to D\tau\bar{\nu}_\tau$ and $B \to D^*\tau\bar{\nu}_\tau$," *Phys. Rev.* **D79** (2009) 092002, arXiv:0902.2660 [hep-ex].

[173] **FlaviaNet Working Group on Kaon Decays** Collaboration, M. Antonelli *et al.*, "Precision tests of the Standard Model with leptonic and semileptonic kaon decays," arXiv:0801.1817 [hep-ph].

[174] M. Antonelli *et al.*, "An evaluation of $|V_{us}|$ and precise tests of the Standard Model from world data on leptonic and semileptonic kaon decays," arXiv:1005.2323 [hep-ph].

[175] A. Czarnecki and W. J. Marciano, "The muon anomalous magnetic moment: A harbinger for 'new physics'," *Phys. Rev.* **D64** (2001) 013014, arXiv:hep-ph/0102122.

[176] M. Knecht, "The anomalous magnetic moment of the muon: A theoretical introduction," *Lect. Notes Phys.* **629** (2004) 37–84, arXiv:hep-ph/0307239.

[177] F. Jegerlehner, "Essentials of the Muon $g-2$," *Acta Phys. Polon.* **B38** (2007) 3021, arXiv:hep-ph/0703125.

[178] J. P. Miller, E. de Rafael, and B. L. Roberts, "Muon $g-2$: Review of Theory and Experiment," *Rept. Prog. Phys.* **70** (2007) 795, arXiv:hep-ph/0703049.

[179] F. Jegerlehner and A. Nyffeler, "The Muon $g-2$," *Phys. Rept.* **477** (2009) 1–110, arXiv:0902.3360 [hep-ph].

[180] J. Prades, "Standard Model Prediction of the Muon Anomalous Magnetic Moment," arXiv:0909.2546 [hep-ph].

[181] **Muon g-2** Collaboration, G. W. Bennett *et al.*, "Final report of the muon E821 anomalous magnetic moment measurement at BNL," *Phys. Rev.* **D73** (2006) 072003, arXiv:hep-ex/0602035.

[182] B. L. Roberts, "Status of the Fermilab Muon $(g-2)$ Experiment," arXiv:1001.2898 [hep-ex].

[183] M. Pospelov and A. Ritz, "Electric dipole moments as probes of new physics," *Annals Phys.* **318** (2005) 119–169, arXiv:hep-ph/0504231.

[184] B. C. Regan, E. D. Commins, C. J. Schmidt, and D. DeMille, "New limit on the electron electric dipole moment," *Phys. Rev. Lett.* **88** (2002) 071805.

[185] M. V. Romalis, W. C. Griffith, and E. N. Fortson, "A new limit on the permanent electric dipole moment of ^{199}Hg," *Phys. Rev. Lett.* **86** (2001) 2505–2508, arXiv:hep-ex/0012001.

[186] W. C. Griffith *et al.*, "Improved Limit on the Permanent Electric Dipole Moment of ^{1}99Hg," *Phys. Rev. Lett.* **102** (2009) 101601.

[187] P. G. Harris *et al.*, "New experimental limit on the electric dipole moment of the neutron," *Phys. Rev. Lett.* **82** (1999) 904–907.

[188] C. A. Baker *et al.*, "An improved experimental limit on the electric dipole moment of the neutron," *Phys. Rev. Lett.* **97** (2006) 131801, arXiv:hep-ex/0602020.

[189] R. D. Peccei and H. R. Quinn, "CP Conservation in the Presence of Instantons," *Phys. Rev. Lett.* **38** (1977) 1440–1443.

[190] R. D. Peccei and H. R. Quinn, "Constraints Imposed by CP Conservation in the Presence of Instantons," *Phys. Rev.* **D16** (1977) 1791–1797.

[191] S. Weinberg, "Larger Higgs Exchange Terms in the Neutron Electric Dipole Moment," *Phys. Rev. Lett.* **63** (1989) 2333.

[192] S. M. Barr, "Measurable T and P odd electron - nucleon interactions from Higgs boson exchange," *Phys. Rev. Lett.* **68** (1992) 1822–1825.

[193] S. M. Barr, "A Review of CP violation in atoms," *Int. J. Mod. Phys.* **A8** (1993) 209–236.

[194] M. Raidal *et al.*, "Flavour physics of leptons and dipole moments," *Eur. Phys. J.* **C57** (2008) 13–182, arXiv:0801.1826 [hep-ph].

[195] D. A. Demir, O. Lebedev, K. A. Olive, M. Pospelov, and A. Ritz, "Electric dipole moments in the MSSM at large tan β," *Nucl. Phys.* **B680** (2004) 339–374, arXiv:hep-ph/0311314.

[196] T. Huber, E. Lunghi, M. Misiak, and D. Wyler, "Electromagnetic logarithms in $\bar{B} \to X_s \ell^+ \ell^-$," *Nucl. Phys.* **B740** (2006) 105–137, arXiv:hep-ph/0512066.

[197] **BABAR** Collaboration, B. Aubert *et al.*, "Measurement of the $B \to X_s \ell^+ \ell^-$ branching fraction with a sum over exclusive modes," *Phys. Rev. Lett.* **93** (2004) 081802, arXiv:hep-ex/0404006.

[198] **Belle** Collaboration, M. Iwasaki *et al.*, "Improved measurement of the electroweak penguin process $B \to X_s \ell^+ \ell^-$," *Phys. Rev.* **D72** (2005) 092005, arXiv:hep-ex/0503044.

[199] Y. A. Golfand and E. P. Likhtman, "Extension of the Algebra of Poincare Group Generators and Violation of p Invariance," *JETP Lett.* **13** (1971) 323–326.

[200] D. V. Volkov and V. P. Akulov, "Possible universal neutrino interaction," *JETP Lett.* **16** (1972) 438–440.

[201] J. Wess and B. Zumino, "Supergauge Transformations in Four-Dimensions," *Nucl. Phys.* **B70** (1974) 39–50.

[202] S. R. Coleman and J. Mandula, "All Possible Symmetries of the S Matrix," *Phys. Rev.* **159** (1967) 1251–1256.

[203] R. Haag, J. T. Lopuszanski, and M. Sohnius, "All Possible Generators of Supersymmetries of the S Matrix," *Nucl. Phys.* **B88** (1975) 257.

[204] P. Van Nieuwenhuizen, "Supergravity," *Phys. Rept.* **68** (1981) 189–398.

[205] M. T. Grisaru, W. Siegel, and M. Rocek, "Improved Methods for Supergraphs," *Nucl. Phys.* **B159** (1979) 429.

[206] N. Seiberg, "Naturalness Versus Supersymmetric Non-renormalization Theorems," *Phys. Lett.* **B318** (1993) 469–475, arXiv:hep-ph/9309335.

[207] P. Fayet and J. Iliopoulos, "Spontaneously Broken Supergauge Symmetries and Goldstone Spinors," *Phys. Lett.* **B51** (1974) 461–464.

[208] L. O'Raifeartaigh, "Spontaneous Symmetry Breaking for Chiral Scalar Superfields," *Nucl. Phys.* **B96** (1975) 331.

[209] J. Scherk and J. H. Schwarz, "Spontaneous Breaking of Supersymmetry Through Dimensional Reduction," *Phys. Lett.* **B82** (1979) 60.

[210] E. Witten, "Dynamical Breaking of Supersymmetry," *Nucl. Phys.* **B188** (1981) 513.

[211] E. Witten, "Constraints on Supersymmetry Breaking," *Nucl. Phys.* **B202** (1982) 253.

[212] I. Affleck, M. Dine, and N. Seiberg, "Dynamical Supersymmetry Breaking in Supersymmetric QCD," *Nucl. Phys.* **B241** (1984) 493–534.

[213] I. Affleck, M. Dine, and N. Seiberg, "Dynamical Supersymmetry Breaking in Four-Dimensions and Its Phenomenological Implications," *Nucl. Phys.* **B256** (1985) 557.

[214] K. A. Intriligator, N. Seiberg, and D. Shih, "Dynamical SUSY breaking in meta-stable vacua," *JHEP* **04** (2006) 021, arXiv:hep-th/0602239.

[215] A. H. Chamseddine, R. L. Arnowitt, and P. Nath, "Locally Supersymmetric Grand Unification," *Phys. Rev. Lett.* **49** (1982) 970.

[216] R. Barbieri, S. Ferrara, and C. A. Savoy, "Gauge Models with Spontaneously Broken Local Supersymmetry," *Phys. Lett.* **B119** (1982) 343.

[217] H. P. Nilles, M. Srednicki, and D. Wyler, "Weak Interaction Breakdown Induced by Supergravity," *Phys. Lett.* **B120** (1983) 346.

[218] L. J. Hall, J. D. Lykken, and S. Weinberg, "Supergravity as the Messenger of Supersymmetry Breaking," *Phys. Rev.* **D27** (1983) 2359–2378.

[219] L. Alvarez-Gaume, J. Polchinski, and M. B. Wise, "Minimal Low-Energy Supergravity," *Nucl. Phys.* **B221** (1983) 495.

[220] M. Dine and W. Fischler, "A Phenomenological Model of Particle Physics Based on Supersymmetry," *Phys. Lett.* **B110** (1982) 227.

[221] L. Alvarez-Gaume, M. Claudson, and M. B. Wise, "Low-Energy Supersymmetry," *Nucl. Phys.* **B207** (1982) 96.

[222] C. R. Nappi and B. A. Ovrut, "Supersymmetric Extension of the SU(3) $\times$ SU(2) $\times$ U(1) Model," *Phys. Lett.* **B113** (1982) 175.

[223] M. Dine and A. E. Nelson, "Dynamical supersymmetry breaking at low-energies," *Phys. Rev.* **D48** (1993) 1277–1287, arXiv:hep-ph/9303230.

[224] M. Dine, A. E. Nelson, and Y. Shirman, "Low-energy dynamical supersymmetry breaking simplified," *Phys. Rev.* **D51** (1995) 1362–1370, arXiv:hep-ph/9408384.

[225] M. Dine, A. E. Nelson, Y. Nir, and Y. Shirman, "New tools for low-energy dynamical supersymmetry breaking," *Phys. Rev.* **D53** (1996) 2658–2669, arXiv:hep-ph/9507378.

[226] G. F. Giudice and R. Rattazzi, "Theories with gauge-mediated supersymmetry breaking," *Phys. Rept.* **322** (1999) 419–499, arXiv:hep-ph/9801271.

[227] E. A. Mirabelli and M. E. Peskin, "Transmission of supersymmetry breaking from a 4-dimensional boundary," *Phys. Rev.* **D58** (1998) 065002, arXiv:hep-th/9712214.

[228] D. E. Kaplan, G. D. Kribs, and M. Schmaltz, "Supersymmetry breaking through transparent extra dimensions," *Phys. Rev.* **D62** (2000) 035010, arXiv:hep-ph/9911293.

[229] Z. Chacko, M. A. Luty, A. E. Nelson, and E. Ponton, "Gaugino mediated supersymmetry breaking," *JHEP* **01** (2000) 003, arXiv:hep-ph/9911323.

[230] L. Randall and R. Sundrum, "Out of this world supersymmetry breaking," *Nucl. Phys.* **B557** (1999) 79–118, arXiv:hep-th/9810155.

[231] G. F. Giudice, M. A. Luty, H. Murayama, and R. Rattazzi, "Gaugino Mass without Singlets," *JHEP* **12** (1998) 027, arXiv:hep-ph/9810442.

[232] L. Girardello and M. T. Grisaru, "Soft Breaking of Supersymmetry," *Nucl. Phys.* **B194** (1982) 65.

[233] P. Fayet, "Spontaneously Broken Supersymmetric Theories of Weak, Electromagnetic and Strong Interactions," *Phys. Lett.* **B69** (1977) 489.

[234] J. R. Ellis, S. Kelley, and D. V. Nanopoulos, "Probing the desert using gauge coupling unification," *Phys. Lett.* **B260** (1991) 131–137.

[235] U. Amaldi, W. de Boer, and H. Furstenau, "Comparison of grand unified theories with electroweak and strong coupling constants measured at LEP," *Phys. Lett.* **B260** (1991) 447–455.

[236] P. Langacker and M.-x. Luo, "Implications of precision electroweak experiments for M_t, ρ_0, $\sin^2\theta_W$ and grand unification," *Phys. Rev.* **D44** (1991) 817–822.

[237] S. Dimopoulos, S. Raby, and F. Wilczek, "Supersymmetry and the Scale of Unification," *Phys. Rev.* **D24** (1981) 1681–1683.

[238] S. Dimopoulos and H. Georgi, "Softly Broken Supersymmetry and SU(5)," *Nucl. Phys.* **B193** (1981) 150.

[239] N. Sakai, "Naturalness in Supersymmetric GUTs," *Zeit. Phys.* **C11** (1981) 153.

[240] G. R. Farrar and P. Fayet, "Phenomenology of the Production, Decay, and Detection of New Hadronic States Associated with Supersymmetry," *Phys. Lett.* **B76** (1978) 575–579.

[241] H. Goldberg, "Constraint on the photino mass from cosmology," *Phys. Rev. Lett.* **50** (1983) 1419.

[242] J. R. Ellis, J. S. Hagelin, D. V. Nanopoulos, K. A. Olive, and M. Srednicki, "Supersymmetric relics from the big bang," *Nucl. Phys.* **B238** (1984) 453–476.

[243] H. E. Haber and G. L. Kane, "The Search for Supersymmetry: Probing Physics Beyond the Standard Model," *Phys. Rept.* **117** (1985) 75–263.

[244] P. Fayet and S. Ferrara, "Supersymmetry," *Phys. Rept.* **32** (1977) 249–334.

[245] J. D. Lykken, "Introduction to supersymmetry," `arXiv:hep-th/9612114`.

[246] S. P. Martin, "A Supersymmetry Primer," `arXiv:hep-ph/9709356`.

[247] D. J. H. Chung *et al.*, "The soft supersymmetry-breaking Lagrangian: Theory and applications," *Phys. Rept.* **407** (2005) 1–203, `arXiv:hep-ph/0312378`.

[248] K. A. Intriligator and N. Seiberg, "Lectures on Supersymmetry Breaking," *Class. Quant. Grav.* **24** (2007) S741–S772, `arXiv:hep-ph/0702069`.

[249] J. Wess and J. Bagger, *Supersymmetry and Supergravity.* Princeton University Press, 1992.

[250] S. Weinberg, *The Quantum Theory of Fields: Volume 3, Supersymmetry.* Cambridge University Press, 2000.

[251] M. Drees, R. M. Godbole, and P. Roy, *Theory and Phenomenology of Sparticles.* World Scientific Publishing Company, 2004.

[252] J. Terning, *Modern Supersymmetry.* Oxford University Press, 2006.

[253] M. Misiak, S. Pokorski, and J. Rosiek, "Supersymmetry and FCNC effects," *Adv. Ser. Direct. High Energy Phys.* **15** (1998) 795–828, `arXiv:hep-ph/9703442`.

[254] J. Rosiek, "Complete Set of Feynman Rules for the Minimal Supersymmetric Extension of the Standard Model," *Phys. Rev.* **D41** (1990) 3464.

[255] J. Rosiek, "Complete set of Feynman rules for the MSSM – ERRATUM," `arXiv:hep-ph/9511250`.

[256] P. Z. Skands *et al.*, "SUSY Les Houches Accord: Interfacing SUSY Spectrum Calculators, Decay Packages, and Event Generators," *JHEP* **07** (2004) 036, `arXiv:hep-ph/0311123`.

[257] B. Allanach *et al.*, "SUSY Les Houches Accord 2," *Comp. Phys. Commun.* **180** (2009) 8–25, `arXiv:0801.0045 [hep-ph]`.

[258] S. Dimopoulos and D. W. Sutter, "The Supersymmetric flavor problem," *Nucl. Phys.* **B452** (1995) 496–512, `arXiv:hep-ph/9504415`.

[259] P. H. Chankowski, S. Pokorski, and J. Rosiek, "Complete on-shell renormalization scheme for the minimal supersymmetric Higgs sector," *Nucl. Phys.* **B423** (1994) 437–496, `arXiv:hep-ph/9303309`.

[260] D. M. Pierce, J. A. Bagger, K. T. Matchev, and R.-j. Zhang, "Precision corrections in the minimal supersymmetric standard model," *Nucl. Phys.* **B491** (1997) 3–67, `arXiv:hep-ph/9606211`.

[261] U. Ellwanger, C. Hugonie, and A. M. Teixeira, "The Next-to-Minimal Supersymmetric Standard Model," `arXiv:0910.1785 [hep-ph]`.

[262] J. R. Ellis, G. Ridolfi, and F. Zwirner, "Radiative corrections to the masses of supersymmetric Higgs bosons," *Phys. Lett.* **B257** (1991) 83–91.

[263] H. E. Haber and R. Hempfling, "Can the mass of the lightest Higgs boson of the minimal supersymmetric model be larger than M_Z ?," *Phys. Rev. Lett.* **66** (1991) 1815–1818.

[264] Y. Okada, M. Yamaguchi, and T. Yanagida, "Upper bound of the lightest Higgs boson mass in the minimal supersymmetric standard model," *Prog. Theor. Phys.* **85** (1991) 1–6.

[265] R. Barbieri, M. Frigeni, and F. Caravaglios, "The Supersymmetric Higgs for heavy superpartners," *Phys. Lett.* **B258** (1991) 167–170.

[266] S. Heinemeyer, W. Hollik, and G. Weiglein, "FeynHiggs: a program for the calculation of the masses of the neutral CP-even Higgs bosons in the MSSM," *Comput. Phys. Commun.* **124** (2000) 76–89, `arXiv:hep-ph/9812320`.

[267] S. Heinemeyer, W. Hollik, and G. Weiglein, "The Masses of the neutral CP - even Higgs bosons in the MSSM: Accurate analysis at the two loop level," *Eur. Phys. J.* **C9** (1999) 343–366, arXiv:hep-ph/9812472.

[268] G. Degrassi, S. Heinemeyer, W. Hollik, P. Slavich, and G. Weiglein, "Towards high-precision predictions for the MSSM Higgs sector," *Eur. Phys. J.* **C28** (2003) 133–143, arXiv:hep-ph/0212020.

[269] M. Frank *et al.*, "The Higgs boson masses and mixings of the complex MSSM in the Feynman-diagrammatic approach," *JHEP* **02** (2007) 047, arXiv:hep-ph/0611326.

[270] R. S. Chivukula and H. Georgi, "Composite Technicolor Standard Model," *Phys. Lett.* **B188** (1987) 99.

[271] L. J. Hall and L. Randall, "Weak scale effective supersymmetry," *Phys. Rev. Lett.* **65** (1990) 2939–2942.

[272] L. J. Hall, V. A. Kostelecky, and S. Raby, "New Flavor Violations in Supergravity Models," *Nucl. Phys.* **B267** (1986) 415.

[273] P. Paradisi, M. Ratz, R. Schieren, and C. Simonetto, "Running minimal flavor violation," *Phys. Lett.* **B668** (2008) 202–209, arXiv:0805.3989 [hep-ph].

[274] G. Colangelo, E. Nikolidakis, and C. Smith, "Supersymmetric models with minimal flavour violation and their running," *Eur. Phys. J.* **C59** (2009) 75–98, arXiv:0807.0801 [hep-ph].

[275] G. Isidori, F. Mescia, P. Paradisi, C. Smith, and S. Trine, "Exploring the flavour structure of the MSSM with rare K decays," *JHEP* **08** (2006) 064, arXiv:hep-ph/0604074.

[276] B. Dudley and C. Kolda, "Supersymmetric Flavor-Changing Sum Rules as a Tool for $b \to s\gamma$," *Phys. Rev.* **D79** (2009) 015011, arXiv:0805.4565 [hep-ph].

[277] M. Wick and W. Altmannshofer, "A Reconsideration of the $b \to s\gamma$ Decay in the Minimal Flavor Violating MSSM," *AIP Conf. Proc.* **1078** (2009) 348–353, arXiv:0810.2874 [hep-ph].

[278] L. Mercolli and C. Smith, "EDM constraints on flavored CP-violating phases," *Nucl. Phys.* **B817** (2009) 1–24, arXiv:0902.1949 [hep-ph].

[279] P. Paradisi and D. M. Straub, "The SUSY CP Problem and the MFV Principle," *Phys. Lett.* **B684** (2010) 147–153, arXiv:0906.4551 [hep-ph].

[280] S. Baek and P. Ko, "Probing SUSY-induced CP violations at B factories," *Phys. Rev. Lett.* **83** (1999) 488–491, arXiv:hep-ph/9812229.

[281] S. Baek and P. Ko, "Effects of supersymmetric CP violating phases on $B \to X_s \ell^+ \ell^-$ and ϵ_K," *Phys. Lett.* **B462** (1999) 95–102, arXiv:hep-ph/9904283.

[282] A. Bartl *et al.*, "General flavor blind MSSM and CP violation," *Phys. Rev.* **D64** (2001) 076009, arXiv:hep-ph/0103324.

[283] J. R. Ellis, J. S. Lee, and A. Pilaftsis, "B-Meson Observables in the Maximally CP-Violating MSSM with Minimal Flavour Violation," *Phys. Rev.* **D76** (2007) 115011, arXiv:0708.2079 [hep-ph].

[284] L. J. Hall, R. Rattazzi, and U. Sarid, "The Top quark mass in supersymmetric SO(10) unification," *Phys. Rev.* **D50** (1994) 7048–7065, arXiv:hep-ph/9306309.

[285] R. Hempfling, "Yukawa coupling unification with supersymmetric threshold corrections," *Phys. Rev.* **D49** (1994) 6168–6172.

[286] M. S. Carena, M. Olechowski, S. Pokorski, and C. E. M. Wagner, "Electroweak symmetry breaking and bottom - top Yukawa unification," *Nucl. Phys.* **B426** (1994) 269–300, arXiv:hep-ph/9402253.

[287] T. Blazek, S. Raby, and S. Pokorski, "Finite supersymmetric threshold corrections to CKM matrix elements in the large $\tan\beta$ regime," *Phys. Rev.* **D52** (1995) 4151–4158, arXiv:hep-ph/9504364.

[288] C. Hamzaoui, M. Pospelov, and M. Toharia, "Higgs-mediated FCNC in supersymmetric models with large $\tan\beta$," *Phys. Rev.* **D59** (1999) 095005, arXiv:hep-ph/9807350.

[289] M. S. Carena, D. Garcia, U. Nierste, and C. E. M. Wagner, "Effective Lagrangian for the $\bar{t}bH^+$ interaction in the MSSM and charged Higgs phenomenology," *Nucl. Phys.* **B577** (2000) 88–120, arXiv:hep-ph/9912516.

[290] K. S. Babu and C. F. Kolda, "Higgs mediated $B^0 \to \mu^+\mu^-$ in minimal supersymmetry," *Phys. Rev. Lett.* **84** (2000) 228–231, arXiv:hep-ph/9909476.

[291] M. S. Carena, D. Garcia, U. Nierste, and C. E. M. Wagner, "$b \to s\gamma$ and supersymmetry with large $\tan\beta$," *Phys. Lett.* **B499** (2001) 141–146, arXiv:hep-ph/0010003.

[292] G. Isidori and A. Retico, "Scalar flavor changing neutral currents in the large $\tan\beta$ limit," *JHEP* **11** (2001) 001, arXiv:hep-ph/0110121.

[293] G. Isidori and A. Retico, "$B_{s,d} \to \ell^+\ell^-$ and $K_L \to \ell^+\ell^-$ in SUSY models with nonminimal sources of flavor mixing," *JHEP* **09** (2002) 063, arXiv:hep-ph/0208159.

[294] A. Dedes and A. Pilaftsis, "Resummed effective Lagrangian for Higgs-mediated FCNC interactions in the CP-violating MSSM," *Phys. Rev.* **D67** (2003) 015012, arXiv:hep-ph/0209306.

[295] A. J. Buras, P. H. Chankowski, J. Rosiek, and L. Slawianowska, "$\Delta M_{d,s}$, $B^0_{d,s} \to \mu^+\mu^-$ and $B \to X_s\gamma$ in supersymmetry at large $\tan\beta$," *Nucl. Phys.* **B659** (2003) 3, arXiv:hep-ph/0210145.

[296] J. Foster, K.-i. Okumura, and L. Roszkowski, "New Higgs effects in B physics in supersymmetry with general flavour mixing," *Phys. Lett.* **B609** (2005) 102–110, arXiv:hep-ph/0410323.

[297] J. Foster, K.-i. Okumura, and L. Roszkowski, "Probing the flavour structure of supersymmetry breaking with rare B processes: A beyond leading order analysis," *JHEP* **08** (2005) 094, arXiv:hep-ph/0506146.

[298] H. Baer, M. A. Diaz, J. Ferrandis, and X. Tata, "Sparticle mass spectra from SO(10) grand unified models with Yukawa coupling unification," *Phys. Rev.* **D61** (2000) 111701, arXiv:hep-ph/9907211.

[299] T. Blazek, R. Dermisek, and S. Raby, "Predictions for Higgs and SUSY spectra from SO(10) Yukawa unification with $\mu > 0$," *Phys. Rev. Lett.* **88** (2002) 111804, arXiv:hep-ph/0107097.

[300] T. Blazek, R. Dermisek, and S. Raby, "Yukawa unification in SO(10)," *Phys. Rev.* **D65** (2002) 115004, arXiv:hep-ph/0201081.

[301] D. Auto *et al.*, "Yukawa coupling unification in supersymmetric models," *JHEP* **06** (2003) 023, arXiv:hep-ph/0302155.

[302] K. Tobe and J. D. Wells, "Revisiting $t - b - \tau$ Yukawa unification in supersymmetric grand unified theories," *Nucl. Phys.* **B663** (2003) 123–140, arXiv:hep-ph/0301015.

[303] S. Antusch and M. Spinrath, "Quark and lepton masses at the GUT scale including SUSY threshold corrections," *Phys. Rev.* **D78** (2008) 075020, arXiv:0804.0717 [hep-ph].

[304] D. Guadagnoli, S. Raby, and D. M. Straub, "Viable and testable SUSY GUTs with Yukawa unification: the case of split trilinears," *JHEP* **10** (2009) 059, arXiv:0907.4709 [hep-ph].

[305] B. A. Dobrescu and P. J. Fox, "Uplifted supersymmetric Higgs region," arXiv:1001.3147 [hep-ph].

[306] G. Isidori and P. Paradisi, "Higgs-mediated $K \to \pi\nu\bar{\nu}$ in the MSSM at large $\tan\beta$," *Phys. Rev.* **D73** (2006) 055017, arXiv:hep-ph/0601094.

[307] J. Hisano, M. Nagai, and P. Paradisi, "Flavor effects on the electric dipole moments in supersymmetric theories: A beyond leading order analysis," *Phys. Rev.* **D80** (2009) 095014, arXiv:0812.4283 [hep-ph].

[308] S. Bertolini, F. Borzumati, A. Masiero, and G. Ridolfi, "Effects of supergravity induced electroweak breaking on rare B decays and mixings," *Nucl. Phys.* **B353** (1991) 591–649.

[309] F. Gabbiani, E. Gabrielli, A. Masiero, and L. Silvestrini, "A complete analysis of FCNC and CP constraints in general SUSY extensions of the standard model," *Nucl. Phys.* **B477** (1996) 321–352, arXiv:hep-ph/9604387.

[310] T. Goto, Y. Okada, and Y. Shimizu, "Flavor changing neutral current processes in B and K decays in the supergravity model," *Phys. Rev.* **D58** (1998) 094006, arXiv:hep-ph/9804294.

[311] S. Baek, T. Goto, Y. Okada, and K.-i. Okumura, "Muon anomalous magnetic moment, lepton flavor violation, and flavor changing neutral current processes in SUSY GUT with right-handed neutrino," *Phys. Rev.* **D64** (2001) 095001, arXiv:hep-ph/0104146.

[312] T. Goto, Y. Okada, T. Shindou, and M. Tanaka, "Patterns of flavor signals in supersymmetric models," *Phys. Rev.* **D77** (2008) 095010, arXiv:0711.2935 [hep-ph].

[313] M. Antonelli *et al.*, "Flavor Physics in the Quark Sector," arXiv:0907.5386 [hep-ph].

[314] S. Bertolini, F. Borzumati, and A. Masiero, "New Constraints on Squark and Gluino Masses from Radiative B Decays," *Phys. Lett.* **B192** (1987) 437.

[315] R. Barbieri and G. F. Giudice, "$b \to s\gamma$ decay and supersymmetry," *Phys. Lett.* **B309** (1993) 86–90, arXiv:hep-ph/9303270.

[316] M. Ciuchini, G. Degrassi, P. Gambino, and G. F. Giudice, "Next-to-leading QCD corrections to $B \to X_s\gamma$: Standard model and two-Higgs doublet model," *Nucl. Phys.* **B527** (1998) 21–43, arXiv:hep-ph/9710335.

[317] M. Ciuchini, G. Degrassi, P. Gambino, and G. F. Giudice, "Next-to-leading QCD corrections to $B \to X_s\gamma$ in supersymmetry," *Nucl. Phys.* **B534** (1998) 3–20, arXiv:hep-ph/9806308.

[318] F. Borzumati, C. Greub, T. Hurth, and D. Wyler, "Gluino contribution to radiative B decays: Organization of QCD corrections and leading order results," *Phys. Rev.* **D62** (2000) 075005, arXiv:hep-ph/9911245.

[319] C. Bobeth, M. Misiak, and J. Urban, "Matching conditions for $b \to s\gamma$ and $b \to s$ gluon in extensions of the standard model," *Nucl. Phys.* **B567** (2000) 153–185, arXiv:hep-ph/9904413.

[320] G. Degrassi, P. Gambino, and G. F. Giudice, "$B \to X_s\gamma$ in supersymmetry: Large contributions beyond the leading order," *JHEP* **12** (2000) 009, arXiv:hep-ph/0009337.

[321] K.-i. Okumura and L. Roszkowski, "Weakened Constraints from $b \to s\gamma$ on Supersymmetry Flavor Mixing Due to Next-To-Leading-Order Corrections," *Phys. Rev. Lett.* **92** (2004) 161801, arXiv:hep-ph/0208101.

[322] M. E. Gomez, T. Ibrahim, P. Nath, and S. Skadhauge, "An improved analysis of $b \to s\gamma$ in supersymmetry," *Phys. Rev.* **D74** (2006) 015015, arXiv:hep-ph/0601163.

[323] G. Degrassi, P. Gambino, and P. Slavich, "QCD corrections to radiative B decays in the MSSM with minimal flavor violation," *Phys. Lett.* **B635** (2006) 335–342, arXiv:hep-ph/0601135.

[324] B. Grinstein and M. B. Wise, "Weak Radiative B Meson Decay as a Probe of the Higgs Sector," *Phys. Lett.* **B201** (1988) 274.

[325] W.-S. Hou and R. S. Willey, "Effects of Charged Higgs Bosons on the Processes $b \to s\gamma$, $b \to sg^*$ and $b \to s\ell^+\ell^-$," *Phys. Lett.* **B202** (1988) 591.

[326] M. Carena, A. Menon, and C. E. M. Wagner, "Minimal Flavor Violation and the Scale of Supersymmetry Breaking," *Phys. Rev.* **D79** (2009) 075025, arXiv:0812.3594 [hep-ph].

[327] S. R. Choudhury and N. Gaur, "Dileptonic decay of B_s meson in SUSY models with large $\tan\beta$," *Phys. Lett.* **B451** (1999) 86–92, arXiv:hep-ph/9810307.

[328] P. H. Chankowski and L. Slawianowska, "$B^0_{d,s} \to \mu^-\mu^+$ decay in the MSSM," *Phys. Rev.* **D63** (2001) 054012, arXiv:hep-ph/0008046.

[329] C. Bobeth, T. Ewerth, F. Kruger, and J. Urban, "Analysis of neutral Higgs boson contributions to the decays $\bar{B}_s \to \ell^+\ell^-$ and $\bar{B} \to K\ell^+\ell^-$," *Phys. Rev.* **D64** (2001) 074014, arXiv:hep-ph/0104284.

[330] C. Bobeth, T. Ewerth, F. Kruger, and J. Urban, "Enhancement of $\mathrm{B}(\bar{B}_d \to \mu^+\mu^-)$ / $\mathrm{B}(\bar{B}_s \to \mu^+\mu^-)$ in the MSSM with minimal flavor violation and large $\tan\beta$," *Phys. Rev.* **D66** (2002) 074021, arXiv:hep-ph/0204225.

[331] A. Dedes, J. Rosiek, and P. Tanedo, "Complete One-Loop MSSM Predictions for $B^0 \to \ell^+\ell'^-$ at the Tevatron and LHC," *Phys. Rev.* **D79** (2009) 055006, arXiv:0812.4320 [hep-ph].

[332] H. E. Logan and U. Nierste, "$B_{s,d} \to \ell^+\ell^-$ in a two Higgs doublet model," *Nucl. Phys.* **B586** (2000) 39–55, arXiv:hep-ph/0004139.

[333] M. Ciuchini *et al.*, "Next-to-leading order strong interaction corrections to the $\Delta F = 2$ effective hamiltonian in the MSSM," *JHEP* **09** (2006) 013, arXiv:hep-ph/0606197.

[334] J. Virto, "Exact NLO strong interaction corrections to the $\Delta F = 2$ effective Hamiltonian in the MSSM," *JHEP* **11** (2009) 055, arXiv:0907.5376 [hep-ph].

[335] A. Crivellin and U. Nierste, "Chirally enhanced corrections to FCNC processes in the generic MSSM," *Phys. Rev.* **D81** (2010) 095007, arXiv:0908.4404 [hep-ph].

[336] A. J. Buras, P. H. Chankowski, J. Rosiek, and L. Slawianowska, "$\Delta M_s/\Delta M_d$, $\sin 2\beta$ and the angle γ in the presence of new $\Delta F = 2$ operators," *Nucl. Phys.* **B619** (2001) 434–466, arXiv:hep-ph/0107048.

[337] M. Gorbahn, S. Jager, U. Nierste, and S. Trine, "The supersymmetric Higgs sector and $B - \bar{B}$ mixing for large $\tan\beta$," arXiv:0901.2065 [hep-ph].

[338] M. Blanke and A. J. Buras, "Lower bounds on $\Delta M_{s,d}$ from constrained minimal flavour violation," *JHEP* **05** (2007) 061, arXiv:hep-ph/0610037.

[339] B. A. Dobrescu, P. J. Fox, and A. Martin, "CP violation in B_s mixing from heavy Higgs exchange," arXiv:1005.4238 [hep-ph].

[340] M. S. Carena, A. Menon, R. Noriega-Papaqui, A. Szynkman, and C. E. M. Wagner, "Constraints on B and Higgs physics in minimal low energy supersymmetric models," *Phys. Rev.* **D74** (2006) 015009, arXiv:hep-ph/0603106.

[341] Y. Nir and M. P. Worah, "Probing the flavor and CP structure of supersymmetric models with $K \to \pi\nu\bar{\nu}$ decays," *Phys. Lett.* **B423** (1998) 319–326, arXiv:hep-ph/9711215.

[342] A. J. Buras, A. Romanino, and L. Silvestrini, "$K \to \pi\nu\bar{\nu}$: A model independent analysis and supersymmetry," *Nucl. Phys.* **B520** (1998) 3–30, arXiv:hep-ph/9712398.

[343] G. Colangelo and G. Isidori, "Supersymmetric contributions to rare kaon decays: Beyond the single mass-insertion approximation," *JHEP* **09** (1998) 009, arXiv:hep-ph/9808487.

[344] A. J. Buras, G. Colangelo, G. Isidori, A. Romanino, and L. Silvestrini, "Connections between ϵ'/ϵ and rare kaon decays in supersymmetry," *Nucl. Phys.* **B566** (2000) 3–32, arXiv:hep-ph/9908371.

[345] A. J. Buras, T. Ewerth, S. Jager, and J. Rosiek, "$K^+ \to \pi^+\nu\bar{\nu}$ and $K_L \to \pi^0\nu\bar{\nu}$ decays in the general MSSM," *Nucl. Phys.* **B714** (2005) 103–136, arXiv:hep-ph/0408142.

[346] Y. Yamada, "$b \to s\nu\bar{\nu}$ decay in the MSSM: Implication of $b \to s\gamma$ at large $\tan\beta$," *Phys. Rev.* **D77** (2008) 014025, arXiv:0709.1022 [hep-ph].

[347] E. Lunghi, A. Masiero, I. Scimemi, and L. Silvestrini, "$B \to X_s\ell^+\ell^-$ decays in supersymmetry," *Nucl. Phys.* **B568** (2000) 120–144, arXiv:hep-ph/9906286.

[348] T. Moroi, "The Muon Anomalous Magnetic Dipole Moment in the Minimal Supersymmetric Standard Model," *Phys. Rev.* **D53** (1996) 6565–6575, arXiv:hep-ph/9512396.

[349] U. Chattopadhyay and P. Nath, "Probing supergravity grand unification in the Brookhaven $g-2$ experiment," *Phys. Rev.* **D53** (1996) 1648–1657, arXiv:hep-ph/9507386.

[350] M. S. Carena, G. F. Giudice, and C. E. M. Wagner, "Constraints on supersymmetric models from the muon anomalous magnetic moment," *Phys. Lett.* **B390** (1997) 234–242, arXiv:hep-ph/9610233.

[351] T. Ibrahim and P. Nath, "Effects of large CP violating phases on $(g-2)_\mu$ in MSSM," *Phys. Rev.* **D62** (2000) 015004, arXiv:hep-ph/9908443.

[352] J. L. Feng and K. T. Matchev, "Supersymmetry and the anomalous anomalous magnetic moment of the muon," *Phys. Rev. Lett.* **86** (2001) 3480–3483, arXiv:hep-ph/0102146.

[353] S. P. Martin and J. D. Wells, "Muon anomalous magnetic dipole moment in supersymmetric theories," *Phys. Rev.* **D64** (2001) 035003, arXiv:hep-ph/0103067.

[354] D. Stockinger, "The muon magnetic moment and supersymmetry," *J. Phys.* **G34** (2007) R45–R92, arXiv:hep-ph/0609168.

[355] S. Marchetti, S. Mertens, U. Nierste, and D. Stockinger, "tan β enhanced supersymmetric corrections to the anomalous magnetic moment of the muon," *Phys. Rev.* **D79** (2009) 013010, arXiv:0808.1530 [hep-ph].

[356] T. Ibrahim and P. Nath, "The chromoelectric and purely gluonic operator contributions to the neutron electric dipole moment in N = 1 supergravity," *Phys. Lett.* **B418** (1998) 98–106, arXiv:hep-ph/9707409.

[357] T. Ibrahim and P. Nath, "The neutron and the electron electric dipole moment in N = 1 supergravity unification," *Phys. Rev.* **D57** (1998) 478–488, arXiv:hep-ph/9708456.

[358] T. Ibrahim and P. Nath, "The neutron and the lepton EDMs in MSSM, large CP violating phases, and the cancellation mechanism," *Phys. Rev.* **D58** (1998) 111301, arXiv:hep-ph/9807501.

[359] D. Chang, W.-Y. Keung, and A. Pilaftsis, "New two-loop contribution to electric dipole moment in supersymmetric theories," *Phys. Rev. Lett.* **82** (1999) 900–903, arXiv:hep-ph/9811202.

[360] A. Bartl, T. Gajdosik, W. Porod, P. Stockinger, and H. Stremnitzer, "Electron and neutron electric dipole moments in the constrained MSSM," *Phys. Rev.* **D60** (1999) 073003, arXiv:hep-ph/9903402.

[361] S. Abel, S. Khalil, and O. Lebedev, "EDM constraints in supersymmetric theories," *Nucl. Phys.* **B606** (2001) 151–182, arXiv:hep-ph/0103320.

[362] A. Pilaftsis, "Higgs-mediated electric dipole moments in the MSSM: An application to baryogenesis and Higgs searches," *Nucl. Phys.* **B644** (2002) 263–289, arXiv:hep-ph/0207277.

[363] O. Lebedev and M. Pospelov, "Electric dipole moments in the limit of heavy superpartners," *Phys. Rev. Lett.* **89** (2002) 101801, arXiv:hep-ph/0204359.

[364] J. Hisano, M. Nagai, and P. Paradisi, "New two-loop contributions to hadronic EDMs in the MSSM," *Phys. Lett.* **B642** (2006) 510–517, arXiv:hep-ph/0606322.

[365] J. Hisano, M. Nagai, and P. Paradisi, "Electric dipole moments from flavor-changing supersymmetric soft terms," *Phys. Rev.* **D78** (2008) 075019, arXiv:0712.1285 [hep-ph].

[366] Y. Li, S. Profumo, and M. Ramsey-Musolf, "A Comprehensive Analysis of Electric Dipole Moment Constraints on CP-violating Phases in the MSSM," arXiv:1006.1440 [hep-ph].

[367] J. R. Ellis, J. S. Lee, and A. Pilaftsis, "Electric Dipole Moments in the MSSM Reloaded," *JHEP* **10** (2008) 049, arXiv:0808.1819 [hep-ph].

[368] T. Ibrahim and P. Nath, "Large CP phases and the cancellation mechanism in EDMs in SUSY, string and brane models," *Phys. Rev.* **D61** (2000) 093004, arXiv:hep-ph/9910553.

[369] S. Dimopoulos and G. F. Giudice, "Naturalness constraints in supersymmetric theories with nonuniversal soft terms," *Phys. Lett.* **B357** (1995) 573–578, arXiv:hep-ph/9507282.

[370] A. G. Cohen, D. B. Kaplan, and A. E. Nelson, "The more minimal supersymmetric standard model," *Phys. Lett.* **B388** (1996) 588–598, arXiv:hep-ph/9607394.

[371] A. Masiero and H. Murayama, "Can ϵ'/ϵ be supersymmetric?," *Phys. Rev. Lett.* **83** (1999) 907–910, arXiv:hep-ph/9903363.

[372] S. Khalil, T. Kobayashi, and A. Masiero, "CP violation in supersymmetric model with nondegenerate A- terms," *Phys. Rev.* **D60** (1999) 075003, arXiv:hep-ph/9903544.

[373] S. Khalil, T. Kobayashi, and O. Vives, "EDM-free supersymmetric CP violation with non-universal soft terms," *Nucl. Phys.* **B580** (2000) 275–288, arXiv:hep-ph/0003086.

[374] S. M. Barr and A. Zee, "Electric Dipole Moment of the Electron and the Neutron," *Phys. Rev. Lett.* **65** (1990) 21–24.

[375] M. Ciuchini *et al.*, "ΔM_K and ϵ_K in SUSY at the next-to-leading order," *JHEP* **10** (1998) 008, arXiv:hep-ph/9808328.

[376] D. Becirevic *et al.*, "$B_d - \bar{B}_d$ mixing and the $B_d \to J/\psi K_S$ asymmetry in general SUSY models," *Nucl. Phys.* **B634** (2002) 105–119, arXiv:hep-ph/0112303.

[377] T. Besmer, C. Greub, and T. Hurth, "Bounds on flavor violating parameters in supersymmetry," *Nucl. Phys.* **B609** (2001) 359–386, arXiv:hep-ph/0105292.

[378] G. L. Kane *et al.*, "$B_d \to \phi K_S$ and supersymmetry," *Phys. Rev.* **D70** (2004) 035015, arXiv:hep-ph/0212092.

[379] M. Ciuchini, E. Franco, A. Masiero, and L. Silvestrini, "$b - - > s$ transitions: A new frontier for indirect SUSY searches," *Phys. Rev.* **D67** (2003) 075016, arXiv:hep-ph/0212397.

[380] J. Foster, K.-i. Okumura, and L. Roszkowski, "Current and future limits on general flavour violation in $b \to s$ transitions in minimal supersymmetry," *JHEP* **03** (2006) 044, arXiv:hep-ph/0510422.

[381] M. Ciuchini and L. Silvestrini, "Upper bounds on SUSY contributions to $b \to s$ transitions from $B_s - \bar{B}_s$ mixing," *Phys. Rev. Lett.* **97** (2006) 021803, arXiv:hep-ph/0603114.

[382] J. Foster, K.-i. Okumura, and L. Roszkowski, "New constraints on SUSY flavour mixing in light of recent measurements at the Tevatron," *Phys. Lett.* **B641** (2006) 452–460, arXiv:hep-ph/0604121.

[383] M. Ciuchini *et al.*, "Soft SUSY breaking grand unification: Leptons versus quarks on the flavor playground," *Nucl. Phys.* **B783** (2007) 112–142, arXiv:hep-ph/0702144.

[384] P. Ko and J.-h. Park, "Implications of the measurements of $B_s - \bar{B}_s$ mixing on SUSY models," *Phys. Rev.* **D80** (2009) 035019, arXiv:0809.0705 [hep-ph].

[385] A. Crivellin and M. Davidkov, "Do squarks have to be degenerate? Constraining the mass splitting with Kaon and D mixing," *Phys. Rev.* **D81** (2010) 095004, arXiv:1002.2653 [hep-ph].

[386] N. Arkani-Hamed and S. Dimopoulos, "Supersymmetric unification without low energy supersymmetry and signatures for fine-tuning at the LHC," *JHEP* **06** (2005) 073, arXiv:hep-th/0405159.

[387] G. F. Giudice and A. Romanino, "Split supersymmetry," *Nucl. Phys.* **B699** (2004) 65–89, arXiv:hep-ph/0406088.

[388] N. Arkani-Hamed, S. Dimopoulos, G. F. Giudice, and A. Romanino, "Aspects of split supersymmetry," *Nucl. Phys.* **B709** (2005) 3–46, arXiv:hep-ph/0409232.

[389] R. Barbieri, E. Bertuzzo, M. Farina, P. Lodone, and D. Pappadopulo, "A Non Standard Supersymmetric Spectrum," arXiv:1004.2256 [hep-ph].

[390] G. F. Giudice, M. Nardecchia, and A. Romanino, "Hierarchical Soft Terms and Flavor Physics," *Nucl. Phys.* **B813** (2009) 156–173, arXiv:0812.3610 [hep-ph].

[391] J. L. Feng, C. G. Lester, Y. Nir, and Y. Shadmi, "The Standard Model and Supersymmetric Flavor Puzzles at the Large Hadron Collider," *Phys. Rev.* **D77** (2008) 076002, arXiv:0712.0674 [hep-ph].

[392] G. Hiller, Y. Hochberg, and Y. Nir, "Flavor Changing Processes in Supersymmetric Models with Hybrid Gauge- and Gravity-Mediation," *JHEP* **03** (2009) 115, arXiv:0812.0511 [hep-ph].

[393] Y. Nir and N. Seiberg, "Should squarks be degenerate?," *Phys. Lett.* **B309** (1993) 337–343, arXiv:hep-ph/9304307.

[394] Y. Nir and G. Raz, "Quark squark alignment revisited," *Phys. Rev.* **D66** (2002) 035007, arXiv:hep-ph/0206064.

[395] M. Leurer, Y. Nir, and N. Seiberg, "Mass matrix models," *Nucl. Phys.* **B398** (1993) 319–342, arXiv:hep-ph/9212278.

[396] M. Leurer, Y. Nir, and N. Seiberg, "Mass matrix models: The Sequel," *Nucl. Phys.* **B420** (1994) 468–504, arXiv:hep-ph/9310320.

[397] L. E. Ibanez and G. G. Ross, "Fermion masses and mixing angles from gauge symmetries," *Phys. Lett.* **B332** (1994) 100–110, arXiv:hep-ph/9403338.

[398] E. Dudas, S. Pokorski, and C. A. Savoy, "Soft scalar masses in supergravity with horizontal $U(1)_X$ gauge symmetry," *Phys. Lett.* **B369** (1996) 255–261, arXiv:hep-ph/9509410.

[399] P. Binetruy, S. Lavignac, and P. Ramond, "Yukawa textures with an anomalous horizontal Abelian symmetry," *Nucl. Phys.* **B477** (1996) 353–377, arXiv:hep-ph/9601243.

[400] E. Dudas, C. Grojean, S. Pokorski, and C. A. Savoy, "Abelian flavour symmetries in supersymmetric models," *Nucl. Phys.* **B481** (1996) 85–108, arXiv:hep-ph/9606383.

[401] K. Agashe and C. D. Carone, "Supersymmetric flavor models and the $B \to \phi K_S$ anomaly," *Phys. Rev.* **D68** (2003) 035017, arXiv:hep-ph/0304229.

[402] A. Pomarol and D. Tommasini, "Horizontal symmetries for the supersymmetric flavor problem," *Nucl. Phys.* **B466** (1996) 3–24, arXiv:hep-ph/9507462.

[403] L. J. Hall and H. Murayama, "A Geometry of the generations," *Phys. Rev. Lett.* **75** (1995) 3985–3988, arXiv:hep-ph/9508296.

[404] R. Barbieri, G. R. Dvali, and L. J. Hall, "Predictions From A U(2) Flavour Symmetry In Supersymmetric Theories," *Phys. Lett.* **B377** (1996) 76–82, arXiv:hep-ph/9512388.

[405] R. Barbieri, L. J. Hall, S. Raby, and A. Romanino, "Unified theories with U(2) flavor symmetry," *Nucl. Phys.* **B493** (1997) 3–26, arXiv:hep-ph/9610449.

[406] R. Barbieri, L. J. Hall, and A. Romanino, "Consequences of a U(2) flavour symmetry," *Phys. Lett.* **B401** (1997) 47–53, arXiv:hep-ph/9702315.

[407] R. Dermisek and S. Raby, "Fermion masses and neutrino oscillations in SO(10) SUSY GUT with $D(3) \times U(1)$ family symmetry," *Phys. Rev.* **D62** (2000) 015007, arXiv:hep-ph/9911275.

[408] S. F. King and G. G. Ross, "Fermion masses and mixing angles from SU(3) family symmetry," *Phys. Lett.* **B520** (2001) 243–253, arXiv:hep-ph/0108112.

[409] S. F. King and G. G. Ross, "Fermion masses and mixing angles from SU(3) family symmetry and unification," *Phys. Lett.* **B574** (2003) 239–252, arXiv:hep-ph/0307190.

[410] G. G. Ross, L. Velasco-Sevilla, and O. Vives, "Spontaneous CP violation and non-Abelian family symmetry in SUSY," *Nucl. Phys.* **B692** (2004) 50–82, arXiv:hep-ph/0401064.

[411] S. Antusch, S. F. King, and M. Malinsky, "Solving the SUSY Flavour and CP Problems with SU(3) Family Symmetry," *JHEP* **06** (2008) 068, arXiv:0708.1282 [hep-ph].

[412] J. A. Casas, A. Lleyda, and C. Munoz, "Strong constraints on the parameter space of the MSSM from charge and color breaking minima," *Nucl. Phys.* **B471** (1996) 3–58, arXiv:hep-ph/9507294.

[413] J. A. Casas and S. Dimopoulos, "Stability bounds on flavor-violating trilinear soft terms in the MSSM," *Phys. Lett.* **B387** (1996) 107–112, arXiv:hep-ph/9606237.

[414] J. A. Casas, "Charge and color breaking," arXiv:hep-ph/9707475.

[415] S. P. Martin and M. T. Vaughn, "Two loop renormalization group equations for soft supersymmetry breaking couplings," *Phys. Rev.* **D50** (1994) 2282, arXiv:hep-ph/9311340.

[416] W. Altmannshofer, "Phenomenology of CP Violation in a Flavor Blind MSSM and Beyond," *AIP Conf. Proc.* **1200** (2010) 867–870, arXiv:0911.0295 [hep-ph].

[417] **MEGA** Collaboration, M. L. Brooks *et al.*, "New Limit for the Family-Number Non-conserving Decay $\mu^+ \to e^+\gamma$," *Phys. Rev. Lett.* **83** (1999) 1521–1524, arXiv:hep-ex/9905013.

[418] L. Calibbi, J. Jones-Perez, and O. Vives, "Electric dipole moments from flavoured CP violation in SUSY," *Phys. Rev.* **D78** (2008) 075007, arXiv:0804.4620 [hep-ph].

[419] L. Calibbi *et al.*, "FCNC and CP Violation Observables in a SU(3)-flavoured MSSM," *Nucl. Phys.* **B831** (2010) 26–71, arXiv:0907.4069 [hep-ph].

[420] S. Bethke, "The 2009 World Average of $\alpha_s(M_Z)$," *Eur. Phys. J.* **C64** (2009) 689–703, arXiv:0908.1135 [hep-ph].

[421] **Tevatron Electroweak Working Group** Collaboration, "Combination of CDF and D0 Results on the Mass of the Top Quark," arXiv:0903.2503 [hep-ex].

[422] K. G. Chetyrkin, J. H. Kuhn, and M. Steinhauser, "RunDec: A Mathematica package for running and decoupling of the strong coupling and quark masses," *Comput. Phys. Commun.* **133** (2000) 43–65, arXiv:hep-ph/0004189.

[423] **CLEO** Collaboration, B. I. Eisenstein *et al.*, "Precision Measurement of B($D^+ \to \mu^+\nu$) and the Pseudoscalar Decay Constant f_{D^+}," *Phys. Rev.* **D78** (2008) 052003, arXiv:0806.2112 [hep-ex].

[424] V. Lubicz and C. Tarantino, "Flavour physics and Lattice QCD: averages of lattice inputs for the Unitarity Triangle Analysis," *Nuovo Cim.* **123B** (2008) 674–688, arXiv:0807.4605 [hep-lat].

[425] C. Aubin, J. Laiho, and R. S. Van de Water, "The neutral kaon mixing parameter B_K from unquenched mixed-action lattice QCD," *Phys. Rev.* **D81** (2010) 014507, arXiv:0905.3947 [hep-lat].

[426] U. Nierste, "Three Lectures on Meson Mixing and CKM phenomenology," arXiv:0904.1869 [hep-ph].

[427] C. R. Allton *et al.*, "B parameters for $\Delta S = 2$ supersymmetric operators," *Phys. Lett.* **B453** (1999) 30–39, arXiv:hep-lat/9806016.

[428] D. Becirevic, V. Gimenez, G. Martinelli, M. Papinutto, and J. Reyes, "B-parameters of the complete set of matrix elements of $\Delta B = 2$ operators from the lattice," *JHEP* **04** (2002) 025, arXiv:hep-lat/0110091.

[429] R. Babich *et al.*, "$K^0 - \bar{K}^0$ mixing beyond the standard model and CP-violating electroweak penguins in quenched QCD with exact chiral symmetry," *Phys. Rev.* **D74** (2006) 073009, arXiv:hep-lat/0605016.

Acknowledgements

I would like to thank all the people who supported me during my PhD time and who contributed to the success of my thesis.

First and foremost I would like to thank my supervisor Andrzej Buras for giving me the opportunity to work in your research group and to do the PhD with you. I am very happy for all your support throughout the last years, for the discussions with you, the many possibilities to go to conferences, workshops and summerschools and of course for your big support in the application for a post doc position.

In particular I would also like to thank Paride Paradisi. Working with you was always a real pleasure for me and from our countless discussions about physics I learned really a lot. I look forward to collaborating with you also in the future.

Many thanks also to all my other collaborators, in particular Patricia Ball, Aoife Bharucha, Stefania Gori, Diego Guadagnoli, David Straub and Michael Wick for the interesting work we did together, for all the inspiring discussions and the efficient collaborations.

Special thanks to my office mate Michael Wick for tolerating me for over 4.5 years now. Working with you was always uncomplicated and relaxed.

Many thanks also to all my other colleagues from T31 and beyond for the very pleasant working environment.

Finally I would like to thank my family and especially my parents for their constant support throughout the years. And last but definitively not least very special thanks to Stefania. I am so glad to have found you.